Department of Chemistry

Characterisation and Treatability of Natural Organic Matter in Groundwaters Used for Drinking Water

Stacey Hamilton

This thesis is presented for the Degree of
Doctor of Philosophy
of
Curtin University

April 2014

Declaration

To the best of my knowledge and belief, this Thesis contains no material previously published by any other person except where due acknowledgement has been made.

This Thesis contains no material which has been accepted for the award of any other degree or diploma in any university.

Signature: _____

Date: _____

Acknowledgements

First and foremost, I would like to offer my deepest gratitude to my Principal Supervisor, A/Prof. Cynthia Joll. Your assistance and encouragement towards my PhD studies, especially during the Thesis preparation stage, will always be appreciated. I know it was a LONG time coming, but it's finally in!

The contribution of my Co-Supervisor, Dr Paul Greenwood, is also gratefully acknowledged, especially in terms of feedback on the pyrolysis data and many chapter reviews. Thank you for all your help over the years.

I would also like to acknowledge Mr Geoff Chidlow, for his invaluable technical assistance in the operation of the GC-MS equipment to allow me to gain a better understanding of the various analytical techniques. Assistance from Mr Peter Chapman for FTIR analyses is also greatly appreciated.

To the staff and students (both past and present) from the Department of Chemistry, thank you for your ongoing support, assistance and friendship over the years. Special thanks must go to Dr Daniel Southam, Amy Bowater, Dr Emma Bartle, Dr Chris May and Lecinda Collins-Brown for their friendship which I am thankful has continued even after our careers have progressed. I would also like to thank the CWQRC crew that I worked with over the years – Dr Brad Allpike, Dr Justin Blythe, Dr Daniel Couton, Dr Ina Kristiana, Hanna Driessen, Michael Alessandrino, Dr Ben Warton, Arron Lethorn, Paul Pringle, Clara Loi, Dr Suzy McDonald, Dr Lyndon Berwick, Dr Francesco Busetti and Andrew Chan for all their help and companionship in the laboratory. I'm guessing the laboratory is pretty quiet now that I am not around.

I would like to thank the staff at the Water Corporation of Western Australia for their assistance in the provision of samples from the Wanneroo Groundwater Treatment Plant, for their technical advice, and for giving useful operational information in relation to my project. Special thanks must go to the Water Treatment Process Expertise Group and the Wastewater Quality Branch, as well as various other staff in the Corporation, for their support as I finalised this Thesis.

I am very grateful to the Cooperative Research Centre for Water Quality and Treatment (now Water Research Australia) for a PhD scholarship to support this study.

Finally, I would like to thank my family and friends for their constant love and support throughout the years. Special thanks go to my parents, Kay and Bob, for all your encouragement, endless questions and reminders to submit my Thesis! I would also like to thank Tahlia (RIP) and Riley for always keeping me company during the long hours sitting at the computer or reading papers.

Publications

Publications arising from the present study:

Conference Presentations (platform), where a conference paper was submitted

Hamilton, S., Joll, C., Greenwood, P. and Kagi, R. (2007) MIEX® treatment of polarity based fractions of natural organic matter from a Western Australian groundwater. *AWWA Water Quality and Technology Conference and Exhibition*, Charlotte, North Carolina, USA, 4-8 November.

Hamilton, S. (2006) Isolation and characterisation of natural organic matter from Perth groundwaters. *CRC Water Quality and Treatment Postgraduate Student Conference,* Melbourne, Victoria, 10-13 July.

Conference Presentations (poster), where a conference abstract was submitted

Hamilton, S., Joll, C.A., Greenwood, P. and Kagi, R.I. (2006) Isolation and characterisation of natural organic matter from Perth groundwaters. *Combined National Conference of the Australian Organic Geochemistry Society and the NOM Interest Group*, Rottnest Island, Western Australia, 12-15 February.

List of Abbreviations

alum	aluminium sulfate
BIF	bromine incorporation factor
DOC	dissolved organic carbon
DBP	disinfection by-product
DBPFP	disinfection by-product formation potential
DMTS	dimethyltrisulfide
EC	enhanced coagulation
EEM	excitation-emission matrix
FAMEs	fatty acid methyl esters
FPD	filter photometric detection
FTIR	Fourier transform infrared
GC-MS	gas chromatography-mass spectrometry
GWTP	groundwater treatment plant
HAA	haloacetic acid
HPI	hydrophilic
HPO	hydrophobic
HPSEC	high pressure size exclusion chromatography
HS SPME	headspace solid-phase microextraction
HU	Hazen units
MIEX®	magnetic ion exchange
MSSV	micro-scale sealed vessel
MW	molecular weight
NOM	natural organic matter
NMR	nuclear magnetic resonance
OCD	organic carbon detection
PAH	polycyclic aromatic hydrocarbon
py-GC-MS	pyrolysis-gas chromatography-mass spectrometry
RO	reverse osmosis
R.T.	retention time
SPME	solid-phase microextraction

SUVA	specific UV absorbance
TIC	total ion chromatogram
TDS	total dissolved solids
THM	trihalomethane
THMFP	trihalomethane formation potential
TMAH	tetramethylammonium hydroxide
TPI	transphilic
TPIB	transphilic base
TPIN	transphilic neutral
UF	ultrafiltration
USGS	United States Geological Survey
UV	ultraviolet

Abstract

Natural organic matter (NOM) is present in all natural water sources and is a heterogeneous, complex mixture of organic compounds derived from the natural environment. NOM significantly affects the properties of the water source and can lead to the formation of unpleasant tastes and odours, impart a brown colour to the water and can act as a substrate for microbial growth. If not effectively removed by treatment, NOM may provide precursors for disinfection by-products (DBPs) during disinfection processes and provide a food source for biological regrowth and biofilm formation in distribution systems. Therefore, NOM directly impacts on source water management, treatment processes and distribution systems.

As NOM represents a complex mixture of compounds derived from plants, animals and microorganisms, structural characterisation of NOM is often difficult and requires a multi-faceted approach. New analytical methods continue to be developed to aid in the structural analysis of NOM, information which can be used to assess the effectiveness of treatment processes. The study described in this Thesis contributes to the body of characterisation studies being conducted to develop a detailed understanding of the origins, structural features and reactivity of NOM in source waters, in order to help predict the impact of this type of NOM on drinking water supplies and to allow optimisation of treatment processes for NOM removal.

In the preliminary investigation presented in Chapter 2, the general water quality of a selection of bores from the Wanneroo borefield in Perth, Western Australia, was assessed to allow selection of the most promising bore for the large scale treatment and characterisation studies presented in Chapters 3-5 of this Thesis. The four bores selected (termed W20, W60, W280 and W300) were located in two distinct regions of the borefield (W20 near W60, W280 near W300). The four bores had a wide range of dissolved organic carbon (DOC) concentrations and UV_{254} absorbance values. The UV absorbance at 254 nm (UV_{254}) is an approximate indicator of the aromatic content of NOM. These ranges in DOC and UV_{254} are due to the diverse hydrogeology of the Wanneroo borefield, but the specific UV_{254} absorbance ($SUVA_{254}$) values of W20 and W60 were similar and of W280 and W300 were

similar. The XAD resin fractionation distributions of NOM in the four samples were relatively similar where each groundwater had a high proportion of hydrophobic and transphilic material, enriched in aromatic moieties compared to the hydrophilic fraction. This suggests that, whilst the general water quality can vary within the borefield, the hydrophobicity of the DOC present in each bore across the borefield was relatively similar. The bore chosen for the further detailed characterisation studies was W300, primarily due to its high DOC concentration, which allowed enough solid material to be collected for the characterisation studies.

After selection of W300, the performance of two NOM isolation methods, ultrafiltration (UF) and XAD-8/XAD-4 resin fractionation, were compared. In Chapter 3, the isolation of a NOM fraction from bore W300 using UF is discussed in detail, and the method for collecting a Raw Water UF solid isolate is described. Desalting of the Raw Water UF fraction was challenging and, even after dialysis, a high ash content remained, hindering characterisation. Even though the quality of the spectra was impeded by the high ash content, FTIR and solid-state ^{13}C NMR spectroscopic analyses indicated a significant aliphatic content in this fraction. Further characterisation by size exclusion chromatography (SEC) also showed a significant contribution from humic substances of relatively high molecular weight.

The Raw Water UF fraction was then treated by a laboratory simulation of the magnetic ion exchange (MIEX®) resin process, a key NOM removal process in operation at the Wanneroo Groundwater Treatment Plant, where water from bore W300 is blended with other Wanneroo bore waters prior to the treatment process. The Raw Water UF fraction was also treated with chlorine to measure the formation of disinfection by-products pre- and post-MIEX® treatment. As the MIEX® process is a relatively new technology in water treatment, the removal effectiveness of the resin for different types of organic matter is not yet well understood. Treatment of the Raw Water UF fraction by MIEX® resin led to only a small reduction in DOC concentration (12 %). The high salt content of the UF fraction may have effectively competed for active ion-exchange sites on the resin, limiting the ability of the MIEX® resin to remove DOC from the UF fraction. Chlorine reactivity of the UF fraction before and after MIEX® treatment where the DOC concentration was normalised to 2 mg L^{-1} prior to chlorine addition showed that the DOC in each

sample had a similar propensity to form trihalomethanes (THMs), but MIEX® treatment of the UF fraction did significantly reduce the propensity for haloacetic acid (HAA) formation.

Characterisation of fractions of NOM from W300 isolated by an XAD-8/XAD-4 resin procedure, and treatment of these fractions by the MIEX® process, is discussed in Chapter 4. Three solid isolates were recovered in the XAD-8/XAD-4 fractionation procedure: hydrophobic (HPO), transphilic base (TPIB) and transphilic neutral (TPIN); and the hydrophilic (HPI) fraction was obtained as a liquid isolate. Desalting of the solid isolates was still challenging, and a high salt content hindered characterisation of the TPIB fraction. Characterisation of the HPO, TPIB and TPIN fractions by FTIR and solid-state ^{13}C NMR spectroscopy revealed significant aliphatic content in these fractions. Further characterisation by pyrolysis-gas chromatography-mass spectrometry (py-GC-MS), thermochemolysis-GC-MS and micro-scale sealed vessel (MSSV)-py-GC-MS revealed that the HPO fraction had a significant contribution of polysaccharide input, whereas the higher nitrogen and oxygen content present in the elemental analysis for the TPIB and TPIN fractions was consistent with more nitrogen- and oxygen-containing groups being observed during the pyrolysis characterisation studies on these two fractions.

The HPO, TPIB and TPIN fractions were then treated by the MIEX® process in a laboratory experiment. MIEX® treatment led to a significant reduction in DOC concentrations (55 – 69 %) and UV_{254} absorbances (57 – 87 %), suggesting that MIEX® was effective for targeting removal of the more non-polar (HPO) and intermediate polarity (TPI) NOM fractions.

The HPO and TPIB fractions, before and after MIEX® treatment, normalised to the same DOC concentration, were treated with chlorine to measure their disinfection by-product formation potential. Both the HPO and TPIB fractions showed similar reactivity with chlorine. The formation of THMs and HAAs for the HPO fraction and the HPO fraction after MIEX® treatment were essentially identical, indicating that the reactivity of the DOC in the two samples was very similar. MIEX® treatment prior to the disinfection studies did not appear to offer an option for selective removal of reactive DBP precursors over non-reactive precursors for the HPO fractions. In contrast, the disinfection study of the TPI fractions did show a reduction

in THMs and HAAs for the post- MIEX® treated sample. This study indicates that the major DBP precursors within the quantitatively significant HPO fraction can not be preferentially removed by MIEX® treatment and should be targeted by additional treatment in order to lower DBP formation from this source water.

To complement the procedure in Chapter 4 whereby W300 water was fractionated by an established XAD resin adsorption method and then treated by the MIEX® resin process on a laboratory-scale, the work undertaken in Chapter 5 involved treating W300 water by a MIEX® resin process first, prior to XAD-8/XAD-4 fractionation of the NOM remaining after MIEX® treatment. Treating the raw water with MIEX® resin first, then fractionation of the remaining NOM, revealed a range of subtle differences in the molecular composition and properties of the fractions isolated, compared to the fractions obtained in Chapter 4. MIEX® pretreatment changed the distribution of the XAD fractions, due to the preferential removal of TPI and HPI material during MIEX® treatment. Characterisation by FTIR and solid-state ^{13}C NMR spectroscopy indicated a significant shift in carbon distribution to aliphatic material compared to the untreated samples in Chapter 4, indicating that the MIEX® treatment had removed some aromatic material from the MIEX® HPO, MIEX® TPIB and MIEX® TPIN samples. Further characterisation by pyrolysis-gas chromatography-mass spectrometry (py-GC-MS), thermochemolysis-GC-MS and micro-scale sealed vessel-py-GC-MS revealed that the MIEX® HPO fraction appeared to have a significant contribution from alkyl phenols and polyaromatic hydrocarbons. The higher nitrogen and oxygen content present in the elemental analysis for the MIEX® TPIB and MIEX® TPIN fractions was consistent with more nitrogen- and oxygen-containing functionalities (such as those derived from proteins and tannins) being observed in the MIEX® TPIB and MIEX® TPIN product mixtures from the three pyrolysis-based methods.

MIEX® treatment prior to fractionation also led to a reduced concentration of THMs and HAAs formed in disinfection by-product formation experiments compared to the corresponding DBP concentrations formed from the raw water HPO and TPI fractions (Chapter 4), but there was a trend towards increasing proportions of brominated species from the XAD fractions of NOM isolated after MIEX® treatment. This can be attributed to the high relative abundance in the MIEX® HPO and MIEX®

TPIB fractions of aliphatic material, as indicated in the FTIR and solid-state ^{13}C NMR spectroscopic analysis, since aliphatic material is generally highly reactive with bromine. This could be significant for any future increased focus on brominated species by DBP regulators.

Using a three-fold research approach to isolate NOM from a local groundwater source containing DOC in high concentration and of a highly hydrophobic nature has contributed to characterisation studies of NOM. The performance of two NOM isolation methods (UF and XAD-8/XAD-4 resin fractionation) has been compared, based on the efficiency with which NOM was collected and separated. Next, the isolated NOM was compared using several analytical methods, to shed light on the variability of molecules contributing to NOM in this highly hydrophobic, high DOC groundwater. The use of a variety of characterisation methods highlighted both the potential value and limitations of the analytical methods used in NOM research. Finally, the chemical composition and reactivity of the NOM isolates has revealed that this particular water source is susceptible to MIEX® treatment, and is highly reactive with chlorine to form DBPs. Treatment processes in addition to the MIEX® process will be required to remove the recalcitrant structural moieties present in the NOM in this water source and this additional treatment may be particularly necessary when DBP formation is an issue.

Table of Contents

ACKNOWLEDGEMENTS i
PUBLICATIONS iii
LIST OF ABBREVIATIONS iv
ABSTRACT vi
TABLE OF CONTENTS xi
LIST OF FIGURES xviii
LIST OF TABLES xxiii

1.0 INTRODUCTION 1
1.1 Natural Organic Matter 1
1.2 Characterisation of Natural Organic Matter 2
1.2.1 Preparative Procedures for the Isolation of Natural Organic Matter 3
1.2.1.1 Resin Adsorption Fractionation 3
1.2.1.1.1 Preparative XAD Resin Techniques 3
1.2.1.1.2 Rapid Fractionation Procedure 5
1.2.1.2 Ultrafiltration 5
1.2.2 Analysis of Isolated Natural Organic Matter 7
1.2.2.1 High Pressure Size Exclusion Chromatography 7
1.2.2.2 Ultraviolet Spectroscopy 8
1.2.2.3 Solid-State ^{13}C Nuclear Magnetic Resonance Spectroscopy 9
1.2.2.4 Fourier Transform Infrared Spectroscopy 9
1.2.2.5 Fluorescence Spectroscopy 10
1.2.2.6 Analytical Pyrolysis 11
1.2.2.7 Thermochemolysis 12
1.2.2.8 Micro-Scale Sealed Vessel Pyrolysis 13
1.2.2.9 Halogen Reactivity 13
1.2.2.9.1 Formation of Disinfection By-Products 15
1.3 Drinking Water Sources of Perth, Western Australia 15
1.4 Drinking Water Treatment for Perth Groundwaters 16

1.4.1 Water Quality Issues in the Wanneroo Source, Treatment and Distribution System 16
1.4.1.1 The Treatment Process at the Wanneroo Groundwater Treatment Plant 17
1.4.1.2 The MIEX® Process 19
1.5 Scope of Thesis 20

2.0 GENERAL CHARACTERISATION OF A SELECTION OF WANNEROO GROUNDWATER SAMPLES 23
2.1 Introduction 23
2.1.1 Scope of This Study 25
2.2 Experimental 25
2.2.1 Water Samples 25
2.2.2 Materials and Methods 26
2.2.2.1 Purified Laboratory Water 26
2.2.2.2 Cleaning Procedures 26
2.2.3 Rapid Fractionation Isolation Procedure 27
2.2.3.1 Cleaning of the Resins 27
2.2.3.2 pH Adjustment of the Water Sample 27
2.2.3.3 Fractionation Process 27
2.2.4 Measurement of Dissolved Organic Carbon Concentration 28
2.2.5 UV/Visible Spectroscopic Measurements 28
2.2.6 Analysis of Bromide Ion Concentration and General Water Quality Parameters 29
2.2.7 High Pressure Size Exclusion Chromatography 29
2.3 Results and Discussion 30
2.3.1 Characterisation of the Groundwater Samples 30
2.3.1.1 General Water Quality Parameters of the Groundwater Samples 30
2.3.1.2 Rapid Fractionation of the Groundwater Samples 31
2.3.1.3 Molecular Weight Distribution of the UV_{254}-Active DOC in the Groundwater Samples 34
2.3.2 Selection of Groundwater Bore for Detailed Study 37
2.3.3 General Water Quality of Groundwater from Bore W300 38
2.4 Conclusions 42

3.0 CHARACTERISATION AND TREATABILITY OF NOM ISOLATED FROM A HIGH HYDROPHOBICITY / HIGH DOC GROUNDWATER BY ULTRAFILTRATION 43
3.1 Introduction 43
3.1.1 Scope of This Study 45
3.2 Experimental 45
3.2.1 Water Sample 45
3.2.2 Cleaning Procedures 45
3.2.3 Ultrafiltration Isolation Protocol 45
3.2.4 MIEX® Treatment of the UF Fraction 46
3.2.4.1 Preconditioning of the MIEX® Resin 46
3.2.4.2 UF Stock Solution 46
3.2.4.3 MIEX® Treatment of UF Solution 47
3.2.5 Characterisation Methodology 47
3.2.5.1 Elemental Analysis 47
3.2.5.2 Fourier Transform Infrared Spectroscopy 47
3.2.5.3 Solid-State ^{13}C Nuclear Magnetic Resonance Spectroscopy 48
3.2.5.4 Fluorescence Spectroscopy 48
3.2.6 Disinfection By-Product Formation Potential Experiments 49
3.2.6.1 Preparation of Chlorine Solution 49
3.2.6.2 Chlorination Experiments 49
3.2.7 Analysis of Disinfection By-Products 50
3.2.7.1 Analysis of Trihalomethanes 50
3.2.7.2 Analysis of Haloacetic Acids 51
3.3 Results and Discussion 52
3.3.1 Isolation of UF Fraction 52
3.3.2 Characterisation of Isolated Solid UF Fraction 53
3.3.2.1 Elemental Analysis 53
3.3.2.2 Fourier Transform Infrared Spectroscopic Analysis 54
3.3.2.3 Solid-State ^{13}C Nuclear Magnetic Resonance Spectroscopic Analysis 56
3.3.2.4 Size Exclusion Chromatographic Analysis 57
3.3.2.5 Overall Characteristics of UF Solid Isolate 59

3.3.3 MIEX® Treatment of the Redissolved UF Fraction 60
3.3.3.1 DOC Concentration, UV_{254} and Colour 60
3.3.3.2 Fluorescence Excitation-Emission Spectroscopy 61
3.3.3.3 Size Exclusion Chromatographic Analysis 65
3.3.3.4 Disinfection By-Product Formation Potential 66
3.3.4 Conclusions 72

4.0 CHARACTERISATION AND TREATABILITY OF NOM ISOLATED FROM A HIGH HYDROPHOBICITY / HIGH DOC GROUNDWATER BY RESIN FRACTIONATION 74
4.1 Introduction 74
4.1.1 Scope of This Study 76
4.2 Experimental 77
4.2.1 Water Samples 77
4.2.2 Cleaning Procedures 77
4.2.3 NOM Resin Fractionation and Isolation Protocol 77
4.2.3.1 Cleaning of Dowex MSC-1 H Resin 77
4.2.3.2 Preparative Fractionation Process 78
4.2.4 MIEX® Treatment of the XAD Isolated Fractions 79
4.2.4.1 Preconditioning of the MIEX® Resin 79
4.2.4.2 Stock Solutions for MIEX® Treatment 79
4.2.4.2.1 Stock Solutions of the HPO, TPIB and TPIN Fractions 79
4.2.4.2.2 Stock Solution of the HPI Fraction 79
4.2.4.3 MIEX® Treatment of Stock Solutions 80
4.2.5 Characterisation Methodology for the XAD Fractions 80
4.2.5.1 Flash Pyrolysis-Gas Chromatography-Mass Spectrometry 80
4.2.5.2 On-line Thermochemolysis-Gas Chromatography-Mass Spectrometry 81
4.2.5.3 Micro-Scale Sealed Vessel Pyrolysis-Gas Chromatography Mass Spectrometry 81
4.2.5.4 Other Spectroscopic Analyses 82
4.2.6 Disinfection By-Product Formation Potential Experiments 82
4.2.6.1 Chlorination Experiments of XAD Fractions Pre- and Post-MIEX® Treatment 82

4.2.7 Analysis of Disinfection By-Products 82
4.3 Results and Discussion 83
4.3.1 Isolation of XAD Fractions 83
4.3.2 Characterisation of Isolated Solid XAD Fractions 85
4.3.2.1 Elemental Analysis and Atomic Ratios 85
4.3.2.2 Fourier Transform Infrared Spectroscopic Analysis 87
4.3.2.3 Solid-State ^{13}C Nuclear Magnetic Resonance Spectroscopic Analysis 89
4.3.2.4 Pyrolysis-Gas Chromatography-Mass Spectrometry 92
4.3.2.5 On-line Thermochemolysis-Gas Chromatography-Mass Spectrometry 100
4.3.2.6 Micro-Scale Sealed Vessel Pyrolysis-Gas Chromatography-Mass Spectrometry 106
4.3.2.7 Overall Characteristics of the HPO, TPIB and TPIN Fractions 111
4.3.3 MIEX® Treatment of the HPO, TPIB and TPIN Fractions 112
4.3.3.1 DOC Concentration, UV_{254} and Colour 112
4.3.3.2 Fluorescence Excitation-Emission Spectroscopy 114
4.3.3.3 Size Exclusion Chromatographic Analysis 120
4.3.3.4 Disinfection By-Product Formation Potential 125
4.3.4 Conclusions 130

5.0 CHARACTERISATION OF RESIN-FRACTIONATED NOM REMAINING AFTER MIEX® TREATMENT OF A HIGH HYDROPHOBICITY / HIGH DOC GROUNDWATER 132
5.1 Introduction 133
5.1.1 Scope of This Study 133
5.2 Experimental 134
5.2.1 Water Samples 134
5.2.2 Cleaning Procedures 134
5.2.3 MIEX® Treatment of the Raw Water 135
5.2.3.1 Preconditioning of the MIEX® Resin 135
5.2.3.2 Treatment of Raw Water by Preconditioned MIEX® Resin 135
5.2.4 NOM Resin Fractionation and Isolation Protocol 135

5.2.4.1 Preparative Fractionation Process 135
5.2.5 Methodology for Characterisation of NOM 137
5.2.6 Disinfection By-Product Formation Potential Experiments 137
5.2.6.1 Stock Solutions of the MIEX® HPO and MIEX® TPIB Fractions 137
5.2.6.2 Chlorination Experiments for the MIEX® HPO and MIEX® TPIB Fractions 137
5.2.7 Analysis of Disinfection By-Products 138
5.3 Results and Discussion 138
5.3.1 MIEX® Resin Preconditioning and MIEX® Treatment of W300 Raw Water 138
5.3.1.1 Size Exclusion Chromatographic Analysis 140
5.3.1.2 Fluorescence Excitation-Emission Spectroscopy 142
5.3.2 Isolation of XAD Fractions from NOM Remaining After MIEX® Treatment 144
5.3.3 Characterisation of Solid XAD Fractions from NOM Remaining After MIEX® Treatment 145
5.3.3.1 Elemental Analysis and Atomic Ratios 145
5.3.3.2 Fourier Transform Infrared Spectroscopic Analysis 147
5.3.3.3 Solid-State ^{13}C Nuclear Magnetic Resonance Spectroscopic Analysis 149
5.3.3.4 Pyrolysis-Gas Chromatography-Mass Spectrometry 152
5.3.3.5 On-line Thermochemolysis-Gas Chromatography-Mass Spectrometry 159
5.3.3.6 Micro-Scale Sealed Vessel Pyrolysis-Gas Chromatography-Mass Spectrometry 165
5.3.3.7 Overall Characteristics of the MIEX® HPO, MIEX® TPIB and MIEX® TPIN Fractions 169
5.3.3.8 Disinfection By-Product Formation Potential 170
5.3.4 Conclusions 174

6.0 SUMMARY OF CHARACTERISATION METHODS, RECOMMENDATIONS AND OVERALL CONCLUSIONS 176
6.1 Comparison of Methods for Concentration of NOM 176
6.2 Comparison of the Chemical Composition of NOM Isolates 178

6.3 Comparison of Methods for NOM Characterisation 181
6.3.1 Elemental Analysis 182
6.3.2 Fourier Transform Infrared Spectroscopy 183
6.3.3 Solid-State ^{13}C Nuclear Magnetic Resonance Spectroscopy 184
6.3.4 Pyrolysis-Gas Chromatography-Mass Spectrometry 185
6.3.5 On-line Thermochemolysis-Gas Chromatography-Mass Spectrometry 187
6.3.6 Micro-Scale Sealed Vessel Pyrolysis-Gas Chromatography Mass Spectrometry 189
6.4 Effects of MIEX® Treatment on the Isolated Fractions 190
6.4.1 DOC Concentration, UV_{254} Absorbance and Colour 190
6.4.2 Fluorescence Excitation-Emission Spectroscopy 191
6.4.3 Size Exclusion Chromatography 192
6.4.4 Disinfection By-Product Formation Potential 193
6.5 MIEX® Treatment Applications 194
6.6 Summary of Characterisation Methods for Water Industry Application 195
6.7 Thesis Conclusions 199

APPENDIX 1 202
APPENDIX 2 211
REFERENCES 220

List of Figures

CHAPTER 1

Figure 1.1 The concentration of a water sample by ultrafiltration. 6

Figure 1.2 A schematic diagram of the two process streams currently operating at the Wanneroo Groundwater Treatment Plant. 18

Figure 1.3 The reversible process of DOC removal by the MIEX® resin (Slunjski et al. 2000, a). 20

CHAPTER 2

Figure 2.1 Location map showing the Perth metropolitan area and some of its water sources. Surface water sources are located to the east of the Darling Fault (modified from Hirschberg (1989)). 24

Figure 2.2 Location of the four groundwater bores W20, W60, W280 and W300 in the Wanneroo Production Borefield (modified from Davidson, 1995). 26

Figure 2.3 Schematic diagram of the XAD-8/XAD-4 resin procedure for rapid DOC fractionation. *Sampling points for the rapid fractionation procedure are shown in red. 32

Figure 2.4 HPSEC-UV_{254} chromatograms of the raw groundwater, XAD-8 eluent and XAD-4 eluent of a) W20; b) W60; c) W280 and d) W300 groundwater samples. Numbers correspond to eight distinct MW regions as described in Huber and Frimmel 1996 and Allpike et al. 2005. 35

Figure 2.5 a) HPSEC-OCD and b) HPSEC-UV_{254} chromatograms of W300 groundwater. Numbers correspond to eight distinct MW regions as described in Huber and Frimmel 1996 and Allpike et al. 2005. 40

CHAPTER 3

Figure 3.1 FT-IR spectrum of the UF fraction. 55

Figure 3.2 Solid-state ^{13}C NMR spectrum for the UF fraction. 56

Figure 3.3 Relative proportions of carbon types based on integration of regions of the solid-state ^{13}C NMR spectrum of the isolated UF NOM sample. 57

Figure 3.4 MW distribution of the UF retentate before dialysis analysed by a) SEC-OCD and b) SEC-UV_{254} detection. Numbers correspond to eight distinct MW regions, as described in Huber and Frimmel 1996 and Allpike et al. 2005. 58
Figure 3.5 Breakdown of fluorescent components (Chen et al. 2003, b). 63
Figure 3.6 Excitation-emission (EEM) fluorescence spectra of the UF fraction a) before and b) after MIEX® treatment. White arrows represent 'humic-like' and yellow arrows represent 'protein-like' components within the spectra. 64
Figure 3.7 MW distribution of the UF sample before and after MIEX® treatment by a) SEC-OCD and b) SEC-UV_{254} detection. Numbers correspond to eight distinct MW regions as described by Huber and Frimmel 1996 and Allpike et al. 2005. 66

CHAPTER 4

Figure 4.1 The treatment, isolation and characterisation methodology for Chapter 4. 77
Figure 4.2 FT-IR spectra for three of the XAD fractions of NOM isolated from W300 groundwater. 88
Figure 4.3 Solid-state ^{13}C NMR spectra for the a) HPO and b) TPIB fractions. 90
Figure 4.4 Relative proportions of carbon types in the solid-state ^{13}C NMR spectra of the isolated NOM fractions. 91
Figure 4.5a Total ion chromatogram from py-GC-MS of the HPO fraction. Peak assignments correspond to products listed in Table 4.4: ■ polysaccharides, ● N/S compounds, □ protein, ◊ lipids, ▲no specific source. The pie chart reflects relative proportions of six major product and precursor types. 95
Figure 4.5b Total ion chromatogram from py-GC-MS of the TPIB fraction. Peak assignments correspond to products listed in Table 4.4: ■ polysaccharides, ● N/S compounds, □ protein, ◊ lipids, ▲no specific source. The pie chart reflects relative proportions of six major product and precursor types. 96
Figure 4.5c Total ion chromatogram from py-GC-MS of the TPIN fraction. Peak assignments correspond to products listed in Table 4.4: ■ polysaccharides, ● N/S compounds, □ protein, ◊ lipids, ▲no specific source. The pie chart reflects relative proportions of six major product and precursor types. 97
Figure 4.6a Total ion chromatogram from thermochemolysis-GC-MS of the HPO fraction. Peak assignments correspond to products listed in Table 4.5: ■ polysaccharides, ● N/S compounds, □ protein, ◊ lipids, ◄ methyl

methoxybenzoates, ►methyl benzoates, ▲no specific source. The pie chart reflects relative proportions of eight major product and precursor groups. 101
Figure 4.6b Total ion chromatogram from thermochemolysis-GC-MS of the TPIB fraction. Peak assignments correspond to products listed in Table 4.5: ■ polysaccharides, ● N/S compounds, □ protein, ◊ lipids, ◄ methyl methoxybenzoates, ►methyl benzoates, ▲no specific source. The pie chart reflects relative proportions of eight major product and precursor groups. 102
Figure 4.6c Total ion chromatogram from thermochemolysis-GC-MS of the TPIN fraction. Peak assignments correspond to products listed in Table 4.5: ■ polysaccharides, ● N/S compounds, □ protein, ◊ lipids, ◄ methyl methoxybenzoates, ►methyl benzoates, ▲no specific source. The pie chart reflects relative proportions of eight major product and precursor groups. 103
Figure 4.7 Total ion chromatograms obtained by MSSV pyrolysis-GC-MS analysis of the a) HPO, b) TPIB and c) TPIN fractions. Peak assignments correspond to products listed in Table 4.6 and Appendix 1. The pie charts reflect relative proportions of eight major product and precursor groups. 108
Figure 4.8 Excitation-emission (EEM) fluorescence spectra of the a) pre and b) post MIEX® treated HPO fraction. White arrows represent 'humic-like' components within the spectra. 'Protein-like' components within the spectra could not be identified due to the high concentration of 'humic-like' material. 117
Figure 4.9 Excitation-emission (EEM) fluorescence spectra of the a) pre and b) post MIEX® treated TPIB fraction. White arrows represent 'humic-like' components within the spectra. 'Protein-like' components within the spectra could not be identified due to the high concentration of 'humic-like' material. 118
Figure 4.10 Excitation-emission (EEM) fluorescence spectra of the a) pre and b) post MIEX® treated TPIN fraction. The intensity of the EEM is represented by contour lines. White arrows represent 'humic-like' components within the spectra. 'Protein-like' components within the spectra could not be identified due to the high concentration of 'humic-like' material. 119
Figure 4.11 MW distribution of the HPO fraction before and after MIEX® treatment detected by a) SEC-OCD and b) SEC-UV_{254}. Numbers correspond to eight distinct MW regions (Huber and Frimmel 1996; Allpike et al. 2005). 121

Figure 4.12 MW distribution of the TPIB fraction before and after MIEX® treatment detected by a) SEC-OCD and b) SEC-UV_{254}. Numbers correspond to eight distinct MW regions (Huber and Frimmel 1996; Allpike et al. 2005). 122
Figure 4.13 MW distribution of the TPIN fraction before and after MIEX® treatment detected by a) SEC-OCD and b) SEC-UV_{254}. Numbers correspond to eight distinct MW regions (Huber and Frimmel 1996; Allpike et al. 2005). 123

CHAPTER 5

Figure 5.1 The treatment, isolation and characterisation methodology for Chapter 5. 134
Figure 5.2 The XAD-8/XAD-4 preparative resin isolation procedure. Four fractions of NOM from the MIEX® treated water were obtained. 136
Figure 5.3 Molecular weight distribution of the raw water before and after MIEX® treatment measured by a) SEC-OCD and b) SEC-UV_{254} detection. Numbers correspond to eight distinct MW regions as described by Huber and Frimmel 1996 and Allpike et al. 2005. 141
Figure 5.4 Excitation-emission (EEM) fluorescence spectra of the a) raw water and b) MIEX® treated water. White arrows represent 'humic-like' components within the spectra. 'Protein-like' components within the spectra could not be identified due to the high concentration of 'humic-like' material. 143
Figure 5.5 FT-IR spectra for the three XAD fractions isolated from MIEX® treated water. 148
Figure 5.6 Solid-state ^{13}C NMR spectra of the a) HPO and b) TPIB fraction isolated from the MIEX® treated water. 150
Figure 5.7 Relative proportions of carbon types in the solid-state ^{13}C NMR spectra of the isolated NOM fractions separated from water after MIEX® treatment. 151
Figure 5.8a Total ion chromatogram from the py-GC-MS of the MIEX® HPO fraction. Peak assignments correspond to products listed in Table 5.5: ■ polysaccharides, ● N/S compounds, □ protein, ◊ lipids, ▲no specific source. The pie chart reflects relative proportions of six major product and precursor types. 154
Figure 5.8b Total ion chromatogram from the py-GC-MS of the MIEX® TPIB fraction. Peak assignments correspond to products listed in Table 5.5: ■ polysaccharides, ● N/S compounds, □ protein, ◊ lipids, ▲no specific source. The pie chart reflects relative proportions of six major product and precursor types 155

Figure 5.8c Total ion chromatogram from the py-GC-MS of the MIEX® TPIN fraction. Peak assignments correspond to products listed in Table 5.5: ■ polysaccharides, ● N/S compounds, □ protein, ◊ lipids, ▲no specific source. The pie chart reflects relative proportions of six major product and precursor types 156
Figure 5.9a Total ion chromatogram from thermochemolysis-GC-MS of the MIEX® HPO fraction. Peak assignments correspond to products listed in Table 5.6: ■ polysaccharides, ● N/S compounds, □ protein, ◊ lipids, ◄ methyl methoxybenzoates, ►methyl benzoates, ▲no specific source. The pie chart reflects relative proportions of eight major product and precursor groups. 160
Figure 5.9b Total ion chromatogram from thermochemolysis-GC-MS of the MIEX® TPIB fraction. Peak assignments correspond to products listed in Table 5.6: ■ polysaccharides, ● N/S compounds, □ protein, ◊ lipids, ◄ methyl methoxybenzoates, ►methyl benzoates, ▲no specific source. The pie chart reflects relative proportions of eight major product and precursor groups. 161
Figure 5.9c Total ion chromatogram from thermochemolysis-GC-MS of the MIEX® TPIN fraction. Peak assignments correspond to products listed in Table 5.6: ■ polysaccharides, ● N/S compounds, □ protein, ◊ lipids, ◄ methyl methoxybenzoates, ►methyl benzoates, ▲no specific source. The pie chart reflects relative proportions of eight major product and precursor groups. 162
Figure 5.10 Total ion chromatograms obtained by MSSV pyrolysis-GC-MS analysis of the a) HPO, b) TPIB and c) TPIN fractions of NOM remaining in the MIEX® treated water. Peak assignments correspond to products listed in Table 5.7 and Appendix 2. The pie charts reflect relative proportions of eight major product and precursor groups. 167

List of Tables

CHAPTER 2

Table 2.1 DOC concentration, UV_{254} and $SUVA_{254}$ data for the four Wanneroo groundwater samples. 30

Table 2.2 Relative contribution of hydrophobic, transphilic and hydrophilic fractions of NOM in the four Wanneroo groundwater samples. 33

Table 2.3 General water quality parameters of W300 groundwater in the current study and as averages of routine borefield sampling events over eight years. 39

CHAPTER 3

Table 3.1 Elemental percentage composition and atomic ratio data for the UF fraction. 53

Table 3.2 DOC concentration, UV_{254}, $SUVA_{254}$ and colour parameters for the UF fraction before and after MIEX® treatment. 60

Table 3.3 Major fluorescent components in the excitation-emission matrix (Leenheer and Croué 2003). 62

Table 3.4 Oxidant demand of the UF fraction and the UF fraction after MIEX® treatment (halogenation conditions: 2 mg L^{-1} DOC, 6 mg L^{-1} Cl_2 dose, 0.2 mg L^{-1} Br^-, pH 7, 25°C, 168 hr). 67

Table 3.5 Concentrations of THMs from chlorination of the UF fraction and the UF fraction after MIEX® treatment (halogenation conditions: 2 mg L^{-1} DOC, 6 mg L^{-1} Cl_2 dose, 0.2 mg L^{-1} Br^-, pH 7, 25°C, 168 hr). 69

Table 3.6 Concentrations of HAAs from chlorination of the UF fraction and the UF fraction after MIEX® treatment (halogenation conditions: 2 mg L^{-1} DOC, 6 mg L^{-1} Cl_2 dose, 0.2 mg L^{-1} Br^-, pH 7, 25°C, 168 hr). 69

Table 3.7 BIF (THMs) and BIF (HAAs) obtained after 7 day chlorination experiment. 71

CHAPTER 4

Table 4.1 Isolated mass and relative proportions of the isolated NOM fractions. 83

Table 4.2 Elemental percentage compositions and atomic ratio data of the three solid XAD fractions. 85
Table 4.3 Elemental composition of the TPIB fraction. 86
Table 4.4 Major pyrolysis products from the XAD fractions and their likely origin. Full list of tentatively identified products can be found in Appendix 1. 98
Table 4.5 Major products from the XAD fractions and their possible origin. Full list of tentatively identified products can be found in Appendix 1. 104
Table 4.6 Major products from MSSV pyrolysis-GC-MS of the XAD fractions. 109
Table 4.7 DOC concentration, UV_{254}, $SUVA_{254}$ and colour parameters for the HPO, TPIB and TPIN fractions before and after MIEX® treatment. 113
Table 4.8 Oxidant demands of the HPO and TPIB fractions before and after MIEX® treatment (halogenation conditions: 2 mg L^{-1} DOC, 6 mg L^{-1} Cl_2 dose, 0.2 mg L^{-1} Br^-, pH 7, 25°C, 168 hours). 125
Table 4.9 Concentrations of THMs from chlorination of the HPO and TPIB fractions before and after MIEX® treatment (halogenation conditions: 2 mg L^{-1} DOC, 6 mg L^{-1} Cl_2 dose, 0.2 mg L^{-1} Br^-, pH 7, 25°C, 168 hours). 126
Table 4.10 Concentrations of HAAs from chlorination of the HPO and TPIB fractions before and after MIEX® treatment (halogenation conditions: 2 mg L^{-1} DOC, 6 mg L^{-1} Cl_2 dose, 0.2 mg L^{-1} Br^-, pH 7, 25°C, 168 hours). 126
Table 4.11 BIF values for THMs and HAAs obtained after a 7 day chlorination period. 129

CHAPTER 5
Table 5.1 DOC concentration, UV_{254}, $SUVA_{254}$ and colour parameters for W300 raw water before and after MIEX® treatment. 138
Table 5.2 Isolated mass and relative proportions of the NOM fractions. 144
Table 5.3 Elemental percentage compositions and atomic ratio data of the solid XAD fractions isolated from the MIEX® treated water. 145
Table 5.4 Elemental composition of the TPIB fraction isolated from the MIEX® treated water. 146
Table 5.5 Major pyrolysis products from the XAD fractions of the NOM isolated from the MIEX® treated water and their likely origin. Full list of tentatively identified products can be found in Appendix 2. 157

Table 5.6 Major products from the XAD fractions of NOM isolated from the MIEX® treated water and their possible origin. Full list of tentatively identified products can be found in Appendix 2. 163
Table 5.7 Major products from MSSV pyrolysis-GC-MS of the XAD fractions of NOM isolated after MIEX® treatment. 168
Table 5.8 Oxidant demands of the MIEX® HPO and MIEX® TPIB fraction (halogenation conditions: 2 mg L^{-1} DOC, 6 mg L^{-1} Cl_2 dose, 0.2 mg L^{-1} Br^-, pH 7, 25°C, 168 hours). 171
Table 5.9 Concentrations of THMs from chlorination of the MIEX® HPO and MIEX® TPIB fractions (halogenation conditions: 2 mg L^{-1} DOC, 6 mg L^{-1} Cl_2 dose, 0.2 mg L^{-1} Br^-, pH 7, 25°C, 168 hours). 172
Table 5.10 Concentrations of HAAs from chlorination of the MIEX® HPO and MIEX® TPIB fractions (halogenation conditions: 2 mg L^{-1} DOC, 6 mg L^{-1} Cl_2 dose, 0.2 mg L^{-1} Br^-, pH 7, 25°C, 168 hours). 172
Table 5.11 BIF values for THMs and HAAs obtained after a 7 day chlorination period. 174

CHAPTER 6

Table 6.1 Analytical methods used to identify different features of NOM. 181
Table 6.2 Summary of analytical methods and their utility for NOM characterisation and applicability to water industry issues. 197

Chapter 1

1.0 Introduction

1.1 Natural Organic Matter

Natural organic matter (NOM) occurs in varying concentrations in essentially all natural water supplies. In aquatic systems, NOM is a complex matrix of organic species, originating from soil, living organisms and/or plant materials, including partial degradation products from any or all of these sources, in natural waters. The concentrations of NOM and of the sub-groups of molecules that contribute to it are usually quantified in terms of the amount of carbon in the molecules (Croué et al. 1999, b). NOM, or total organic carbon (TOC), encompasses all organic matter in the watershed: insoluble particulate matter, including microorganisms, colloidal material and macro-scale plant and animal detritus, collectively referred to as particulate organic carbon (POC), as well as dissolved organic carbon (DOC) (Thurman 1985). DOC is an operationally defined term used to describe all the organic material able to pass through a 0.45 μm filter (Aiken and Leenheer 1993). It has been asserted (Thurman, 1985) that approximately 90 % of NOM in water is present as DOC. The DOC fraction of NOM can be further divided into humic and non-humic material (Beck and Jones 1992).

Aquatic humic substances are heterogeneous, yellow to black organic materials that are reported to include most of the naturally occurring dissolved organic matter in water (Franson 1998) and to comprise up to 60 % of NOM in source waters (Smith et al. 2003). They are generally defined based on their solubility properties in aqueous solutions. The generalized terms, humic acids, fulvic acids and humins, cover the major fractions distinguished on the basis of their solubility in acid/base and are used to describe humic substance components (Piccolo 2001). Humic acids are insoluble below pH 2, fulvic acids are soluble at all pH levels and humins are insoluble at any pH level (Franson 1998). Humic acids and fulvic acids, like NOM, cannot be regarded as single chemical entities; hence, chemical structures can only be

illustrated by model structures based on compositional, structural, functional and behavioural data (Franson 1998).

The structure of NOM varies based on its origin, as well as its chemical reactivity and biological breakdown (Chen et al. 2002). Difficulties have been encountered in determining the exact composition of NOM because it is comprised of a wide range of compounds, which can only be characterised broadly into generic groupings (Drikas 1997). Aquatic NOM is present in all source waters and on its own is not typically harmful. However, some of the compounds of which NOM is comprised affect water treatment by interacting with chemicals during treatment, thus adversely affecting water quality. For example, aquatic NOM in source waters can lead to the formation of unpleasant tastes and odours, impart a brown colour in water and can act as a substrate for microbial growth. If not effectively removed by treatment, NOM may provide precursors for disinfection by-products (DBPs) and provide a food source for biological regrowth and biofilm formation in the distribution system. NOM directly impacts, therefore, on source water management, treatment processes and distribution systems.

1.2 Characterisation of Natural Organic Matter

The characterisation of NOM is a complex and demanding analytical challenge due to the heterogeneous and variable nature of the material (Piccolo 2001; Her et al. 2003). Analytical methods range from simple, rapid methods requiring little or no sample preparation, but which provide only basic information, to methods that are complicated, expensive and laborious, but which provide detailed structural chemical information. No single technique exists to determine the chemical structure and functionality of NOM, and all methods have considerable limitations and drawbacks; generally, the more complex the technique, the more detailed the information that is yielded. To enable improved understanding of the types of organic compounds present in source waters and after treatment, a number of established and complementary characterisation techniques are typically used. Other analytical methods continue to be developed to aid the structural analysis of NOM and assess the effectiveness of treatment processes. A detailed understanding of the origins, structural features and reactivity of NOM in source waters will help minimise

detrimental impacts of NOM in potable water systems. Understanding the nature of NOM and its potential behaviour in water treatment continues to be a high priority for water utilities and researchers.

1.2.1 Preparative Procedures for the Isolation of Natural Organic Matter

Characterisation of NOM is often hampered by its inherent chemical complexity (Aiken et al. 1992). A large number of protocols have been developed to isolate aquatic organic matter (Leenheer 1981; Thurman and Malcolm 1981) which is typically the first step in the characterisation protocol. Isolation is often accompanied or followed by separation into more analytically amenable fractions. Two techniques commonly used for the isolation and fractionation of aquatic NOM are resin adsorption chromatography and ultrafiltration (Kitis et al. 2002; Leenheer 1981).

1.2.1.1 Resin Adsorption Fractionation

It is desirable to have an isolation approach based on the chemical properties of the material of interest. Adsorption chromatography on non-ionic macroporous resins (such as XAD-8 and XAD-4 resins) has been successfully employed for the isolation of NOM fractions, with most of the emphasis placed on hydrophobic organic acids (Aiken and Leenheer 1993). Sorption of humic substances is determined by the aqueous solubilities of the solutes and the solution pH (Thurman et al. 1978). At low pH, weak acids are protonated and adsorbed on the resin; at high pH, weak acids are ionised and desorption is favoured. Samples are generally acidified with mineral acids, such as hydrochloric acid (HCl), and passed through a column of XAD-8 resin (a methyl methacrylate resin). Adsorbed organic acids are then recovered by eluting the column with a basic solution.

1.2.1.1.1 Preparative XAD Resin Techniques

An XAD-8 method developed by the United States Geological Survey (USGS) research group (Leenheer 1981; Thurman and Malcolm 1981) has now been widely adopted as a standard method (Ma et al. 2001; Croué et al. 1999, a) for the isolation of humic substances. With this approach, the humic fraction of NOM (the hydrophobic fraction: HPO) is selectively adsorbed at acidic pH onto the XAD-8

resin column, whereas the non-humic fraction (the hydrophilic fraction: HPI) elutes through the XAD-8 resin. Using this technique, up to 60 percent of DOC can be isolated (Leenheer et al. 2000).

Another approach to the fractionation of organic matter in a water sample is to use a two-column array of XAD-8 and XAD-4 resins (Aiken et al. 1992; Andrews et al. 1994; Croué et al. 1993, a; Malcolm and MacCarthy 1992; Marhaba et al. 2003; Sharp et al. 2006, c). The two column array is an extension of the method of Thurman (1981) and allows for the isolation and separation of both the hydrophobic (HPO) fraction and a portion of the organic matter which is more hydrophilic. The fraction obtained from the XAD-4 resin (a styrene-divinylbenzene resin) is referred to as the transphilic fraction (TPI) because the compounds in this fraction are of intermediate polarity. The following fractions of DOC can be obtained using this approach: HPO, TPI and HPI, whereby the HPI fraction is material that passes through both columns. The main advantage associated with the XAD-8/XAD-4 chromatographic method of fractionation over the XAD method is that totals of approximately 55 – 90 % of the DOC from a variety of aquatic environments have been isolated (Aiken et al. 1992).

In addition to the capacity to isolate NOM from a variety of aquatic environments, the XAD-8/XAD-4 chromatographic method also allows the fractionation of the water to be carried out without using a pre-concentration step, which helps maintain fractionation reproducibility and comparability between samples (Aiken and Leenheer 1993). Disadvantages of the approach include potential structural alteration of NOM constituents due to the use of various solvents and the alternating pH conditions necessary to bring about the sorption/desorption of the compounds of interest. The fractions of organic matter obtained using the preparative methods are operationally controlled and are not sharply defined. Some overlap between fractions can occur. The preparative XAD-8/XAD-4 isolation procedure can also be time consuming due to resin cleaning and the quantities of water that need to be processed in order to obtain significant quantities of humic substances for characterisation purposes (Malcolm 1989).

A further extension of the XAD-8/XAD-4 fractionation method has been developed based on the charge characteristics of NOM (Leenheer 1981; Leenheer et al. 2000).

This fractionation scheme separates NOM into six fractions: hydrophobic acids (HPOA), hydrophobic bases (HPOB), hydrophobic neutrals (HPON), hydrophilic acids (HPIA), hydrophilic bases (HPIB) and hydrophilic neutrals (HPIN) (Marhaba et al. 2000; Croué et al. 2000). Isolating the hydrophobic and hydrophilic material occurs by the same method as the two column array of XAD-8/XAD-4 resins. However, in this extended method, the hydrophobic and hydrophilic material isolated from the two column array is further fractionated into acid, base and neutral components by the use of ion exchange resins and successive elution with different solvents.

1.2.1.1.2 Rapid Fractionation Procedure

A rapid characterisation technique, utilising a small-scale arrangement of the XAD-8/XAD-4 resins with an analysis time of less than 12 hours, has more recently been developed to assist water treatment operators to determine the relative percentage of XAD-based fractions of NOM in water samples (Chow et al. 2004). This rapid characterisation technique is based on the full-scale fractionation scheme reported by Croué et al. (1994) and Bolto et al. (1999) for the determination of the concentration of four organic fractions: very hydrophobic acids (VHA), slightly hydrophobic acids (SHA), hydrophilic charged (CHA) and hydrophilic neutral (NEU). This analytical procedure measures the organic carbon concentrations of the raw, XAD-8 effluent, XAD-4 effluent and IRA-958 (an anion exchange resin) effluent. The organic carbon concentration of each fraction is calculated from the concentrations of organic carbon before and after contact with the various resins. Results are presented either as actual DOC concentration or as a relative percentage.

1.2.1.2 Ultrafiltration

Ultrafiltration (UF) is an established separation process which utilizes permeable membrane filters to separate the components of solutions by molecular size (Amy et al. 1987). Ultrafiltration membranes typically use pore sizes in the range of 0.0015 to 0.2 microns (Best et al. 2001) and are usually made of polymeric films with molecular weight cut-off (MWCO) values between 200 – 1000 or 1000 – 10,000 Daltons (Da) (Lee et al. 2005). UF conveniently handles large volumes of water

samples and has been widely used for the concentration and fractionation of NOM (Assemi et al. 2004; Cai 1999; Francioso et al. 2002; Lankes et al. 2008).

The solution to be processed is brought in contact with a suitable ultrafiltration membrane that will retain the large molecules. Pressure is applied until half the volume has passed through the membrane. The large molecules are retained in half of the original volume (known as the retentate), which also contains half the salt molecules. The filtrate (known as the permeate) contains the other half of the salt molecules but no organic molecules above the MW cut off of the membrane. A schematic of the process of ultrafiltration is shown in Figure 1.1.

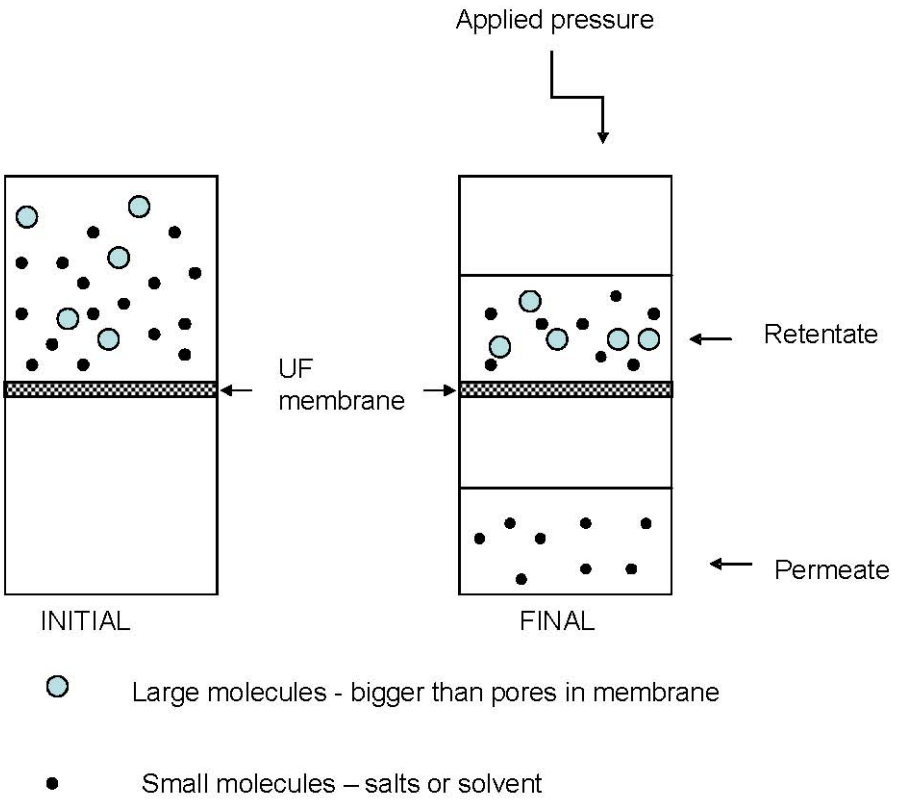

Figure 1.1 The concentration of a water sample by ultrafiltration.

UF concentrates the large organic molecules, whilst liquid and salts are removed (Figure 1.1). The salt molecule to volume ratio in the retentate and the ionic strength of the concentrated solution both remain relatively constant. The ionic strength of the concentrated solution is measured by its conductivity, which is the ability of an aqueous solution to carry an electric current. This ability depends on a number of factors including the presence, mobility, valence and concentration of ions, as well as

the temperature of the water (Franson 1998). The ionic strength of the retentate solution can subsequently be reduced by "washing" the remaining salt out of the retentate, in a process called diafiltration or "desalting". This is essentially a dilution process and is performed in conjunction with a concentration process. It involves washing out the original salts in the retentate by adding water to the retentate at the same rate filtrate is being generated. Diafiltration is a fast and effective desalting technique which minimises the risk of sample loss or contamination compared to other conventional salt removal techniques. After diafiltration, the concentrated high MW material is freeze dried to obtain a solid NOM sample.

1.2.2 Analysis of Isolated Natural Organic Matter

The characterisation of NOM is challenging because of the heterogeneous size, structure and functional chemistry of its constituent compounds due to variation with source, climate and other environmental factors (Wong et al. 2002). A combination of characterisation techniques is typically required to establish the structural elements of aquatic NOM. The techniques used for the characterisation of NOM in this Thesis are discussed in the following subsections.

1.2.2.1 High Pressure Size Exclusion Chromatography

Molecular weight (MW) distribution is one of the fundamental properties required to understand the physical and chemical characteristics of NOM. The MW distribution affects the behaviour of NOM with respect to adsorption, metal binding, hydrophobic organic partitioning, electrostatic effects, bioreactivity and water treatment (Zhou et al. 2000).

High pressure size exclusion chromatography (HPSEC) is a separation method based on the hydrodynamic molecular size of analytes (Vuorio et al. 1998). It is commonly used to determine the MW distribution of NOM in water. Separation by HPSEC is based on differential permeation of molecules of various sizes into a porous matrix. The largest molecules, which cannot penetrate the gel pores, elute first, whilst the smallest molecules exit the column last (Vuorio et al. 1998).

HPSEC is an attractive option for determining the MW distribution of NOM, due to its ease of operation, simplicity of sample preparation and high sensitivity requiring

minimal sample volumes (Allpike et al. 2005). In particular, HPSEC has become very useful for NOM characterisation during different steps in drinking water treatment (Fabris et al. 2008; Allpike et al. 2007; Chow et al. 2009). However, the technique has several significant limitations that need to be considered during data interpretation. Firstly, a series of non-ideal interactions between the column stationary phase can contribute to separation (Allpike et al. 2005). Further, most existing methods of HPSEC use UV detection of the DOC, usually at a wavelength of 254 nm (HPSEC-UV_{254}). These detectors are sensitive only to UV-absorbing species. Many organic compounds absorb at different intensities in the UV spectrum, and some do not at all, hence, this method is not quantitative. For this reason, DOC-specific detection methods have been developed (HPSEC-OCD) (Allpike et al. 2005; Amy and Her 2004; Huber and Frimmel 1996) The advantages of these methods are that the detector signal is directly proportional to the concentration of organic carbon, so all carbon species can be detected, irrespective of functionality. However, due to the intricacies of detecting trace amounts of DOC online, and the inherent cost in the recently manufactured instruments, there are presently only a small number of research groups worldwide with HPSEC-OCD capacity.

1.2.2.2 Ultraviolet Spectroscopy

Dissolved organic matter absorbs light, and the absorption behaviour of NOM in the UV region (190 – 800 nm) gives information regarding the relative number and types of functional groups (Korshin et al. 1997). The degree of aromaticity of NOM is reported to correlate with absorbance of the humic fraction of NOM in the UV region at 254 nm (UV_{254}) (Barrett et al. 2000). UV_{254} has also been used as a surrogate parameter for the concentration of DOC, as it is less time consuming and costly than direct DOC measurement (Chow et al. 1999). Similarly, the specific UV_{254} absorbance ($SUVA_{254}$), the ratio of the absorbance at 254 nm (m^{-1}) over the concentration of DOC (mg L^{-1}), is used as an indicator of the aromatic character of NOM (Barrett et al. 2000). From a practical point of view, UV spectroscopic analysis of NOM is popular due to its ease of operation and the minimal sample preparation necessary. However, compared to other analytical methods, UV spectra are fairly featureless and may provide only limited information on the chemical structure of NOM.

1.2.2.3 Solid-State ^{13}C Nuclear Magnetic Resonance Spectroscopy

Solid-state ^{13}C nuclear magnetic resonance (NMR) spectroscopy has been used in a number of characterisation studies of NOM (Kögel-Knabner 2000; Cook 2004; Hatcher et al. 2001; Lankes et al. 2008; Li et al. 2009; Templier et al. 2005). Solid-state NMR spectroscopy has many advantages over its liquid-state counterpart including: no solvent effects, minimal sample handling and whole sample analysis. Solid-state ^{13}C NMR spectroscopy is now routinely applied with cross-polarisation-magic-angle-spinning (CP-MAS). The technique is non-destructive and provides information on the chemical environment surrounding individual carbon atoms (Gélinas et al. 2001). Solid-state ^{13}C NMR spectra of NOM samples can be broadly divided into five chemical shift regions. Signals for carbon atoms surrounded by carbon-carbon bonds are expressed in the aliphatic region of 0 – 60 ppm. A second aliphatic region of 60 – 90 ppm shows carbons bonded to oxygen atoms, including ether, alcohol and carbohydrate carbons. Aromatic and olefinic carbons occur in the region 90 – 160 ppm, with carboxyl carbons (mainly carboxylic acid carbons) present in the region 160 – 190 ppm. Signals in the region between 190 – 220 ppm represent the carbonyl carbons of aldehydes and ketones (Kögel-Knabner 2000; Knicker and Nanny 1997).

In a ^{13}C NMR spectroscopic study of river NOM isolates, Croué et al. (1999, a) was able to observe two major structural differences between transphilic and hydrophobic acid fractions, isolated by the XAD-8/XAD-4 chromatographic method. The transphilic fraction had the higher carboxyl and heteroaliphatic carbon content (carbon singly bonded to oxygen in aliphatic alcohols, ethers and esters). Another difference was that the hydrophobic acid fraction had the greater aromatic carbon content. These trends have also been shown in other studies (Aiken et al. 1992; De Paolis and Kukkonen 1997; Wong et al. 2002).

1.2.2.4 Fourier Transform Infrared Spectroscopy

Infrared spectroscopy has been widely used for the investigation of humic substances and has provided valuable insight into the nature, reactivity and structural arrangement of oxygen-containing functional groups in humic substances (Stevenson 1994). Infrared spectra of humic substances contain a variety of bands that are

indicative of the absorption of different functional groups present in the complex mixture (Davis et al. 1999). FTIR spectroscopy is still limited in its application to NOM or humic substances characterisation because these samples are comprised of extremely complex mixtures of organic compounds and the spectrum represents many superimposed signals of the many different functional groups. This can also result in significant spectral overlap, peak shifts and peak broadening, leading to only a few resolvable spectral bands. Broad featureless spectra can cause difficulties in assignment of spectral regions to specific functional groups. Despite its limitations, FTIR spectroscopy has been one of the more common methods of NOM characterisation (Christy and Egeberg 2000; Davis et al. 1999; Ludlow et al. 1999; Kanokkantapong et al. 2006; Her et al. 2007) as the unique information provided can complement data from other characterisation techniques.

Hydrophobic and hydrophilic NOM samples have been shown to have dominant carboxyl peaks near 1725 cm^{-1} in their infrared spectra (Leenheer et al. 2000), with the hydrophilic NOM sample having a greater relative absorption from alcohol groups (1045 cm^{-1}). FTIR spectroscopy has also revealed differences between humic and fulvic acids, with the latter having dominant carboxylic acid and ester group bands and the former more intense peaks attributed to aliphatic and aromatic stretching (De Paolis and Kukkonen 1997). Colloidal organic matter has been distinguished from hydrophobic and hydrophilic material by FTIR spectroscopy, with colloidal material producing signals due to the presence of amide groups (1655 cm^{-1} and 1545 cm^{-1}), as well as methyl groups (1382 cm^{-1}) and broad O-H (3402 cm^{-1}) and C-O (1045 cm^{-1}) bands (Leenheer et al. 2000).

1.2.2.5 Fluorescence Spectroscopy

Aquatic NOM has distinctive spectrophotometric properties in terms of both absorption of light and fluorescence. Many studies have investigated the fluorescence and size distribution of aquatic NOM (Belin et al. 1993; Alberts and Takács 2004; Marhaba 2000; Smart et al. 1976; Swietlik and Sirorska 2004). Fluorescence has been reported to be sensitive to molecular and quantitative aspects of the chemistry of fulvic acid and its interactions with metal ions and organic chemicals (Senesi 1990). The high sensitivity and non-destructive nature of fluorescence techniques are well suited for studies of the chemical and physical

properties of NOM. In general, relatively low DOC concentrations (< 20 mg L^{-1}) are suitable for fluorescence spectroscopic analysis (Chen et al. 2003, a). Fluorescence spectra are usually obtained either by analysing the intensity of emitted light as a function of its wavelength (emission spectra) or by analysing the intensity of light emitted at a fixed wavelength (excitation spectra). Recent advances in fluorescence spectroscopy permit the rapid detection of organic matter at a wide range of excitation and emission wavelengths to produce an excitation-emission matrix covering a range from 200 nm to 500 nm. Specific wavelengths or fluorescence centres may be attributed to NOM groups such as humic and fulvic acids as well as proteins (Baker and Spencer 2004; Amy 2007). Humic and fulvic acids are seen in the excitation and emission wavelengths of 300 – 600 nm, whilst proteins are seen in the emission region below 350 nm and excitation region below 305 nm (Leenheer and Croué 2003).

1.2.2.6 Analytical Pyrolysis

Many of the organic compounds in humic substances are insoluble macromolecules, which can not be analysed at the molecular level without a degradation step (Hatcher et al. 2001). Pyrolysis is a common degradation technique which in combination with gas chromatography-mass spectrometry (py-GC-MS) allows analysis of complex, heterogeneous high molecular weight compounds that are difficult to analyse in their polymeric form. Pyrolysis typically involves rapidly heating a sample in an inert environment. The large amount of incident thermal energy causes the macromolecules to fragment, and volatile low MW fragments can be separated by GC and identified by MS. The fragments produced from pyrolysis may reflect moieties of the parent macromolecule in the NOM from which they are released. Therefore, some structural features of the parent molecules can be deduced from identification and quantification of the pyrolysates produced (Hatcher et al. 2001; Leenheer and Croué 2003; Templier et al. 2005). Pyrolysis is only semi-quantitative, but can be used to estimate the relative proportions of source diagnostic NOM components (Bruchet et al. 1990).

Due to the structural complexity of NOM, and the potential for secondary reactions during the application of pyrolysis (usually at 500 – 600 ºC) (Filley et al. 2006), the interpretation of pyrolysis data can be challenging. In order to simplify the results,

products in NOM pyrolysates are commonly grouped into different classes, based on the source biopolymers from which the fragments most likely originated. Common biopolymer precursors of NOM pyrolysis products include carbohydrates, proteins, lignin, amino sugars and polyhydroxy aromatic compounds (Christy et al. 1999; Lu et al. 2000). Pyrolysis products may directly derive from parent structures or may be structurally modified secondary products. The latter typically provide little evidence of source and can complicate interpretation and classification of pyrolysis data.

1.2.2.7 Thermochemolysis

Thermochemolysis is used to chemically degrade higher molecular weight molecules at an elevated temperature, releasing fragments that may be volatile enough for GC-MS analysis (Hatcher et al. 2001). Using the most common thermochemolysis reagent, tetramethylammonium hydroxide (TMAH), thermochemolysis involves base-catalysed reactions at elevated temperatures, reportedly including hydrolysis and methylation of labile C-O bonds such as esters and some ether and glycosidic bonds, as well as amide bonds. Functional groups containing acidic protons, such as carboxylic acids and phenols, may also be simultaneously methylated, whereas esters are transesterified to the corresponding methyl esters (Frazier et al. 2003). Many of the resulting products are volatile enough to be separated by GC and analysed by MS. Methylation of otherwise undetectable polar constituents represents an advantage over conventional pyrolysis. Highly polar carboxylic acids have poor chromatographic behaviour and are prone to decarboxylation during direct pyrolysis (Saiz-Jimenez et al. 1993). Therefore, thermochemolysis is a useful adjunct to analytical pyrolysis studies, providing complementary information on the structure and composition of macromolecules.

Alternative chemical reagents, such as tetrabutylammonium hydroxide (TBAH) (Challinor 1989), tetramethylammonium acetate (TMAAc) (Joll et al. 2004) tetraethylammonium acetate (TEAAc) (Guignard et al. 2005) and trimethyl(triflouro-*m*-tolyl)ammonium hydroxide (Challinor 1996), have also been investigated, but TMAH remains the most widely utilised thermochemolysis reagent.

1.2.2.8 Micro-Scale Sealed Vessel Pyrolysis

Micro-scale sealed vessel (MSSV) pyrolysis can complement more traditional pyrolysis techniques, such as flash pyrolysis. MSSV pyrolysis uses relatively lower pyrolysis temperatures (300 – 360ºC) over longer time periods (several days) than the high temperatures (> 500ºC) and rapid heating rates associated with flash pyrolysis (Berwick et al. 2007). MSSV pyrolysis uses microgram amounts of sample in sealed tubes (Greenwood et al. 2006). MSSV pyrolysis can provide additional speciation information for establishing the structures of, and source inputs of, recent organic matter. This method has been widely applied to the kinetic study of petroleum generation from source organic compounds by simulating the thermal alteration of sedimentary hydrocarbons that occurs naturally over millions of years (Mycke et al. 1994). Characterisation of more recent organic material, such as NOM, however, has received relatively little attention. Thermal maturation of organic matter can induce a multitude of complex chemical reactions, many more than with rapid pyrolysis. Few of these secondary processes are well understood, but often lead to high yields of small sized, non-polar hydrocarbon products easily analysed by GC-MS. Low MW fragments are produced by thermal cracking of the precursor biomacromolecules, whilst certain functional groups may be removed by redox or other selective processes according to thermodynamic equilibrium (Greenwood et al. 2006). Several low MW products detected from MSSV pyrolysis have recently been investigated to understand the sources, and mechanisms of formation of these products (Berwick 2009; Berwick et al. 2010, a; Berwick et al. 2010, b).

1.2.2.9 Halogen Reactivity

Microbiological safety of drinking water is generally achieved by treating the water with a chemical disinfectant, such as chlorine. While chemical disinfectants are effective in destroying harmful microorganisms, they can also react with organic (such as NOM) and inorganic (such as bromide and iodide) materials in treated waters leading to the formation of disinfection by-products (DBPs). When chlorine is added to water during disinfection, molecular chlorine undergoes rapid and almost complete hydrolysis to form the chloride ion and hypochlorous acid (HOCl) (Equation 1.1), existing in equilibrium with its unprotonated form, hypochlorite ion (OCl^-) (Equation 1.2) (White 1999).

$$Cl_2 + H_2O \longrightarrow HOCl + H^+ + Cl^- \quad \textit{Equation 1.1}$$

$$HOCl \rightleftharpoons H^+ + OCl^- \quad \textit{Equation 1.2}$$

Bromide, and to a lesser extent iodide, ions are naturally present in many source waters (Hua et al. 2006). Naturally occurring bromide and iodide can be rapidly oxidised to hypobromous acid (HOBr) and hypoiodous acid (HOI) during disinfection (White 1999). These oxidants then react with NOM to form brominated and iodinated DBPs in an analogous way to the formation of chlorinated DBPs from hypochlorous acid (HOCl). Hence, in the presence of bromide ion and NOM, chlorination of water can result in the formation of brominated, chlorinated and mixed bromo-chloro DBPs (Singer 1999).

The first group of DBPs, the trihalomethanes (THMs), were discovered in 1974 (Bellar et al. 1974; Rook 1974). In the presence of bromide, four THMs are normally found: chloroform ($CHCl_3$), bromodichloromethane ($CHBrCl_2$), dibromochloromethane ($CHBr_2Cl$) and bromoform ($CHBr_3$). In the absence of bromide, only chloroform is found. The latest revision of the Australian Drinking Water Guidelines (NHMRC 2011) has set the guideline value for total THMs in Australian drinking water supplies to be less than 250 μg L^{-1}.

A number of factors affect the rate and extent of DBP formation: e.g. the characteristics and concentration of NOM, bromide ion concentration, the type and concentration of the disinfectant, the contact time between the disinfectant and the water, temperature and pH (Harrington et al. 1996; Liang and Singer 2003). Different NOM components react with aqueous chlorine species at different rates (Harrington et al. 1996). Reckhow et al. (1990) indicated that the nature of the aromatic sites, and especially the relative abundance of activated and non-activated rings, markedly governs the reactivity of NOM with chlorine. This is due to chlorine reacting with aromatic rings through electrophilic aromatic substitution. For electrophilic aromatic substitution reactions, a group that releases electrons (such as a methoxy group $–OCH_3$) activates the ring, and a group that withdraws electrons (such as a nitro group $–NO_2$) deactivates the ring (Morrison and Boyd 1992).

Chlorine demand measurements examine the consumption of chlorine dosed into a water sample over a period of time (usually 72 hours or 7 days). The chlorine

demand of the water is a non-specific measure of the total organic and inorganic components that will react with chlorine in the sample, giving a partial indication of the reactive fraction of NOM in the sample. The chlorine demand can also reveal the chlorine dose required to achieve a specified disinfectant residual after a specified time.

1.2.2.9.1 Formation of Disinfection By-Products

The chemical reactivity of NOM with chlorine can provide a qualitative assessment of NOM character. The reactivity of NOM and chlorine can be measured with the trihalomethane formation potential (THMFP) method. The reactivity of NOM is directly proportional to the concentration of THMs produced. The more hydrophobic (HPO) and acidic fractions of NOM, and polyhydroxy aromatic structures in particular, have been reported to be the main THM precursors (Norwood et al. 1987; Croué et al. 2000). Haloacetic acids (HAAs) have not been studied as extensively as THMs, but in several waters they have been found at mass concentrations equal to or greater than the mass concentrations of the THMs (Singer 2002). The relative distributions of HAAs, along with the THMs, are reported to be influenced by the HPO and HPI distribution of NOM (Liang and Singer 2003). Nine HAAs can be produced if chlorine and indigenous bromide ion are present in the water. Of these, chloroacetic acid, dichloroacetic acid and trichloroacetic acid are the most extensively studied, with Australian Drinking Water Guideline values of 150 μg L^{-1} for chloroacetic acid, and 100 μg L^{-1} each for dichloroacetic and trichloroacetic acid (NHMRC 2011).

1.3 Drinking Water Sources of Perth, Western Australia

Perth, the capital city of Western Australia, has a population of 1.75 million ("Australian Bureau of Statistics" 2012) and sources its drinking water from surface, sea and groundwater supplies. Surface water is obtained from nine separate reservoirs in the Darling Range, situated in largely uninhabited Jarrah forests growing on low-nutrient lateritic sediment. Groundwater is sourced from shallow subsurface aquifers or deeper aquifers in the sands of the Swan Coastal Plain

(Davidson 1995). The Perth Seawater Desalination Plant, commissioned in 2006, produces up to 45 gigalitres per day (GL d^{-1}) of potable water, which is supplied into Perth's Integrated Water Supply Scheme. Most of the source water for Perth is located in groundwater borefields in the northern suburbs. Recent low water levels in the reservoirs have increased the amount of groundwater needed to supply water to the community. Currently, 35 – 50 % of Perth's drinking water is supplied by groundwater sources ("Water Corporation of Western Australia" 2010). The local shallow groundwater resources are usually highly coloured and contain relatively high concentrations of dissolved organic carbon (DOC, 10 – 50 mg L^{-1}), sulfide (0.5 – 5 mg L^{-1}) and dissolved iron (1 – 4 mg L^{-1}) (Davidson 1995), such that these resources require substantial treatment to produce drinking water which complies with the Australian Drinking Water Guidelines (NHMRC 2011).

1.4 Drinking Water Treatment for Perth Groundwaters

In drinking water treatment, removal of NOM early in the treatment process is desirable, in order to achieve more effective water treatment. The type and extent of treatment required is dependent on the source water quality. The local Perth groundwater supplies use a multi-step treatment process to satisfy community requirements for water quality, as well as to control various parameters to levels recommended by the Australian Drinking Water Guidelines (NHMRC 2011). Groundwater is treated at six major groundwater treatment plants (GWTPs) located at Wanneroo, Mirrabooka, Jandakot, Gwelup, Neerabup and Lexia. Each of these GWTPs receives water from a variety of bores (from both confined and unconfined aquifers), which individually have varying quality, but are mixed in such a way as to achieve a relatively stable composition, which, upon treatment, will produce water that meets current drinking water guidelines (NHMRC 2011).

1.4.1 Water Quality Issues in the Wanneroo Source, Treatment and Distribution System

Groundwater to be treated at the Wanneroo GWTP is extracted from 50 bores from various unconfined and confined aquifers. Due to the large number of bores in this

borefield, and each bore containing variable water quality, considerable complexity exists within the Wanneroo distribution system. Raw water entering the Wanneroo GWTP can be blended from several bores to produce a consistent water quality, however, the nature and concentration of other components, which are not individually monitored, can vary widely. The variable composition of NOM in these bores has led to the occurrence of aesthetic water issues in the distribution system that have stemmed from the Wanneroo GWTP. The high concentrations of DOC in these groundwaters have been shown to indirectly contribute to the formation of an objectionable, 'swampy' odour in the distribution system (Wajon et al. 1985; Franzmann et al. 2001; Heitz 2002). Wajon et al. (1985) first described the formation of this 'swampy' odour in the Perth distribution system and their research established that the odour was caused by dimethyltrisulfide (DMTS). DMTS is formed in zones of the distribution system where the chlorine residuals fall below critical levels (Smith et al. 2003). Franzmann et al. (2001) established a relationship between the 'swampy' odour formed in distributed water and groundwater sources, probably due to the high concentrations of DOC and sulfide in certain groundwaters. Subsequent research (Heitz 2002) established a relationship between DMTS formation and the occurrence of biofilms in the distribution system.

1.4.1.1 The Treatment Process at the Wanneroo Groundwater Treatment Plant

The Wanneroo Groundwater Treatment Plant (GWTP), Perth's largest GWTP, processes up to 225 megalitres per day (ML d^{-1}). Historically, treatment has involved a conventional process of aeration, enhanced coagulation, sand filtration and chlorine disinfection. In 2001, the world's first large-scale magnetic ion exchange (MIEX®) treatment plant was installed to improve water quality and odour issues in the Wanneroo distribution system. The MIEX® treatment process has been designed specifically for the removal of DOC from source waters containing high concentrations of DOC. At the Wanneroo plant, the goal of the MIEX® process is to reduce the concentration of DOC entering the distribution system, thus reducing chlorine usage and disinfection by-product formation. The reduction in chlorine demand has also provided a more stable chlorine residual and minimized biological activity within the distribution system. The current treatment scheme at the

Wanneroo GWTP, comprised of two parallel treatment streams (MIEX®–coagulation and enhanced coagulation), is shown in Figure 1.2.

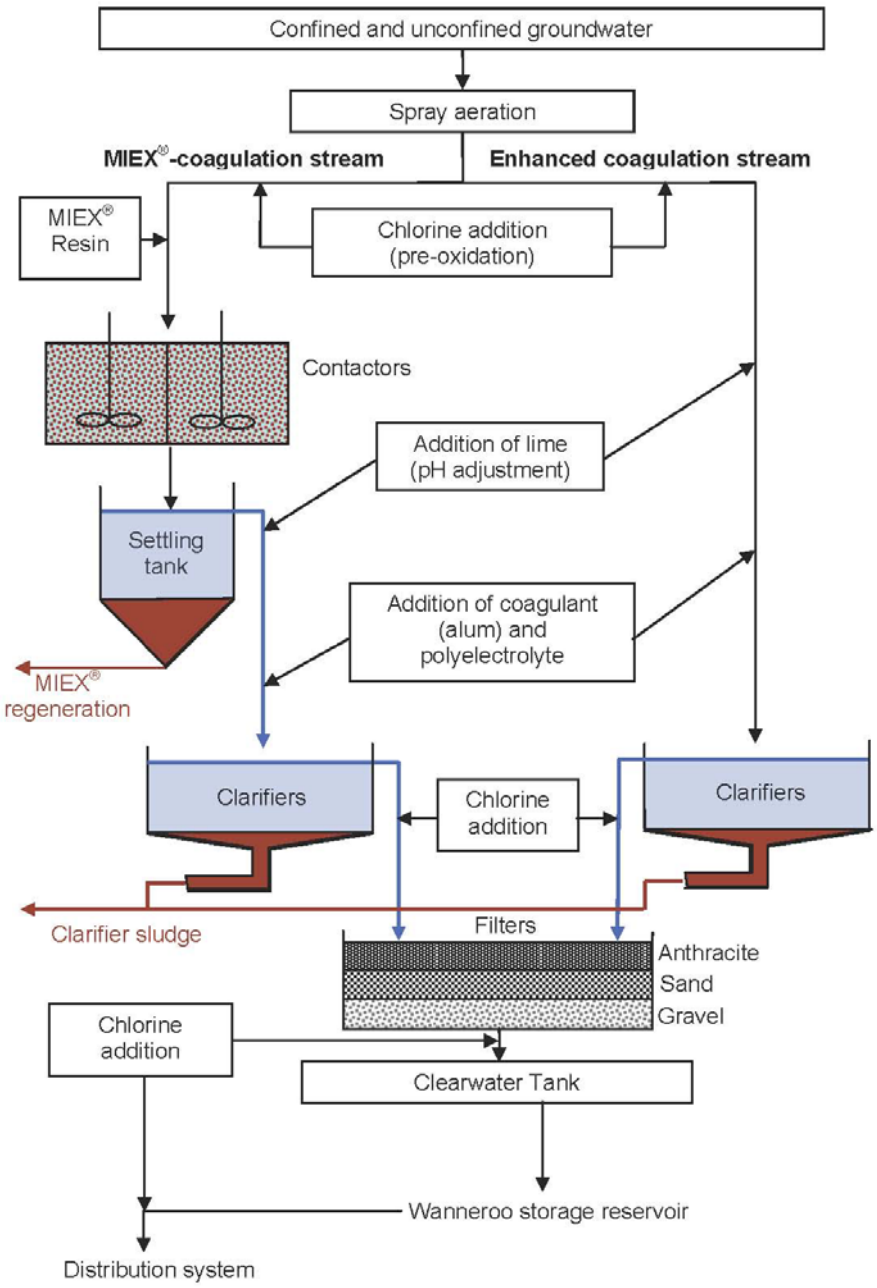

Figure 1.2 A schematic diagram of the two process streams currently operating at the Wanneroo Groundwater Treatment Plant.

The source water entering the plant is first aerated to remove dissolved hydrogen sulfide. In summer, when water demand is high and the Wanneroo plant is running at full capacity, the aerated water is split between the MIEX®–coagulation process stream and the enhanced coagulation process stream. In winter, when the water demand is lower, the inlet water often flows only into the MIEX®–coagulation

stream, which has a capacity of 112 ML d^{-1}. In the MIEX®–coagulation stream (Figure 1.2), following aeration, chlorine (0.5 mg L^{-1}) is added to oxidise iron (II) to iron (III). The water is subsequently mixed with the MIEX® resin in the contactors for 30 minutes, and after that the water-resin slurry is transferred to the settlers. In the settlers, the magnetic properties of the resin allow the resin to separate from the water at a fast settling rate, facilitating the recycling of the resin back to the contactors. The remainder of the water entering the treatment plant is treated by the parallel enhanced coagulation process and is pre-chlorinated (0.5 mg L^{-1}) prior to enhanced coagulation. Coagulation with alum (aluminium sulfate) occurs in both treatment streams with typical doses of 30 – 40 mg L^{-1} for the MIEX®–coagulation process (pH 6.7), and 70 – 80 mg L^{-1} for the enhanced coagulation stream pH 6.0 – 6.4). Polyelectrolyte (a flocculation aid), at a dose of 0.25 mg L^{-1} for the MIEX®–coagulation stream and 0.4 – 0.6 mg L^{-1} for the enhanced coagulation stream, is added as the water enters one of three clarifiers. Supernatant water from the clarifiers in all treatment streams is recombined before flowing through up to twelve concrete filters, comprising anthracite coal, sand and gravel, (filters are backwashed with chlorinated water every 72 hours). After filtration, the water is chlorinated (3 – 5 mg L^{-1}) and fluoridated (0.9 mg L^{-1}) before entering the clearwater tank and is then pumped to the Wanneroo storage reservoir. At the reservoir outlet, the water is re-chlorinated to maintain a free chlorine residual of 0.6 to 1.5 mg L^{-1}, prior to distribution to consumers ("Water Corporation of Western Australia" 2010; "Department of Water" 2010).

1.4.1.2 The MIEX® Process

The MIEX® resin has a polyacrylic macroporous structure which contains a high concentration of quaternary ammonium functional groups. The resin structure contains a magnetic component such that resin beads act individually as weak magnets. Their very small particle size (approximately 180 μm) provides a high relative surface area, allowing rapid adsorption kinetics (Slunjski et al. 2000, b).

Negatively charged DOC is removed from the water by exchange with chloride ions on the active sites of the resin surface, as shown in Figure 1.3. The DOC sorption phase of the exchange cycle is based on a high affinity of the resin for anionic DOC (Slunjski et al. 2000, b). This allows DOC to be preferentially removed from raw

waters containing low levels of DOC and other naturally occurring anions. DOC desorption from the resin (resin regeneration) is achieved by reversing the sorption reaction. For this, the resin is treated with 10 % aqueous brine (NaCl) solution. The high chloride ion concentration displaces DOC from the resin via ion exchange.

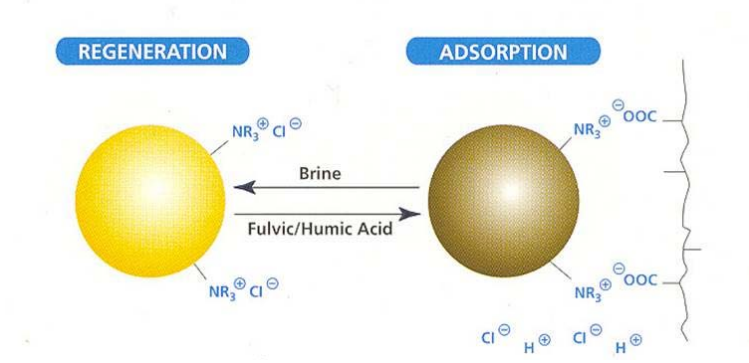

Figure 1.3 The reversible process of DOC removal by the MIEX® resin (Slunjski et al. 2000, a).

1.5 Scope of Thesis

Natural organic matter (NOM) represents a complex mixture of compounds derived from plants, animals and microorganisms, and its interactions with various chemicals affects all aspects of water treatment and water quality. NOM directly impacts, therefore, on source water management, treatment processes and distribution systems. The study described in this Thesis contributes to the body of characterisation studies which provide a detailed understanding of the origins, structural features and reactivity of NOM in source waters, along with its behaviour in drinking water treatment processes, ultimately allowing improved catchment management practices and optimisation of treatment processes.

In Chapter 2, a preliminary investigation of a selection of bores in the Wanneroo borefield in terms of general water quality and NOM polarity distribution was performed to select the most promising bore to be used for larger scale treatment and characterisation. From analysis of the respective bore data, groundwater from bore W300 was selected to undergo further detailed characterisation.

Isolation of a W300 NOM fraction by ultrafiltration is discussed in detail in Chapter 3. The method for collecting a Raw Water UF solid isolate fraction is described, as

well as information on the character of the organic matter isolated in this fraction. The Raw Water UF fraction was then treated by a laboratory simulation of the MIEX® process. As MIEX® is a new technology in water treatment, the effect of the resin on different types of organic matter is not well understood. The MIEX® treated Raw Water UF fraction was then treated with chlorine and the formation of disinfection by-products measured. This information allowed structural features of the organic matter in this fraction to be identified and correlated with disinfection behaviour.

Characterisation of W300 fractions isolated by an XAD-8/XAD-4 resin procedure and treatment of these fractions by the MIEX® process is discussed in Chapter 4. The hydrophobic, transphilic and hydrophilic fractions were analytically characterised before and after MIEX® treatment to establish the susceptibility of these fractions to removal during MIEX® treatment. By isolating and treating separate fractions rather than a bulk water source, insights into structural characteristics, such as the broad functional group distribution and molecular weight distribution, which may affect the removal of the fractions during MIEX® treatment, were provided.

In a related study, treatment of a large volume of W300 water by the MIEX® process, followed by isolation of NOM fractions from the treated water by the XAD-8/XAD-4 resin procedure, is reported in Chapter 5. To complement the procedure undertaken in Chapter 4, whereby W300 water was fractionated by an established XAD resin adsorption method and then treated by MIEX®, the work undertaken in this chapter involved treating W300 water by a MIEX® treatment process prior to XAD-8/XAD-4 resin fractionation of the NOM remaining in the treated water, to investigate the reactivity of the recalcitrant material remaining after MIEX® treatment. The fractions isolated from the MIEX® treated water were compared to the fractions isolated in the work described in Chapter 4 to examine the relatively treatable versus recalcitrant nature of the different NOM fractions. This comparison aids in the understanding of MIEX® treatment of various fractions, potentially allowing improved treatment strategies, and ultimately contributing to the improved quality of drinking water to consumers.

Chapter 6 gives the overall conclusions from this study, together with specific recommendations for the MIEX® treatment process. Chapter 6 also provides

recommendations on the isolation and characterisation methods used in this Thesis, together with comments on their application to water treatment issues.

Chapter 2

2.0 General Characterisation of a Selection of Wanneroo Groundwater Samples

2.1 Introduction

The Perth region lies almost entirely within the Swan Coastal Plain (Davidson 1995). The Swan Coastal Plain covers an area of 4000 km^2 and is bounded by Gingin Brook to the north, the Murray River to the south, the Darling Scarp to the east and the Indian Ocean to the west (Davidson 1995). The important groundwater resources in this area include the unconfined superficial aquifer, incorporating the Gnangara and Jandakot mounds (Figure 2.1), as well as the semi-confined and confined Rockingham, Kings Park, Mirrabooka, Leederville and Yarragadee aquifers. The work described in this Thesis has exclusively involved water samples from the unconfined superficial aquifer. Accordingly, a detailed description of this aquifer follows.

The superficial unconfined aquifer supplies for the Wanneroo borefield are located within the Gnangara mound in the Swan Coastal Plain (Davidson 1995). There is temporal variation in the quality of the groundwater in this aquifer. Salinity ranges from 130 – 12 000 mg L^{-1}, measured as total dissolved solids (TDS), but rarely exceeds 1000 mg L^{-1} which Davidson (1995) attributed to sodium chloride arising from the presence of Bassendean Sand in the aquifer. Groundwater within the Bassendean Sand formation is generally acidic (pH 4.0 – 6.5). The acidity is due to a high organic acid component in the NOM, arising from decomposed vegetation in the swampy environment. NOM, appears to be transferred to the superficial aquifer from swampy lakes which are in hydraulic contact with the aquifer, such that concentrations of DOC in the aquifer can range up to 50 mg L^{-1}. The characteristic

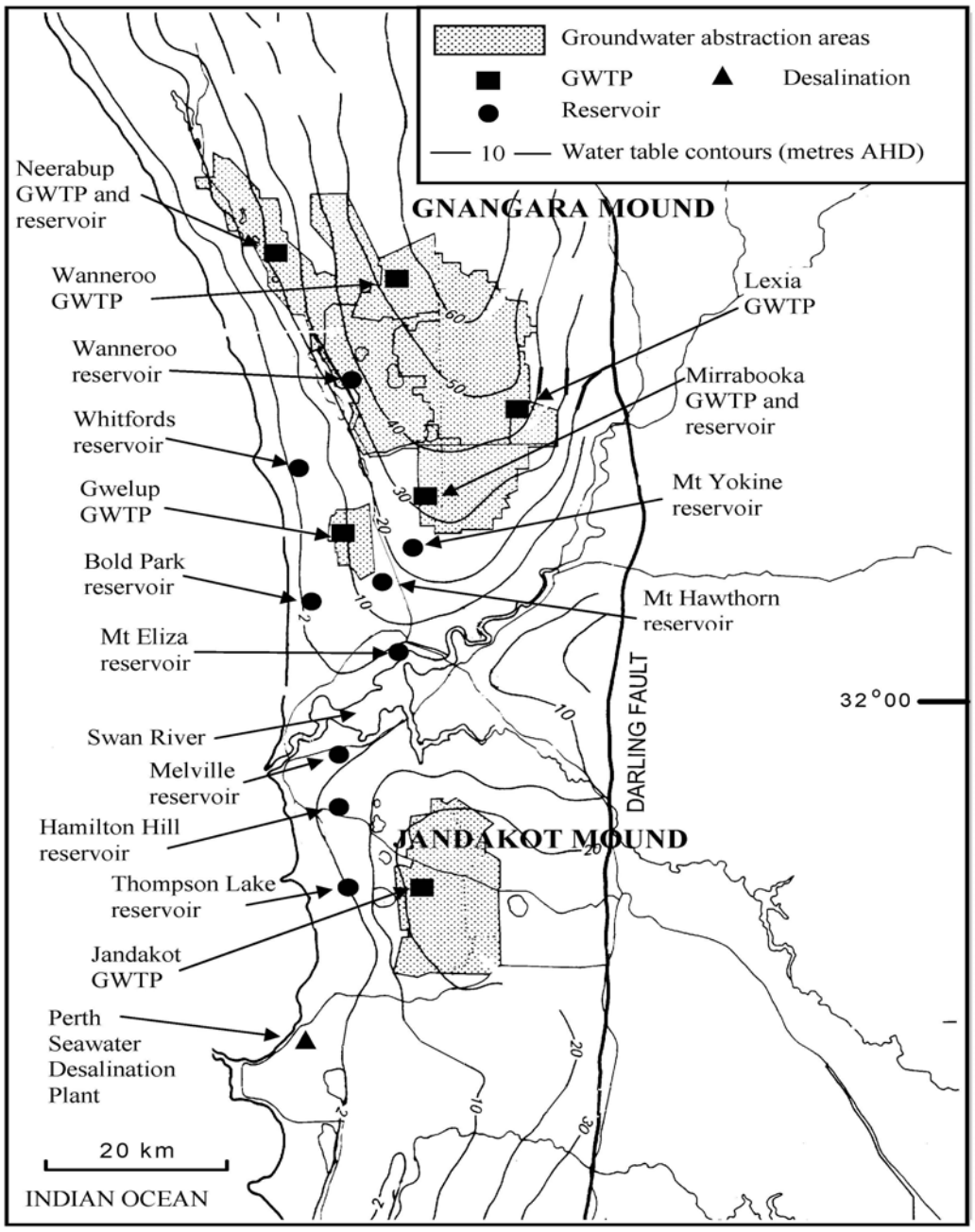

Figure 2.1 Location map showing the Perth metropolitan area and some of its water sources. Surface water sources are located to the east of the Darling Fault (modified from Hirschberg (1989)).

brown colour of the water is due to the presence of organic compounds which are concentrated near the water table. Colour can be used as an indicator of the content of organic matter in natural waters (Bennett and Drikas 1993; Edwards and Amirtharajah 1985), and the colour in the Wanneroo borefield varies significantly, with the highest values due to leaching of organic matter from vegetation and peat deposits on the surface passing through the water table due to infiltration (Davidson

1995). The hardness of the water varies between less than 50 and greater than 300 mg L^{-1}, expressed in terms of an equivalent quantity of calcium carbonate ($CaCO_3$). From the hardness scale, the groundwater for the superficial aquifer can vary from very soft (<50 mg L^{-1} as $CaCO_3$) to very hard (> 300 mg L^{-1} as $CaCO_3$). Sulfate concentrations are usually less than 100 mg L^{-1}. The dissolved iron concentration is usually less than 1 mg L^{-1}, but has been reported higher than 50 mg L^{-1} and this variation can be attributed to the presence of pyrite (Davidson 1995). The dissolved iron is present as ferrous ion, which is readily oxidised to ferric ion on contact with air. Water in the confined or semi-confined aquifers is considerably different in quality to the superficial aquifer: generally it is lower in colour, salinity, hardness, iron and sulfate (Davidson 1995).

2.1.1 Scope of This Study

A preliminary investigation on a selection of bores in the Wanneroo borefield in terms of general water quality was performed to select the most promising bore to be used for larger scale treatment and characterisation. The DOC concentration, UV absorbance and molecular weight distribution of the UV_{254}-active DOC were determined for each bore water. A fractionation procedure based on the longer resin fractionation procedure (Chow et al. 2004) was employed to qualitatively characterise the NOM for each bore water. The water samples were passed through this small-scale, modified, rapid XAD-8/XAD-4 fractionation procedure, to determine the polarity distribution of the major fractions of NOM present in these groundwaters. The characterisation of the four bores from this initial investigation was used to determine the bore to be chosen for larger scale treatment and characterisation.

2.2 Experimental

2.2.1 Water Samples

Water samples (10 L) were obtained from bores labeled W20, W60, W280 and W300 in the Wanneroo groundwater production borefield on July 21st 2004. The locations of these four bores are shown in Figure 2.2. The groundwater samples were subjected to filtration through a 0.45 μm filter (Millipore) and stored at 4ºC.

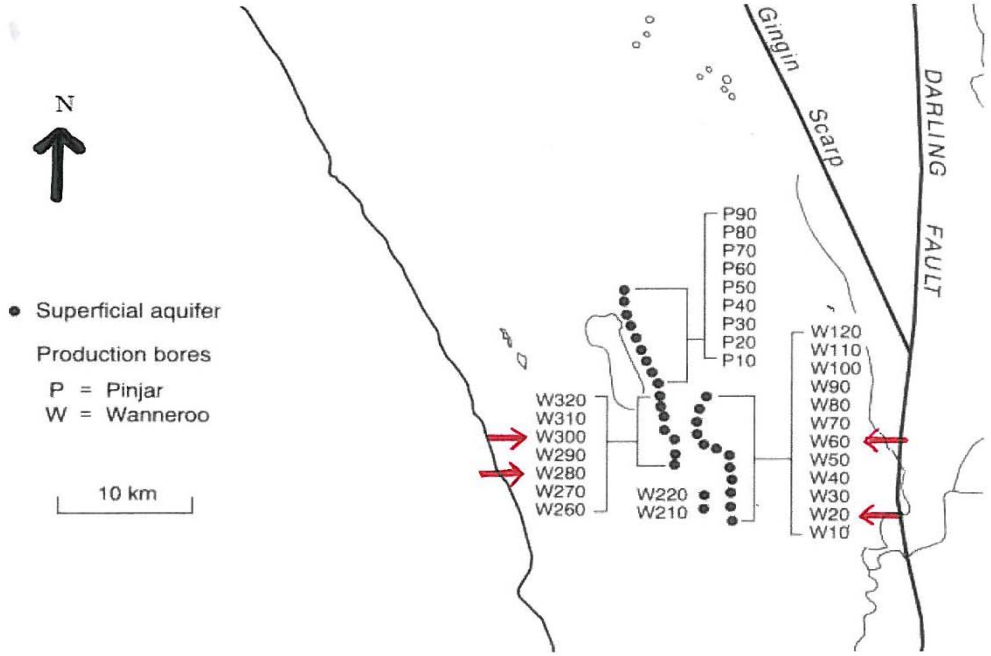

Figure 2.2 Location of the four groundwater bores W20, W60, W280 and W300 in the Wanneroo Production Borefield (modified from Davidson, 1995).

2.2.2 Materials and Methods

2.2.2.1 Purified Laboratory Water

Purified laboratory water was obtained by passing tap water first through an Ibis® reverse osmosis system which included a 5 μm pre-filter followed by an activated charcoal filter and two mixed-bed ion exchange purification packs arranged in series. Product water was then passed through a reverse osmosis membrane and the permeate water was stored in a 60 L polypropylene tank. Water from the storage tank was then fed to an Elga Purelab Ultra Analytic purification system, comprising microfiltration, mixed bed ion exchange and final UV disinfection, as required, to produce high purity water with a conductivity of 18.2 mΩ and a total organic carbon concentration of 1 μg L^{-1}. This high purity water is referred to in this Thesis as MilliQ water.

2.2.2.2 Cleaning Procedures

All non-volumetric glassware was washed with Pyroneg® detergent, rinsed with deionised water (3 ×) and annealed overnight at 600°C prior to use. All glassware that could not be annealed (volumetric flasks and syringes) was washed with ethanol,

dichloromethane, methanol and MilliQ water, with up to six separate washes with each solvent or liquid. All 0.45 μm filters were pre-washed with MilliQ water (500 mL) followed by sample water (50mL).

2.2.3 Rapid Fractionation Isolation Procedure

A small-scale, rapid XAD-8/XAD-4 resin fractionation procedure, modified from the longer resin fractionation procedure of Chow et al. (2004), was employed to quantitatively characterise the main polar moieties of the NOM in the four groundwater samples. The adapted procedures for cleaning of the resins and fractionation of the NOM are outlined in the following subsections.

2.2.3.1 Cleaning of the Resins

Slurries of XAD-8 Resin (Rohm and Hass, 40 mL) and XAD-4 resin (Sigma Aldrich, 40 mL) in aqueous sodium hydroxide solution (0.1 M, 100 mL) were prepared. The fines were removed by decantation and the remainder of the resin was stored in the sodium hydroxide solution for 24 hours. The resin slurry was then rinsed with MilliQ water and organic resin contaminants were removed by sequential 48 hour Soxhlet extractions with methanol, acetonitrile, and diethyl ether. Clean resin was then stored in methanol until required.

2.2.3.2 pH Adjustment of the Water Sample

Just prior to fractionation, the pH of the sample was adjusted by the addition of aqueous hydrochloric acid solution (0.1 M) while stirring. Once the pH decreased to 2.2, the water sample was stirred to achieve equilibrium, upon which aqueous hydrochloric acid solution (0.1 M) was added until the pH reached 2.0, and the water sample was then stirred for a further 5 minutes.

2.2.3.3 Fractionation Process

Glass columns (10 mm diameter; 300 mm length) with a glass frit were packed with water-resin slurry and the resin column was rinsed with MilliQ water to remove methanol. The resin was cleaned further with an acetonitrile/MilliQ mixture (75:25 % v/v, 100 mL) followed by MilliQ water until the DOC concentration was less than

0.5 mg L^{-1}. Final preparation of the resin involved cleaning with hydrochloric acid solution (0.1 M, 200 mL).

The water sample (2.5 L) was passed through the XAD-8 resin (40 mL). After 1 L of the sample was passed through the resin, a 100 mL aliquot of eluent was collected for analysis. The remaining XAD-8 eluent was passed through the XAD-4 resin (40 mL) and, after 1 L, a 100 mL aliquot of eluent was collected for analysis. The remainder of the XAD-4 eluent was discarded.

2.2.4 Measurement of Dissolved Organic Carbon Concentration

Water samples were filtered using an IC Acrodisc filter (0.45 μm). The filtered water was collected in a glass vial (40 mL) and analysed using a Shimadzu TOC-V-Ws Total Organic Carbon Analyser using a non-purgeable organic carbon (NPOC) method. The NPOC parameters included: 3 to 5 injections of 2.5 mL of sample (with a maximum standard deviation of 0.05 mg L^{-1}). An aliquot of aqueous phosphoric acid solution (75 μL, 17 %) was added and the sample sparged with nitrogen gas for 3 minutes. An aliquot of an aqueous persulfate oxidiser solution (1.5 mL, 20 % sodium persulfate and 17 % phosphoric acid) was added and the sample irradiated by UV light to oxidise organic carbon. The resulting carbon dioxide was detected using an infrared detector.

2.2.5 UV/Visible Spectroscopic Measurements

Measurements at 254 nm were conducted using a Shimadzu Pharmaspec UV-1700 Spectrophotometer with a 5 cm quartz cell. Background measurements were performed with MilliQ water, and all samples were filtered through a 0.45 μm IC Acrodisc filter prior to analysis.

All UV_{254} absorbances in this Thesis were calculated per centimetre (cm^{-1}) after converting the absorbance recorded using a 5 cm cell and after including any dilution factors.

2.2.6 Analysis of Bromide Ion Concentration and General Water Quality Parameters

Bromide ion analyses were conducted using ion chromatography with a limit of quantification of 0.02 mg L^{-1}. The Chemistry Centre of Western Australia performed these analyses under a commercial arrangement.

Analysis of a series of general water quality parameters was carried out by SGS Laboratory Services Pty Ltd.

2.2.7 High Pressure Size Exclusion Chromatography

High pressure size exclusion chromatography (HPSEC) was performed according to a previously described method (Allpike et al. 2005). Detectors used for HPSEC were UV_{254} and OCD (organic carbon detection). Briefly, the HPSEC-UV_{254} system was comprised of a TSK G3000SW_{xl} (TOSOH BioSep, 5 µm particle size, 250 Å pore size, 7.8 mm diameter, 300 mm length) column and a Hewlett Packard 1090 Series II HPLC instrument with filter photometric detection (FPD) at a wavelength of 254 nm. For organic carbon detection, the organic carbon in the eluent was separated and converted into carbon dioxide according to the procedure described by Allpike et al. (2007). Detection of the carbon dioxide was achieved using a Balzers Instrument Thermostar Mass Spectrometer operating in SIM mode (Warton et al. 2008). The HPSEC column had a void volume (V_0) of 5.5 mL (determined with dextran blue) and a permeation volume (V_p) of 13.3 mL (determined with acetone). The eluent was a 20 mM phosphate buffer (1.36 g L^{-1} KH_2PO_4 and 3.58 g L^{-1} Na_2HPO_4, pH 6.85, with an ionic strength of 40 mM). Samples were injected manually using a Rheodyne 7125 6-port injection valve equipped with a 100 µL sample loop and a flow rate of 1 mL/minute. HP Chemstation software was used for data analysis of the FPD signal, while Bruker Opus software was used to record the signal from the FTIR detector. Calibration was carried out using a series of polystyrene sulphonate standards with molecular weights between 840 – 81800 Da, and potassium hydrogen phthalate was used as a quantification standard for OCD.

2.3 Results and Discussion

2.3.1 Characterisation of the Groundwater Samples

2.3.1.1 General Water Quality Parameters of the Groundwater Samples

Four groundwater bores (W20, W60, W280 and W300) from the Wanneroo borefield were sampled for preliminary NOM characterisation to select the most promising bore to be used for larger scale treatment and characterisation. The DOC concentration, UV_{254} absorbance and specific UV_{254} absorbance ($SUVA_{254}$) for these four groundwater samples are shown in Table 2.1.

Table 2.1 DOC concentration, UV_{254} and $SUVA_{254}$ data for the four Wanneroo groundwater samples.

Bore	DOC concentration (mg L^{-1})	UV_{254} absorbance (cm^{-1})	$SUVA_{254}$ (m^{-1} L / mg C)
W20	6.4	0.232	3.7
W60	11.2	0.427	3.8
W280	14.3	0.716	5.0
W300	23.4	1.349	5.8

The DOC concentrations and UV_{254} absorbance of the four groundwater samples varied considerably from 6 to 24 mg L^{-1} and 0.24 to 1.34 cm^{-1}, respectively. The high DOC concentrations measured here are consistent with the high concentrations (10 – 50 mg L^{-1}) in Wanneroo groundwaters reported by Davidson (1995). The large variation between bores is likely due to the hydrogeology of the borefield, as discussed in detail in Section 2.1. The groundwater samples showed smaller variation in $SUVA_{254}$. W20 and W60 had the same $SUVA_{254}$ value despite different DOC concentrations and UV_{254} absorbances. This indicates that the chemical nature of the DOC within these bores may show some similarities despite the large variation in DOC concentration. A previous study of fulvic acids (a major fraction of NOM, soluble at all pH levels) showed a strong correlation between $SUVA_{254}$ and aromatic carbon (Chin et al. 1994). A good relationship has also been established between $SUVA_{254}$ and the aromatic carbon content of NOM fractions isolated from natural waters using the XAD-8/XAD-4 isolation protocol (Aiken et al. 1992; Croué et al. 1999, a), with $SUVA_{254}$ of the whole water sample largely dependent on the amount

and $SUVA_{254}$ of the hydrophobic (HPO) fraction (Croué et al. 1999, a). Another study by Croué et al. (2001) showed that the correlation between $SUVA_{254}$ and the aromatic carbon content is still valid when considering fractions isolated from both raw and treated waters. Typically $SUVA_{254} < 3$ m^{-1} L / mg C is reported to correspond to largely non-humic material, whereas $SUVA_{254}$ in the range of 4-5 m^{-1} L / mg C is reported to indicate mainly humic material (Hwang et al. 1999). $SUVA_{254}$ is therefore a good predictor of the aromatic carbon content of NOM, and can be used to estimate the chemical nature of the DOC at a given location. The higher $SUVA_{254}$ value from the other two bores (W280 and W300) may indicate a higher content of aromatic carbon in the NOM in these samples. The similarities and differences in $SUVA_{254}$ between W20/W60 and W280/W300 are consistent with the location of W20 and W60 on one north-south transect, and W280 and W300 on another, through the aquifer. The variations in $SUVA_{254}$ from the different water samples (such as W20/W60 and W280/W300) based on their spatial variability are reportedly often found to be reflected in differences in both the fractionation patterns and the quality of the material contained in the fractions (Croué et al. 1999, a).

2.3.1.2 Rapid Fractionation of the Groundwater Samples

The NOM contained within the Wanneroo groundwater samples (2.5 L each) was fractionated by a modified version of the rapid XAD-8/XAD-4 procedure (Chow et al. 2004) shown schematically in Figure 2.3, with the sampling points for the procedure shown in red.

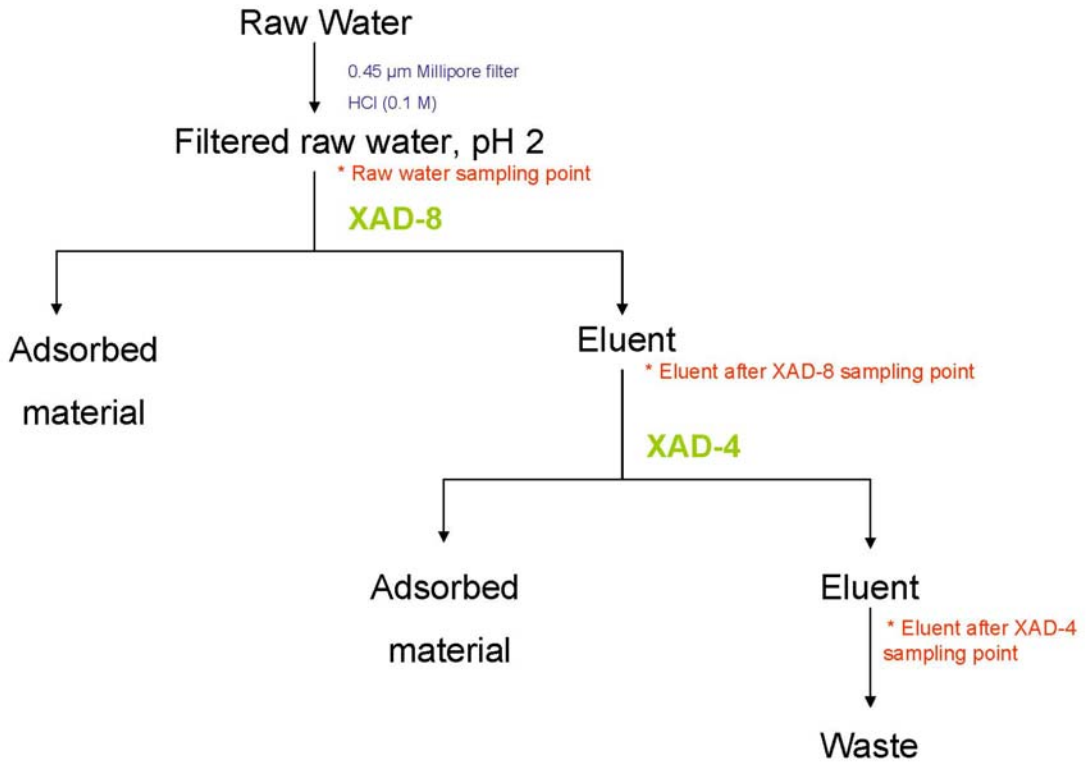

*Figure 2.3 Schematic diagram of the XAD-8/XAD-4 resin procedure for rapid DOC fractionation. *Sampling points for the rapid fractionation procedure are shown in red.*

The relative proportions of three fractions of NOM within the DOC of each sample were measured in this technique, calculated from the differences in DOC concentrations between column influents and column effluents. This procedure allowed a semi-quantitative assessment of the proportion of hydrophobic, transphilic and hydrophilic material in each groundwater sample. The proportion of hydrophobic material (HPO) was calculated based on the DOC concentration difference between the 'Raw Water DOC' and the sampling point 'Eluent after XAD-8, relative to the Raw Water DOC concentration (Equation 2.1). The proportion of transphilic material (TPI) was calculated based on the DOC concentration difference between the 'Eluent after XAD-8' and the 'Eluent after XAD-4', relative to the Raw Water DOC concentration (Equation 2.2). The proportion of hydrophilic material (HPI), which is not adsorbed onto either resin, was calculated as the DOC concentration of the 'Eluent after XAD-4' relative to the DOC concentration of the raw water (Equation 2.3).

$$HPO = \left(\frac{\text{'Raw Water DOC'} - \text{'Eluent after XAD-8'}}{\text{'Raw Water DOC'}} \right) \times 100\% \qquad \textit{Equation 2.1}$$

$$\text{TPI} = \left(\frac{\text{'Eluent after XAD - 8' - 'Eluent after XAD - 4'}}{\text{'Raw Water DOC'}} \right) \times 100\% \qquad \textit{Equation 2.2}$$

$$\text{HPI} = \left(\frac{\text{'Eluent after XAD - 4'}}{\text{'Raw Water DOC'}} \right) \times 100\% \qquad \textit{Equation 2.3}$$

For each sample, the proportion of each fraction (hydrophobic, transphilic and hydrophilic) was calculated and the proportions are shown in Table 2.2. The proportions of each fraction for all four groundwater samples were similar to that found in a previous rapid fractionation study of a Wanneroo groundwater from a deep underground source (Bolto et al. 2002), where 80 % was measured to be hydrophobic (cf. 70 – 80 % in the current study), 9 % transphilic (cf. 10 – 15 %) and 11 % hydrophilic (cf. 10 – 18 %). The small disparity between the XAD fraction distribution between the samples of this study and the study of Bolto et al. (2002) is likely due to the waters being taken from different locations within the aquifer of the Wanneroo borefield in the two studies. In another study (Croué et al. 1999, a), a slight variation in DOC distribution due to sampling time for a surface water source in France was observed. During winter sampling, the hydrophobic material accounted for 51 % of the DOC, with the transphilic and hydrophilic material being 24 and 25 %, respectively. During spring, the hydrophobic material accounted for 60 % of the DOC, with the transphilic and hydrophilic material being 19 and 21 %, respectively (Croué et al. 1999, a). In each case, the hydrophobic fraction was the largest fraction in the DOC distribution, which was also observed in the current study.

Table 2.2 Relative contribution of hydrophobic, transphilic and hydrophilic fractions of NOM in the four Wanneroo groundwater samples.

Bore	% Hydrophobic NOM	% Transphilic NOM	% Hydrophilic NOM	% Hydrophobic + Transphilic NOM
W20	70	12	18	82
W60	80	12	10	92
W280	79	10	11	89
W300	75	15	10	90

The high $SUVA_{254}$ values measured for the four groundwaters (Table 2.1), suggestive of the NOM in these groundwaters being comprised of mainly humic

material, are supported by the high proportion of HPO and TPI fractions seen for each groundwater (Table 2.2). It has been previously observed in the XAD-8/XAD-4 resin isolation protocol (Croué et al. 1999, a; Aiken et al. 1992) that generally the humic-type material (HPO and TPI) is enriched in aromatic moieties compared to the HPI fraction. Since the Wanneroo groundwaters have a high proportion of HPO/TPI fractions (82 – 92 % of the total DOC), they most likely have a high degree of aromatic character, which is distinctly different to other water sources (Bolto et al. 2002). Mash et al. (2004) showed that the amount of hydrophobic compounds, defined as the fraction of dissolved organic matter (DOM) retained on XAD-8 resin at pH 2, expressed as a percentage of the total DOC from three freshwater reservoirs in the USA varied between 25 – 58 %, significantly lower than the HPO/TPI fractions in the Wanneroo groundwaters. The variation in hydrophobic compounds was reported to be a reflection of the source of the NOM, and whether it was of predominantly vegetative or microbial origin (Bolto et al. 2002). The high hydrophobic content of Wanneroo groundwaters can influence the behaviour of NOM in water treatment. The high amount of aromatic character can influence the removal of NOM by coagulation, as coagulation is influenced by the proportion of humic/non-humic fractions, the HPO/HPI character and the MW of NOM constituents (Chow et al. 2006). Therefore, the characterisation of NOM is extremely important to the water industry, and considerable research has been undertaken worldwide to establish links between NOM character and treatability of the water in drinking water treatment processes (Croué et al. 1994; Owen et al. 1995; Gjessing et al. 1998; Chow et al. 2000; van Leeuwen et al. 2002; Warton et al. 2007, a).

2.3.1.3 Molecular Weight Distribution of the UV_{254}-Active DOC in the Groundwater Samples

The molecular weight (MW) distributions of the UV_{254}-active fractions of DOC within the groundwater samples and their rapid fractionation eluents were analysed by HPSEC-UV_{254}. The HPSEC system was calibrated with polystyrene sulfonate standards of various MW to correlate the log of the MW and the distribution coefficient (K_d'). The calibration curve was used to convert each measured chromatogram to a plot of absorbance vs. MW, with the converted chromatograms of

the four groundwater samples and the rapid fractionation eluents shown in Figure 2.4.

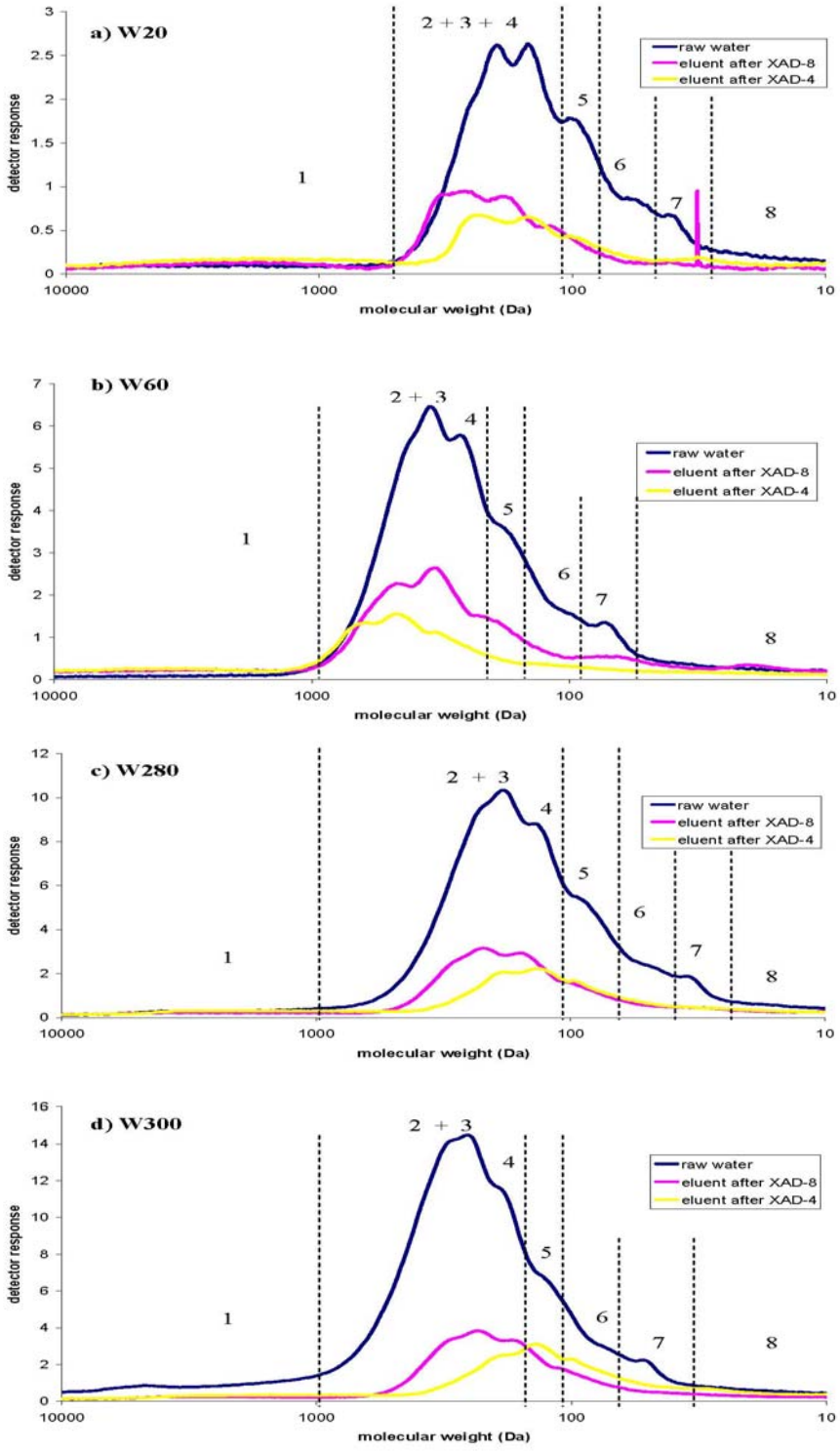

Figure 2.4 HPSEC-UV$_{254}$ chromatograms of the raw groundwater, XAD-8 eluent and XAD-4 eluent of a) W20; b) W60; c) W280 and d) W300 groundwater samples. Numbers correspond to eight distinct MW regions as described in Huber and Frimmel 1996 and Allpike et al. 2005.

In Figure 2.4a – 2.4d, the MW regions are numbered from 1 – 8, according to the numbering system proposed by Huber and Frimmel (1996) and used by our group previously (Allpike et al. 2005), with the numbering corresponding to the elution order of the peaks. Each of these MW sub-regions still represents a complex mixture of organic compounds. The MW profiles for the raw water samples in Figure 2.4 are consistent with previous studies showing broad MW distribution for raw water samples from Finland (Peuravuori and Pihlaja 1997; Vrijenhoek et al. 1998) as well as for raw water samples from the Wanneroo GWTP (Warton et al. 2007, a; Allpike et al. 2005). Region 1, which elutes as a broad range of poorly resolved material in all four chromatograms, has been reported in earlier studies of Wanneroo borefield-derived samples to potentially consist of sulphur species associated with organic matter, either in solution or colloidal form as elemental sulfur, and other inorganic substances (Allpike et al. 2005). Although samples were filtered (0.45 μm) prior to injection onto the SEC column, previous workers (Huber and Frimmel 1996) observed similar characteristics in a German lake water which similarly was attributed to an early eluting fraction of colloidal material. Regions 2 – 4, which elute as two partially resolved peaks for all four groundwater samples (Figure 2.4a – Figure 2.4d), are reported to be likely enriched in humic substances of relatively high molecular weight (Huber and Frimmel 1996). Humic substances are considered to be rich in aromatic functional groups, which are easily detected by both DOC specific and UV absorbance detectors. Regions 5 – 7 reportedly correspond to the fractions comprising lower molecular weight monoprotic organic acids such as fulvic acids, conjugated unsaturated acids or keto-acids (Huber and Frimmel 1996). Region 8 eluted as a broad band of poorly resolved material and comprised organic matter of the lowest apparent MW.

Comparison of the HPSEC-UV_{254} profiles of the groundwater samples after resin fractionation showed that the MW distribution of the UV_{254}-active DOC remaining in the water after elution through the XAD-8 resin was similar for each bore. The large proportion of HPO fraction, adsorbed on the XAD-8 resin, can also be observed by the large difference between the chromatograms for the raw water and the eluent after XAD-8. The UV_{254}-active material remaining after elution through the XAD-8 resin was predominantly of high MW (500 - 1000 Da), presumably humic, in nature. This is consistent with NOM fractions isolated by rapid

fractionation from Myponga reservoir that showed a high amount of humic/fulvic and polysaccharide/protein material (Soh et al. 2007). The preferential retention of UV_{254}-active NOM on the XAD-8 resin (the difference between the chromatograms of raw water and eluent from XAD-8) confirms that the XAD-8 resin favours the adsorption of the higher MW NOM fractions (the most hydrophobic), which are the most aromatic in nature (Croué 2004). The higher MW portion of the material in the eluent after XAD-8 was adsorbed onto the XAD-4 resin, corresponding to the portion of NOM referred to as transphilic material. The hydrophilic fraction (remaining after elution through the XAD-4 resin; 'Eluent After XAD-4') of each groundwater showed less UV_{254}-activity than the component remaining after elution through the XAD-8 resin, consistent with previous studies (Soh et al. 2007; Buchanan et al. 2005). The hydrophilic fraction of all of the bore waters included some humic character in the MW range of 500 – 200 Da.

The small differences in relative amounts and profiles of the eight distinct MW regions (Allpike et al. 2005; Huber and Frimmel 1996) for the raw water and two eluents of the four groundwater samples, observed in the HPSEC-UV_{254} chromatograms may reflect subtle changes in the general water chemistry of the four groundwater samples. Future HPSEC-UV_{254}-OCD analysis would enable the complete range of DOC in the water samples to be investigated.

2.3.2 Selection of Groundwater Bore for Detailed Study

The general water quality data of the four groundwater samples showed a range of DOC concentrations and UV absorbance values likely due to the hydrogeology of the borefield. The variation evident in $SUVA_{254}$ values was not reflected by the relatively similar XAD resin fractionation distribution for the four groundwaters, where each groundwater had a high proportion of hydrophobic and transphilic material, enriched in aromatic moieties compared to the hydrophilic fraction. These results suggested that, whilst the general water quality can vary (such as DOC concentration, UV_{254}, $SUVA_{254}$); the hydrophobicity of the DOC present in each bore is relatively similar. HPSEC-UV_{254} analysis for the four groundwaters showed small differences in profiles in the raw waters. The MW profiles of W280 and W300 were almost identical, with the majority of the MW distribution between 1000 – 100 Da representing humic substances of a highly aromatic nature (Huber and Frimmel

1996). W60 had a high proportion of MW material in the 1000 – 100 Da range as seen in W280 and W300, more material in this range was of higher MW than in W280 and W300. W20 still had a high amount of humic material in the 1000 – 100 Da range, but there was a higher proportion of MW material between 100 – 10 Da for this sample, thought to represent monoprotic low MW acids such as fulvic acids (Huber and Frimmel 1996). These differences in MW distribution of the UV_{254}-active material may reflect subtle changes in the general water chemistry of the four groundwater samples, based on their location in the borefield. Understanding the NOM present in the raw water samples is important as the types of organic compounds collected by different isolation processes can differ based on the samples isolated. Inferences about the entire NOM pool in the source water are often drawn based on the analysis of material collected (Croué et al. 1999, b). After consideration of the NOM present in the water samples having relatively similar MW distributions from the HPSEC-UV_{254} profiles, groundwater from bore W300 was chosen for further detailed characterisation. This bore contained the highest DOC concentration and a high amount of aromatic DOC (based on the relative contribution of hydrophobic, transphilic and hydrophilic fractions) which will assist in isolation of sufficient quantities of DOC fractions for treatment and characterisation.

2.3.3 General Water Quality of Groundwater from Bore W300

Following selection of bore W300 for treatment and characterisation studies, groundwater (1000 L) from bore W300 was collected, filtered (0.45 μm) and stored at 4ºC. The general water quality parameters of the groundwater sample were analysed and the results are presented in Table 2.3.

The general water quality parameters measured for W300 water in the current study were largely consistent with average annual sampling data reported over almost a decade by Ash et al. (2012). The exceptions to this were the very low turbidity and the higher colour in the current study, compared to the average annual data. This modest disparity in the physical properties of colour and turbidity could reflect differences in water quality at the time of sampling or differences in the manner of sampling. Organic compounds in water can result in a characteristic brown colour. Turbidity due to colloidal material from clay minerals in the sediments is extremely variable because of the thin beds of clay present throughout the Wanneroo borefield

Table 2.3 General water quality parameters of W300 groundwater in the current study and as averages of routine borefield sampling events over eight years.

Water Quality Parameters	W300 Sample (current study)	Average Borefield Sampling Data from W300 from 2003 – 2011 (Ash et al. 2012)
Total Alkalinity concentration as $CaCO_3$ (mg L^{-1})	15	19
Chloride concentration (mg L^{-1})	76	72
Colour (TCU)	220	164
Conductivity (mS cm^{-1})	310	324
Hardness concentration (mg L^{-1})	45	42
Bromide concentration (mg L^{-1})	0.23	0.20
Iodide concentration (mg L^{-1})	0.03	• ND
Sulphate concentration (mg L^{-1})	21	21
Total Dissolved Solids concentration (mg L^{-1})	310	318
Nitrate concentration (mg L^{-1})	< 0.2	0.024
Nitrite concentration (mg L^{-1})	< 0.1	<0.011
pH	5.9	5.64
Total Filtered Solids concentration (mg L^{-1})	176	234
Aluminium concentration (mg L^{-1})	< 1	0.5
Calcium concentration (mg L^{-1})	5.4	5.2
Iron concentration (mg L^{-1})	< 0.5	0.37
Potassium concentration (mg L^{-1})	< 5	2.5
Magnesium concentration (mg L^{-1})	7.1	6.7
Manganese concentration (mg L^{-1})	< 0.20	0.003
Sodium concentration (mg L^{-1})	44	44
Silicon concentration (mg L^{-1})	6	10
Turbidity (NTU)	8	51
DOC concentration (mg L^{-1})	24	23
UV_{254} (cm^{-1})	0.97	1.04

• *ND – not determined*

area within the Leederville aquifer (Davidson 1995). Therefore, depending on depth and seasonal time of the year, the turbidity and colour can vary. The salinity (measured as total dissolved solids) of W300 groundwater (310 mg L^{-1}) lies in the range reported for the Leederville aquifer (176 – 2511 mg L^{-1}) by Davidson (1995).The salinity of the water is due to the sodium chloride arising from the Bassendean Sand present in the aquifer. The pH (5.9) indicates acidic water, probably due to the decomposition of vegetation in the swampy environment. The water was of low hardness (15 mg L^{-1} as $CaCO_3$) according to the hardness scale in Davidson (1995) (< 50 mg L^{-1} as $CaCO_3$). The low dissolved iron concentration (<0.5 mg L^{-1}) is consistent with the low concentration of iron in water from the same groundwater bore reported by Ash et al. (2012). The low sulfate concentration (21 mg L^{-1}) is consistent with the reported Leederville aquifer concentrations (<50 mg

L^{-1}) (Davidson 1995). The DOC concentration measured for this W300 sample (24 mg L^{-1}) is consistent with the high concentrations (10 – 50 mg L^{-1}) reported by Davidson (1995). Overall, the general water quality of W300 is consistent with previous studies (Davidson 1995, Ash et al. 2012) on this bore and the Leederville aquifer in general.

Size exclusion chromatography with organic carbon detection (SEC-OCD) and ultraviolet detection at 254 nm (SEC-UV_{254}) was performed on the sampled groundwater to examine the MW distribution of the DOC in this water source and the chromatograms are shown in Figure 2.5. In Figures 2.5a and 2.5b, the peaks are numbered from 1 – 8, as described in Section 2.3.1.3, with the numbering corresponding to the elution order of the peaks.

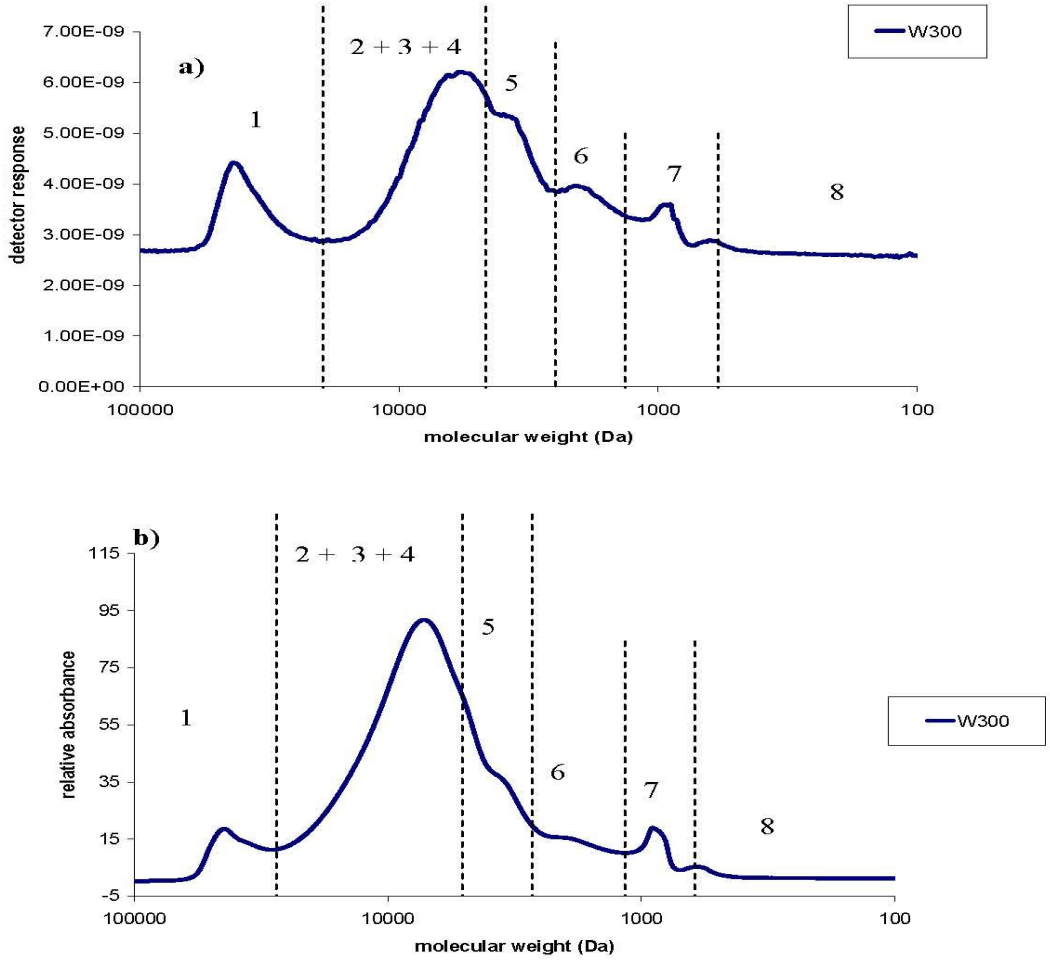

Figure 2.5 a) HPSEC-OCD and b) HPSEC-UV_{254} chromatograms of W300 groundwater. Numbers correspond to eight distinct MW regions as described in Huber and Frimmel 1996 and Allpike et al. 2005.

The MW distributions of both the UV_{254}-active DOC and total DOC in the W300 sample were similar in nature, as shown by the chromatograms derived using both UV_{254}-specific (Figure 2.5b) and DOC-specific detectors (Figure 2.5a), respectively. The MW profiles were consistent with MW profiles of raw water entering the Wanneroo GWTP as seen in previous studies (Wong et al. 2007; Warton et al. 2007, a; Heitz 2002; Warton et al. 2008). It is likely that the material represented by Region 1 was colloidal in nature and may also have been comprised of some inorganic substances, as discussed in Section 2.3.1.3 and seen previously for Wanneroo groundwaters (Allpike et al. 2005; Allpike 2008), as well as other groundwater sources in Western Australia such as water sourced from the Jandakot Mound (Chow et al. 2006). The later eluting UV_{254}-active and DOC regions (regions 2 – 8 in Figures 2.5a and 2.5b) are more alike than the earlier eluting region. Regions 2 – 4, which eluted as one unresolved peak in Figures 2.5a and 2.5b, are likely to be enriched in humic substances of relatively high MW (Allpike et al. 2005). Humic substances are considered to be rich in aromatic functional groups (Collins et al. 1986) and so these fractions tend to be "over-represented" by UV_{254} detection. This can be observed in Figure 2.5 where these fractions form an apparently greater proportion of the sample in Figure 2.5b than in Figure 2.5a. SEC-OCD analysis shows great benefits in giving a more quantitative representation of the MW distribution of the DOC in water samples. In the W300 sample, regions 5 – 7, had moderate UV absorbance and DOC concentration; these regions reportedly correspond to the fractions comprising lower MW monoprotic organic acids, such as fulvic acids, conjugated unsaturated acids or keto-acids (Huber and Frimmel 1996; Specht and Frimmel 2000). Region 8 eluted as a broad band of poorly resolved material and was comprised of organic matter of the lowest apparent MW. The lowest MW fractions are thought to be important in drinking water treatment as these are poorly removed by conventional processes and are considered to be bioavailable (Volk and LeChevallier 2000).

The general water quality of W300 was largely consistent with the quality reported for this bore during routine sampling (Ash et al. 2012). HPSEC analysis showed a similar MW distribution by both UV_{254}-active DOC and total DOC detection.

2.4 Conclusions

Four groundwater samples (W20, W60, W280 and W300) were collected from the Wanneroo borefield to investigate characteristics of each water sample in order to determine the most promising bore for further characterisation studies. The bore chosen for further detailed characterisation was W300. W300 was primarily chosen due to its high DOC concentration, which should allow enough solid material to be collected for characterisation studies, and its relatively high proportion of aromatic components (based on the relative contribution of hydrophobic, transphilic and hydrophilic fractions from XAD-8/XAD-4 resin fractionation).

The general water quality of W300 from the large sampling event (1000 L) was consistent with 8-year-average annual sampling data for the bore for the vast majority of water quality parameters (Table 2.3; Ash et al. 2012). Isolation of the DOC present in the groundwater sample W300 using ultrafiltration and resin chromatography, followed by characterisation of the DOC fractions, will be presented in the following Chapters.

Chapter 3

3.0 Characterisation and Treatability of NOM Isolated from a High Hydrophobicity / High DOC Groundwater by Ultrafiltration

3.1 Introduction

NOM characterisation remains a priority for the water treatment industry, because such characterisation holds the key to understanding, predicting and controlling NOM reactivity under water treatment conditions. A large number of protocols have been developed to isolate aquatic NOM (Thurman 1985; Aiken and Leenheer 1993). These protocols are based on two different approaches: 1) concentration and fractionation, and 2) concentration only. Adsorption chromatography (such as XAD resins) and membrane filtration (such as ultrafiltration and nanofiltration) are the most commonly applied isolation methods (Croué et al. 1999, a). In this Thesis, one of each of these types of isolation methods (XAD resins and ultrafiltration) will be investigated and compared for isolation of NOM for characterisation purposes. Among the membrane filtration methods available, ultrafiltration (UF) has been the most widely used to fractionate aquatic NOM for characterisation studies (Francioso et al. 2002; Christensen et al. 1998; Koechling and Summers 1996; Cai 1999; Assemi et al. 2004), hence ultrafiltration was chosen to isolate the organic matter present in W300 in this study. UF has also been useful to examine the compositional variability of NOM samples from different sources based on an estimation of DOC distributions in different nominal molecular weight (NMW) fractions (Newcombe et al. 1997). Another study using ultrafiltration to fractionate NOM (Koechling and Summers 1996) showed a correlation between the NMW of NOM and its potential to

produce DBPs, with the lower the NMW, the higher the potential to produce THMs upon chlorination.

The advantages of membrane techniques over adsorbent-based NOM techniques are: firstly, that a comparatively large volume of water can be processed in a short period of time, and secondly, the NOM is never subjected to extreme pH values that could alter its structural properties (Croué et al. 1999, b). Unlike adsorbent-based NOM techniques, which rely on certain chemical properties of NOM, membrane filtration is based on the molecular weight/size of the NOM components. The fractionation mechanism characterising membrane filtration is based on membrane pore size and the difference in size of the NOM molecules in the water (Amy et al. 1987). In theory, the membrane will retain NOM molecules larger than the maximum pore size of the membrane and the smaller molecules will pass through the pores (Assemi et al. 2004). Since the NOM components are fractionated as a function of their molecular size/shape without any reference to specific chemical composition or characteristics, there is no specific term for NOM fractions obtained from these membrane filtration methods. Therefore, each fraction of NOM is only distinguished from the other fractions by its NMW. However, it must be noted that the NMW of the NOM fractions produced from the membrane separation is not a true molecular weight, as there is some uncertainty in the range of the molecular weight of the NOM which will pass through a membrane of a particular NMW (Cho et al. 1999). This is because the application of membrane filtration may lead to filter polarisation, in which smaller materials can be trapped in the larger molecules and so the larger molecules can act as a filter themselves (Peuravuori and Pihlaja 1997).

The major drawback of membrane concentration is that the membrane concentration techniques usually concentrate inorganic salts along with the NOM, albeit not necessarily with the same efficiency (Croué et al. 1999, b), and concentrated samples must be repeatedly diluted with purified water and subjected to further membrane filtration steps in order to reduce the concentration of inorganic salts in the fractions. Another problem with the use of membranes for NOM concentration is the possibility of membrane fouling by NOM (Croué et al. 1999, a).

3.1.1 Scope of This Study

For this study, ultrafiltration was employed to isolate the fraction of NOM from a sample of W300 raw water which did not pass through the membrane. The efficiency and practicality of ultrafiltration for isolation of NOM from a high hydrophobicity / high DOC groundwater was investigated. The isolated fraction was then characterised by a variety of NOM characterisation techniques, allowing new information to be determined about the characteristics in terms of structure and functionality of NOM from a high hydrophobicity / high DOC groundwater.

The isolated fraction was also separately treated by a laboratory simulation of the magnetic ion exchange (MIEX®) treatment process to determine the effectiveness of MIEX® treatment for removal of this fraction from water. The characteristics of the NOM in the fraction were investigated before and after MIEX® treatment. As MIEX® is a relatively new technology in water treatment, the removal effectiveness of the resin for different types of organic matter is not yet well understood. New information was obtained on the treatability of a highly hydrophobic DOC fraction by the MIEX® process.

3.2 Experimental

3.2.1 Water Sample

Groundwater (1000 L) from bore W300 in the Wanneroo groundwater production borefield was collected on 31st March 2005. The groundwater sample was subjected to filtration through a 0.45 μm filter and the filtrate was stored at 4°C prior to use.

3.2.2 Cleaning Procedures

The procedure for cleaning of glassware was the same as that described in Section 2.2.2.2.

3.2.3 Ultrafiltration Isolation Protocol

Filtered raw water (W300, 75 L) was passed through a 1 kDa nominal molecular weight (NMW) tangential flow ultrafiltration cartridge (Millipore). The retentate was

refiltered until the volume of the retentate was reduced to 4 L, and retentate and permeate sub-samples were collected in 30 mL glass vials. These samples were immediately analysed for their conductivity values and subsequently analysed for their DOC concentrations. MilliQ water was then added to increase the volume to 75 L and the filtering process repeated until the retentate was again reduced to 3 L and retentate and permeate sub-samples (30 mL) collected for analysis of conductivity and DOC concentration. Rotary evaporation further reduced the volume of the retentate to 400 mL. Since the conductivity of the concentrated retentate was approximately 880 μS cm^{-1}, indicating the presence of significant amount of inorganic salts, dialysis using a 1 kDa Spectra/Por 6 regenerated cellulose membranes was performed until the conductivity of the dialysis retentate was approximately 50 – 60 μS cm^{-1}. The 1 kDa dialysis membrane was chosen to keep a consistent NOM NMW fraction while maximising salt removal. The sample was then freeze dried to obtain a solid sample of NOM of NMW > 1000 Da. This sample is referred to as the UF sample or fraction.

3.2.4 MIEX® Treatment of the UF Fraction

3.2.4.1 Preconditioning of the MIEX® Resin

Raw water (W300, 1.65 L) was stirred with virgin MIEX® resin (16.6 mL) for 30 minutes. The resin was then regenerated by stirring with 10 % aqueous sodium chloride solution (600 mL) for 30 minutes. Lastly, the resin was stirred with MilliQ water (600 mL) for 10 minutes. After each process the solvent/solution was decanted from the settled resin.

3.2.4.2 UF Stock Solution

A stock solution (1 L) of the UF fraction was produced by initial dissolution of the dried isolate (100 mg) in aqueous sodium hydroxide solution (0.01 M, 1 mL) followed by addition of MilliQ water. The solution was filtered through a 0.45 μm glass fibre filter and the DOC concentration measured, as outlined in Section 2.2.4, to be 17.5 mg L^{-1}.

3.2.4.3 MIEX® Treatment of UF Solution

UF stock solution (400 mL, [DOC] = 17.5 mg L^{-1}) was stirred with MilliQ water (total volume 1 L) and preconditioned and regenerated MIEX® resin (2.1 mL) for 15 minutes, and the aqueous layer was decanted from the resin. The aqueous layer represented the UF after MIEX® treatment sample.

3.2.5 Characterisation Methodology

DOC concentration, UV/Visible spectroscopy and HPSEC were analysed as outlined in Sections 2.2.4, 2.2.5 and 2.2.7, respectively.

3.2.5.1 Elemental Analysis

Elemental analysis for carbon (C), hydrogen (H), nitrogen (N), sulfur (S), oxygen (O) and ash was performed on the dry UF isolate by micro-combustion. Chemical and Micro Analytical Services Pty. Ltd performed this analysis under a commercial arrangement. Carbon, hydrogen and nitrogen were liberated from the sample via combustion (1800 °C) and detected as CO_2, H_2O and NO_x, respectively, by gas chromatography. Sulfur was converted to SO_2 via explosive heating with subsequent ion chromatography with detection using a sulfate ion-selective electrode. Oxygen was liberated by heating (800 °C) in an anoxic environment in the presence of a platinum/nickel catalyst with detection as CO_2 via gas chromatography. Ash content was determined gravimetrically after heating (815 °C).

3.2.5.2 Fourier Transform Infrared Spectroscopy

Fourier transform infrared (FTIR) spectra were collected in the transmission mode using a Bruker IFS-66 spectrometer. Approximately 2 mg of dried UF isolate was ground and potassium bromide (300 mg) was mixed with the ground material, and the mixture was pressed into a small disc. FTIR analyses were carried out by collecting 4 background scans followed by 4 scans of the sample. All FTIR spectra were scanned between 4000 and 7000 cm^{-1} and data analysis performed with OPUS software.

3.2.5.3 Solid-State ^{13}C Nuclear Magnetic Resonance Spectroscopy

The solid-state ^{13}C cross polarization magic angle spinning NMR spectra were obtained at a frequency of 50.3 MHz on a Varian Unity 200 spectrometer. The samples were packed in a 7 mm diameter cylindrical zirconia rotor with Kel-F end-caps and spun at 5000 ± 100 Hz in a Doty Scientific MAS probe. The spectra were acquired using a 1 millisecond contact time and a 1 second recycle delay. Between 24K and 61K scans were collected, representing a total run time of 7 to 17 hours. The free induction decays (FIDs) were acquired with a sweep width of 40 kHz; 1216 data points were collected over an acquisition time of 15 milliseconds. The FID was zero-filled to 32768 data points and processed with a 50 Hz Lorentzian line broadening and a 0.01 second Gaussian broadening. The chemical shift was externally referenced to the methyl resonance of hexamethylbenzene at 17.36 ppm. Spectra were corrected for background signal by subtracting the spectrum acquired for an empty rotor under the same acquisition conditions.

These analyses were performed under a collaborative arrangement by Dr Ron Smernick in the School of Earth and Environmental Sciences at the University of Adelaide, Australia.

3.2.5.4 Fluorescence Spectroscopy

Fluorescence excitation-emission (EEM) measurements were conducted using a Varian Cary Eclipse Fluorescence Spectrophotometer with a quartz cuvette of 1 cm path length. The spectrometer displayed a maximum emission intensity of 1000 arbitrary units (AU). The spectrometer used a xenon excitation source and excitation and emission slits were set to a 5 nm band-pass. To obtain fluorescence EEMs, excitation wavelengths were incrementally increased from 190 to 380 nm at 2 nm increments. The emission wavelength range was 280 – 500 nm with 1 nm increments. Data acquisition and processing was computer controlled with Sigma Plot software.

3.2.6 Disinfection By-Product Formation Potential Experiments

3.2.6.1 Preparation of Chlorine Solution

A stock solution of chlorine in water (approximately 1000 mg L^{-1}) was prepared by dilution of a commercial sodium hypochlorite solution (125 g L^{-1}) with MilliQ water. Due to the instability of chlorine solutions, the free chlorine concentration of the stock solution was measured prior to every set of experiments. The chlorine concentration was initially determined iodometrically against standardised sodium thiosulphate solution and excess potassium iodide (Franson 1998). The chlorine concentration obtained by titration was compared to the response given by a HACH chlorine colorimeter. The colorimeter was then used to determine the free Cl_2 equivalent concentration (mg L^{-1}) of subsequent chlorine solutions.

3.2.6.2 Chlorination Experiments

UF stock solution and UF after MIEX® stock solution (diluted to 2 mg L^{-1} DOC concentration) and bromide ion stock solution (200 µL, 1000 mg L^{-1}) were separately added into amber glass bottles, the pH was adjusted to 7.0 through the addition of phosphate buffer, and the solutions diluted with MilliQ water and dosed with a concentrated chlorine solution (6 mL, 1000 mg L^{-1}) to produce an initial chlorine concentration of 6 mg L^{-1} (total volume 1 L), a similar concentration to what is applied for disinfection at the Wanneroo GWTP. The reaction mixtures were stored in the dark at 25°C for 7 days. At various times over 7 days, the residual chlorine equivalent concentrations were measured in duplicate and aliquots (~40 mL) of each reaction mixture were quenched with an aqueous sodium sulfite solution (500 µL, 100 g L^{-1}) and stored in the dark at 5°C until THM analysis was performed. After 7 days, an additional aliquot (40 mL) of each reaction mixture was quenched with an aqueous sodium sulfite solution (500 µL, 100 g L^{-1}) and stored in the dark at 5°C until HAA analysis was performed.

3.2.7 Analysis of Disinfection By-Products

3.2.7.1 Analysis of Trihalomethanes

THMs were extracted from the samples and concentrated via automated headspace-solid-phase microextraction (HS SPME) as per the procedure published by Kristiana et al. (2010) on a Gerstel Multipurpose Sampler MPS2, which was interfaced to an Agilent Technologies Series II 6890N/5973N GC Mass Selective Detector for analysis. HS SPME was carried out on 30 mL of sample in a 40 mL vial. Anhydrous sodium sulfate (5 g) and internal standard solution (30 µL of 50 mg L^{-1} 1,2-dibromopropane in methanol) were added to the sample. Samples were agitated for 15 minutes prior to the introduction of a Supelco® divinyl/carboxen/ polydimethylsiloxane fibre (50/30 µm) into the headspace of the vial. The fibre was exposed to the headspace for 15 minutes to allow extraction of THMs. The SPME fibre was desorbed at 270°C for 10 minutes in the injector port of the GC. Separation of the analytes was achieved using a 60 m × 0.25 mm i.d. × 0.25 µm film thickness Phenomenex DB-5MS fused silica 5% phenyl/95% dimethylpolysiloxane GC column. Helium carrier gas was used at a constant flow of 1.0 mL/minute. The oven temperature was initially 35°C held for 5 minutes, then ramped at 10°C/minute to 200°C, then 20°C/minute to 310°C and held for a final 10 minutes. Selected-ion-monitoring (SIM) of m/z 83, 85, 96, 121, 123, 127, 129, 131, 173 and 175 was performed. Each sample was analysed in duplicate.

Calibration of THM concentrations was achieved by analysis of a series of external standards ($CHCl_3$, $CHBrCl_2$, $CHBr_2Cl$ and $CHBr_3$; AR grade, Aldrich). A stock standard solution with each THM present at a concentration of 2 g L^{-1} in methanol was prepared. A working standard solution (10 mg L^{-1}) was then prepared. For the calibration standards, aliquots of the working standard solution were diluted with MilliQ water (30 mL) following the addition of the internal standard solution (10 µL, 50 mg L^{-1} 1,2-dibromopropane in methanol) and sodium sulfate (1.67g). Extraction by HS SPME and analysis by GC-MS was performed as described above. Each standard was analysed in duplicate.

3.2.7.2 Analysis of Haloacetic Acids

Analysis of HAAs was conducted by liquid-liquid extraction, derivatisation to the methyl esters and analysis of the esters by GC-MS as per the procedure published by Kristiana et al. (2010). The pH of the quenched reaction mixture (30 mL) was lowered to < 0.5 via the addition of concentrated sulfuric acid. Sodium sulfate (13 g) and methyl *tertiary*-butyl ether (MTBE) (3 mL) were then added. The MTBE layer (~2 mL) was collected and 10 % sulfuric acid in methanol (2.5 mL) was added. The mixture was heated at 60°C for 2 hours then cooled to room temperature. The mixture was washed with aqueous sodium sulfate solution (7 mL, 150 g L^{-1}) and saturated sodium bicarbonate solution (1 mL). The organic layer was then dried (magnesium sulfate) and an aliquot (15 µL, 50 mg L^{-1} 1,2-dibromopropane in methanol) of the internal standard solution added.

The final solution was analysed using a Hewlett Packard (HP) 6890 GC interfaced to a HP 5973N Mass Selective Detector. A cool-on-column injector system was used with helium carrier gas at a constant flow of 1.0 mL/minute. Separation of the analytes was achieved using a fused silica 60 m × 0.25 mm i.d. × 0.25 µm film thickness Phenomenex ZB-5MS 5% phenyl/95% dimethylpolysiloxane GC column. The initial oven temperature was 35°C which was held for 10 minutes, then ramped at 5°C/minute to 135°C with 5 minute hold times at each of 75°C, 100°C and 135°C, then increased at 20°C/minute to a final 300°C, and held for 10 minutes. Selected-ion-monitoring (SIM) of m/z 59, 83, 85, 93, 95, 108, 117, 119, 121, 123, 127, 129, 161, 163, 171, 173, 205, 209, 251 and 253 was performed.

Calibration of HAA concentrations was achieved by analysis of a series of external standards. A working standard solution containing all 9 HAAs (concentration range of 1 – 500 µg L^{-1}) was prepared by dilution of the commercially available HAA mixture in MTBE (EPA 552.2 Acids Calibration Mix, HAAs concentration range of 200 – 2000 µg L^{-1}, Supelco), into methanol. For the calibration standard solutions, aliquots of the working standard solution were added to MilliQ water (30 mL). The standard sample was then extracted, derivatised and analysed as described above. Each standard was analysed in duplicate.

3.3 Results and Discussion

3.3.1 Isolation of UF Fraction

In the first part of a comparison study of NOM isolation techniques, NOM from 75 L of a high hydrophobic / high DOC concentration (23 mg L^{-1}) groundwater from a bore in the Wanneroo borefield (W300) was isolated and fractionated by ultrafiltration. Pre-filtered (0.45 μm) W300 water was passed through the ultrafiltration system (1 kDa NMW membrane), during which the concentration of DOC in both the permeate and retentate were monitored. From the first pass through the UF system (total DOC: 1725 mg), the DOC contained in the permeate was calculated to be 123 mg, and the DOC in the retentate was 1580 mg, resulting in retention of 92 % of the DOC and only 8 % of the DOC being transferred to the permeate, with 1 % loss of DOC, presumably on the membrane. After passing the retentate through the system for a second time, the DOC contained in the retentate was 1060 mg, and the DOC contained in the permeate was 130 mg, resulting in 68 % retention of the DOC from the first retentate in the second retentate, 8 % of the DOC from the retentate from the first pass being transferred to the permeate during the second pass, with 25 % of the DOC from the first retentate being lost during the second ultrafiltration pass, presumably due to adsorption of DOC onto the membrane. Overall, the UF procedure retained 61 % of the total DOC after two passes. From previous work in our laboratory (Allpike 2008), approximately 65 – 70 % of the DOC from a Wanneroo groundwater sample was retained during ultrafiltration using a 1000 NMW Da Millipore membrane, which was comparable to the recovery in the combined retentate in the current study. Practical considerations in NOM isolation limit the NOM recovery currently achievable to 70 – 90 % for freshwater samples (Croué et al. 1999, b) with the major limitation imposed by the presence of salts. Due to time constraints in the current study, a solid isolate fraction (UF fraction) was obtained by freeze-drying the retentate after the second pass through the UF membrane after desalting by dialysis (1000 Da). The UF fraction was characterised by a number of techniques, which are described below.

3.3.2 Characterisation of Isolated Solid UF Fraction

3.3.2.1 Elemental Analysis

Elemental analysis is generally the first technique applied to the study of NOM (Croué et al. 2000). The elements analysed include carbon, hydrogen, nitrogen, oxygen and sulfur, and the fraction of NOM which is not oxidised is referred to as 'ash' and indicates the amount of inorganic species present (Croué et al. 2000). The results of these analyses are usually given in percent by weight and also specific ratios of elements present. The elemental analysis and atomic ratio data for the UF fraction is shown in Table 3.1.

Table 3.1 Elemental percentage composition and atomic ratio data for the UF fraction.

Sample	% C	% O	% H	% N	% S	% Ash	H/C	O/C	N/C
UF	13.86	35.58	3.13	0.56	0.98	35.07	2.69	1.93	0.03

The UF fraction was found to have a high ash content (Table 3.1). Ash includes heteroatomic compounds (eg. P), halogens (e.g. Cl, Br) and metals present in the raw water and is generally an indication of total inorganic content within the sample. Dialysis was performed to reduce the amount of inorganic salts in this fraction, but the ash content indicated that the remaining salt concentration was still very high compared to the carbon content. The high ash content present in the UF fraction was likely due to insufficient transfer of salt into the permeates during the ultrafiltration and dialysis processes. As ultrafiltration is primarily used to determine molecular weight of organic matter in water samples (Aiken 1985), solid NOM isolates from the retentates of ultrafiltration separations have rarely been obtained. Hence, there are few previous reports of elemental composition of ultrafiltration fractions. Abbt-Braun and Frimmel (1999) did report the isolation of ultrafiltration retentate fractions and reverse osmosis retentate fractions from various NOM samples from different origins (surface water, lakes and controlled catchments) from Norway. The ultrafiltration retentate fractions produced similar elemental compositions (except for O and H) to those in the current study, i.e. for the Norwegian samples: C 14.36 – 15.64 %, H 1.36 – 1.49 %, N 0.90 – 1.81 %, O 24.5 – 27.7 % and ash 24.21 – 57.56 % (Abbt-Braun and Frimmel 1999). The substantial amount of ash present in these

isolates reportedly caused the C content to be low and prevented the effective analysis of oxygen. With samples containing high ash levels (such as in the current study), it is important to use sufficiently high combustion temperatures (usually > 1000°C) to decompose any carbonates that may be present in the sample or formed during combustion. If carbonates are present, the carbon value obtained represents total carbon, and carbonate carbon must be determined by treating the sample with a strong mineral acid (Huffman Jr and Stuber 1985). As oxygen is usually calculated by difference, the inefficient removal of salts may have contributed to some variation in measured elemental composition (Nanny 1997; Abbt-Braun and Frimmel 1999).

The type of water sample from which the NOM has been isolated by UF may also influence the elemental composition as surface water lakes and dams, groundwater and river waters have been reported to produce NOM fractions with different elemental composition (Thurman 1985). H/C, O/C and N/C ratios are fundamental quantities used in describing and understanding geochemical substances (Huffman Jr and Stuber 1985). The high H/C ratio relative to the O/C and N/C ratios is indicative of an aliphatic rich character (Christensen et al. 1998) in the present UF sample.

3.3.2.2 Fourier Transform Infrared Spectroscopic Analysis

The Fourier transform infrared (FTIR) spectrum of the UF fraction solid sample, shown in Figure 3.1, is characterised by a number of absorption bands, exhibiting variable relative intensity. The FTIR spectrum (Figure 3.1) shows similarities to those of humic substances isolated from both soil and aquatic environments (Senesi 1990; Leenheer et al. 1995; Kim et al. 2006), including four solid NOM isolates from water collected from various treatment stages at the Wanneroo GWTP (Allpike 2008). Peak assignment includes a very broad absorption band at 3500 – 2500 cm^{-1} (shown as the green region of Figure 3.1), due to hydrogen bonded hydroxyl groups of carboxylic acids, as well as phenols and alcohols (Takács and Alberts 1999), from carbohydrate material (Barber et al. 2001). Broad bands at 3000 – 2800 cm^{-1} (yellow region) are representative of C-H stretching from methyl and methylene carbons, from petroleum products and/or lipids present in the NOM fraction (Barber et al. 2001). Other prominent bands in the spectrum include carboxylic and ketonic carbonyl stretching at 1710 cm^{-1} (pink region) due to the presence of carboxylic, ketonic, aldehydic or ester carbonyl groups, which all have a strong absorbance at

this wavelength. These stretches occur at this wavelength typically for aliphatic and aromatic acids, fulvic and humic acids, as well as amino acids (Barber et al. 2001). The strong band at 1630 cm^{-1} (purple region) is due to aromatic carbon stretches. Moderate bands at 1400 cm^{-1} (orange region) are characteristic of asymmetric and symmetric bending of CH_3 and CH_2 groups associated with carbonyl moieties, such as those of ketones, esters and carboxylic acids. A significant feature of the FTIR spectrum was absorbance bands centred at 1250 cm^{-1} (blue region), as several functional groups give signals in this region, including bands due to C-O stretching of alcohols, C-O stretching and O-H deformations of carboxylic acids, C-O stretching of esters and C-O-C stretching of ethers (Aiken et al. 1985; Stevenson 1994). FTIR can also serve as an assay of purity of NOM fractions because it allows bicarbonate, carbonate, nitrate, phosphate, silicate and sulfate salts in the sample to be readily detected (Croué et al. 1999, b). The FTIR spectrum of the UF sample indicates detectable inorganic constituents such as carbonates, nitrates, phosphates, silica and sulfates were still present in the sample post dialysis, indicated by the detectable peaks in the 800 – 500 cm^{-1} region. Hence, careful assignment of the peaks at 1630 cm^{-1} and 1400 cm^{-1} is necessary as they can be influenced by small changes in salt content (Takács and Alberts 1999), a likely outcome for this sample.

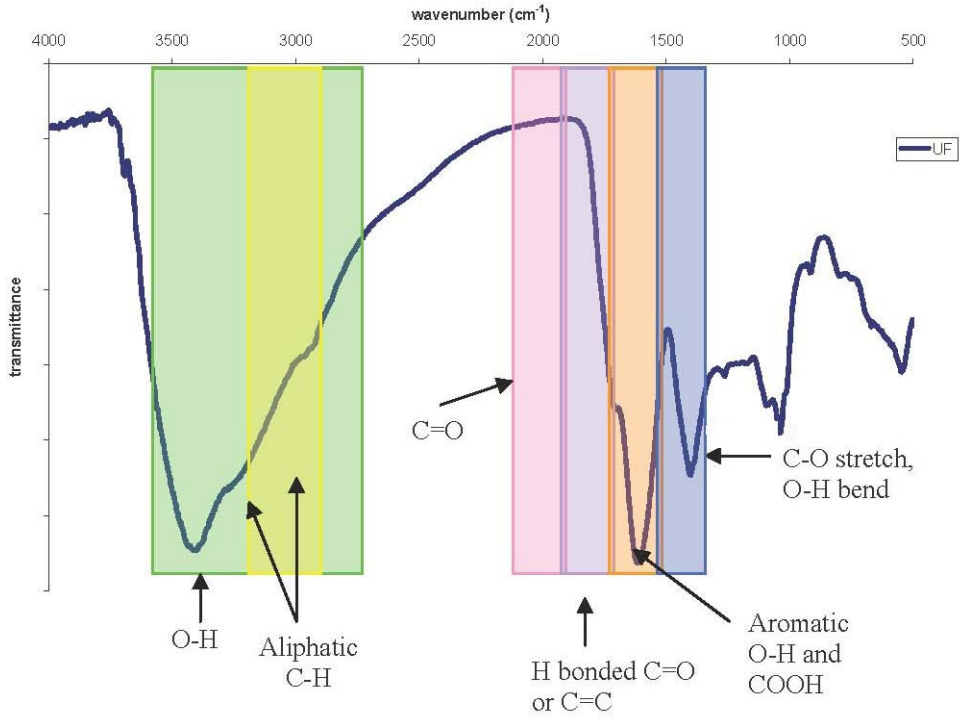

Figure 3.1 FT-IR spectrum of the UF fraction.

3.3.2.3 Solid-State ^{13}C Nuclear Magnetic Resonance Spectroscopic Analysis

The solid-state ^{13}C NMR spectrum for the UF fraction solid sample is shown in Figure 3.2. The low carbon and high ash contents of the fraction contribute to a poorly resolved spectrum. Nevertheless, several small broad peaks were attributable to aliphatic carbon (0 – 45 ppm, green in Figure 3.2), oxygenated aliphatic carbon (45 – 110 ppm, shaded yellow), aromatic carbon (110 – 160 ppm, pink shading), and carbonyl carbon (160 – 190 ppm, purple shading) structures (Li et al. 2004). The relative proportions of these different types of carbon atoms, based on integration of the UF fraction solid-state ^{13}C NMR spectrum, are shown in Figure 3.3.

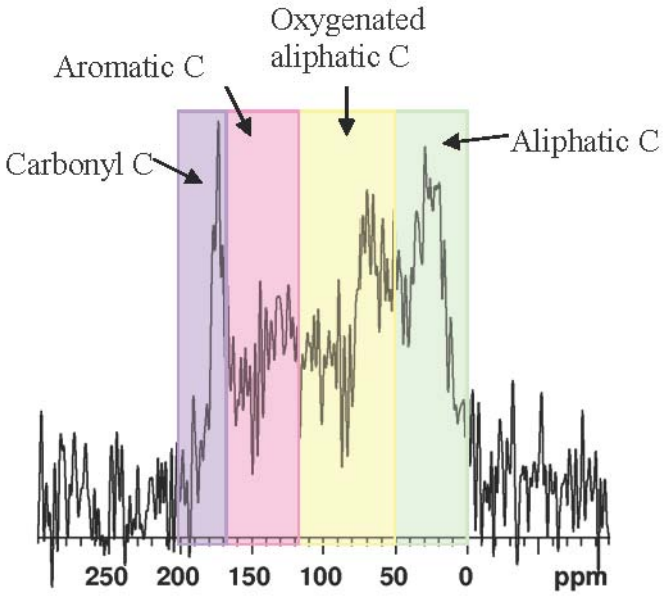

Figure 3.2 Solid-state ^{13}C NMR spectrum for the UF fraction.

The relatively strong aliphatic carbon signal (0 – 45 ppm) is likely due to methyl, methylene and methine carbons (Wilson 1989) from lipid and biopolymer precursors (Dria et al. 2002). As the aliphatic signal is very broad, it indicates that the aliphatic components are short in chain length and or highly branched (Wilson et al. 1981). In a previous study, a hydrophobic NOM sample obtained from a MIEX® pilot plant process operating at the Wanneroo GWTP, a sample removed from the MIEX® resin representing the material removed by ion exchange, showed a similarly pronounced aliphatic peak (Wong et al. 2002). The moderate peak of the oxygenated aliphatic carbon region, is typical of a wide variety of alcohol, ether and ester carbons (Wilson et al. 1981). In a previous study of a highly coloured surface water from South Australia (Newcombe et al. 1997), ultrafiltration was used to isolate NOM into five

MW fractions and study the structural characteristics by solid-state ^{13}C NMR spectroscopy. Newcombe et al. (1997) found that oxygenated aliphatic carbon was also the dominant signal by solid-state ^{13}C NMR spectroscopy. The sharp peak at 170 ppm, also seen in the previous study by Wong (2002), may be due to either carboxyl, ester or amide carbons (Desmukh et al. 2001), with all of these types of carboxyl carbon being found in humic substances (Wilson et al. 1981).

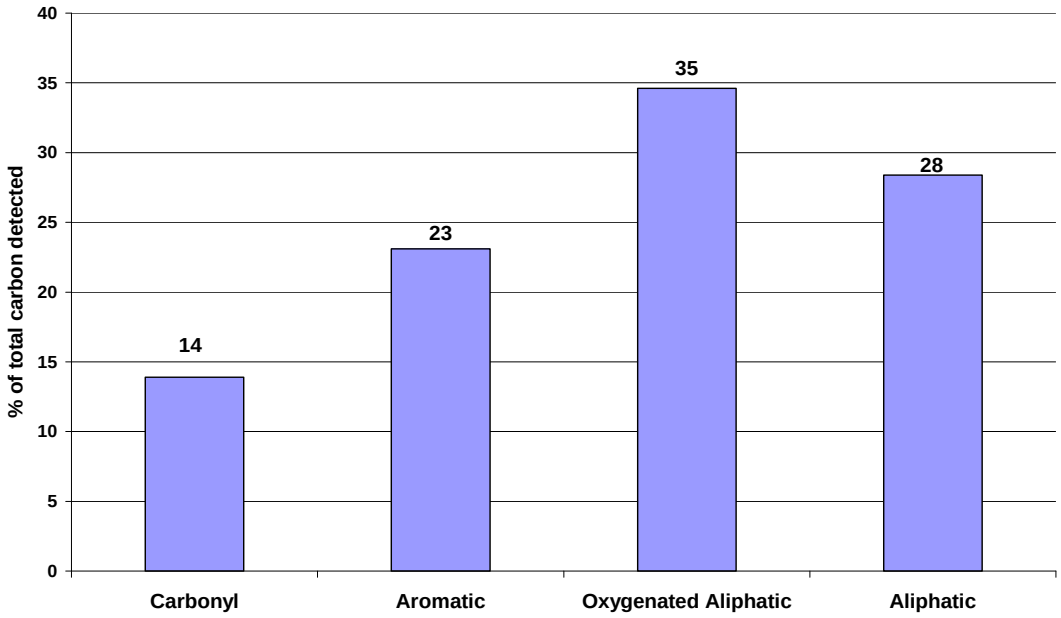

Figure 3.3 Relative proportions of carbon types based on integration of regions of the solid-state ^{13}C NMR spectrum of the isolated UF NOM sample.

For comparative purposes, the relative signal areas measured for the sample were divided into four broad regions (Figure 3.3). Overall, the distribution of types of carbons from solid-state ^{13}C NMR spectroscopy were similar to other fractions isolated from Wanneroo groundwater (Allpike 2008). For the UF sample, the major carbon type was oxygenated aliphatic carbon, with aliphatic carbon the second most abundant carbon type. Carbonyl carbon was the least abundant carbon type as found in the previous study (Allpike 2008).

3.3.2.4 Size Exclusion Chromatographic Analysis

Size exclusion chromatography with organic carbon detection (SEC-OCD) and ultraviolet detection at 254 nm (SEC-UV_{254}) was performed on the UF retentate of the raw water, prior to dialysis, to examine the molecular weight (MW) distribution of the organic matter in this fraction. DOC detection data is shown in Figure 3.4a and

SEC-UV_{254} data in Figure 3.4b, with different MW regions numbered from 1 – 8 according to a previously reported numbering system (Allpike et al. 2005; Huber and Frimmel 1996). Similar MW distributions were detected by both methods, and the distributions were consistent with the MW distribution using UV_{254} detection of the W300 raw water profile reported in Section 2.3.3, as well as the MW distribution indicated by a chromatogram from a typical groundwater in Finland (Nissinen et al. 2001).

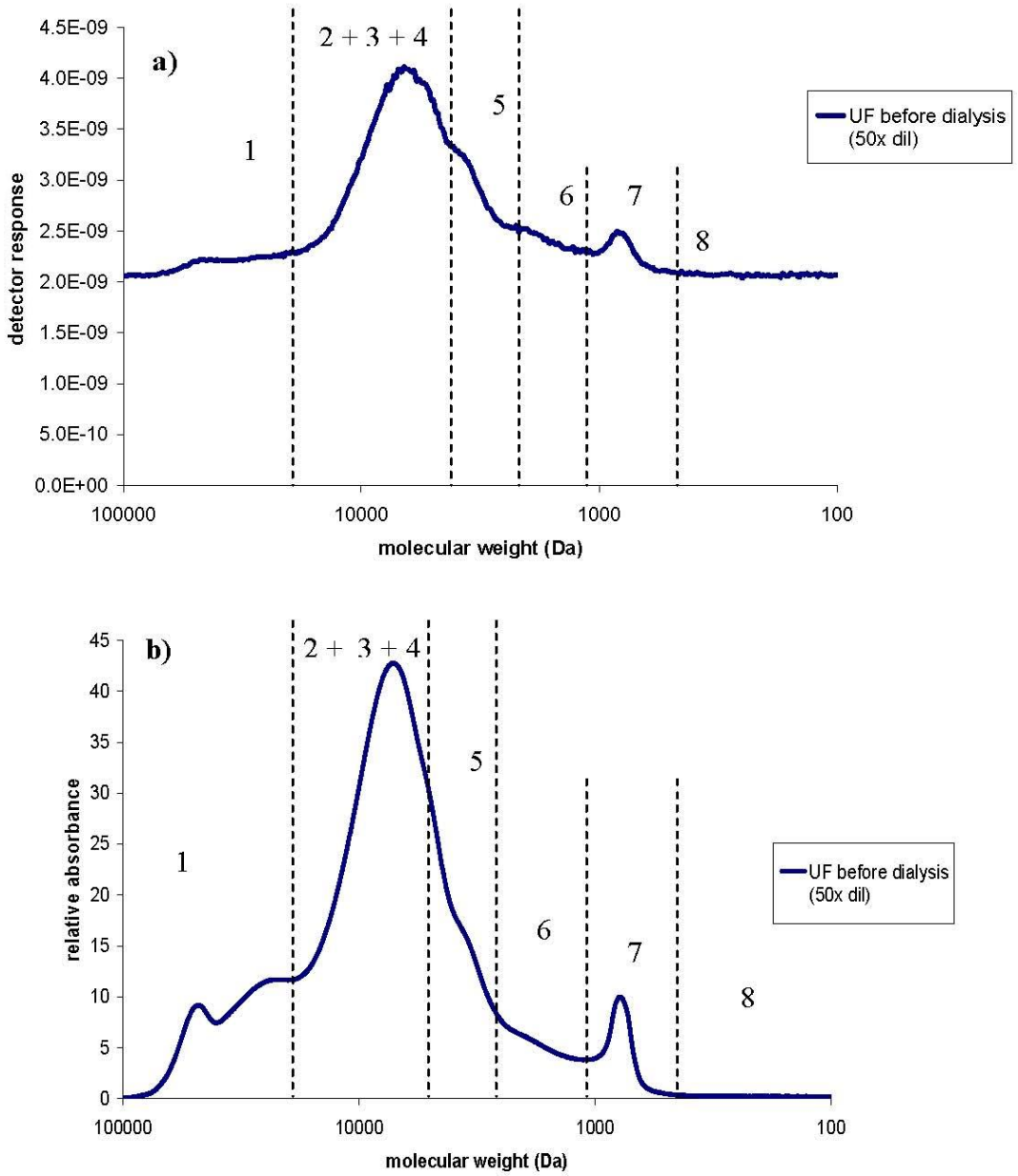

Figure 3.4 MW distribution of the UF retentate before dialysis analysed by a) SEC-OCD and b) SEC-UV_{254} detection. Numbers correspond to eight distinct MW regions, as described in Huber and Frimmel 1996 and Allpike et al. 2005.

As size exclusion chromatographic analysis can not be performed on a solid sample, a sub-sample of the UF retentate of the raw water, prior to dialysis, was used. The high ash content (approximately 35 %, Table 3.1) of the solid UF fraction, post dialysis, correlates with a high salt content in the UF retentate post-dialysis. Because the sample for SEC characterisation was taken pre-dialysis, the salt content of this fraction would presumably have been higher than the post-dialysis sample. In high salt conditions, two elution modes are reported to be operating in SEC: separation based on size and the column interaction mode (Vuorio et al. 1998). These two elution modes have an effect on purification of the sample. The high salt content, causing an interaction between the salt in the sample and the column, resulted in the MW distribution of the UF sample being only broadly bimodal in nature, as shown by chromatograms using both UV_{254}-specific and OCD-specific detectors (Figure 3.4). The peak denoted as region 1 in these samples, which eluted as a broad range of poorly resolved material, has been reported in earlier studies of Wanneroo borefield-derived samples to potentially consist of colloidal organic and inorganic substances (Allpike et al. 2005; Huber and Frimmel 1996; Warton et al. 2007, a). Regions 2 – 4, which eluted as one partially resolved peak, have been reported to be likely enriched in humic substances of relatively high molecular weight (Huber and Frimmel 1996). Regions 5 – 7 reportedly correspond to the fractions comprising lower molecular weight monoprotic acids, such as fulvic acids, conjugated unsaturated acids or keto-acids (Huber and Frimmel 1996). Region 8 eluted as a broad band of poorly resolved material and comprised organic matter of the lowest apparent MW.

3.3.2.5 Overall Characteristics of UF Solid Isolate

Isolation of W300 NOM by ultrafiltration produced a solid freeze-dried sample. Desalting the fraction was challenging, and even after dialysis, a high ash content remained, hindering characterisation. While the quality of the spectra was impeded by the high ash content of the sample, FTIR and solid-state ^{13}C NMR spectroscopic analyses indicated that the sample may have a significant aliphatic content, presumably from lipid and biopolymer precursors. Further characterisation by SEC revealed the UF fraction to have a significant contribution from humic substances of relatively high molecular weight. NOM from groundwaters is reported to contain molecules originating from the breakdown of large molecules: carbohydrate residues,

plant residues, plus the breakdown of lipids, fats and proteins (Caron and Smith 2011). Hence, characterisation of the UF fraction has shown the fraction to be typical of groundwater-derived NOM.

3.3.3 MIEX® Treatment of the Redissolved UF Fraction

Virgin MIEX® resin was obtained from the Wanneroo GWTP at the time of raw water sampling. The virgin MIEX® resin was preconditioned with raw water (W300) to preload the resin with W300 NOM in a laboratory simulation of the plant treatment process. Preconditioning was carried out using a Jar Test Protocol developed by Orica Advanced Water Technologies (Holmquist 2006) which closely models full-scale MIEX® treatment at the Wanneroo GWTP.

The isolated UF fraction was redissolved in MilliQ water and separately treated by preconditioned MIEX® resin. A UF solution (approximately 8 mg L^{-1} DOC) was treated with 2 mL of MIEX® resin for 15 minutes in a simulation of the full-scale plant at Wanneroo. The characteristics of the UF fraction before and after MIEX® treatment were then compared.

3.3.3.1 DOC Concentration, UV_{254} and Colour

The DOC concentration, UV_{254}, $SUVA_{254}$ and colour of the UF fraction before and after MIEX® treatment are shown in Table 3.2. A comparison of water quality from the Wanneroo GWTP at the time of sampling is also shown in Table 3.2.

Table 3.2 DOC concentration, UV_{254}, $SUVA_{254}$ and colour parameters for the UF fraction before and after MIEX® treatment.

Sample	DOC (mg L^{-1})	UV (cm^{-1})	$SUVA_{254}$ (m^{-1} L / mg C)	Colour (HU)
UF	7.7	0.878	2.2	37
UF after MIEX®	6.7	0.628	1.8	27
Wanneroo raw water	6.8	0.430	6.3	55
MIEX® treated water	3.5	0.250	7.1	27

The DOC concentration was only slightly reduced (12 %) by the laboratory MIEX® treatment, compared to the DOC removal (49 %) at the time of sampling through the MIEX® treatment process at the Wanneroo GWTP. Extensive batch, pilot plant and

full scale testing of the MIEX® process in Australia and the USA have shown that removal of DOC can vary between 9 – 89 % (Singer et al. 2007, b). Factors affecting DOC removal include resin dose, resin concentration, quality of DOC and the presence of competing anions. The resin concentration and dose used to treat the UF fraction in a simulated-fashion to the Wanneroo GWTP was based on the plant conditions at the time of water sampling. In the elemental analysis of the solid UF fraction (Section 3.3.2.1), the ash content was approximately 2.5× larger than the % C. Anions (such as chloride and sulfate) in this sample may have effectively competed for the active sites on the resin. The minimal MIEX® removal of DOC (2%) from the HPI fraction of a surface water source was attributed to the large retention of salts in the sample (Lee et al. 2002).

The absorbance at 254 nm (UV_{254}) is a useful surrogate for DOC concentration. MIEX® treatment of the UF fraction showed a 28 % reduction in the UV_{254} absorbance, correlating reasonably well with the slight reduction in DOC after MIEX® treatment. There was a reasonable reduction in UV_{254} (50 %) from the MIEX® treatment process at the Wanneroo GWTP, consistent with the DOC concentrations of the samples. The $SUVA_{254}$, the ratio of UV absorption at 254 nm relative to the DOC concentration, for the UF fraction showed a small decrease with MIEX® treatment (18 %). This decrease showed that the MIEX® resin removed relatively more UV absorbing components of the DOC present in the fraction (Budd et al. 2005). In a previous pilot plant study on MIEX® treatment using raw water with a low $SUVA_{254}$ (<2) and high total dissolved solid content, from Southern Nevada Water Authority, USA (Singer et al. 2007, b) the reduction in $SUVA_{254}$ was larger than the reduction in DOC concentration, as found in the current study. Colour refers to the 'true' colour; i.e. the colour of the sample with the turbidity removed. The colour values were strongly correlated with the respective UV_{254} and DOC concentrations, with the UF fraction colour reduced by 27 % and the MIEX® treated water colour reduced by almost 50 %, respectively, after treatment.

3.3.3.2 Fluorescence Excitation-Emission Spectroscopy

Fluorescence spectroscopy is useful for monitoring changes in the molecular structure of humic substances. Humic substances, regardless of their origin, exhibit characteristic fluorescence spectra which have been attributed to the presence of

aromatic fluorophores with electron-donating functional groups (Chen et al. 2003, a). The major fluorescent components present in the excitation-emission matrix (EEM) are shown in Table 3.3 (Leenheer and Croué 2003), whereby the EEM peaks have been associated with humic-like, tyrosine-like, tryptophan-like, or phenol-like organic compounds. The spectral breakdown of fluorescent components and their excitation and emission characteristics are shown in Figure 3.5 (Chen et al. 2003, b) where the operationally defined excitation and emission boundaries for the five regions are largely based upon supporting literature (Chen et al. 2003, b). In general, peaks at shorter excitation wavelengths (< 250 nm) and shorter emission wavelengths (< 350 nm) are related to simple aromatic proteins such as tyrosine (Regions I and II; Figure 3.5). Peaks at intermediate excitation wavelengths (250 – ~ 280 nm) and shorter emission wavelength (< 380 nm) are related to soluble microbial by-product-like material (Region IV). Peaks at longer excitation wavelengths (≥ 280 nm) and longer emission wavelengths (> 380 nm) are related to humic-acid like organic material (Region V) (Chen et al. 2003, b). Peaks with shorter excitation wavelengths (< 250 nm) and longer emission wavelengths (> 350 nm) are related to fulvic acid-like materials (Region III) (Chen et al. 2003, b).

Table 3.3 Major fluorescent components in the excitation-emission matrix (Leenheer and Croué 2003).

Range of excitation (nm)	**Range of emission (nm)**	**Component type**
330 – 350	420 – 480	Humic-like
250 – 260	380 – 480	Humic-like
310 – 320	380 – 420	Marine humic-like
270 – 280	300 – 320	Tyrosine-like, protein-like
270 – 280	320 – 350	Tryptophan-like, protein-like or phenol-like

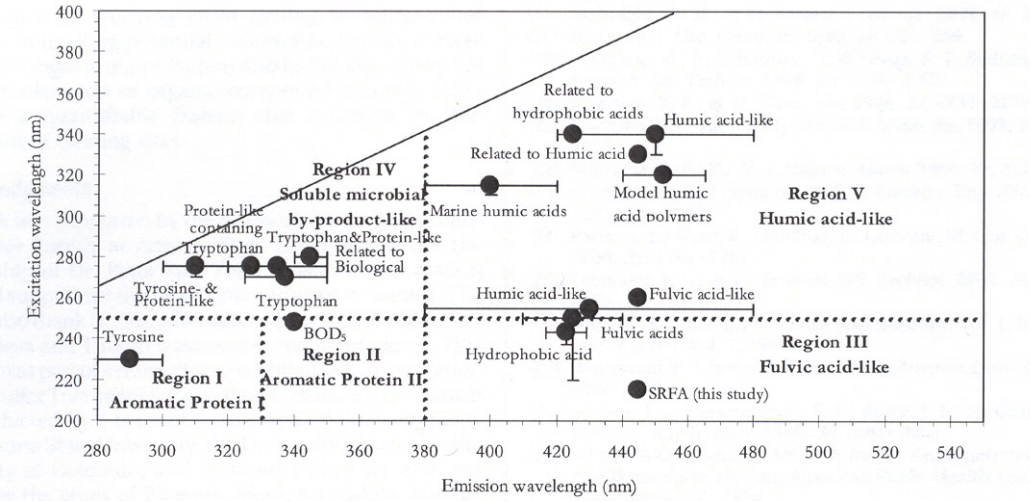

Figure 3.5 Breakdown of fluorescent components (Chen et al. 2003, b).

The EEM spectra of the UF fraction before and after MIEX® treatment are shown in Figures 3.6a and b, respectively. The peaks running diagonally through the emission range of 400 – 500 nm at an excitation range of 200 – 260 nm are instrument artefacts of glass and water interactions present in all excitation-emission spectra. The peaks running diagonally through the emission range of 250 – 380 nm at an excitation range of 270 – 290 nm are due to Rayleigh/Tyndall scattering lines (Caron and Smith 2011). The intensity scale for Figure 3.6 was chosen to be consistent with the intensity scales for the EEM fluorescence profiles in Chapter 4 (Figures 4.8 – 4.10) and Chapter 5 (Figure 5.4) to allow comparison of all EEM fluorescence spectra in Chapter 6. Fluorescence spectroscopy shows that treatment of the UF fraction by the MIEX® process removed humic and fulvic type material. The fluorescence intensities of the humic and fulvic regions in the spectrum from the UF fraction (Figure 3.6a) are large, relative to the MIEX® treated fraction which showed minimal humic and fulvic fluorescence (Figure 3.6b). The decrease in fluorescing components may also be consistent with the decrease in UV_{254}-active species observed with treatment (Table 3.2). A small residual of soluble microbial by-product like material and aromatic proteins (Figure 3.6b) was visible in the water sample after MIEX® treatment, which was not seen in the pre-treated sample. There has been no other reports of EEM spectra of MIEX® treated UF samples, so this is the first study of MIEX® treatment in this area. The microbial by-product like

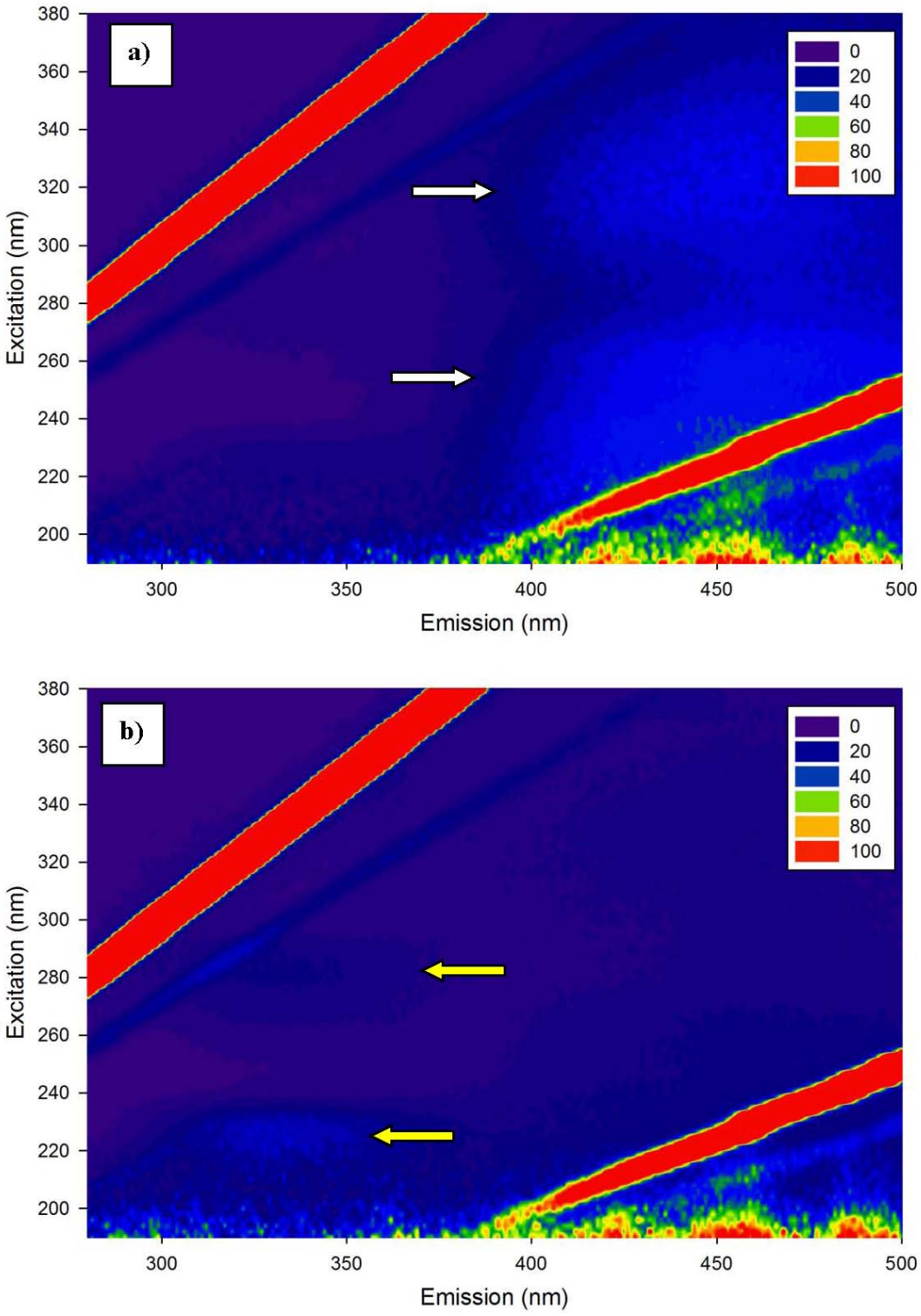

Figure 3.6 Excitation-emission (EEM) fluorescence spectra of the UF fraction a) before and b) after MIEX® treatment. White arrows represent 'humic-like' and yellow arrows represent 'protein-like' components within the spectra.

material present after treatment, which was not seen pre-treatment, can not be easily explained. The presence of soluble microbial by-products after treatment indicates

that the MIEX® process is less effective at removing protein-derived structures. A previous fluorescence EEM study of a wastewater impacted drinking water source (Amy 2007) demonstrated effective removal of humic-like organic matter and ineffective removal of protein-like organic matter after coagulation treatment.

3.3.3.3 Size Exclusion Chromatographic Analysis

The SEC-OCD and SEC-UV254 chromatograms of the UF fraction (post-dialysis and redissolved in MilliQ water), before and after MIEX® treatment, are shown in Figures 3.7a and 3.7b. Separate MW regions are numbered from 1 – 8 as described in Section 2.3.1.3. Organic carbon detection showed a small proportion of the DOC over a wide MW range was removed by MIEX® treatment, consistent with the low removal of DOC (12 %, Table 3.2). Previous studies (Humbert et al. 2007; Comstock et al. 2003; Fearing et al. 2004; Lee et al. 2002; Drikas et al. 2011) of water from Lake Allatoona (Georgia, USA), a high DOC (6 mg L^{-1}) surface water from the Villejean/Rennes drinking WTP in Brittany (France) and various surface waters in the USA with differing alkalinity and TOC concentrations, as well as a long term case study of MIEX® treatment from Mt Pleasant WTP in South Australia, have shown that organic matter in the MW range of 1000 – 10000 Da was removed by MIEX® resin, with higher MW material poorly removed, consistent with the results of the current study.

The MW distribution of both UV_{254}-active DOC and total DOC in the UF fraction post dialysis is consistent with previous studies of Wanneroo groundwater (Allpike 2008; Allpike et al. 2005; Warton et al. 2007, a). Region 1 with the high MW seems to be peculiar to local Western Australian waters (Warton et al. 2007, a), and was poorly removed by the MIEX® process. This lack of removal of the likely colloidal organic and inorganic substances in region 1 by MIEX®, also seen in previous studies of Wanneroo raw water (Allpike et al. 2005; Warton et al. 2007, a), is consistent with the idea that colloids would not be removed by an anion exchange process (Vrijenhoek et al. 1998). Material in regions 2 – 4, was only slightly removed by MIEX® treatment. Since the NOM in groundwaters from the Wanneroo borefield is thought to consist largely of tannin-derived substances (Heitz 2002), composed predominantly of phenolic moieties with relatively minor carboxylic content, the low removal of material is consistent with phenolic moieties not being

amenable to removal by ion exchange. Material represented by regions 5 – 7 was removed slightly by the MIEX® process, suggesting that these fractions are probably enriched in negatively charged species and these anionic species are more readily removed by ion exchange (Allpike et al. 2005). Poor chromatographic resolution for region 8 hindered any quantification of this fraction, as per the previous study by Allpike et al. (2005).

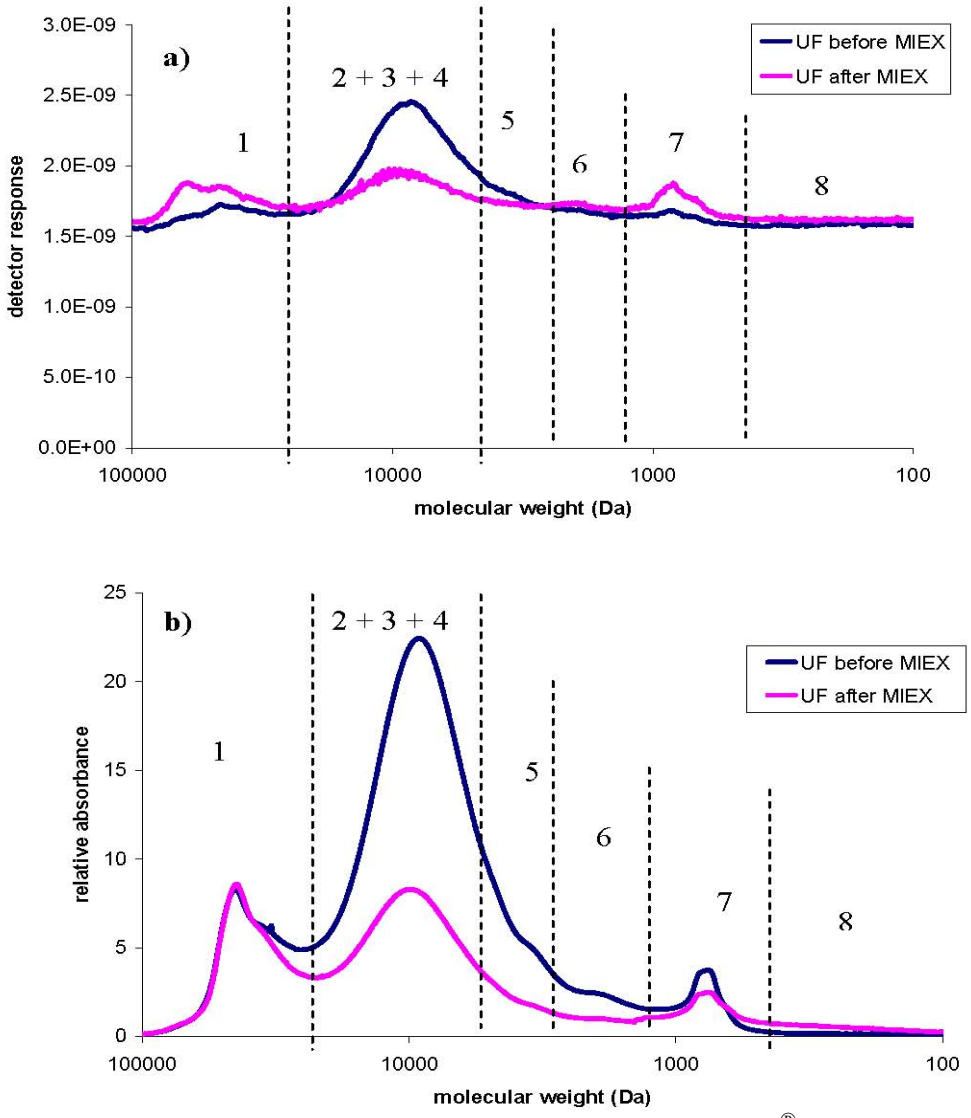

Figure 3.7 MW distribution of the UF sample before and after MIEX® treatment by a) SEC-OCD and b) SEC-UV_{254} detection. Numbers correspond to eight distinct MW regions as described by Huber and Frimmel 1996 and Allpike et al. 2005.

3.3.3.4 Disinfection By-Product Formation Potential

The chemical reactivity of NOM with chlorine as measured by the disinfection by-product formation potential (DBPFP) can provide a qualitative assessment of NOM character. Prior to DBPFP measurement, aqueous samples of the UF fraction (post

dialysis, redissolved in MilliQ water) and the UF fraction after MIEX® treatment were diluted to achieve DOC concentrations of 2 mg L^{-1}, typical of the DOC concentration leaving the Wanneroo GWTP, and bromide ion was added at a concentration of 0.2 mg L^{-1}, typical of bromide concentrations of raw W300 water (Table 2.3, Section 2.3.3). The pore size of ultrafiltration membranes allows bromide to pass into the permeate (Chow et al. 2005), so the UF retentate fraction itself should have contained minimal bromide. This was confirmed by analysis of bromide in the UF fraction by ion chromatography with a detection limit of 10 μg L^{-1}, where bromide was found to be below the limit of detection of the analysis. Disinfection experiments involved addition of chlorine to achieve an initial concentration of 6 mg L^{-1} (a similar chlorine dose to that applied to the treated water leaving the Wanneroo GWTP), addition of buffer to achieve pH 7 and temperature control to 25 ºC, and analysis of the concentration of trihalomethanes (THMs) and haloacetic acids (HAAs) after 7 days. The 7-day oxidant demands of the UF fraction and the UF after MIEX® treatment fraction are shown in Table 3.4, with the 7-day individual and total THM concentrations shown in Table 3.5, and the corresponding HAA concentrations shown in Table 3.6.

Table 3.4 Oxidant demand of the UF fraction and the UF fraction after MIEX® treatment (halogenation conditions: 2 mg L^{-1} DOC, 6 mg L^{-1} Cl_2 dose, 0.2 mg L^{-1} Br^-, pH 7, 25°C, 168 hours).

Sample	Oxidant demand (mg L^{-1} free chlorine)	Specific oxidant demand (mg free chlorine/mg C)
UF	3.7	1.9
UF after MIEX®	2.8	1.4

The oxidant demand (expressed as a free chlorine equivalent concentration; commonly referred to as chlorine demand) examines the consumption of oxidant concentration over a period (usually 7 days). The oxidant concentration gives a measure of the amount of organic and inorganic components in the water sample with the capacity to react with the oxidant. Consumption of the oxidant (the oxidant demand) then gives an indication of the oxidant-reactive (here chlorine- and bromine-reactive) fraction of NOM in the water sample. Oxidant demands are useful for determination of the oxidant residual (often termed ‘chlorine residual’) required to achieve a specific disinfectant residual during water treatment.

MIEX® treatment resulted in a lower oxidant demand (Table 3.4), indicating that the MIEX® treatment preferentially removed the oxidant-reactive (chlorine- and bromine-reactive) fraction of NOM. Since the DOC concentration of each sample has been normalised to 2 mg L^{-1} prior to the disinfection experiments, the oxidant demand concentration is already in essence normalised to the DOC concentration. The oxidant demand data was completely normalised to the DOC concentration by dividing by the DOC concentration to produce a specific oxidant demand (mg free chlorine/mg C) to compare the current results to other MIEX® treatment studies. The study by Warton et al. (2007, a) described the behaviour of the MIEX® process on a full scale plant level using several parameters to assess its performance. Combining MIEX® with coagulation resulted in a higher quality water than simply coagulation in an enhanced mode, as measured by DOC concentration, UV_{254} absorbance, chlorine demand and specific chlorine demand, THMFP, turbidity and colour (Warton et al. 2007, a). In another study on two reservoir waters in South Australia, Drikas et al. (2003) found a lower specific chlorine demand for MIEX® treated waters (MIEX® 6 mL L^{-1}, 15 minute contact time), and combined alum/MIEX® coagulation (6 mL L^{-1}, 10 minute contact time, 20 mg L^{-1} alum/pH 6), compared to other treatment strategies including alum coagulation without pH adjustment and alum coagulation at pH 6. The slower chlorine decay for the MIEX® treatment alone compared with the combined alum/MIEX® treatment was thought to be due to the higher resin dose or longer resin contact time used with MIEX® treatment alone, but additional experiments confirmed the same chlorine decay rate was observed when the same MIEX® treatment conditions were used for both options. Similar trends were also seen at higher temperatures; the only difference was a faster chlorine decay (Drikas et al. 2003). Incorporating MIEX® into a treatment scheme may allow preferential removal of the oxidant-reactive fraction of NOM, resulting in a reduced chlorine consumption and likely correspondingly lower THM formation.

Table 3.5 Concentrations of THMs from chlorination of the UF fraction and the UF fraction after MIEX® treatment (halogenation conditions: 2 mg L^{-1} DOC, 6 mg L^{-1} Cl_2 dose, 0.2 mg L^{-1} Br^-, pH 7, 25°C, 168 hours).

Sample	Concentration of Individual THMs (µg L^{-1})				Total THMFP (µgL^{-1})	Specific THMFP (µg/mg C)
	$CHCl_3$	$CHBrCl_2$	$CHBr_2Cl$	$CHBr_3$		
UF	99	106	71	7	283	142
UF after MIEX®	129	104	52	5	290	145

Table 3.6 Concentration of HAAs from chlorination of the UF fraction and the UF fraction after MIEX® treatment (halogenation conditions: 2 mg L^{-1} DOC, 6 mg L^{-1} Cl_2 dose, 0.2 mg L^{-1} Br^-, pH 7, 25°C, 168 hours).

Sample	Concentration of Individual HAAs (µg L^{-1})									Total HAAFP (µg L^{-1})	Specific HAAFP (µg/mg C)
	MCAA	MBAA	DCAA	TCAA	BCAA	DBAA	BDCAA	CDBAA	TBAA		
UF	ND*	ND*	44	82	34	15	92	27	ND*	294	147
UF after MIEX®	ND*	ND*	13	6	21	21	19	19	10	108	54

* ND – not detected

The 7-day THMFPs of the UF fraction and the UF fraction after MIEX® treatment, each with DOC concentrations normalised to 2 mg L^{-1}, were essentially identical, indicating that the reactivity of DOC for THM formation in the two samples was the same and that the MIEX® treatment did not preferentially remove THM precursors from the UF fraction. This is not surprising given the low (12 %) DOC removal by MIEX® treatment in this case. As NOM is the principal precursor of organic DBPs, DBP formation is directly proportional to the concentration and characteristics of the NOM (Singer et al. 2007, b). In this DBPFP study, the DOC concentration was normalised to 2 mg L^{-1} for both samples to study the propensity to form DBPs for each sample. From both the UF fraction and the UF fraction after MIEX® treatment, the total THMs produced after 7 days were above the ADWG of 250 µg L^{-1}, indicating that the NOM in this water type has a high propensity to form THMs. Even though the total THMs produced for both samples was higher than the maximum recommended concentration of 250 µg L^{-1}, it should not be of concern as DBPFP experiments are generally considered to represent a worst-case scenario (Warton et al. 2007, a). The ADWG guidelines were also exceeded in a previous study on eight apparent MW fractions of a Western Australian surface water which were isolated by preparative SEC, where the initial DOC concentrations were also

normalised to 2 mg L^{-1} in disinfection experiments (Kristiana et al. 2010). At the Wanneroo GWTP, water is extracted from a variety of bores (from both confined and unconfined aquifers), which individually have varying quality. Although blending of the bores at the treatment plant results in the major water quality parameters being comparatively constant, the nature and concentration of other components, which are not individually monitored, can vary widely. Hence, while the NOM in W300 is very prone to THM formation as seen in Table 3.5, this bore water is blended with other higher quality bore waters as it enters the Wanneroo GWTP, such that the actual THM concentrations in distributed water are likely to be well below the THMFP measured in this experiment.

Chlorination is widely utilized in drinking water disinfection and THMs and HAAs have been reported to be two of the most important DBPs formed (Rodriguez et al. 2004). THMs are identified as the main DBPs, and, as such, HAAs have not been studied as extensively, but, in a number of systems, they have been found to occur at similar concentrations to THMs (Singer 2002). There are nine bromine- and chlorine-containing HAAs: two are monohalogenated species [monochloroacetic acid (MCAA) and monobromoacetic acid (MBAA)]; three are dihalogenated species [dichloroacetic acid (DCAA), bromochloroacetic acid (BCAA) and dibromoacetic acid (DBAA)], and four are trihalogenated species [trichloroacetic acid (TCAA), bromodichloroacetic acid (BDCAA), chlorodibromoacetic acid (CDBAA) and tribromoacetic acid (TBAA)]. BDCAA was the most abundant HAA product (in mass concentration) from the untreated UF fraction, with BCAA and DBAA equally abundant from the MIEX® treated UF fraction (Table 3.6). The UF after MIEX® fraction showed a shift towards brominated HAAs, as TBAA was only detected in the UF after MIEX® fraction. But, MIEX® treatment of the UF fraction did significantly reduce the potential for HAA formation, indicating preferential removal of HAA precursors by MIEX® treatment. Again, it should be emphasised that in this DBPFP study, the DOC concentration was normalised to 2 mg L^{-1} for both samples to study their propensity to form DBPs. The HAAFP of the UF fraction was very high and similar in mass concentration to its THMFP, but the concentrations of individual HAAs did not exceed the ADWG maximum concentrations. The ADWG only has maximum recommended concentrations for three HAAs: 150 μg L^{-1} for monochloroacetic acid (MCAA), and 100 μg L^{-1} each for dichloroacetic (DCAA)

and trichloroacetic acid (TCAA) (NHMRC 2011). Overall, these results demonstrated the high reactivity of the NOM fractions from this Wanneroo bore water for the formation of DBPs.

Relative distributions of brominated and chlorinated DBPs can be compared through the 'Bromine Incorporation Factor' (BIF) parameter introduced by Boyer and Singer (2005). The 'BIF' is a parameter used to measure the extent of bromine substitution within a DBP class, as classified by the ratio of moles of bromine to moles of total halogen incorporated into the various DBP classes (Boyer and Singer 2005). The BIF parameter (Obolensky and Singer 2005; Boyer and Singer 2005) allows interclass comparisons of the extent of bromine substitution, by normalising the values to a range between 0 and 1, with zero representing no incorporation and 1 representing full bromine incorporation. In particular, the formula for THMs, where the concentrations of the individual THMs are expressed in molar units, is (Boyer and Singer 2005):

$$\mathrm{BIF}(\mathrm{THMs}) = \left(\frac{[\mathrm{CHCl_2Br}] + 2[\mathrm{CHClBr_2}] + 3[\mathrm{CHBr_3}]}{3\{[\mathrm{CHCl_3}] + [\mathrm{CHCl_2Br}] + [\mathrm{CHClBr_2}] + [\mathrm{CHBr_3}]\}} \right)$$

The formula for HAAs, where the concentrations of the individual HAAs are expressed in molar units, is (Boyer and Singer 2005):

$$\mathrm{BIF\,(HAAs)} = \left(\frac{[\mathrm{MBAA}] + [\mathrm{BCAA}] + 2[\mathrm{DBAA}] + [\mathrm{BDCAA}] + 2[\mathrm{CDBAA}] + 3[\mathrm{TBAA}\}}{6\{[\mathrm{MCAA}] + [\mathrm{MBAA}] + [\mathrm{DCAA}] + [\mathrm{TCAA}] + [\mathrm{BCAA}] + [\mathrm{DBAA}] + [\mathrm{BDCAA}] + [\mathrm{CDBAA}] + [\mathrm{TBAA}]\}} \right)$$

The BIFs for THMs and HAAs for the UF fraction and the UF after MIEX® treatment are shown in Table 3.7.

Table 3.7 BIF (THMs) and BIF (HAAs) obtained after 7 day chlorination experiment.

Sample	BIF (THMs)	BIF (HAAs)
UF	0.31	0.12
UF after MIEX®	0.26	0.23

For both THMs and HAAs, the extent of bromine substitution varied for the UF and UF after MIEX® treatment fractions. During disinfection, the initial concentration of bromide ion and the extent of bromide ion oxidation to hypobromous acid (HOBr), have been found to affect the distribution of DBP species (Harrington et al. 1996). In addition, HOBr is reportedly more reactive to aliphatic precursors (Liang and Singer 2003), and as bromine incorporation reduced for THMs after MIEX® treatment, this suggests that MIEX® treatment preferentially removed aliphatic precursors present in the fraction (Section 3.3.1). Aliphatic precursors are more significant for THM formation than HAA formation (Kanokkantapong et al. 2006). The increased BIF values for the HAAs in the UF fraction after MIEX® treatment reflects a shift towards the brominated HAAs. A MIEX® pilot plant study on four raw waters with varying water qualities in various locations across the United States (Singer et al. 2007, b) reported a similar shift towards brominated HAAs after MIEX® treatment.

From the DBPFP experiments, the UF fraction and the UF after MIEX® fraction have been demonstrated to be highly reactive to the formation of DBPs. The total THM concentrations of the UF fraction and the UF fraction after MIEX® treatment were comparable, indicating that the reactivity of DOC for THM formation in the two fractions was the same, suggesting MIEX® treatment has not preferentially removed THM precursors from the UF fraction. But, MIEX® treatment of the UF fraction did significantly reduce the potential for HAA formation.

3.3.4 Conclusions

Isolation of NOM from a local high hydrophobic / high DOC groundwater source using ultrafiltration was shown to have some success. The solid freeze-dried UF isolate obtained from 75 L of a high DOC concentration (23 mg L^{-1}) groundwater had a low carbon content (14 %) and a high ash content (35 %). Desalting of the UF isolate was challenging, hindering characterisation of this fraction by the analytical methods employed in this study. While the quality of the spectra were impeded by the high ash content of the sample, FTIR and solid-state ^{13}C NMR spectroscopic analyses indicated that the sample may have a significant aliphatic content, with some carboxylic acid groups present.

Treatment of the UF fraction by preconditioned MIEX® resin led to only small reductions in DOC concentration (12 %), UV_{254} absorbance (28 %) and colour (27 %). The high salt content of the UF fraction, indicated by the high ash content of the solid sample, may have effectively competed for active ion-exchange sites on the resin surface, limiting the ability of the preconditioned MIEX® resin to remove DOC from the UF fraction.

Chlorine reactivity of the UF fraction before and after MIEX® treatment showed that the DOC in each fraction had a similar propensity to form THMs, but MIEX® treatment of the UF fraction did significantly reduce the potential for HAA formation. However, there was a notable post MIEX® shift towards brominated HAAs, attributed to the selective reactivity of HOBr towards aliphatic precursors of these DBPs. The possibility of a shift towards more brominated HAAs after MIEX® treatment should be monitored in plant-scale applications of MIEX® treatment, since brominated DBPs are reported to be of greater health concern than their chlorinated analogues (Richardson 2003).

Ultrafiltration was used with limited success for the isolation of NOM from W300, as the salt concentration limited the quality of the characterisation that could be performed on the isolated fraction. Nevertheless, the isolated UF fraction was able to be treated with MIEX® resin, and was demonstrated to be highly reactive to the formation of DBPs. A comparison of the UF fraction to fractions isolated by an adsorption chromatographic isolation method (XAD-8/XAD-4 resin method) will be presented in Chapter 4.

Chapter 4

4.0 Characterisation and Treatability of NOM Isolated from a High Hydrophobicity / High DOC Groundwater by Resin Fractionation

4.1 Introduction

The first step of many analytical protocols for characterisation of NOM is the fractionation process. Fractionation refers to chemical or physical processes that separate components of environmental mixtures into more homogeneous groupings based upon chemical or physical properties (Leenheer 2009). Since the purpose of isolating and fractionating NOM is to elucidate chemical properties, it is desirable to have an approach based on the chemical and reactive properties of the material of interest. Presently, the procedure used most extensively for isolation and fractionation of NOM is sorption onto XAD-type resins. These non-ionic macroporous resins combine relatively high adsorption affinities for NOM, with high elution efficiencies and very low affinities for inorganic salts (Croué et al. 1999, b). An attraction of sorption-based isolation techniques is their ability to simultaneously concentrate, isolate and fractionate NOM (Thurman and Malcolm 1981). Over three decades ago, Leenheer and Huffman (1976) proposed using XAD and ion exchange resins in a hierarchical fractionation procedure to characterise NOM molecules based on their hydrophobic-hydrophilic and acid-base properties. This approach was developed further in subsequent years, and a version of the protocol, first proposed by researchers at the United States Geological Survey (USGS) research group in 1981, discussed in detail in Section 1.2.1.1., has become a reference method for the isolation of humic and fulvic acid fractions of NOM (Leenheer 1981; Thurman and Malcolm 1981). The approach has been further expanded and modified since then

(Aiken and Leenheer 1993; Malcolm and MacCarthy 1992), but still provides the basic framework for most fractionation studies. In this Chapter, the preparative two column array of XAD-8 and XAD-4 resins was chosen to fractionate the highly hydrophobic organic matter present in a high DOC water source on the basis of polarity (Croué et al. 1993, a). This protocol separates aquatic NOM into hydrophobic, transphilic and hydrophilic fractions and was preferred to the standard XAD-8 method which isolates just two fractions (hydrophobic and hydrophilic). The chosen fractionation method was also directly compared to the isolation method of ultrafiltration, reported in Chapter 3. Previous investigations of NOM from a variety of sources have led to some generalisations about the characteristics of NOM molecules in different environments. For instance, environments in which water is exposed to mineral surfaces that complex and adsorb NOM contain low concentrations of dissolved NOM, especially humic acids (Croué et al. 1999, b). NOM in lakes and reservoirs of moderate to high trophic status are often dominated by material generated in the water body (autochthonous material), whereas low-order rivers and streams usually carry more NOM that is generated exterior to the water body (allochthonous NOM). Allochthonous NOM has large C/N ratios, is highly coloured, and has significant aromatic carbon content, whereas autochthonous NOM has lower C/N ratios, is almost colourless, and has lower aromatic carbon content (Aiken et al. 1992). Isolating NOM from a high hydrophobicity / high DOC groundwater source from Western Australia will contribute to the body of characterisation studies being conducted to develop a detailed understanding of the origins, structural features and reactivity of NOM.

There are two primary advantages associated with chromatographic methods of fractionation and isolation. First, it is possible to fractionate and isolate a total of approximately 55 to 90 % of the DOC from a variety of aquatic environments (Aiken et al. 1992). Secondly, the fractionation can be carried out on the original water sample without using a pre-concentration step (such as reserve osmosis), thereby maintaining fractionation consistency and comparability between samples (Croué et al. 1999, a). However, there are several potential drawbacks in NOM fractionation using XAD resins. First, the fractions isolated by XAD-8/XAD-4 fractionation may not fully represent the actual chemical properties of the NOM mixture because the use of strong acids and bases in the fractionation procedure potentially alters the

chemical characteristics of the NOM. Secondly, the distribution of each fraction can be affected by the sample preparation, as storage methods and filter type may contribute to variations in fractionation outcomes (Gadmar et al. 2005). Thirdly, fractions of organic matter obtained using these isolation methods are not sharply defined and thus overlapping and operational variations can occur (Gadmar et al. 2005).

For the potable water industry, the major goal of NOM characterisation is to understand and predict the behaviour and/or reactivity of NOM or its fractions in specific water treatment processes. The need for concentration and/or isolation of NOM is largely driven by the sensitivity of the characterisation methods: if it were possible to use the characterisation methods effectively on unconcentrated and unfractionated samples, many problems associated with the analysis (e.g. reactions among molecules in concentrates that are different from those in dilute samples; losses upon concentration and/or isolation) could be avoided (Croué 2004). Unfortunately, at the present time, many characterisation methods are not sufficiently sensitive to be applied to unmodified raw water.

4.1.1 Scope of This Study

This Chapter presents a study of the treatability of XAD-separated NOM fractions isolated from the Wanneroo groundwater bore W300. The NOM fractions were separately treated by a laboratory simulation of the MIEX® process to investigate the removal of the different fractions. The hydrophobic, transphilic and hydrophilic fractions were analytically characterised before and after MIEX® treatment to establish the susceptibility of these fractions, all still relatively complex chemical mixtures, to the treatment. A schematic of the treatment, isolation and characterisation process is shown in Figure 4.1. Isolation and treatment of separate fractions rather than a bulk water source was designed to provide insights into structural characteristics, such as the broad functional group distribution and molecular weight distribution, which may affect the removal of the fractions during MIEX® treatment. The goal was to propose optimisation of treatment processes based on the various fractions of NOM, rather than only the removal of total NOM, ultimately contributing to improved drinking water quality to consumers.

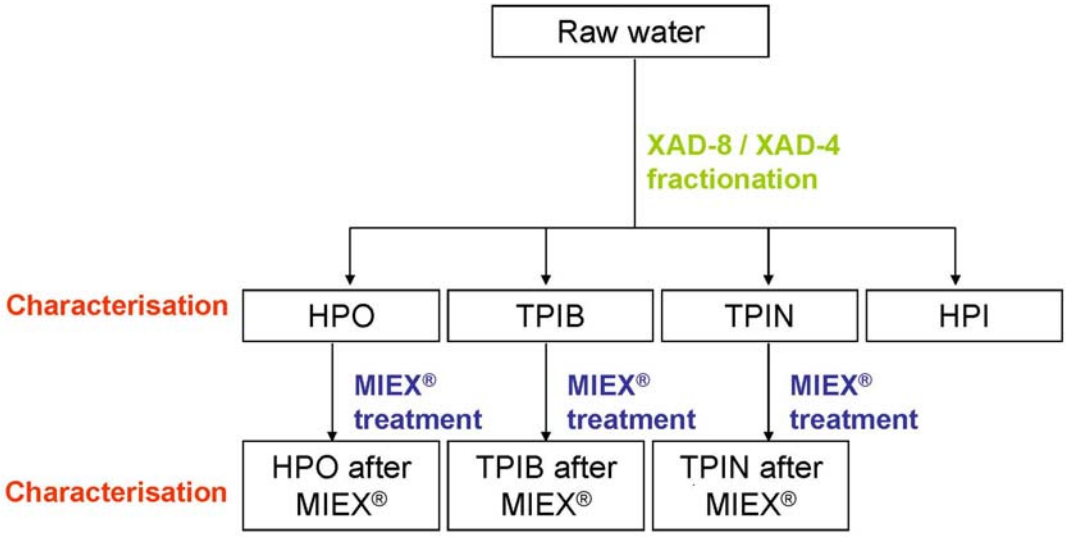

Figure 4.1 The treatment, isolation and characterisation methodology for Chapter 4.

4.2 Experimental

4.2.1 Water Samples

The collection, filtration and storage of the water samples used in this study was described in Section 3.2.1.

4.2.2 Cleaning Procedures

The procedure for cleaning of glassware was the same as that described in Section 2.2.2.2.

4.2.3 NOM Resin Fractionation and Isolation Protocol

The XAD-8/XAD-4 resin preparation, cleaning and pH adjustment are described in detail in Section 2.2.3.

4.2.3.1 Cleaning of Dowex MSC-1 H Resin

The strong acid cation exchange resin (Dowex MSC-1 H) was prepared as a slurry in methanol. The fines were removed by decantation and the remainder of the resin was stored in methanol for 24 hours. Organic resin contaminants were removed by

Soxhlet extraction with methanol for 48 hours. Clean resin was then stored in methanol until required.

4.2.3.2 Preparative Fractionation Process

The XAD-8/XAD-4 resin fractionation procedure employed in this Chapter was modified from the fractionation procedure of Croué et al. (1993, a). Three glass columns (50 mm diameter; 300 mm length) with Teflon frits were each packed with a water-resin slurry (XAD-8, XAD-4 and Dowex MSC-1 H) and the resin column was then rinsed with MilliQ water to remove methanol. The XAD-8 and XAD-4 resins (500 mL) were further cleaned with an acetonitrile/MilliQ mixture (75:25 % v/v, 500 mL) followed by MilliQ water until the DOC concentration was less than 0.5 mg L^{-1}. Final preparation of the resin involved cleaning with hydrochloric acid solution (0.1 M, 500 mL).

The Dowex MSC-1 H resin (250 mL) was further cleaned with aqueous hydrochloric acid solution (3M, 2 L) followed by MilliQ water (4 L), prior to sample application.

Filtered W300 water (0.45 µm, 33 L) was passed sequentially through the XAD-8 and XAD-4 resin columns in series. The sample was followed by a pH 2-formic acid (2.5 L) rinse until the conductivity of the column effluent was the same as the conductivity of the column influent.

The hydrophobic NOM sample was then desorbed from the XAD-8 resin by elution with acetonitrile/MilliQ water (75:25 % v/v) until the eluent was colourless (2.5 L). The solvent was removed from the eluent by rotary evaporation and freeze-drying, yielding the solid hydrophobic NOM fraction (HPO). The isolated mass of HPO was 1900 mg.

One transphilic NOM sample was desorbed from the XAD-4 resin using acetonitrile/MilliQ water (75:25 % v/v) until the eluent was colourless (2.5 L). The solvent was removed by rotary evaporation and freeze-drying, yielding the solid transphilic neutral NOM fraction (TPIN). The isolated mass of TPIN was 200 mg. The other transphilic NOM fraction was desorbed from the XAD-4 resin using aqueous sodium hydroxide solution (0.1 M, 1 L). The eluent was passed through Dowex MSC-1 H resin. The eluent from the Dowex MSC-1 H resin was then

concentrated by rotary evaporation and freeze-dried to yield the solid transphilic base fraction (TPIB). The mass of TPIB fraction recovered was 595 mg.

The hydrophilic NOM fraction (33 L), which passed through both XAD-8 and XAD-4 resins was subsequently concentrated by reverse osmosis. The retentate was recycled through the membrane until its volume was reduced to 2 L. Dialysis (100 Da Spectra/Por Biotech Cellulose Ester membranes) was performed to minimise salts (conductivity of final retentate was approximately 50 – 60 μS cm), and the volume of the dialysed retentate reduced to 500 mL by rotary evaporation to obtain a concentrated isolate of the hydrophilic fraction (HPI) in water.

The fractionation procedure was repeated four times (4 × 33 L) in order to provide sufficient material (approximately 200 mg) of the least abundant transphilic base fraction (TPIB), as well as the other two fractions, for the detailed treatment and characterisation purposes of this study.

4.2.4 MIEX® Treatment of the XAD Fractions

4.2.4.1 Preconditioning of the MIEX® Resin

Preconditioning of the MIEX® resin was conducted as described in Section 3.2.4.1.

4.2.4.2 Stock Solutions for MIEX® Treatment

4.2.4.2.1 Stock Solutions of the HPO, TPIB and TPIN Fractions

Stock solutions (1 L) of the HPO, TPIB and TPIN fractions in water were produced by initial dissolution of the dried isolate (50 – 100 mg) in aqueous sodium hydroxide solution (0.01 M, 1 mL) followed by the addition of MilliQ water. The solutions were filtered through a 0.45 μm glass fibre filter and the respective DOC concentrations measured, as described in Section 2.2.4, to be 18.1 mg L^{-1}, 8.8 mg L^{-1} and 89.6 mg L^{-1}.

4.2.4.2.2 Stock Solution of the HPI Fraction

A stock solution of the HPI fraction (500 mL) was prepared after the HPI isolate obtained in the preparative fractionation process (Section 4.2.3.2) was filtered

through a 0.45 µm glass fibre filter. The DOC concentration of this solution was measured to be 13.6 mg L^{-1}.

4.2.4.3 MIEX® Treatment of Stock Solutions

The HPO (386 mL, 18.1 mg L^{-1}), TPIB (676 mL, 8.8 mg L^{-1}), TPIN (89 mL, 89.6 mg L^{-1}) and HPI (147 mL, 13.6 mg L^{-1}) stock solutions were all separately stirred with MilliQ water (total volume for each fraction 1 L) in a 2 L beaker with preconditioned and regenerated MIEX® resin (2.1 mL) for 15 minutes, and the aqueous layer was decanted from the resin. The aqueous layer represented the corresponding post MIEX® solutions.

4.2.5 Characterisation Methodology for the XAD Fractions

Elemental analyses of the solid isolates (HPO, TPIB and TPIN) were measured by the procedure outlined in Section 3.2.5.1. DOC concentration, UV/Visible spectroscopy, bromide ion concentration, and HPSEC were all analysed as outlined in Sections 2.2.4 – 2.2.7.

4.2.5.1 Flash Pyrolysis-Gas Chromatography-Mass Spectrometry

Flash pyrolysis-GC-MS was carried out using a Chemical Data Systems 160 pyroprobe. The solid NOM isolates (0.5 – 1 mg) were introduced into a quartz capillary with a plug of pre-annealed glass wool at one end and the capillary was placed inside the NiChrome coil of the Pyroprobe which was inserted into the Pyroprobe housing. The coil was heated at 650 ºC for 10 seconds. The pyroprobe-GC interface temperature was maintained at 250 ºC. Pyrolysis products were cryofoccused at -170 °C at the front of the GC column for 2 minutes prior to elution. Analysis was performed by GC-MS on a Hewlett Packard HP 5890 Series II GC with a HP 5971 mass selective detector (MSD) operating in the EI mode. Full scan m/z 50 – 550 mass spectra were acquired at 4 scans/second with an ionization energy of 70 eV. Separation of pyrolysis products was achieved using a fused silica capillary column: 30 m × 0.25 mm i.d. × 1 µm film thickness ZB-5MS GC column. Helium was used as the carrier gas at a pressure of 11 psi, flow rate of 1 mL/minute and a split of 30 mL/minute. The GC temperature program was increased from an initial 40 ºC (2 minutes isothermal) at 4 ºC/minute to a final 310 ºC (15 minutes isothermal).

Data was collected using Chemstation software and mass spectra obtained were correlated with the Wiley 275 mass spectral library and published data.

4.2.5.2 On-line Thermochemolysis-Gas Chromatography Mass Spectrometry

Each dried isolate (0.5 mg) was transferred into a pre-annealed quartz tube sealed at one end. The thermochemolytic reagent tetramethylammonium hydroxide (TMAH) was added as a methanolic solution (5 μL, 25% w/w) and the open end sealed with a pre-annealed glass wool plug. The tube was placed into the coil of a Chemical Data Systems 160 Pyroprobe which in turn was loaded into a dedicated pyroprobe chamber installed on the GC injector. Thermochemolysis was performed at 650 ºC for 10 seconds. The temperature of the interface was maintained at 150 ºC. The products were cryofocussed (-170 ºC) at the front of the GC column for 2 minutes prior to commencement of GC-MS analysis. Conditions for GC-MS analysis were as described for flash pyrolysis-GC-MS (Section 4.2.5.1) except that the GC temperature program was increased from the initial 40 ºC (2 minutes isothermal) at 4ºC/minute to 200 ºC, then 10 ºC/minute to a final 310 ºC (7 minutes isothermal).

4.2.5.3 Micro-Scale Sealed Vessel Pyrolysis-Gas Chromatography-Mass Spectrometry

Each dried isolate (~ 0.5 mg) was loaded into the middle of a glass tube (length 5 cm, i.d. 5 mm). Glass beads were used to fill the void above and below each sample. The tubes were flame sealed, with care taken to avoid direct heating of the sample, and placed in an oven at 300°C for 72 hours. Each sealed vessel, containing a thermally matured sample, was then loaded into a dedicated MSSV injector (300°C) installed on top of the GC oven. The MSSV tube was cracked with a plunger and the volatile products were transferred by helium carrier gas (6 psi) to the GC column. The products were initially cryogenically trapped (-170°C) at the beginning of the column for 2 minutes. GC-MS analysis commenced on removal of the liquid nitrogen trap and was performed as described for flash pyrolysis-GC-MS (Section 4.2.5.1) except that a 40 m × 0.32 mm i.d. × 0.25 μm film thickness ZB-5MS GC column and a split of 20 mL/minute were used, and the GC temperature was programmed to increase from an initial 40 ºC (2 minutes isothermal) at 4 ºC/minute to a final 300 ºC (15 minutes isothermal).

4.2.5.4 Other Spectroscopic Analyses

FTIR, solid-state ^{13}C NMR and fluorescence spectroscopic analyses were conducted as outlined in Sections 3.2.5.2 – 3.2.5.4.

4.2.6 Disinfection By-Product Formation Potential Experiments

The various solutions used for DBP formation potential measurement were prepared as outlined in Sections 3.2.6.1 and 4.2.4.2.1.

4.2.6.1 Chlorination Experiments of XAD Fractions Pre- and Post-MIEX® Treatment

Aliquots of the HPO (110 mL, 18.1 mg L^{-1}), TPIB (226 mL, 8.8 mg L^{-1}), HPO after MIEX® (209 mL, 9.5 mg L^{-1}) and TPIB after MIEX® (500 mL, 3.9 mg L^{-1}) stock solutions were added into separate amber glass bottles and bromide ion stock solution (200 µL, 1000 mg L^{-1}) was added into each bottle. The pH was adjusted to 7.0 with the addition of phosphate buffer, and the solutions diluted with MilliQ water and dosed with stock chlorine solution (6 mL, 1000 mg L^{-1}) to produce an initial chlorine concentration of 6 mg L^{-1} (total volume 1 L), a similar concentration to that applied for disinfection at the Wanneroo GWTP. The reaction mixtures were stored in the dark at 25°C for seven days. At various times over 7 days, the residual chlorine equivalent concentrations were measured in duplicate, and aliquots (~40 mL) of each reaction mixture were quenched with an aqueous sodium sulfite solution (500 µL, 100 g L^{-1}) and stored in the dark at 5 °C until THM analysis was performed. After 7 days, an additional aliquot (40 mL) of each reaction mixture was quenched with a sodium sulfite solution (500 µL, 100 g L^{-1}) and stored in the dark at 5°C until HAA analysis was performed. The initial free chlorine equivalent concentration was chosen so as to produce a final 7-day free chlorine equivalent concentration of 0.5 – 1.5 mg L^{-1} for each sample.

4.2.7 Analysis of Disinfection By-Products

HS SPME-GC-MS analysis of the THMs, and liquid-liquid extraction and derivatisation followed by GC-MS analysis of the HAAs, were conducted as described in Section 3.2.7.

4.3 Results and Discussion

4.3.1 Isolation of XAD Fractions

In the second part of a comparison study of ultrafiltration (Chapter 3) and resin fractionation techniques for NOM isolation, NOM from 132 L of a high DOC concentration (23 mg L^{-1}) groundwater from a bore in the Wanneroo borefield (W300) was isolated and fractionated by the XAD-8/XAD-4 resin procedure. The hydrophobic (HPO) fraction was adsorbed onto the XAD-8 resin, eluted by acetonitrile/water and the solvent removed by rotary evaporation and freeze-drying. The transphilic (TPI) fraction was adsorbed onto the XAD-4 resin, and two TPI isolates, a transphilic base (TPIB) fraction, eluted with sodium hydroxide (and passed through the Dowex MSC-1 H resin), and a transphilic neutral (TPIN) fraction, eluted with acetonitrile/water, were recovered after rotary evaporation and freeze-drying of the solvents. The hydrophilic (HPI) fraction, which did not adsorb on either XAD-8 or XAD-4 resin, was obtained as an aqueous isolate. The mass and relative proportions of the isolated XAD fractions are shown in Table 4.1.

Table 4.1 Isolated mass and relative proportions of the isolated NOM fractions.

Sample	Isolated Mass (mg)	Calculated Weight of C in Isolate based on Elemental Analysis % C (mg)	Proportion of Total Recovered C as a Percentage^
HPO	1900	944	89 %
TPIB	595	22	2 %
TPIN	200	77	7 %
HPI	13*	N/A	1 %

N/A – not calculated
^ Based on mg C of each isolate (from the elemental analysis) / total mass of C of all isolates (from the elemental analysis)
*This fraction was not isolated as a solid form. The isolated mass was calculated to be 13 mg of organic carbon based on the concentration of DOC in the aqueous isolate.

The goal of comprehensive NOM isolation is, of course, 100 % recovery of NOM in desalted fractions, however practical considerations limit the recovery currently achievable to 70 – 90 % for freshwater samples (Croué et al. 1999, b). The total carbon recovered from the XAD-8/XAD-4 resin isolation method was 1056 mg,

equating to a carbon recovery of 35 %, which is consistent with the recovery achieved in some previous resin fractionation studies, including a previous study in the USA on various lakes, swamps and rivers (Leenheer et al. 1987), where the amount of DOC recovered varied between 20 – 71 % for the various samples. In comparison to the DOC recovery (61 %) achieved using the UF isolation method in Chapter 3, the XAD-8/XAD-4 resin procedure used in this Chapter did not allow a higher recovery of total DOC.

The proportions of HPO, TPI and HPI fractions of rivers, lakes, groundwaters and swamps are typically in the range of 23 – 78 %, 7 – 33 % and 8 – 70 %, respectively (Chow et al. 2005), and the results from the XAD-8/XAD-4 resin fractionation (Table 4.1) show that the groundwater bore W300 has a very high amount of HPO NOM present within this water source. The high proportion of HPO material is expected, as preliminary rapid fractionation results (Chapter 2, Table 2.2, Section 2.3.1.2) showed the HPO fraction to be the largest fraction in the DOC distribution, and the high $SUVA_{254}$ values measured in the groundwater (Chapter 2, Table 2.1, Section 2.3.1.1), suggestive of mainly humic material, are consistent with the high proportion of HPO fraction isolated in this study. In previous studies (Croué et al. 1999, a; Aiken et al. 1992) using XAD-8/XAD-4 resin isolation protocols, the humic-type material (HPO) has been noted to be generally enriched in aromatic moieties. Since W300 has a high proportion of HPO material (89 %), which is likely to have a high degree of aromatic character, this is distinctly different to other water sources (Bolto et al. 2002). The proportion of each fraction in the current study was similar to that found in a previous rapid fractionation study of a Wanneroo groundwater from a deep underground source (Bolto et al. 2002), where 80 % was measured to be HPO material, 9 % TPI and 11 % HPI material, based upon differences in DOC concentrations between column influents and effluents, rather than isolated mass as reported in current study. The modest disparity of the DOC distribution between this study and the study of Bolto et al. (2002) is likely to be due to the waters being taken from different aquifers in the Wanneroo borefield. In another study (Croué et al. 1999, a), a slight variation in DOC distribution due to sampling time for a surface water source was observed. During winter sampling, the HPO material accounted for 51 % of the DOC, with the TPI and HPI material being 24 and 25 %, respectively. During spring, the HPO material accounted for 60 % of

the DOC, with the TPI and HPI 19 and 21 %, respectively. In each case, the HPO fraction was the largest fraction in the DOC distribution, consistent with the distribution in the current study.

4.3.2 Characterisation of Isolated Solid XAD Fractions

4.3.2.1 Elemental Analysis and Atomic Ratios

General compositional information was provided by the elemental analysis of the solid fractions. The elemental analysis and atomic ratio data of the HPO, TPIB and TPIN solid fractions is shown in Table 4.2.

Table 4.2 Elemental percentage compositions and atomic ratio data of the three solid XAD fractions.

Sample	% C	% O	% H	% N	% S	% Ash	H/C	O/C	N/C
HPO	49.73	40.56	5.19	1.75	0.85	3.10	1.24	0.61	0.01
TPIB	3.71	6.42	6.95	22.63	0.38	5.43	22.32	1.29	5.23
TPIN	38.71	ND*	5.48	5.92	0.51	ND*	1.69	ND*	0.13

* ND - Not determined due to insufficient sample for analysis

The elemental composition values were largely consistent with other reports of similar data typical of NOM from groundwater sources (Thurman 1985; Grøn et al. 1996; Christensen et al. 1998), however HPO from W300 was slightly enriched in oxygen compared to other groundwater samples from Germany (36.50 %, (Frimmel and Abbt-Braun 1999)). It is critical that NOM fractions are separated from inorganic salt hydrates before elemental analysis is conducted (Leenheer 2009). As the ash content of the HPO sample was < 5 %, the XAD isolation procedure was relatively successful in removing inorganic components from the samples. It is also important that NOM fractions have low ash content, especially for oxygen analyses, as oxygen is commonly reported by difference between 100% minus the sum of the other major elements determined. The external laboratory reported percentage errors associated with the elemental analysis procedure are as follows for the elements analysed: C ± 0.2 %, O ± 0.2 %, H ± 0.3 %, N ± 0.3 %, S ± 0.3 % and ash ± 0.2 %. Hence, as the HPO sample reported an oxygen percentage of 40.56 ± 0.2 %, this fraction is enriched in oxygen compared to other groundwater samples from

Germany (36.50 ± 0.2 %, Frimmel and Abbt-Braun 1999) after taking into account the experimental error for oxygen analysis. The low sample amount (200 mg) of the TPIN fraction prohibited measurement of oxygen and ash content, and without these results the elemental composition of the TPIN fraction was similar to other reported TPIN fractions of NOM (Mash et al. 2004; Croué et al. 2003; Croué 1999).

The low ash content for the HPO and TPIB fractions compared to the ash content seen in the UF fraction (Chapter 3, Table 3.1, 35 %) suggests that the XAD isolation procedure was relatively successful in removing inorganic components from the samples. However, the measured mass of the TPIB fraction (C, O, H, N, S, ash) elementally accounted for only 45.5 % recovery, indicating other elements that were not measured as part of the elemental analysis were present in significant quantities. A sub-sample of the TPIB fraction was dissolved in MilliQ water, the DOC concentration of this sample was determined and concentrations of selected metals and other ions in the TPIB fraction, measured by atomic absorption spectroscopy, are listed in Table 4.3. The results suggest that the TPIB fraction contained relatively high concentrations of the elements sodium and chlorine, which would have been volatilised at the combustion temperature used during the elemental analysis. The high concentrations of sodium and chlorine in the TPIB fraction suggest inefficient cleaning of the Dowex MSC-1 H resin, prior to sample application. Desalting the TPIB sample was considered, but as it a very laborious technique, with the risks including possible sample alteration and lower sample recovery, the decision was made to use the TPIB fractions as obtained.

Table 4.3 Elemental composition of the TPIB fraction.

Sample	**Concentration (mg L^{-1})**										
	Na	**K**	**Mg**	**Ca**	**Al**	**Si**	**Fe**	**Mn**	**Cu**	**Cl**	**DOC**
TPIB	148	0.25	0.13	1.55	0.03	0.75	0.05	0.0	0.06	105	5.9

According to Abbt-Braun and Frimmel (1999), the H/C ratio is an indication of the aromatic/aliphatic character of NOM samples. A high H/C ratio indicates greater aliphatic content, while lower H/C ratios indicate greater aromatic character (Abbt-Braun and Frimmel 1999). The values of the H/C ratio were in order of TPI > HPO which is typical of the respective hydrophilic character of these two types of NOM fractions (Croué 2004). As NOM becomes more hydrophilic, it is more enriched in

nitrogenous structures and oxygenated functional groups. The TPI fractions were more nitrogen-enriched than the HPO fraction (Table 4.2), which is consistent with the expected increase in the polar moiety content for the TPI fractions, with decreasing hydrophobicity with higher H/C values (Aiken et al. 1992). The relatively high carbon and nitrogen concentrations of the TPIN fraction are consistent with other studies of XAD fractions (Aiken et al. 1992) and can be attributed to the high structural polarity and low hydrophobicity of this fraction. The high O/C atomic ratio for the HPO fraction indicates a high content of carboxylic acid groups or hydroxylated functional groups (Christensen et al. 1998), which is supported by the prominent carboxyl peak (C=O) peak in the infrared spectrum (Section 4.3.2.2, Figure 4.2).

4.3.2.2 Fourier Transform Infrared Spectroscopic Analysis

FTIR spectra of humic substances typically contain a variety of discrete bands which can be attributed to specific molecular structures (Stevenson 1994), although some chemical absorbances can be difficult to resolve (Chen et al. 2002). FTIR spectra of the HPO and two TPI fractions are presented in Figure 4.2. Although each fraction had several distinguishing features in its infrared spectrum, the broadness of the infrared absorption bands indicated that each fraction contained a mixture of polyfunctional compounds. The HPO fraction gave an infrared spectrum very similar to that of a soil fulvic acid (Schnitzer and Ghosh 1979), as well as humic substances isolated from aquatic environments (Leenheer 1981; Kim et al. 2006) and four solid NOM isolates taken at various treatment stages from the Wanneroo GWTP (Allpike 2008). The three fractions showed similar IR absorptions, reflecting qualitatively similar structural and functional group features. Nevertheless, the relative intensity of several absorbances did differ. The most prominent features in the spectrum of the HPO fraction were the aliphatic hydrocarbon absorption bands at 3000 – 2800 cm^{-1} (yellow region), representative of C-H stretching from methyl and methylene carbons, accompanied by signals in the 1450 cm^{-1} (orange region) characteristic of C-H deformation of methyl and methylene groups. FTIR absorbance spectra of humic substances are often dominated by O-H group stretches, as well as C=O group stretches and C-O stretches (Leenheer 2009), all of which were evident in the spectrum of the HPO fraction (Figure 4.2). The high oxygen content in the HPO

fraction measured in the elemental analysis (Table 4.2) was further evident in the prominent carboxyl peak C=O at 1715 cm^{-1} in the infrared spectrum (Figure 4.2, pink region), due to C=O stretching of carboxylic and carbonyl groups (Takács and Alberts 1999). This strong carboxyl peak was accompanied by the major band at 1621 cm^{-1} (purple region) which can be assigned to aromatic C=C stretching and asymmetric C=O stretching in COO^- groups (Rivero et al. 1998). The more hydrophilic fractions (TPIB and TPIN) were characterised by strong O-H stretching absorption bands from 3500 – 2500 cm^{-1} (green region) and C-O stretching bands from 1050 – 1250 cm^{-1} (blue region). The TPIB fraction showed relatively high aliphatic C-H stretching (yellow region) and prominent carboxylic and ketonic carbonyl stretching (pink region). The sharp peak at approximately 1400 cm^{-1} may be indicative of high salt content (Takács and Alberts 1999).

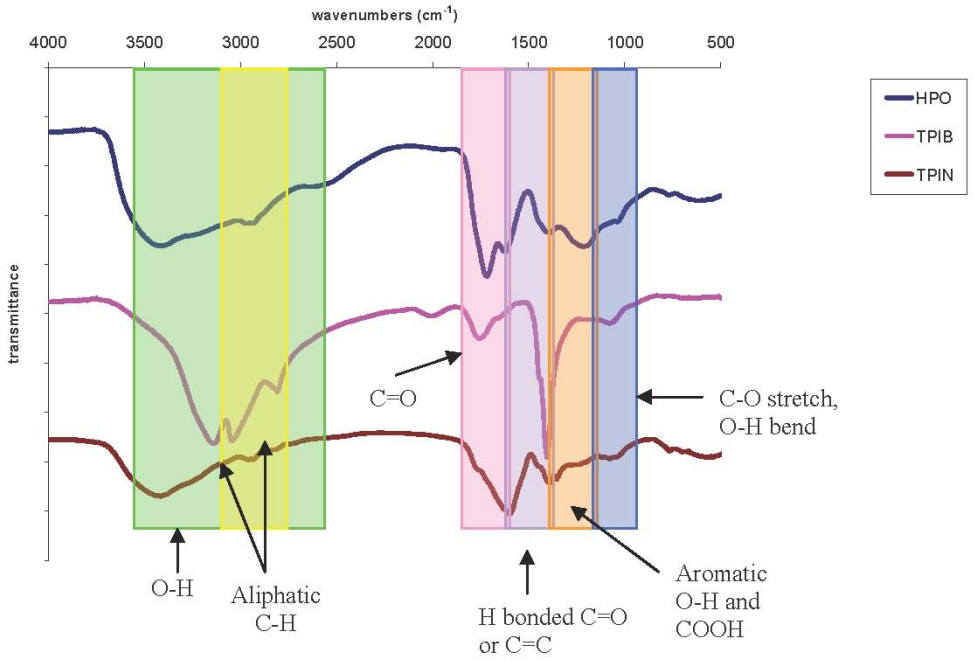

Figure 4.2 FT-IR spectra for three of the XAD fractions of NOM isolated from W300 groundwater.

4.3.2.3 Solid-State ^{13}C Nuclear Magnetic Resonance Spectroscopic Analysis

NMR spectroscopy has been proposed to be one of the most useful spectroscopic methods for investigation of NOM structure because qualitative and quantitative organic structural information for certain organic moieties can be generated in both solution and solid state under non-degradative conditions (Knicker and Nanny 1997). The solid-state ^{13}C NMR spectra for the HPO and TPIB solid fractions are shown in Figure 4.3. Due to the limitation in collected sample size, the TPIN fraction could not be analysed by solid-state ^{13}C NMR spectroscopy. The HPO and TPIB fractions were relatively noisy due to the limited sample sizes available for analysis and showed several broad peaks at very low intensity. The most significant peaks in the HPO fraction were a broad aliphatic carbon signal at 10 – 60 ppm (green region), and a more sharply resolved aromatic signal at 150 – 170 ppm (pink shading). Smaller signals at 60 – 100 ppm and 100 – 140 ppm (yellow region) were attributed to carbon singly bonded to oxygen and unsaturated carbon. The TPIB fraction contained less aliphatic (green region) and unsaturated carbon (yellow region) and more aromatic carbon (pink region) than the HPO fraction, consistent with previous solid-state ^{13}C NMR spectroscopic analyses of NOM isolated from a Wanneroo groundwater (Wong et al. 2002). In this previous study (Wong et al. 2002), the ^{13}C NMR spectrum of the HPO material was dominated by a strong and broad aliphatic carbon signal at 10 – 60 ppm, with less intense signals at 70 – 90 ppm and 120 – 140 ppm, attributable to carbon singly bonded to oxygen (or some other heteroatom) and unsaturated (olefinic and aromatic) carbon, respectively. The TPI fraction contained relatively less aliphatic and unsaturated carbon and more carbonyl carbon than the HPO fraction (Wong et al. 2002), as observed in the current study.

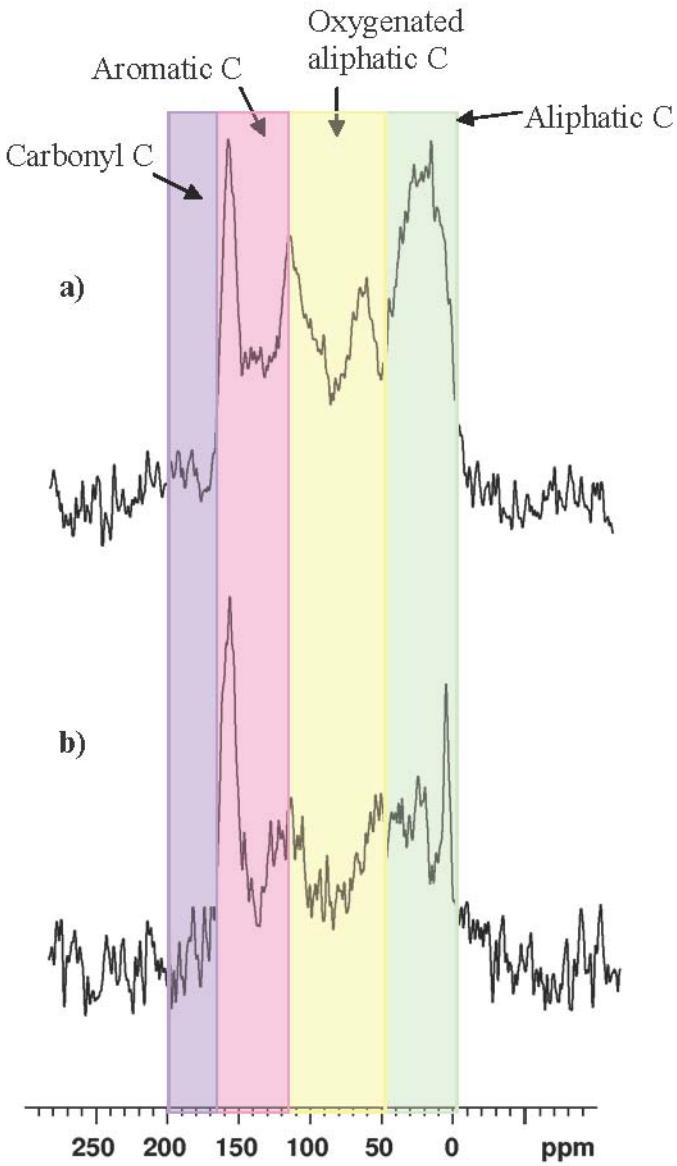

Figure 4.3 Solid-state ^{13}C NMR spectra for the a) HPO and b) TPIB fractions.

To better compare the two spectra in Figure 4.3, functional group types were assigned to the various chemical shift ranges based on previous work by Croué et al. (2000) and Hatcher et al. (2001), where solid-state ^{13}C NMR spectroscopy was used for the characterisation of aquatic NOM. The spectra were integrated over four broad regions 0 – 45, 45 – 110, 110 – 160 and 160 – 190 ppm. These spectral regions were then attributed to the following functionalities: 0 – 45 ppm to aliphatic carbons, 45 – 110 ppm to oxygenated aliphatic carbons, 110 – 160 ppm to aromatic carbons and 160 – 190 ppm to carbonyl carbons (Hatcher et al. 2001; Croué et al. 2000). The relative proportions of carbon types from integration of the two spectra are shown in Figure 4.4.

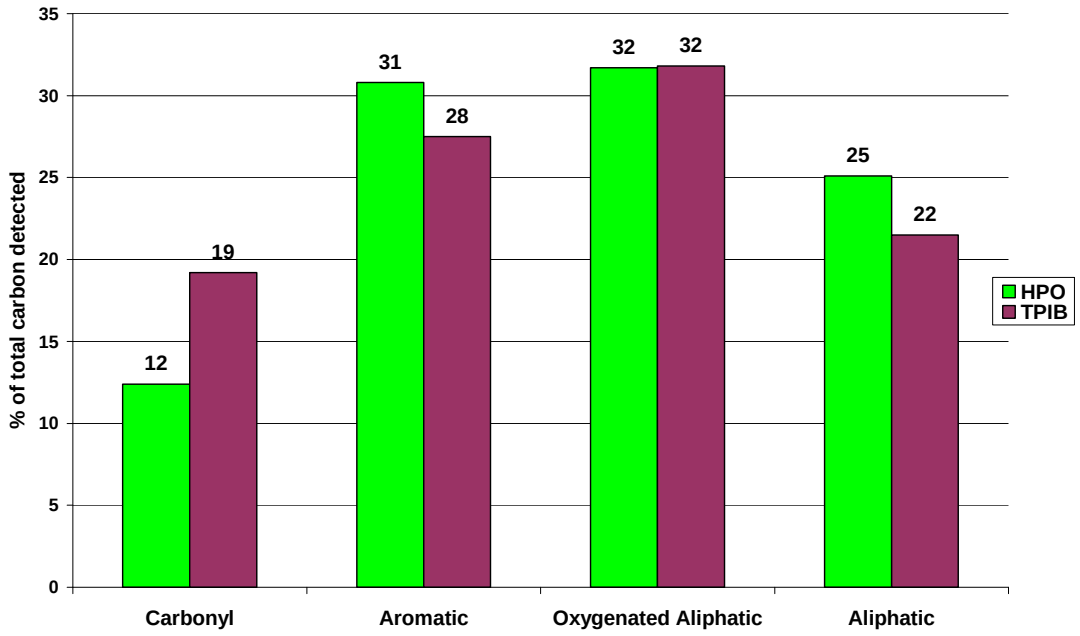

Figure 4.4 Relative proportions of carbon types in the solid-state ^{13}C NMR spectra of the isolated NOM fractions.

Overall, the distributions of types of carbon from solid-state ^{13}C NMR spectroscopy were similar for the two fractions, and similar to other NOM fractions isolated from Wanneroo groundwater (Allpike 2008), as well as the isolated UF fraction studied in Chapter 3 (Figure 3.2). The major carbon type for the HPO and TPI fractions was oxygenated aliphatic carbon (32 %), which was found in a similar proportion in the UF fraction (Figure 3.3, 35 %) and also in a highly coloured surface water from the Myponga reservoir (39 %) in a study by Newcombe et. al (1997). Oxygenated aliphatic carbons incorporate carbons in the alcohol, ester and ether functional groups (Wilson et al. 1981). For the HPO and TPI fractions, the aromatic carbon type was the second most abundant carbon type (31 and 28 %, respectively). Carbonyl carbon was the least abundant carbon type in both fractions: HPO (12 %) and TPIB (19 %), similar to the results observed in previous studies on NOM isolated from Wanneroo groundwater (Allpike 2008) and the UF fraction isolated in Chapter 3.

The solid-state ^{13}C NMR spectra of the HPO and TPI fractions exhibit the general features of aliphatic, oxygenated aliphatic, aromatic and carbonyl carbons. The HPO fraction had higher aliphatic and aromatic carbon content, coupled with less carbonyl carbon than the TPI fraction (Figure 4.4). These features are consistent with the elemental analysis and the low H/C ratio (Table 4.2) in this study, as a high level of unsaturation for the HPO fraction is implied from the low H/C ratio. In general,

greater aromaticity can be directly correlated with increased hydrophobicity, with the highest aromatic content reported to be found in the HPO fractions (Aiken et al. 1992).

Humic substances have been reported to arise largely from the decomposition of vegetable matter, and four main classes of compounds have been reported as potential precursors, namely, carbohydrates, lipids, amino acids and lignin (Wilson et al. 1981). Carbohydrates contain considerable amounts of oxygenated aliphatic carbon (Croué et al. 2001), and lignin is aromatic, so it is quite reasonable to suppose that the ^{13}C oxygenated and aryl resonances arise from these components or their microbial degradation products (Wilson et al. 1981). Carbonyl groups are components of amino acids and lipids which are also present in humic material. Hence, the carbonyl resonance could in part arise from these components. But, more likely, the major proportion of the carbonyl resonance may arise from carboxylic carbon (COOH) formed from microbiological oxidation of lignin and lipid material (Wilson et al. 1981). Further characterisation of the fractions using degradative techniques is discussed in Sections 4.3.2.4 – 4.3.2.6 to determine potential moieties present within the fractions.

4.3.2.4 Pyrolysis-Gas Chromatography-Mass Spectrometry

Most constituents of humic substances are too large or polar for GC analysis (Berwick et al. 2010, a; Hatcher et al. 2001). Strategies to overcome these challenges include chemical or thermal degradation to release macromolecular fragments that may be sufficiently volatile for GC-MS analysis. These may include structural fragments of the parent humic substance, although inevitably there will be some thermally altered secondary products. Conventional flash pyrolysis-GC-MS was performed at 650°C for 10 seconds on the solid samples of the HPO, TPIB and TPIN fractions of NOM isolated from W300 bore water. The total ion chromatograms from py-GC-MS of these fractions are shown in Figure 4.5a – c, respectively. The major pyrolysis products from these fractions together with their likely biological precursor are listed in Table 4.4. The full suite of tentatively identified products for each fraction is listed in Appendix 1.

Approximately 50 % of the pyrolysis products of NOM can usually be assigned to a specific biochemical precursor (Leenheer 2009). The HPO fraction showed a relatively high abundance of aromatic hydrocarbons (15, 20, 25), alkylphenols (31, 37) and PAHs (28, 33, 47, 54, 60). Aromatic hydrocarbons are reported to be common flash pyrolysis products of aquatic NOM and can derive from several biomolecular sources, hence they offer limited source diagnostic value (Templier et al. 2005). Alkylphenols are often attributed to intact or partially degraded lignin and tannin constituents of plant tissues (McIntyre and McRae 2005). Polycyclic aromatic hydrocarbons (such as alkyl naphthalenes and alkyl benzenes) derive from land plant terpenoids present in plant resins, bark and leaf tissues, which are recognised as a major source of aromatic humic substances (Schulten and Gleixner 1999). It is proposed that PAHs (such as alkyl benzenes) are primary structural units of humic substances, but can also derive in pyrolysis experiments from secondary thermal alteration of other NOM constituents (Schulten and Gleixner 1999; del Rio et al. 1998; Page et al. 2003).

In contrast to the HPO fraction, the distribution of the pyrolysis products from the TPIB and TPIN fractions contained higher proportions of nitrogen- and oxygen-containing products, consistent with previous pyrolysis studies of XAD resin fractions (Croué 2004; Krasner et al. 1996). The higher nitrogen content of the pyrolysis products from the TPI fraction compared to the HPO fraction was also reflected by the elemental analysis data (Table 4.2) and probably relates to a higher abundance of protein-derived material in this fraction (Croué et al. 1993, a). Templier et al. (2005) showed a higher proportion of nitrogenous pyrolysis products from a TPI fraction, rather than the HPO fraction, of NOM isolated from the Gartempe River in France, despite similar nitrogen content (1.9 %) in each of the XAD fractions. In a study of various NOM fractions isolated by XAD-type resins, Croué et. al (1999, b) found that the most hydrophilic fractions included up to 40 % of the identified pyrolysis product area as protein-derived material. Amino acid and peptide functional groups can form H bonds with surrounding water molecules which gives rise to significant hydrophilic character (Gadmar et al. 2005). Heterocyclic nitrogenous compounds have also been produced by pyrolysis of chitosan, a biomolecule containing *N*-acetyl sugars similar to those in bacterial cell walls (Gadmar et al. 2005). Acetamide (peak 28 in Table A.3, Appendix 1) identified

in the TPIN pyrolysate, likely originates from aminosugars (Gadmar et al. 2005). Aminosugars have previously been detected in peptidoglycans, naturally present in microbial and fungal cell walls, algae and aquatic animals (Bruchet et al. 1990).

The pyrolysis products analysed from the XAD fractions were generally consistent with pyrolysis products analysed in a previous study of unfractionated Wanneroo NOM (Heitz et al. 2001). In the previous study, groundwater NOM was found to typically contain high contributions of phenol and alkylphenols, aromatic hydrocarbons and thiophenes (Heitz et al. 2001). Sulfur-containing products (such as thiophenes) were only detected in the HPO fraction (peaks 16 and 21 in Table A.1, Appendix 1). The structural precursors of sulfur compounds are not well documented, probably due to the low concentrations in which they have been detected in studies of NOM using pyrolysis and other methods (Lu et al. 2001). The intrinsic polarity of sulfur (and oxygen) groups can limit the GC resolution of structurally intact sulfur and oxygen pyrolysis products from flash pyrolysis (Templier et al. 2005). These compounds can also undergo complex thermal reactions, such as decarboxylation, rearrangement and condensation, which can lead to loss of structural information and underestimation of their structural contribution to NOM (del Rio et al. 1998; Saiz-Jimenez 1994).

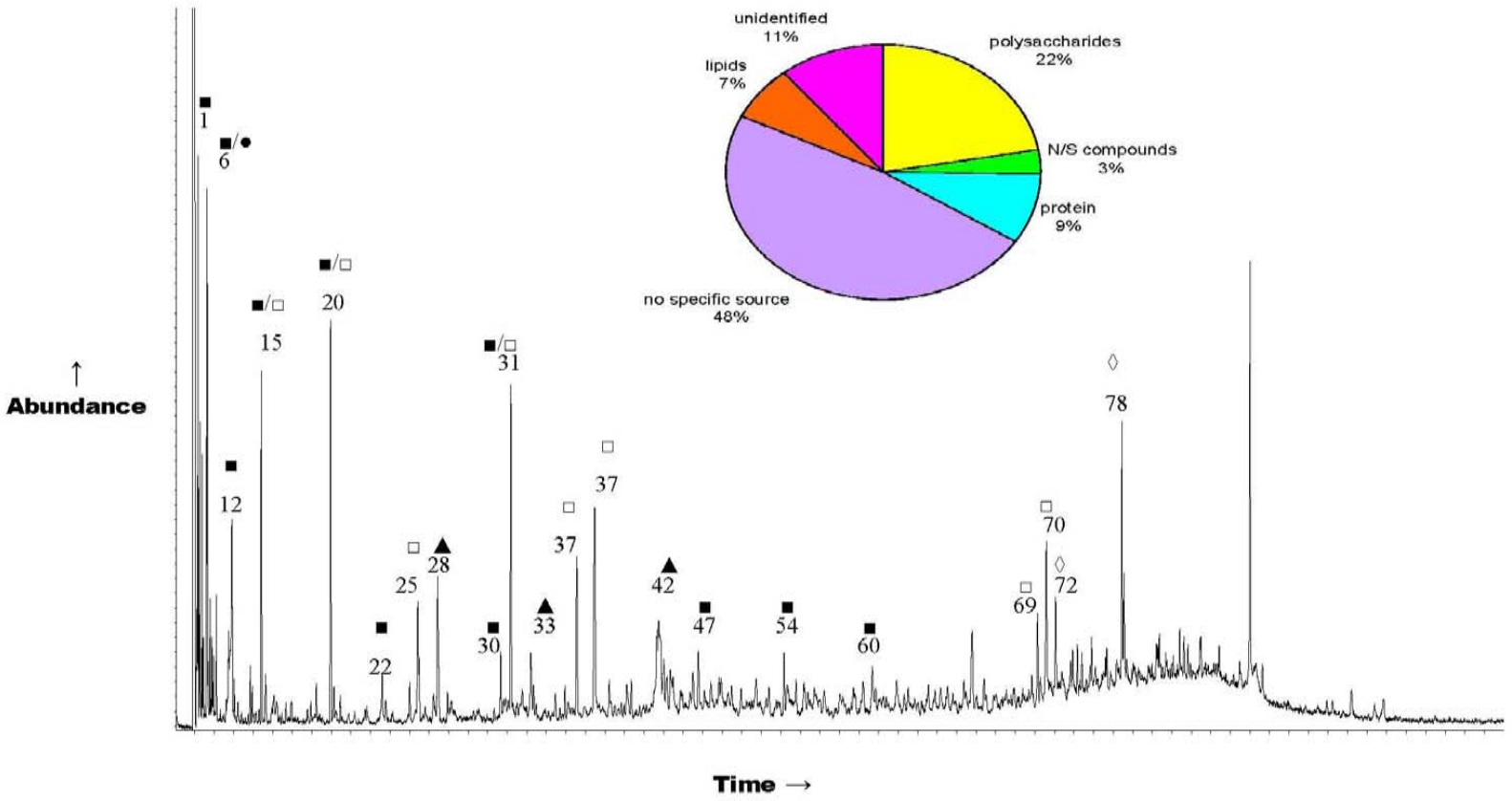

Figure 4.5a Total ion chromatogram from py-GC-MS of the HPO fraction. Peak assignments correspond to products listed in Table 4.4: ■ *polysaccharides,* ● *N/S compounds,* □ *protein,* ◊ *lipids,* ▲*no specific source. The pie chart reflects relative proportions of six major product and precursor types.*

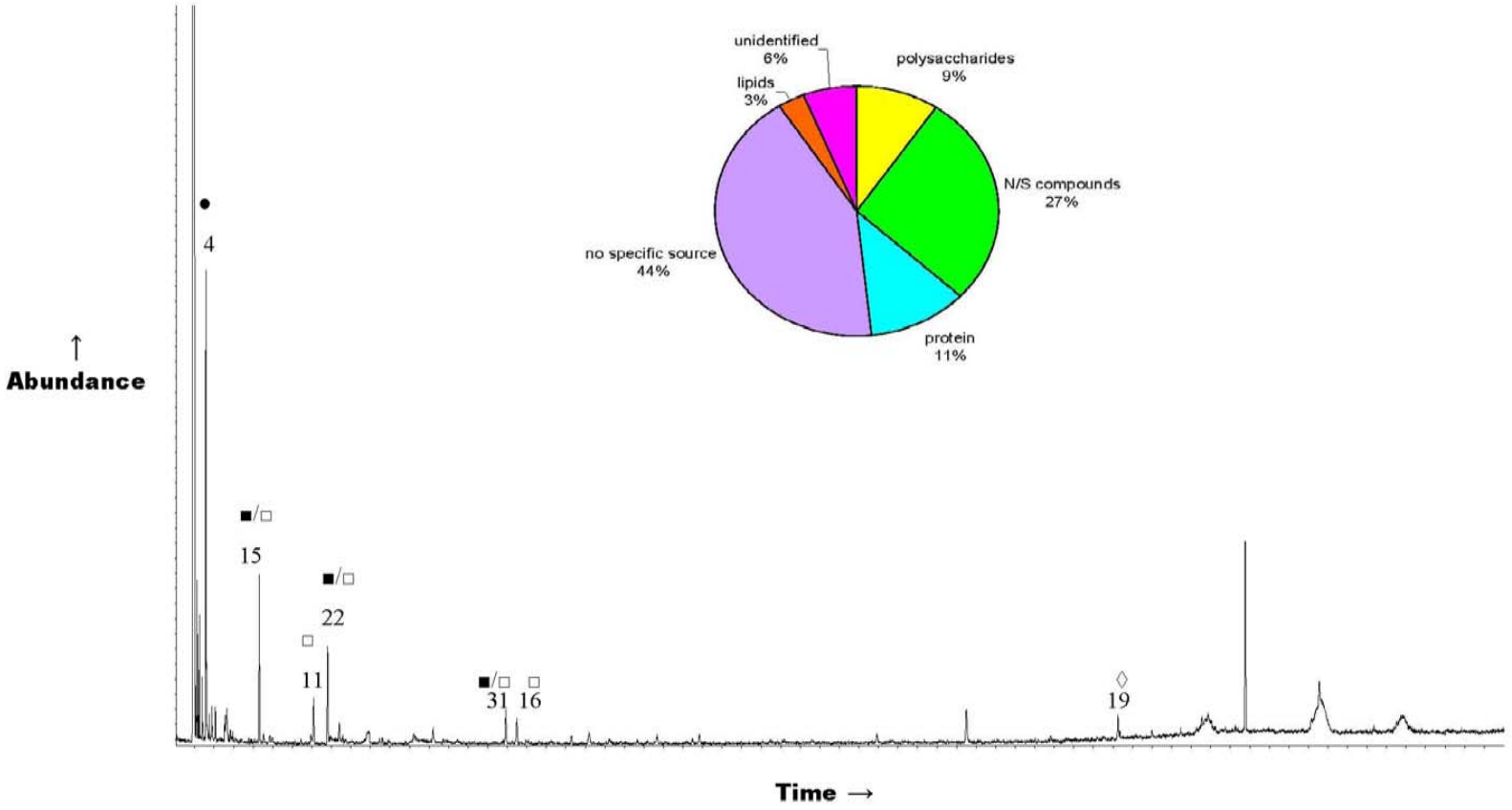

Figure 4.5b Total ion chromatogram from the py-GC-MS of the TPIB fraction. Peak assignments correspond to products listed in Table 4.4: ■ polysaccharides, ● N/S compounds, □ protein, ◊ lipids, ▲no specific source. The pie chart reflects relative proportions of six major product and precursor types.

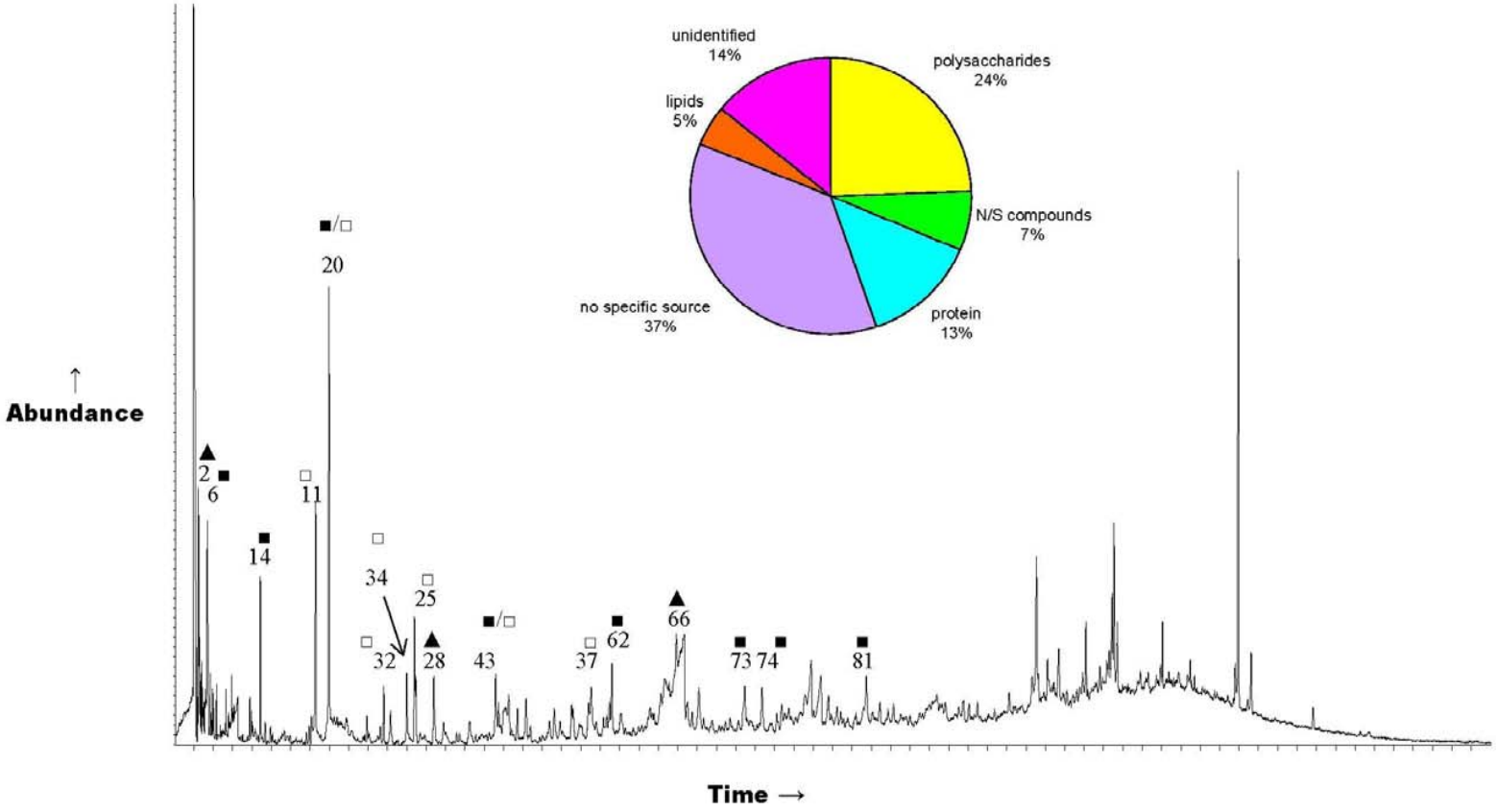

Figure 4.5c Total ion chromatogram from the py-GC-MS of the TPIN fraction. Peak assignments correspond to products listed in Table 4.4: ■ polysaccharides, ● N/S compounds, □ protein, ◊ lipids, ▲no specific source. The pie chart reflects relative proportions of six major product and precursor types.

Table 4.4 Major pyrolysis products from the XAD fractions and their likely origin. Full list of tentatively identified products can be found in Appendix 1.

Peak N°.	**Compound**	**Possible Origin**
1	acetaldehyde / methyl propene / 1,3-butadiene	polysaccharides / no specific source
2	methyl propene / 1,3-butadiene	polysaccharides / no specific source
4	acetonitrile	N/S compounds
6	acetone/acetonitrile	polysaccharides / N/S compounds
11	pyrrole	protein
12	2-butanone	polysaccharides
14	2-butenone	polysaccharides
15	benzene	polysaccharides / protein / lignin
16	benzonitrile	protein
19	decanoic acid	lipids
20	toluene	polysaccharides / protein / lignin
22	furan	polysaccharides
25	xylene	protein / lignin
28	styrene	no specific source
30	2-cyclopenten-1-one	polysaccharides
31	phenol	polysaccharides / protein / lignin
32	methylpyrrole	protein
33	C_3 benzene	no specific source
34	ethylbenzene	protein / lignin
37	cresol	lignin / tannin / protein
42	methylbenzyl alcohol	no specific source
43	ethyltoluene	polysaccharides / protein/ lignin
47	naphthalene	polysaccharides
54	methylnaphthalene	polysaccharides
60	dimethylnaphthalene	polysaccharides
62	furandione	polysaccharides
66	benzoic acid	no specific source
69	3,3,6,9,9,10-hexamethyl-2,10 diazabicyclo[4.4.0]-1-decene	protein
70	2,4-diphenyl-4-methyl-2(*Z*)-pentene	protein
72	tetradecanoic acid	lipids
73	ethylacetophenone	polysaccharides
74	*trans*-benzalacetone	polysaccharides
78	hexadecanoic acid	lipids
81	diacetylbenzene	polysaccharides

Guaiacol and other methoxyphenol products diagnostic of lignin were not detected in any of the pyrolysates of the XAD fractions, nor were they detected in the pyrolysate in the previous study of a Wanneroo groundwater (Heitz et al. 2001). The absence of

any syringyl, guaiacyl or *p*-hydroxyphenyl moieties within the pyrolysates suggest that there was minimal lignin input into the sample, or that the NOM sample had undergone sufficient environmental degradation such that any lignin character within the NOM sample has been lost. Lignin-derived pyrolysis products have been previously reported to be not usually present in high concentrations in pyrolysates from groundwater NOM (Sihombing et al. 1996; Gadel and Bruchet 1987). One disadvantage of the pyrolytic technique (and other chemical degradative techniques) is that the yields of products which can be analysed are often low, i.e., < 25% of the original sample is usually recovered as products which can be analysed (Gaffney et al. 1996). So, as only a fraction of the sample is represented in the pyrolysis products, conclusions regarding the original structure of the groundwater fractions must be drawn with caution (Kögel-Knabner 2000).

The tentatively identified pyrolysis products for the three different fractions were compared in a modified version of the classification system of Bruchet and colleagues (Bruchet et al. 1989; Bruchet et al. 1990). Each of the products were assigned to one of six groups, four of which related to distinct biological origin or chemical structure, with two other categories referring to those products known to be derived from multiple sources and those that could not be identified by GC-MS. The proportion of species within these categories was determined by summing the areas of all peaks within a category and calculating the ratio of this total category peak area to the total area of detected peaks as a percentage. This process was carried out in an identical manner for all three samples, providing a consistent method for comparison. The relative proportions of these groups expressed as a percentage of the total pyrolysis product peak area are shown as pie charts in Figure 4.5a – c. Hence, this semi-quantitative approach adds to the chemical assessment of different samples, and revealed distinct differences between the three XAD derived fractions of W300 NOM. The HPO fraction was rich in polysaccharides (furans, cyclopentenes) and lipids, with minimal input from protein or nitrogen- or sulfur-containing (N/S) compounds. The high abundance of polysaccharides present was reflected by the high oxygenated-aliphatic and aromatic carbon content seen in ^{13}C NMR spectroscopic analysis (Figure 4.4), and was consistent with the separation expected by use of the XAD-8/XAD-4 resin fractionation method and the elemental analysis (Table 4.2) in this study. The TPIB fraction was rich in tannins (e.g.

alkylphenols), protein (N/S compounds, eg. acetonitrile, propanenitrile, pyrroles) and polysaccharides (e.g. furans). The higher abundance of oxygenated and nitrogenous products was consistent with the high oxygenated-aliphatic content shown by the ^{13}C NMR data (Figure 4.4) and the higher organic nitrogen content and N/C ratio (Table 4.2) found in the elemental analysis.

4.3.2.5 On-line Thermochemolysis-Gas Chromatography-Mass Spectrometry

Conventional pyrolysis gives little information about carboxylic acid structures in NOM, since decarboxylation occurs readily during pyrolysis (del Rio et al. 1998). Thermochemolysis-GC-MS with tetramethylammonium hydroxide (TMAH) or other methylating reagents combines thermal degradation and chemical derivatisation, ideally in a single process termed "thermochemolysis". Thermochemolysis may be performed either as an on-line or an off-line technique, with on-line thermochemolysis the most frequently employed thermochemolysis method (Filley et al. 2006). Degradation occurs mainly through a base catalysed hydrolysis reaction at elevated temperature. Thermochemolysis offers the advantage over conventional pyrolysis of preservation of carboxylic acid and ester structures, since acidic protons, such as those found on carboxylic acids and some phenols, are methylated simultaneously, and esters are transesterified into the corresponding methyl esters (Hatcher et al. 2001). In earlier work conducted in our laboratory (Couton 2010), on-line TMAH thermochemolysis of NOM samples was conducted at various temperatures (300, 400, 500 and 650 °C), and use of 650 °C was found to produce a vastly different product distribution compared to the other temperatures, indicating that, at 650 °C, in addition to thermochemolysis, pyrolysis may have also been occurring, resulting in the additional production of alkyl benzenes and phenols from the groundwater NOM sample. To obtain the most structural information possible, the temperature of 650 °C was therefore adopted in the current study. On-line thermochemolysis with TMAH was conducted at 650 °C for 10 seconds on the HPO, TPIB and TPIN solid fractions. The total ion chromatograms from thermochemolysis-GC-MS analysis of these fractions are shown in Figure 4.6a – c, respectively. Major products and their likely origin are listed in Table 4.5. The full suite of tentatively identified products for each fraction is listed in Appendix 1.

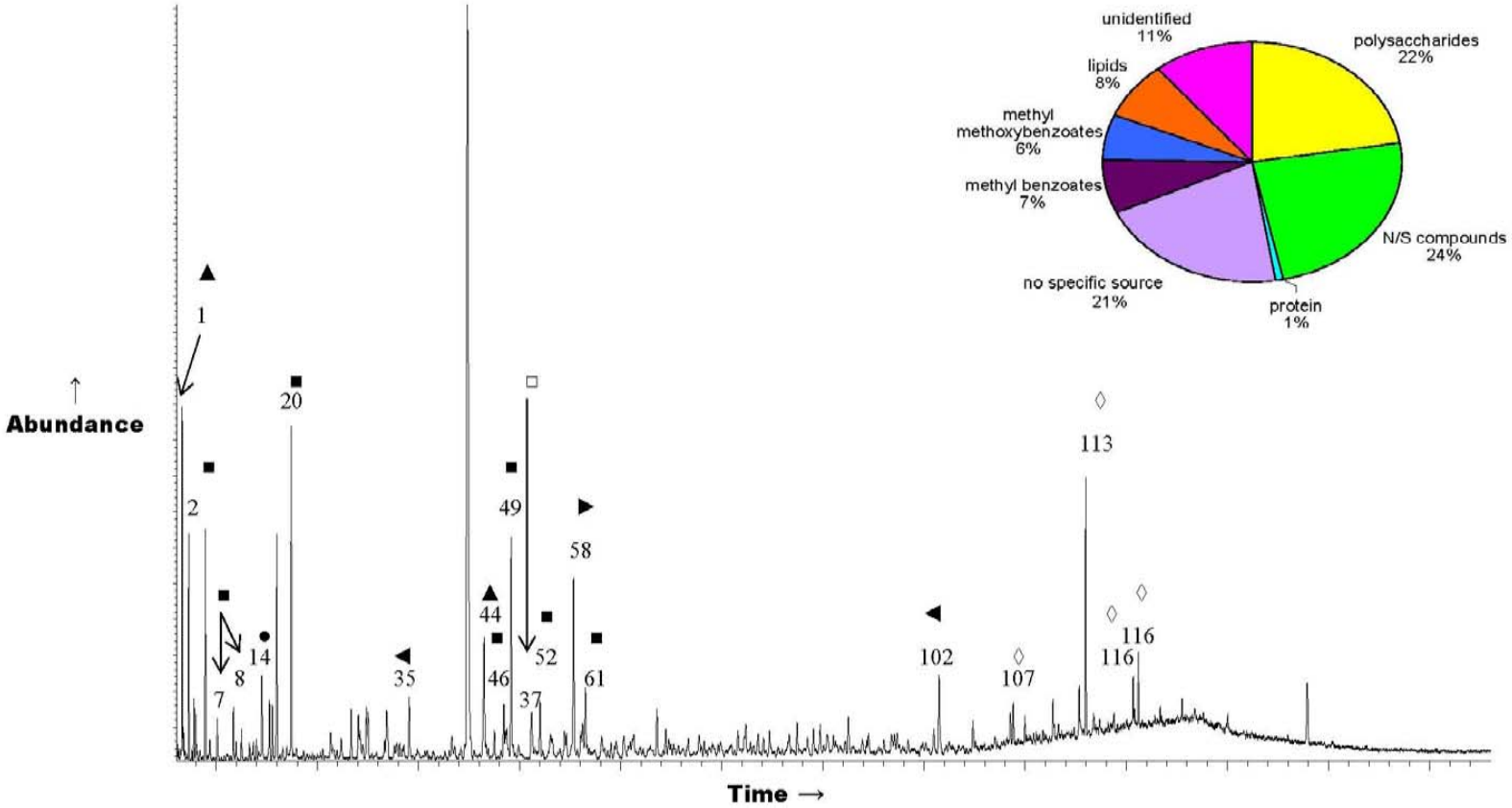

Figure 4.6a Total ion chromatogram from thermochemolysis-GC-MS of the HPO fraction. Peak assignments correspond to products listed in Table 4.5: ■ polysaccharides, ● N/S compounds, □ protein, ◊ lipids, ◄ methyl methoxybenzoates, ►methyl benzoates, ▲no specific source. The pie chart reflects relative proportions of eight major product and precursor groups.

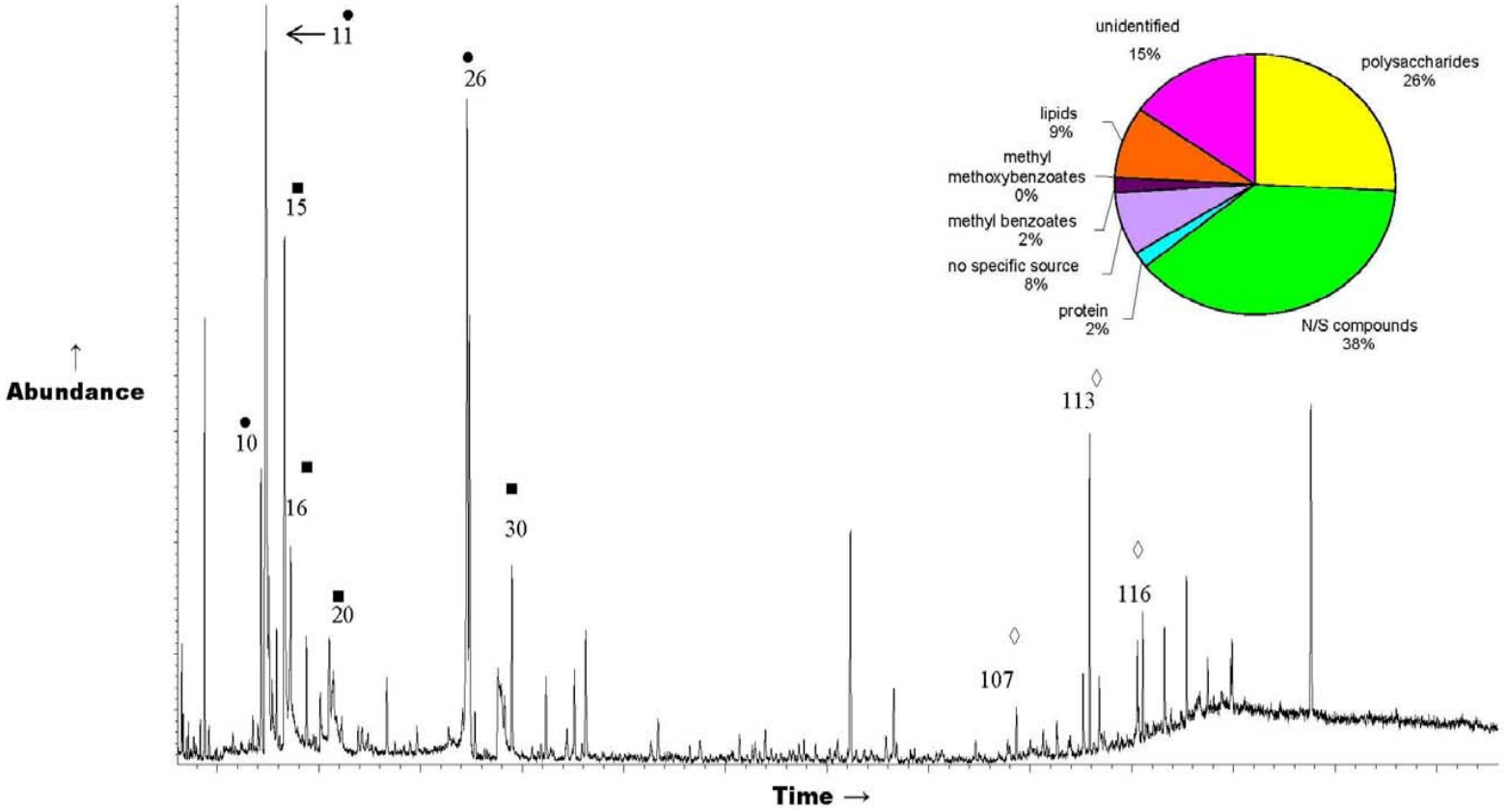

Figure 4.6b Total ion chromatogram from thermochemolysis-GC-MS of the TPIB fraction. Peak assignments correspond to products listed in Table 4.5: ■ polysaccharides, ● N/S compounds, □ protein, ◊ lipids, ◄ methyl methoxybenzoates, ►methyl benzoates, ▲no specific source. The pie chart reflects relative proportions of eight major product and precursor groups.

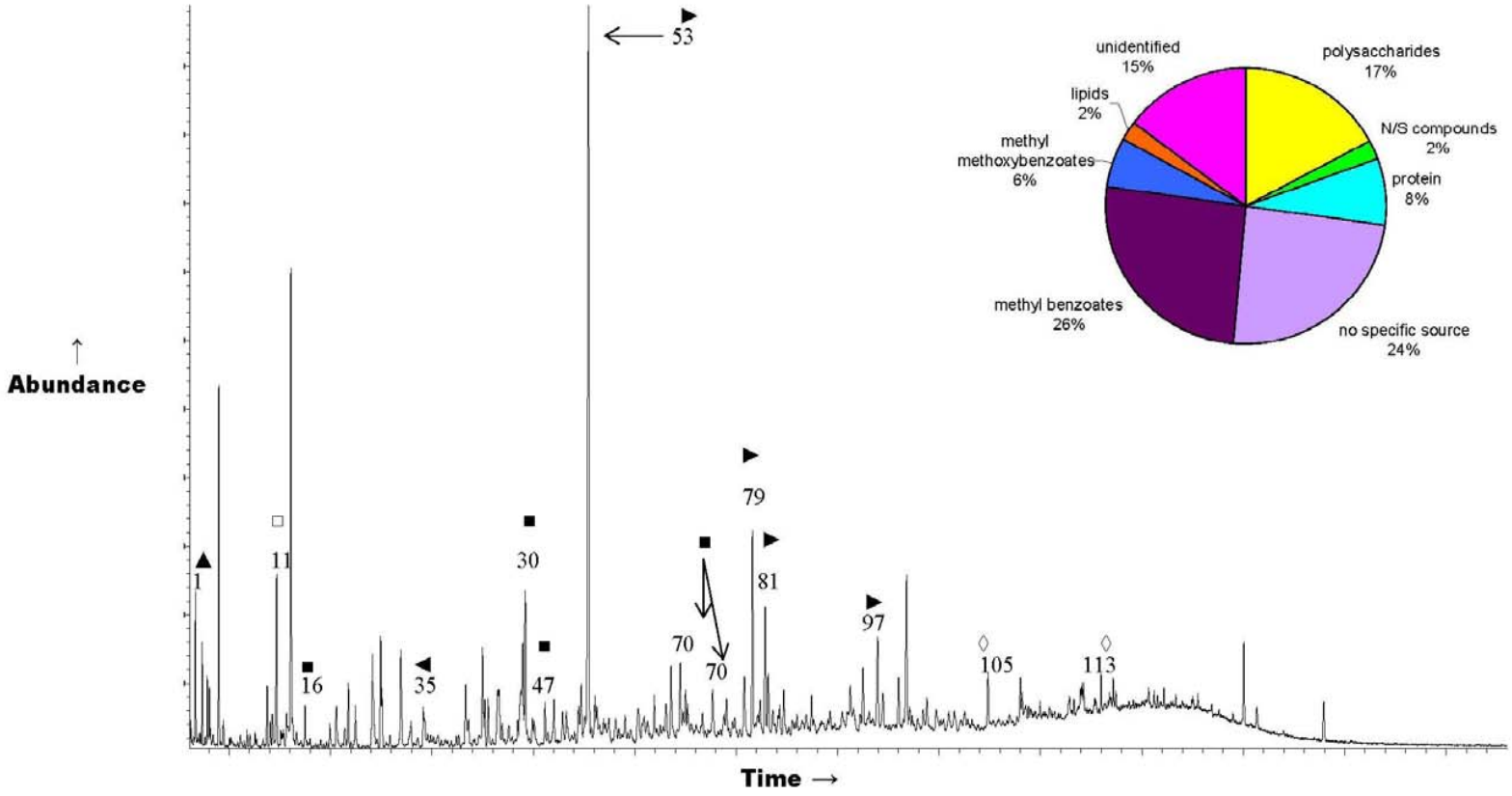

Figure 4.6c Total ion chromatogram from thermochemolysis-GC-MS of the TPIN fraction. Peak assignments correspond to products listed in Table 4.5: ■ polysaccharides, ● N/S compounds, □ protein, ◊ lipids, ◄ methyl methoxybenzoates, ►methyl benzoates, ▲no specific source. The pie chart reflects relative proportions of eight major product and precursor groups.

Table 4.5 Major products from the XAD and their possible origin. Full list of tentatively identified products can be found in Appendix 1.

Peak Nº.	Compound	Possible Origin
1	methyl acrylate	no specific source
2	methyl propanoate	no specific source
7	methyl isobutyrate	polysaccharides
8	methyl methacrylate	polysaccharides
10	dimethylaminoacetonitrile	N/S compounds
11	dimethylcyanamide	N/S compounds
14	dimethylaminoacetonitrile	N/S compounds
15	butyl ethylene	polysaccharides
16	2-methoxypropionic acid methyl ester	polysaccharides
20	2-methoxypropionic acid methyl ester	polysaccharides
26	hexahydro-1,3,5-trimethyl-1,3,5-triazine	N/S compounds
30	dimethyl succinate	polysaccharides
35	anisole	lignin
37	cresol	lignin / tannin / protein
44	trimethylbenzene	no specific source
46	methyl fumarate	polysaccharides
47	dimethyl methyl succinate	polysaccharides
49	dimethyl succinate	polysaccharides
52	methyl 4,4-dimethoxy-2-methyl butanoate	polysaccharides
53	benzonitrile	protein
58	methyl benzoate	methyl benzoates
61	glycine methyl ester/ methyl benzofuran	polysaccharides
70	methyl toluate	polysaccharides / protein / lignin
79	methyl dimethyl benzoate	methyl benzoates
81	ethyl benzoic acid methyl ester	methyl benzoates
97	methyl acetylbenzoate	methyl benzoates
102	methyl dimethoxybenzoate	methyl benzoates
105	decanedioic acid methyl ester	lipids
107	tetradecanoic acid methyl ester	lipids
113	hexadecanoic acid methyl ester	lipids
116	octadecanoic acid methyl ester	lipids
1	methyl acrylate	no specific source
2	methyl propanoate	no specific source
7	methyl isobutyrate	polysaccharides
8	methyl methacrylate	polysaccharides
10	dimethylaminoacetonitrile	N/S compounds

The product suites from on-line thermochemolysis complement the conventional flash pyrolysis analysis (Figure 4.4a – c), with the detection of additional acids (as methyl esters) such as methyl propanoate, methyl isobutyrate and 2-

methoxypropionic acid methyl ester, which were not detected by flash pyrolysis. There were also a number of peaks (11 – 15 % of the total peak area) that could not be identified in each of the three chromatograms. While a number of these peaks had mass spectra that gave an indication of the likely structure, firm identifications could not be made.

The methyl esters of low MW saturated and unsaturated acids (e.g. methyl acrylate, methyl propanoate) were detected in relatively high abundance. Low MW acids and polymethoxybenzenes are common thermochemolysis products of NOM (Frazier et al. 2003; Templier et al. 2005) and are usually attributed to cross linking units between phenolic structures of humic macromolecules (Martin et al. 1995). Several fatty acid methyl esters (FAMEs), generally formed by transesterification of triglycerides and other lipids (Challinor 1991), were also detected in moderate proportions. The FAMEs ranged from C_8 to octadecanoic acid (C_{18}) and several mono-unsaturated and branched chain isomers were also detected. FAMEs are likely to have been chemically bound to the humic macromolecule through ester linkages (del Rio et al. 1998) and are generally attributed to microbial sources (Frazier et al. 2005). The C_{16} and C_{18} FAMEs were the most dominant lipids for each of the HPO, TPIB and TPIN fractions, consistent with similar studies of other groundwater NOM samples (Desmukh et al. 2001).

The major products from the HPO fraction included methylbenzene carboxylic acid products and non acidic phenolic products. These are likely to be products of direct pyrolysis (Hatcher et al. 2001). However additional methoxy analogues (detected as methyl esters) can be attributed to TMAH thermochemolysis. Methyl esters of butanedioic and hexanedioic acids indicated the release of aliphatic compounds. Methyl esters of diacids such as methyl butanedioic acid were also detected in high relative abundance. These are typical thermochemolysis products of humic and fulvic acids (del Rio et al. 1998; Templier et al. 2005) and are thought to link phenolic units in cross-linked macromolecules (Templier et al. 2005). These acids are common metabolites of plant, microbial and macro-faunal sources (Martin et al. 1995).

A small number of oxygenated cyclic compounds, largely comprised of 2-cyclopenten-1-one and its methyl derivatives, were detected in the HPO and TPI

fractions. TMAH does promote detection of nitrogen- and oxygen-containing structures which are known to concentrate in the TPI fraction (Templier et al. 2005).

The high amount of total TMAH thermochemolysis products detected compared to flash pyrolysis products highlights the low suitability of flash pyrolysis to the large polar moiety of humic substances such as that found in NOM (Hatcher et al. 2001). A modified classification system used for the tentative flash pyrolysis products was applied to the TMAH thermochemolysis product distribution and the relative percentages of eight discrete product and precursor groups are shown as pie charts in Figure 4.6a – c. The eight product groups were comprised of: polysaccharides, N/S compounds, proteins, lipids, methyl benzoates, methoxy benzoates, other products which are known to be derived from multiple sources and those products that could not be identified.

Several qualitative differences were evident between the relative proportions of product/precursor categories for the HPO, TPIB and TPIN fractions. The HPO fraction was rich in the categories of polysaccharides (eg. methyl methacrylate), lignins/tannins (cresol), methyl methoxybenzoates (methyl dimethoxybenzoate), methyl benzoates (methyl benzoate) and lipids (hexadecanoic acid methyl ester). The TPIB fraction was much richer in N/S products, with still significant contributions of polysaccharide and lipid precursors. The higher nitrogen content was reflected by an abundance of N products (such as methyl acetamide), as well as proteinaceous material (such as pyridine, methyl pyrrole), in Figure 4.6b. The TPIN fraction was also rich in the category of protein, as well as the categories of polysaccharides, lignin/tannin material, methyl benzoates and methyl methoxybenzenes. As NOM becomes enriched in nitrogenous compounds (indicated by e.g. acetonitrile, pyridine, and pyrrole in the thermochemolysate) it becomes more hydrophilic, consistent with the higher relative contribution of N compounds in the thermochemolysates from the TPIB and TPIN fractions and the results of elemental analysis (Table 4.2).

4.3.2.6 Micro-Scale Sealed Vessel Pyrolysis-Gas Chromatography-Mass Spectrometry

Micro-scale sealed vessel (MSSV) pyrolysis can complement the analytical characterisation afforded by more traditional pyrolysis techniques (e.g. flash

pyrolysis). Performed in a closed system using moderate temperatures (typically 250 – 350 ºC) over long time periods (e.g. days), MSSV pyrolysis can provide additional speciation information useful for establishing the structures and source inputs to recent organic material (Berwick et al. 2010, b). MSSV removes oxygenated functional groups that give rise to chemical complexity, leaving the core hydrocarbon structures that may have less mixture complexity (Leenheer 2009). MSSV pyrolysis was conducted at 300°C for 72 hours on the HPO, TPIB and TPIN solid fractions. Total ion chromatograms from MSSV pyrolysis followed by GC-MS analysis of the HPO, TPIB and TPIN fractions are shown in Figure 4.7. Major products assigned on the basis of mass spectral interpretation are listed in Table 4.6 and all products are listed in Appendix 1.

The major products of each fraction were alkyl substituted benzenes, phenols and naphthalenes. As found in the pyrolysis-GC-MS and thermochemolysis-GC-MS chromatograms, the HPO and TPIN fractions formed products in greater abundances and number than the TPIB fraction, with the high salt content present in the TPIB fraction (Table 4.2) reducing the NOM content in the sample and therefore the product abundance, as well as possibly inhibiting product formation in the MSSV pyrolysis-GC-MS technique. The chromatogram from analysis of the HPO fraction was dominated by alkylphenols (peaks 95, 110, 122), as well as low MW short chain aliphatic compounds (peaks 2, 9). These products can be derived from a range of organic precursors, hence they provide only limited information about source and origin (Greenwood et al. 2006). Monomethyl phenols were also prominent flash pyrolysis products (Figure 4.5a); however the higher MW alkyl ($\geq C_2$) phenols were detected in much lower abundance in flash pyrolysis compared to MSSV pyrolysis-GC-MS. Alkylphenols are very common pyrolysis products of aquatic and terrestrial humic substances and are often attributed to intact or partially degraded lignin structures (Saiz-Jimenez and De Leeuw 1986; Bruchet et al. 1990; Templier et al. 2005). The broad distribution of alkylphenols from the HPO fraction likely reflects contribution from other sources apart from lignin, as guaiacol and other methoxyphenol products diagnostic of lignin were not detected, as discussed in Section 4.3.2.4, suggesting that there was minimal lignin input into the sample.

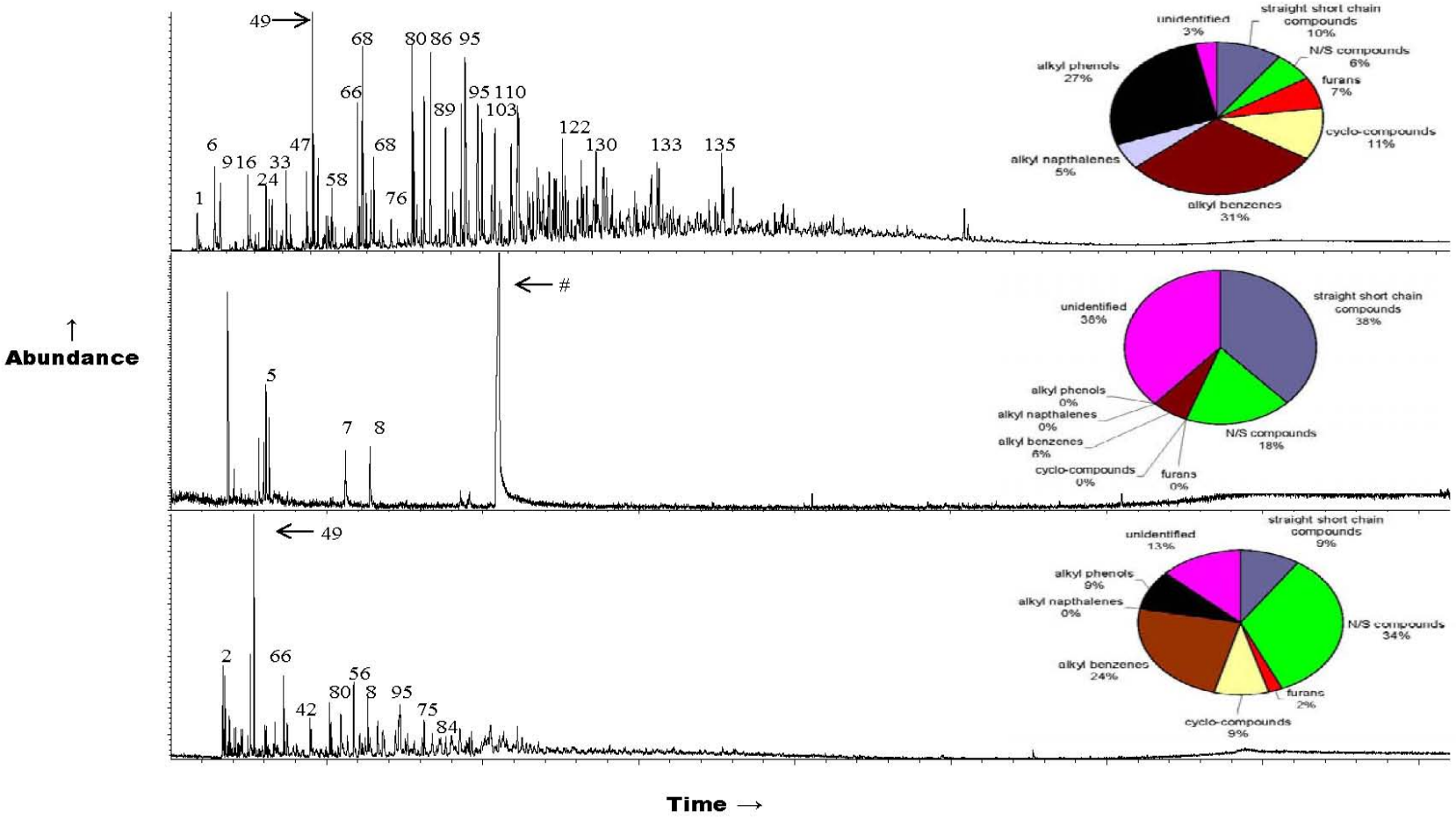

Figure 4.7 Total ion chromatograms obtained by MSSV pyrolysis-GC-MS analysis of the a) HPO, b) TPIB and c) TPIN fractions. Peak assignments correspond to products listed in Table 4.6 and Appendix 1. The pie charts reflect relative proportions of eight major product and precursor groups.

Table 4.6 Major products from MSSV pyrolysis-GC-MS of the XAD fractions.

Peak N°.	Compound	Possible Origin
1	butene	short chain compounds
2	butene / methyl propene / methanethiol	short chain compounds
5	methyl heptene	short chain compounds
6	propanal	short chain compounds
7	benzonitrile	N/S compounds
8	ethyl hexanol	short chain compounds
9	pentene	short chain compounds
16	butanone	short chain compounds
24	methyl cyclopentene	cyclic compounds
33	heptane	short chain compounds
42	dimethylpyrrole	N/S compounds
47	trimethyl cyclopentene isomer	cyclic compounds
49	toluene	alkyl benzenes
56	ethylmethylpyrrole	N/S compounds
58	trimethyl cyclopentene isomer	cyclic compounds
66	ethylbenzene	alkyl benzenes
68	xylene	alkyl benzenes
75	dimethylbenzamine	N/S compounds
76	isopropylbenzene	alkyl benzenes
80	ethyl toluene	alkyl benzenes
84	dimethylbenzofuran	furans
86	trimethylthiophene	N/S compounds
89	C3 benzene	alkyl benzenes
95	cresol	phenols
103	methylbenzofuran	furans
110	dimethylphenol	phenols
122	ethylmethylphenol	phenols
130	methylnaphthalene	naphthalenes
133	dimethylnaphthalene	naphthalenes
135	trimethylnaphthalene	naphthalenes
#	azepan-2-one	contaminant

* Full list of products are included in Appendix 1

Lehtonen et al. (2000, a) attributed alkylphenols in the product mixture from thermochemolysis-GC-MS of lake humic substances to carbon-carbon bound alkyl aromatic networks, as opposed to phenolic-carboxylic acid structures characteristic of degraded tannins. The origins of these alkylphenols were attributed to algal-derived compounds, including tyrosine moieties of proteins and selectively preserved phenolic biomolecules (phlorotannins) (Lehtonen et al. 2000, a). Alkylphenols have been postulated to be more strictly bound macromolecular components than esterified or acidic lignin phenols not containing alkyl groups (Lehtonen et al. 2000,

b). The softer thermal release of covalently bound alkylphenols by MSSV pyrolysis-GC-MS may partially preserve their alkyl substitution patterns (Lehtonen et al. 2000, b) and contribute to the higher concentration of more highly substituted alkyl (C_2 – C_4) phenols than were evident in flash pyrolysis.

High abundances of polycyclic aromatic hydrocarbons, including alkyl naphthalenes (peaks 130, 133, 135) and alkyl benzenes (peaks 66, 68, 76, 80, 89) and indanes (Appendix 1), were detected from MSSV pyrolysis of the HPO fraction. Flash pyrolysis, in contrast, yielded very low concentrations of these products. Previous MSSV pyrolysis research (Berwick 2009) strongly correlated alkyl naphthalenes with higher plant terpenoids. Many cyclic higher plant terpenoids undergo aromatisation during natural or artificial maturation (Lu et al. 2003). A high aliphatic ^{13}C NMR signal was observed for the HPO fraction (Figure 4.4) and aromatisation of alicyclic terpenoids during MSSV thermal treatment may contribute to the high concentrations of aromatic hydrocarbon products. Alkyl benzenes likely include both primary alkyl-linked aromatic structures (Schulten and Gleixner 1999), as well as secondary products from the thermal alteration of other NOM moieties. Thermochemolysis of the HPO fraction also produced several aromatic carboxylic acids (as their methyl esters; Section 4.3.2.5).

MSSV pyrolysis-GC-MS also yielded several cyclic oxygen-containing products, including alkyl furans (peak 84) and other cyclic compounds (peaks 24, 47, 58), from the HPO fraction. These products were detected in lower relative abundance than the alkylphenolic and aromatic hydrocarbon products. Major sources of furans and cyclic compounds (such as cyclopentene and indane) include carbohydrates, such as simple sugars (e.g. glucose, fructose), polysaccharides and their microbial metabolites (Almedros et al. 2000).

The anoxic and sulfidic condition of the groundwater source was reflected by the relatively high concentration of a thiophene derivative (peak 86). The TPIN fraction showed large distributions of alkylated pyrroles, pyridines and pyrazines (Appendix 1, Table A.9), which is consistent with nitrogen being reported to typically concentrate in the more polar HPI or TPI fractions of NOM (Croué et al. 2003), and was evident in the py-GC-MS (Figure 4.4 b – c) and on-line thermochemolysis data

(Figure 4.5 b – c). The high concentrations of heterocyclic N-products probably represent primary or secondary pyrolysates of diagenetically degraded proteinaceous material (Berwick et al. 2010, a), which is supported by previous chemical degradation and pyrolysis-MS data from soil, aquatic and recent sedimentary environments (Schulten and Gleixner 1999; Mao et al. 2007). Analysis of the TPIB fraction included the identification of azepan-2-one (#) which was attributed to contamination from the gloves used to handle the samples.

A semi-quantitative modified classification as discussed in Section 4.3.2.4 (Bruchet et al. 1989; 1990) of common MSSV pyrolysis product groups is shown as pie charts in Figure 4.7. Many of the abundant alkyl aromatic hydrocarbons of the HPO fraction can be derived from a range of organic precursors and therefore provide limited information about their source of origin. Alkyl benzenes and alkyl naphthalenes are generally attributed to algal or plant input (Greenwood et al. 2006). The alkylphenols are usually attributed to tannin or lignin precursors (Templier et al. 2005). There was a lower proportion of N-containing compounds in the HPO fraction compared to the TPIN fraction (Figure 4.7), which is consistent with previous studies on the HPO and TPI fractions of a French river source (Gadmar et al. 2005; Templier et al. 2005) and selected RO-isolates which were then fractionated by an XAD-8 resin fractionation method using water from various Nordic surface water locations (Gadmar et al. 2005). Compared to flash pyrolysis-GC-MS (Table 4.4), MSSV pyrolysis-GC-MS (Table 4.6) provides more information about the N-containing organic compounds and the heteroatom compounds in general (Berwick et al. 2010, a).

4.3.2.7 Overall Characteristics of the HPO, TPIB and TPIN Fractions

Isolation of NOM from W300 groundwater by XAD-8/XAD-4 fractionation produced three solid freeze-dried samples, termed HPO, TPIB and TPIN. Reduction of salt concentrations within these fractions was challenging, and a high salt content hindered characterisation of the TPIB fraction. Characterisation of the fractions by FTIR and solid-state ^{13}C NMR spectroscopic analysis indicated that the samples had a significant aliphatic content, from lipid and biopolymer precursors. Further characterisation by py-GC-MS, thermochemolysis-GC-MS and MSSV pyrolysis-

GC-MS revealed that the HPO fraction had a significant precursor contribution from alkylphenols and polyaromatic hydrocarbons. The higher nitrogen and oxygen content of the TPIB and TPIN fractions than the HPO fraction found in the elemental analysis was consistent with more nitrogen- and oxygen- containing groups (such as proteins and tannins) being observed in the TPIB and TPIN product mixtures.

4.3.3 MIEX® Treatment of the HPO, TPIB and TPIN Fractions

Virgin MIEX® resin was obtained from the Wanneroo GWTP at the time of raw water sampling, and the virgin resin was preconditioned with raw water (W300) to preload the resin with W300 NOM in a laboratory simulation of the plant treatment process, as discussed in detail in Section 3.2.4.1. The isolated solid HPO, TPIB and TPIN samples were separately redissolved in MilliQ water and treated by preconditioned MIEX® resin to investigate the removal achieved by the MIEX® process of the different organic polarity-based fractions. Solutions of HPO, TPIB and TPIN fractions (DOC concentrations ranging from 5 – 9 mg L^{-1}) were treated with 2 mL of MIEX® resin for 15 minutes in a simulation of the full-scale plant at Wanneroo. The characteristics of the fractions before and after MIEX® treatment were then compared.

4.3.3.1 DOC Concentration, UV_{254} and Colour

The DOC concentration, UV_{254}, $SUVA_{254}$ and colour of the HPO, TPIB and TPIN fractions both before and after MIEX® treatment are shown in Table 4.7. This work focused on the HPO and TPI fractions, since the high concentration of inorganic salts compared to DOC concentration in the HPI fraction was likely to interfere in DOC removal by the MIEX® process. Reverse osmosis and dialysis were performed to reduce the amount of inorganic salts in this fraction but the conductivity (9600 μS cm^{-1}) of the resulting sample indicated that the remaining salt concentration was still very high compared to the DOC concentration of 13.6 mg L^{-1}. The separation of inorganic salts from HPI NOM fractions is known to be particularly challenging, and the ratio of DOC to salt concentration is frequently the determining factor in the recovery of this fraction (Croué et al. 1999, a).

Table 4.7 DOC concentration, UV_{254}, $SUVA_{254}$ and colour parameters for the HPO, TPIB and TPIN fractions before and after MIEX® treatment.

Sample	DOC (mg L^{-1})	UV (cm^{-1})	$SUVA_{254}$ (m^{-1} L / mg C)	Colour (HU)
HPO	7.01	0.32	4.6	46
HPO after MIEX®	2.23	0.08	3.6	12
TPIB	5.96	0.22	3.7	4
TPIB after MIEX®	1.83	0.03	1.6	3
TPIN	8.81	0.14	1.5	9
TPIN after MIEX®	3.94	0.06	1.5	4

MIEX® treatment significantly reduced the DOC concentration in each of the fractions on a laboratory scale: HPO (68 % reduction), TPIB (69 %) and TPIN (55 %). A previous study (Lee et al. 2003) focussed on MIEX® treatment of surface waters in the USA with varying TOC and alkalinity concentrations, where significant reductions in both the TOC and UV absorbance for the HPO, TPI and HPI fractions were observed after MIEX® pre-treatment, with three of the four waters showing similar percentage removals of the HPO and TPI fractions (Lee et al. 2003). This is consistent with the current study, where the HPO and TPI fractions were removed to a similar extent. The UV_{254} absorbance data showed similar trends to DOC removal, with reductions between 57-87 % for the three main fractions. Similar reductions in both DOC (60 %) and UV_{254} (78 %) were observed for MIEX® treated waters from the Maytum WTP in the USA (Budd et al. 2005), as well as four raw drinking waters in California, with reductions in DOC (36 – 72 %) and UV_{254} (54 – 83 %) after MIEX® treatment (Boyer and Singer 2005).

$SUVA_{254}$, the ratio of UV absorption at 254 nm relative to the DOC concentration, decreased for the HPO (21 %) and TPIB (56 %) fractions after MIEX® treatment, with no change in $SUVA_{254}$ observed for the TPIN fraction. Treatment processes such as ion exchange (i.e. MIEX®) are reported to be more effective at removing UV_{254}-absorbing materials in raw waters with a high $SUVA_{254}$ (> 3 m^{-1} L/ mg C, as

seen in the HPO and TPIB fractions), and is less effective in waters with a lower $SUVA_{254}$ (< 3 m^{-1} L/ mg C such as the TPIN fraction) (Boyer and Singer 2005).

The range of reduction of DOC concentration, UV_{254} absorbance and $SUVA_{254}$ for the NOM fractions after MIEX® treatment was observed to be 21 – 75 % for the HPO fraction, 56 – 87 % for the TPIB fraction and 0 – 57 % for the TPIN fraction. The higher reductions in these parameters achieved for the TPIB fraction are thought to be due to the higher affinity for MIEX® towards this fraction than other fractions (Boyer et al. 2008, b). Any improved performance of MIEX® over conventional treatments (such as coagulation) is reported to be due to the higher removal of the transphilic and hydrophilic fractions (Bond et al. 2010, Sharp et al. 2006, a), with the degree of anionic charge the key factor in removal (Bond et al. 2010). While the exact chemical identity of transphilic acids are unknown, they are assumed to be more hydrophilic than the hydrophobic acids and with a high proportion of carboxylic acid functionality (Aiken et al. 1992). Multiple dissociated carboxylic acid groups are necessary for the high removals reported for transphilic acids by coagulation and MIEX® treatment (Bond et al. 2010). This increased hydrophilic character was observed in Section 4.3.2.3 (Figure 4.4), as the TPIB fraction had a greater relative abundance of carboxylic acid signal area in the ^{13}C NMR spectrum compared to the HPO fraction. The lower percentage reductions for the TPIN fraction compared to the HPO and TPIB fractions after MIEX® treatment were likely due to physicochemical properties of the fraction, as the degree of anionic charge within this fraction is reported to be low (Bond et al. 2010), and anionic charge is the key factor to removal by MIEX® treatment (Bond et al. 2010).

4.3.3.2 Fluorescence Excitation-Emission Spectroscopy

Fluorescence spectroscopy provides sensitive and non-destructive analysis of the structure, functional groups, conformation and heterogeneity of humic substances, as well as dynamic properties relating to their intramolecular and intermolecular interactions (Chen et al. 2003, a). Fluorescence excitation-emission matrices (EEM) of the XAD fractions before and after MIEX® treatment are shown in Figures 4.8 – 4.10, with all supporting literature explaining the major fluorescent components discussed in detail in Section 3.3.2. Humic acid material seen in fluorescent EEM

spectra represents NOM that is refractory to oxidation and is highly conjugated (Caron and Smith 2011). Fulvic acid material is described as being more functionalised than humic acids but with a lower MW (Caron and Smith 2011). Proteinaceous material represents NOM originating in the build up or breakdown of biomass (Caron and Smith 2011). The fluorescent bands running diagonally through the emission range of 400 – 500 nm at an excitation range of 200 – 260 nm were present in all spectra and were artefacts of glass and water interactions. The peaks positioned diagonally through the emission range of 250 – 380 nm at an excitation range of 270 – 290 nm were due to Rayleigh/Tyndall scattering lines (Caron and Smith 2011). The XAD fractions showed several distinct EEM spectral differences before and after MIEX® treatment. This is the first report of EEM spectra of MIEX® treated XAD fractions.

Before treatment, the HPO fraction (Figure 4.8a) showed high humic and fulvic acid signal intensity at Ex: 330 nm – Em: 450 nm and Ex: 250 nm – Em: 450 nm. These areas were significantly reduced in intensity by MIEX® treatment (Figure 4.8b), mirroring the reductions in DOC (68%) and UV_{254} (75%) by MIEX® treatment (Table 4.7). The reduction in intensity for the humic and fulvic acid material is due to the removal of carbonyl, hydroxyl and alkoxyl containing substituents present within the HPO fraction (Senesi 1990) as these components are easily removed by the ion exchange process (Bond et al. 2010).

The untreated TPIB fraction (Figure 4.9a) showed similar humic and fulvic acid signals to the HPO fraction (Figure 4.8a), with MIEX® treatment of the TPIB fraction completely removing these signals (Figure 4.9b). Transphilic material was expected to be preferentially removed by MIEX® treatment, due to its higher hydrophilic character, as discussed in Section 4.3.3.1 (Bond et al. 2010). However, a low intensity signal at Ex: 270 nm – Em: 320 nm and Ex: 333 nm – Em: 380nm, indicative of soluble microbial metabolites (Chen et al. 2003, a) remained after MIEX® treatment. A similar component of the UF fraction also proved recalcitrant to MIEX® treatment (Section 3.2.2), consistent with the idea that the MIEX® process is less effective at removing protein-derived structures (Amy 2007).

Fluorescence spectroscopy shows that treatment of the TPIN fraction by the MIEX® process removed a small proportion of humic and fulvic acid type material (Figure 4.10b). The different chemical composition of the TPIN fraction compared to the TPIB and HPO fractions is key to the low removal of the fluorescent signals for the TPIN fraction. The TPIN fraction had a reduced aromatic character compared to the other two fractions (as seen in the elemental analysis data, Section 4.3.2.1) and this fraction is reported to generally consist of lower MW components such as polysaccharides and proteins (Leenheer 1981). Only very small amounts of the TPIN material were removed by any treatment (MIEX®, coagulation) in the study of Drikas et al. (2011). van Leeuwen et al. (2002) also identified neutral material as recalcitrant following fractionation and coagulation of two waters. A pilot-plant study of MIEX® treatment on estuarine water using size exclusion chromatographic analysis also showed MIEX® to be ineffective at removal of neutral polysaccharides and protein-like organic material (Booth et al. 2006).

In a previous study of fifty-six Missouri lakes (Hua et al. 2007), it was observed that waters with abundant fluorescent signals also exhibited high THMFP. In Figures 4.8 – 4. 10, the untreated HPO, TPIB and TPIN fractions exhibited abundant fluorescent signals, which may indicate a high propensity to form disinfection by-products. The DBPFP of each fraction will be discussed in detail in Section 4.3.3.4.

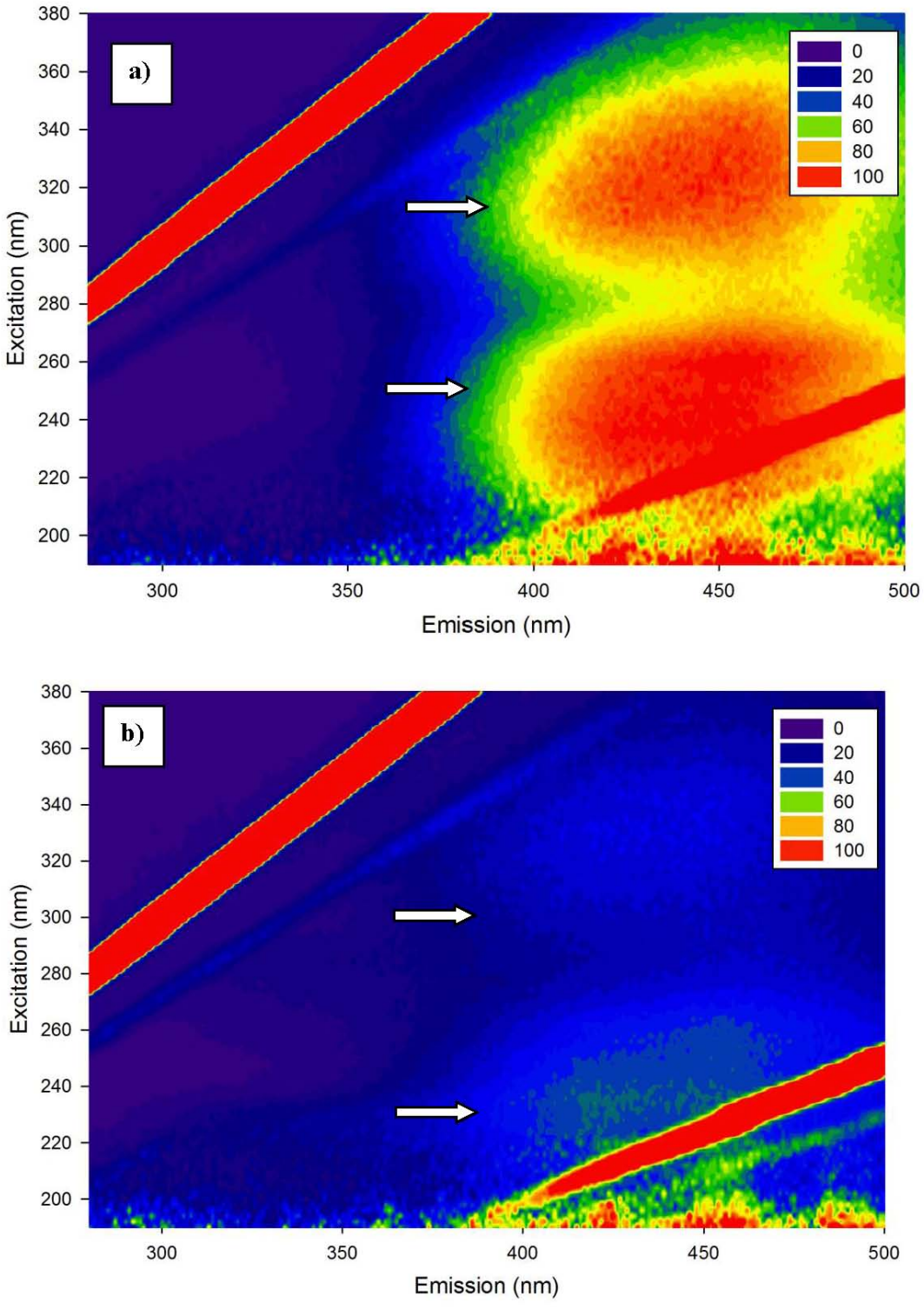

Figure 4.8 Excitation-emission (EEM) fluorescence spectra of the a) pre and b) post MIEX® treated HPO fraction. White arrows represent 'humic-like' components within the spectra. 'Protein-like' components within the spectra could not be identified due to the high concentration of 'humic-like' material.

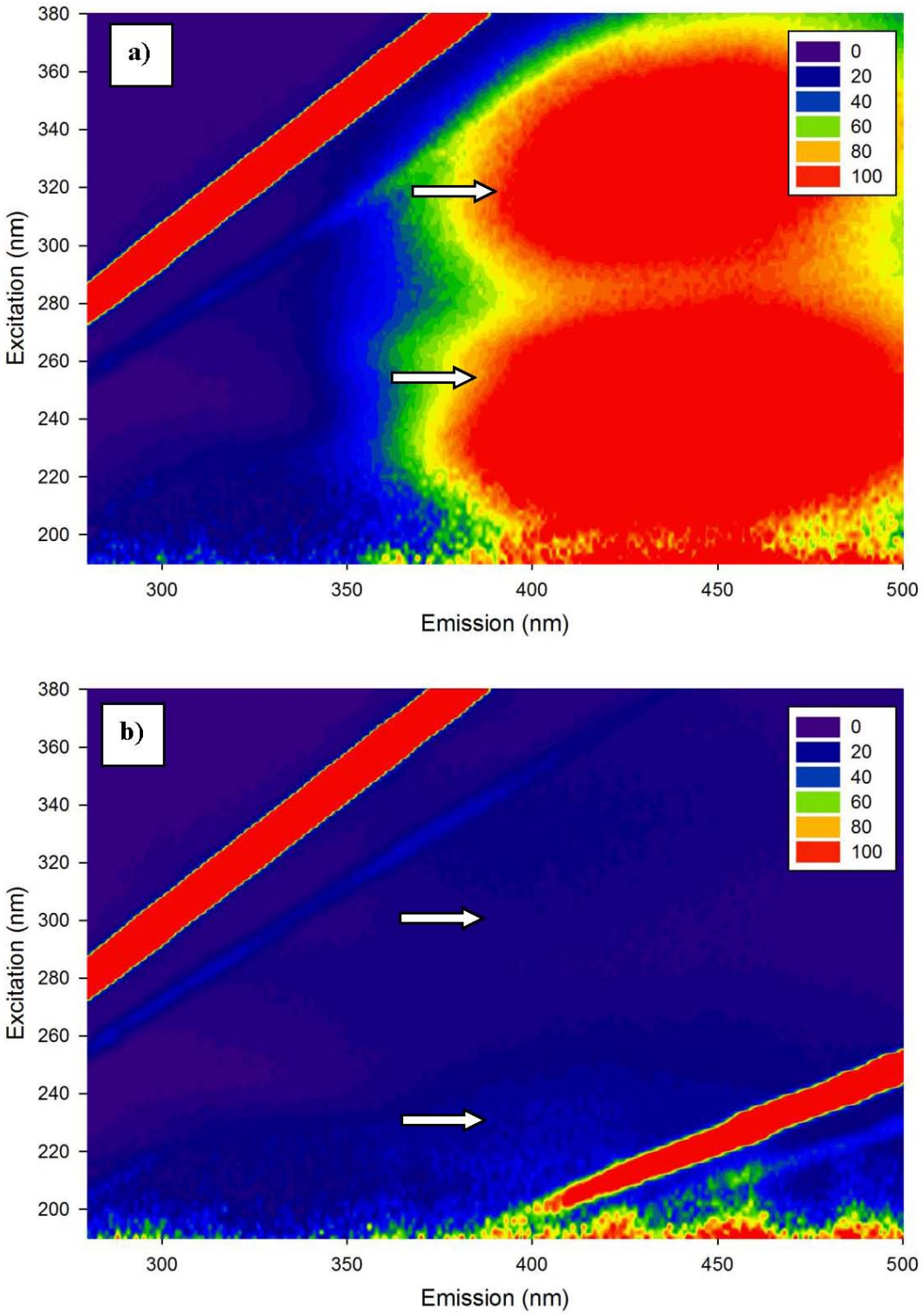

Figure 4.9 Excitation-emission (EEM) fluorescence spectra of the a) pre and b) post MIEX® treated TPIB fraction. White arrows represent 'humic-like' components within the spectra. 'Protein-like' components within the spectra could not be identified due to the high concentration of 'humic-like' material.

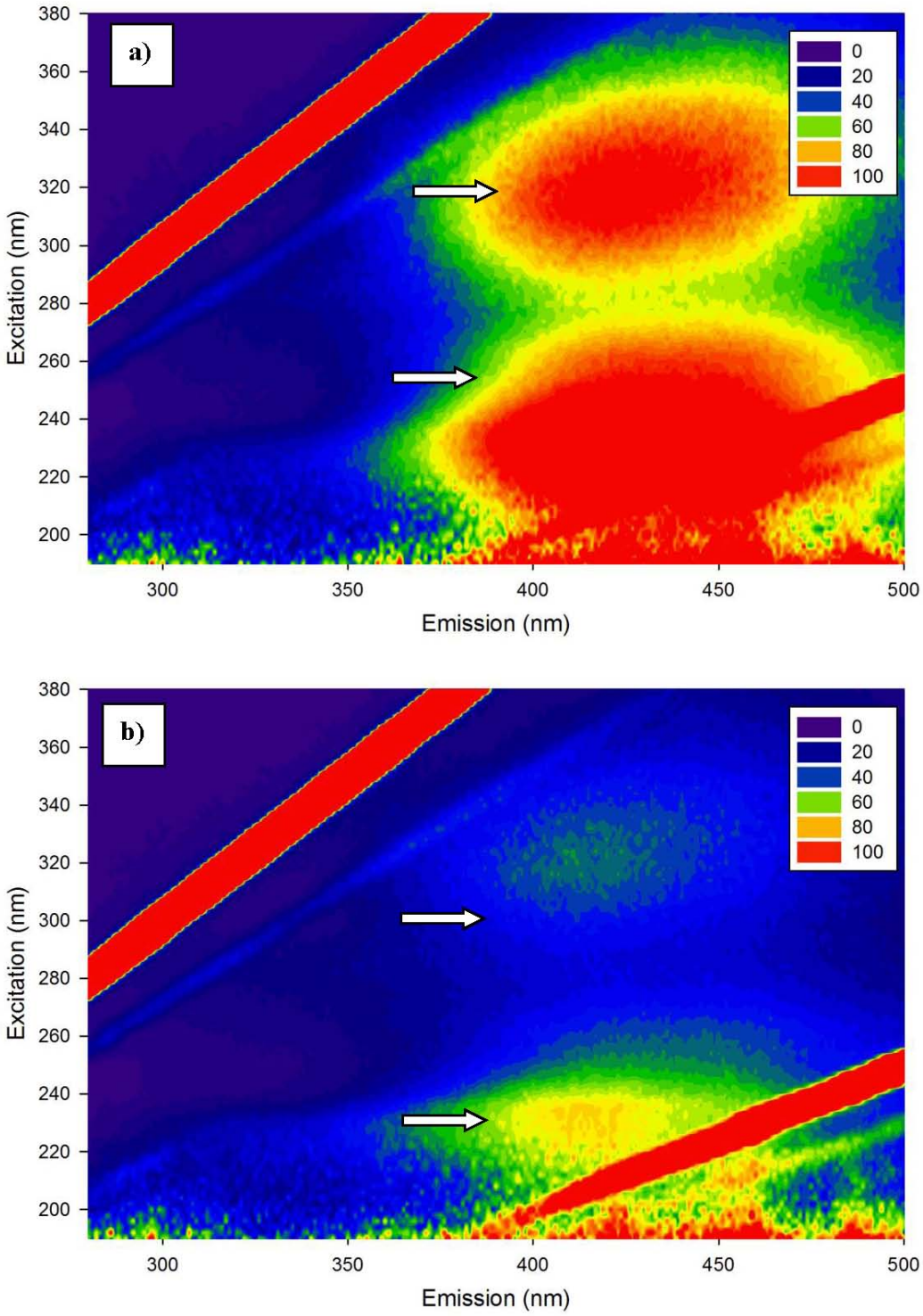

Figure 4.10 Excitation-emission (EEM) fluorescence spectra of the a) pre and b) post MIEX® treated TPIN fraction. The intensity of the EEM is represented by contour lines. White arrows represent 'humic-like' components within the spectra. 'Protein-like' components within the spectra could not be identified due to the high concentration of 'humic-like' material.

4.3.3.3 Size Exclusion Chromatographic Analysis

Size exclusion chromatography analysis, with both organic carbon detection (OCD) and UV_{254} absorbance detection, was performed on solutions of the HPO and TPI fractions before and after MIEX® treatment to examine the molecular weight distribution in these samples (Figures 4.11 – 4.13). In Figures 4.11 – 4.13, the different MW regions are numbered from 1 – 8 according to a previously reported numbering system (Allpike et al. 2005; Huber and Frimmel 1996). Each of these fractions is comprised of a variety of individual organic compounds. Region 1, which elutes as a broad band of poorly resolved material in both the HPO and TPI fractions, has been reported to potentially consist of sulphur species associated with organic matter, either in colloidal form as elemental sulfur or in solution, or as colloidal in nature, and may be comprised of some inorganic substances (Allpike et al. 2005). Regions 2 – 4, which elute as three partially resolved peaks for the HPO fraction before MIEX® treatment (Figure 4.11), and as one unresolved peak for the TPIB (Figure 4.12) and TPIN fractions (Figure 4.13), are reported to be likely to be enriched in humic substances of relatively high MW (Huber and Frimmel 1996). Humic substances are considered to be rich in aromatic functional groups, and these are easily detected by both DOC specific and UV_{254} absorbance detectors. Regions 5 – 7 reportedly correspond to the fractions comprising lower MW monoprotic organic acids such as fulvic acids, conjugated unsaturated acids or keto acids (Huber and Frimmel 1996). Region 8 is comprised of DOC of the lowest apparent MW, which eluted as a broad band of poorly resolved material.

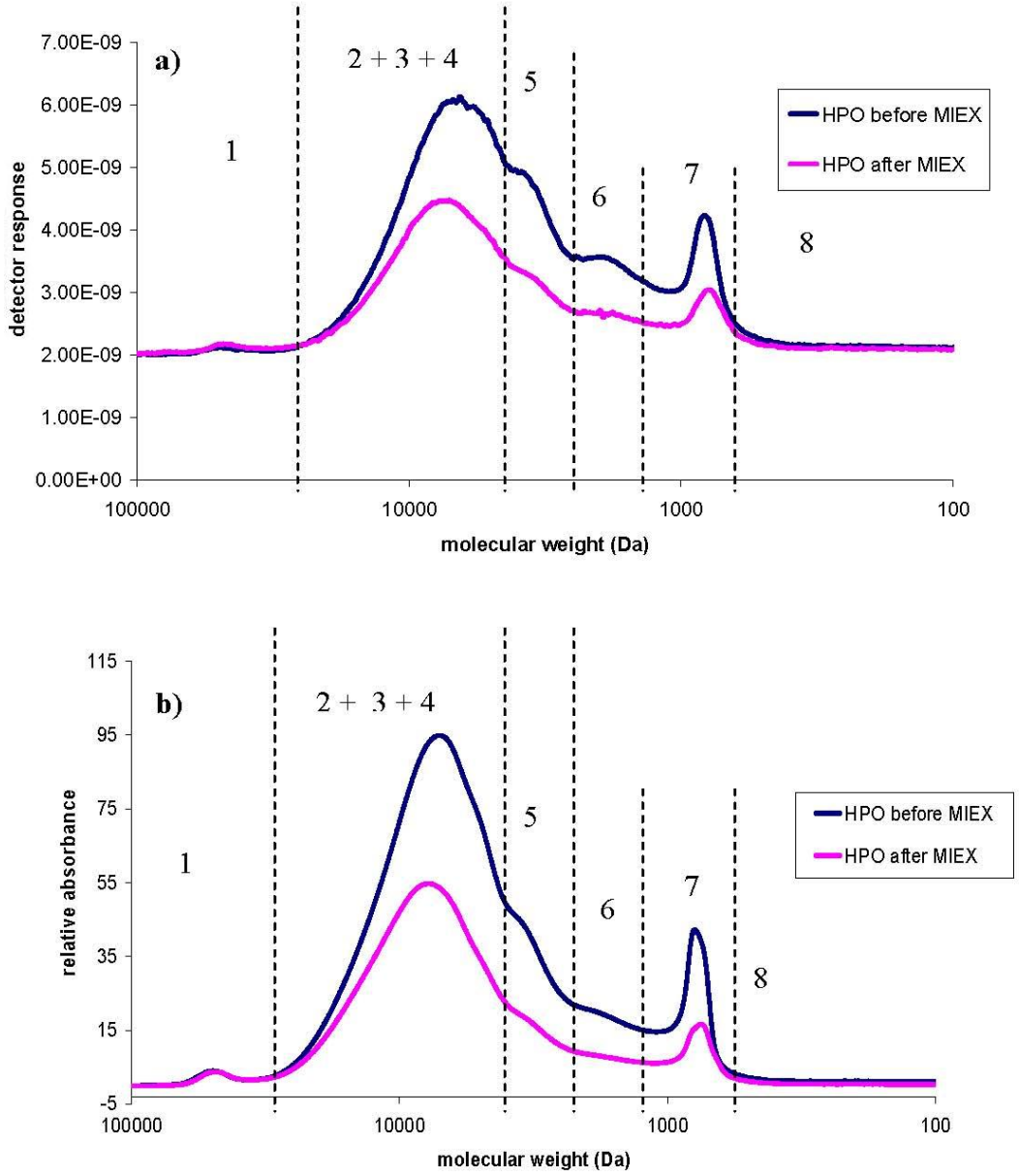

Figure 4.11 MW distribution of the HPO fraction before and after MIEX® treatment detected by a) SEC-OCD and b) SEC-UV_{254}. Numbers correspond to eight distinct MW regions as described by Huber and Frimmel 1996 and Allpike et al. 2005.

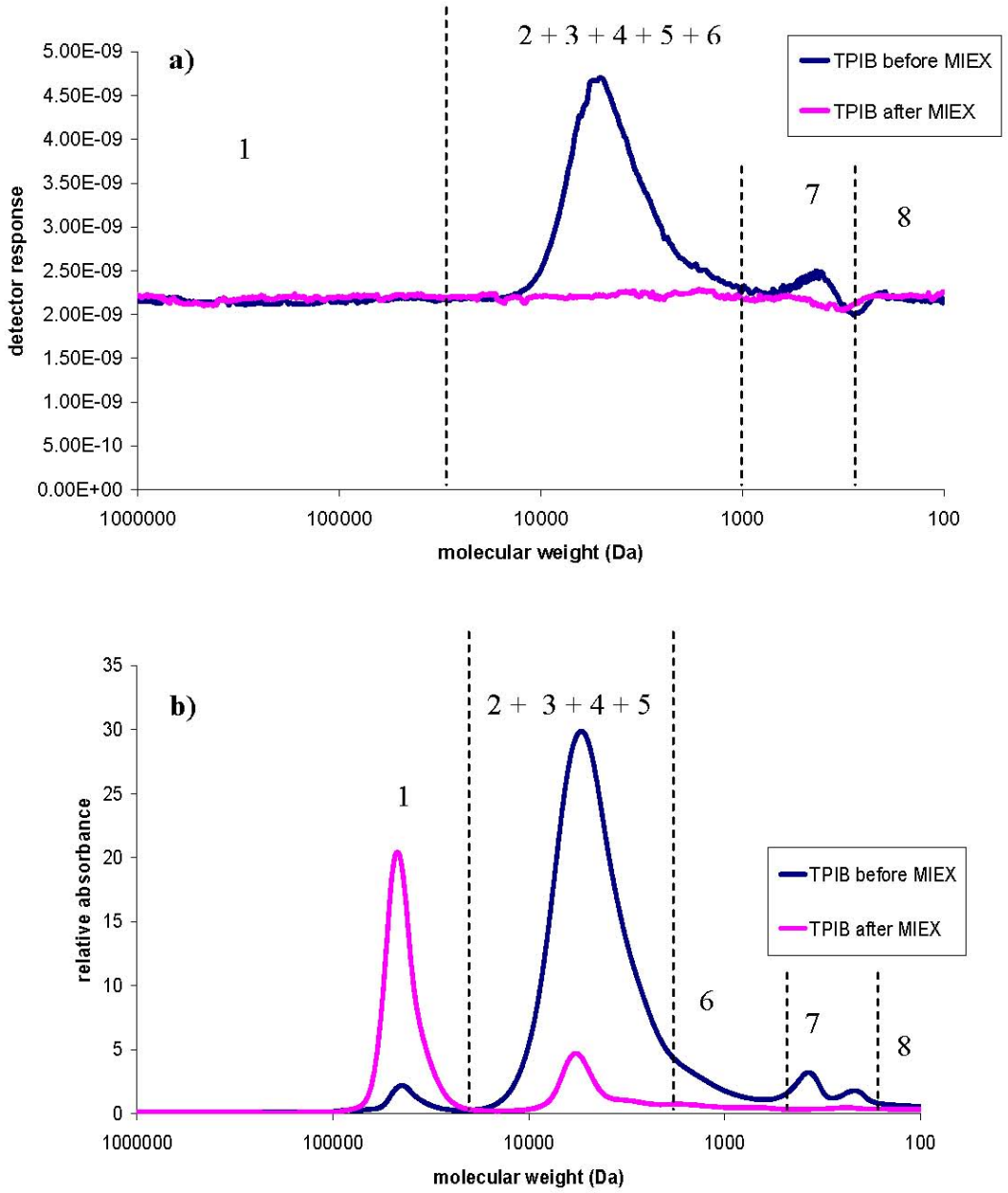

Figure 4.12 MW distribution of the TPIB fraction before and after MIEX® treatment detected by a) SEC-OCD and b) SEC-UV_{254}. Numbers correspond to eight distinct MW regions as described by Huber and Frimmel 1996 and Allpike et al. 2005.

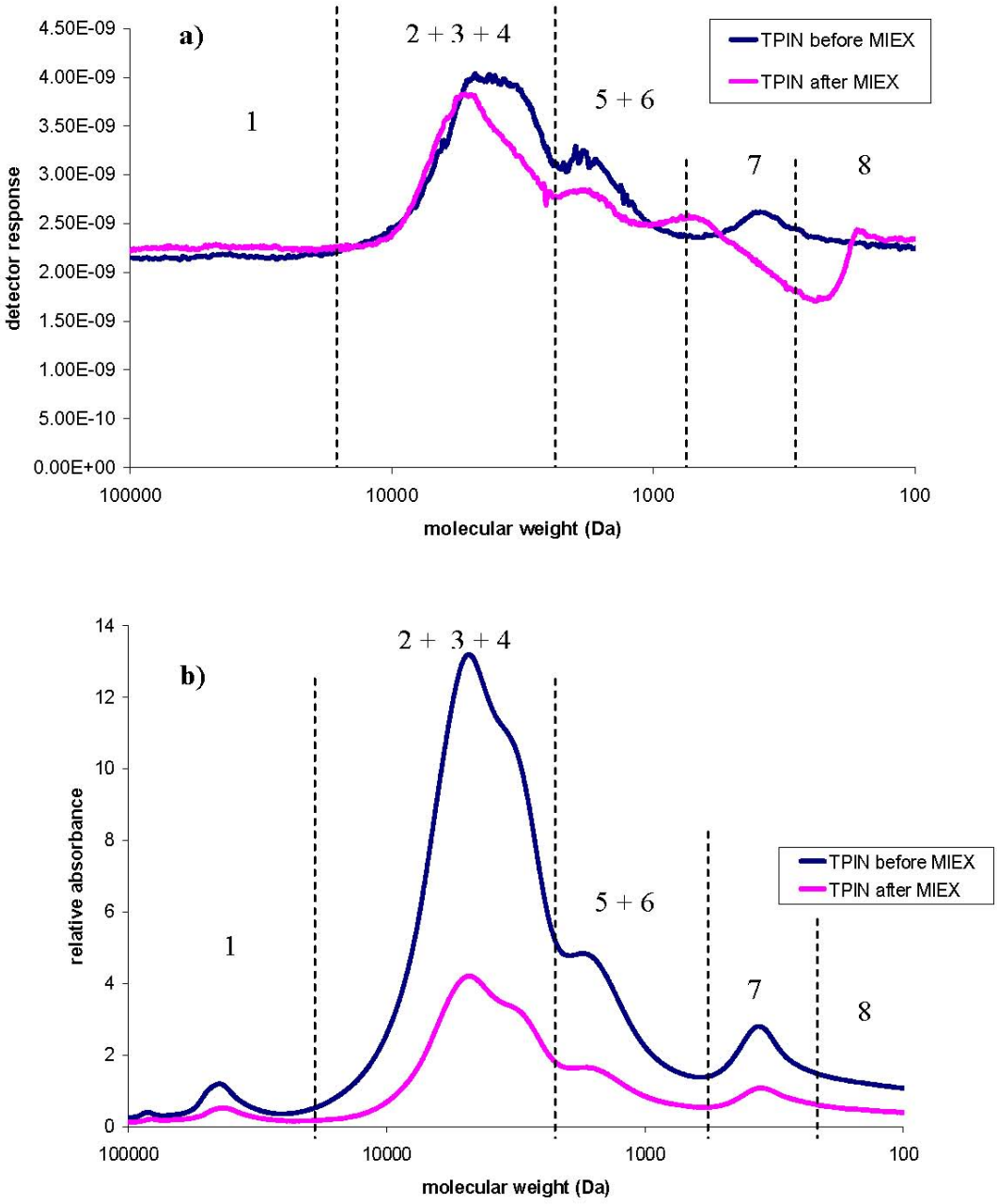

Figure 4.13 MW distribution of the TPIB fraction before and after MIEX® treatment detected by a) SEC-OCD and b) SEC-UV_{254}. Numbers correspond to eight distinct MW regions as described by Huber and Frimmel 1996 and Allpike et al. 2005.

Analysis by SEC-OCD and SEC-UV_{254} showed that a significant proportion of the material in all of the regions was removed by MIEX® treatment for the HPO fraction. From Figure 4.11, it appears that the MIEX® resin removed organic matter over a wide range of apparent MW for the HPO fraction, with particularly good removal of the high molecular weight material. This is consistent with a previous study of MIEX® treatment of Wanneroo GWTP raw water (Allpike et al. 2005).

The DOC concentrations of the various components of the TPIB fraction after MIEX® treatment (total DOC concentration after treatment 1.8 mg L^{-1}) were too close to the detection limit of the SEC-OCD instrument to observe the remaining material in the various regions (Figure 4.12a). The aromatic-sensitive UV_{254} detection showed some signal in the sample after treatment and there was significant removal of material with MW in regions 2 – 4, indicative of removal of high MW humic substances (Huber and Frimmel 1996). The removal of these organic components probably also accounts for the significant reduction in fluorescence of the TPIB fraction after MIEX® treatment (Figure 4.9). Interestingly, the SEC-UV_{254} chromatogram (Figure 4.12b) showed a large increase in region 1 after MIEX® treatment. The high $SUVA_{254}$ of this peak is suggestive of aromatic humic substances, but it is more likely to be colloidal with some inorganic substances (Huber and Frimmel 1996). Colloidal material can permeate the 0.45 μm membranes used to filter the sample prior to injection on the SEC column and has high UV absorbance activity due to light scattering effects (Huber and Frimmel 1996). Similar characteristics evident in the SEC characterisation of a German lake water were attributed to early eluting inorganic colloidal material (Huber and Frimmel 1996).

SEC-OCD and SEC-UV_{254} analysis of the TPIN fraction (Figure 4.13) also showed a significant proportion of the material in all the MW regions was removed by MIEX® treatment. The negative detector response between 100 and 1000 Da evident in the SEC-OCD chromatogram (Figure 4.13a) is probably due to salt interference, since the separation at the salt boundary can cause interactions between the sample and the persulfate oxidiser (Soh et al. 2007). In order to reduce the salt boundary peak, an ionic strength adjustment is required as a pre-treatment step for optimal HPSEC chromatograms (Soh et al. 2007). Nevertheless, SEC-OCD which measures the total MW distribution, as opposed to the aromatic-sensitive SEC-UV_{254}, indicated removal over a wide range of apparent MWs, with particularly good removal of high molecular weight material. A study of the ion exchange treatment of NOM (Amy 2007) also showed relatively efficient removal of humic substances and low molecular weight acids (regions 2 – 4).

4.3.3.4 Disinfection By-Product Formation Potential

A common laboratory approach to assess the possible formation of DBPs during chlorination in drinking water treatment is the DBP formation potential (DBPFP) procedure (Franson 1998). This test is performed by spiking waters of interest at pH 7.0 – 8.3 and incubating them at 20 or 25ºC for a specific time period (days). In this test, the reactivity of chlorine and NOM is examined to predict the potential DBPs of finished waters (Chow et al. 2005).

Prior to DBPFP measurement, aqueous samples of the HPO and TPIB fractions (produced by initial dissolution of the dried isolate in MilliQ water) and the HPO and TPIB fractions after MIEX® treatment were diluted to achieve DOC concentrations of 2 mg L^{-1}, typical of the DOC concentration at the outlet of the Wanneroo GWTP, and bromide ion (0.2 mg L^{-1}) was added to simulate the bromide concentrations of raw W300 water (Table 2.3, Section 2.3.3). Disinfection experiments involved addition of chlorine to achieve an initial concentration of 6 mg L^{-1} (a similar chlorine dose to what is applied for disinfection of water at the Wanneroo GWTP), addition of buffer to achieve pH 7 and temperature control to 25 ºC, and analysis of the concentration of trihalomethanes (THMs) and haloacetic acids (HAAs) after 7 days. The oxidant demands of the HPO and TPIB fractions before and after MIEX® treatment are shown in Table 4.8, with the 7-day individual and total THM concentrations produced shown in Table 4.9, and the corresponding HAA concentrations shown in Table 4.10.

Table 4.8 Oxidant demand of the HPO and TPIB fractions before and after MIEX® treatment (halogenation conditions: 2 mg L^{-1} DOC, 6 mg L^{-1} Cl_2 dose, 0.2 mg L^{-1} Br^-, pH 7, 25^oC, 168 hours).

Sample	Oxidant demand (mg L^{-1} free chlorine)	Specific oxidant demand (mg free chlorine/mg C)
HPO	5.7	2.9
HPO after MIEX®	4.8	2.4
TPIB	5.1	2.6
TPIB after MIEX®	4.1	2.1

Table 4.9 Concentrations of THMs from chlorination of the HPO and TPIB fractions before and after MIEX® treatment (halogenation conditions: 2 mg L^{-1} DOC, 6 mg L^{-1} Cl_2 dose, 0.2 mg L^{-1} Br^-, pH 7, 25°C, 168 hours).

Sample	Concentration of Individual THMs (µg L^{-1})				Total THMFP (µgL^{-1})	Specific THMFP (µg/mg C)
	$CHCl_3$	$CHBrCl_2$	$CHBr_2Cl$	$CHBr_3$		
HPO	164	90	28	1	283	142
HPO after MIEX®	166	95	33	2	296	148
TPIB	133	100	54	5	292	146
TPIB after MIEX®	49	79	60	10	198	99

Table 4.10 Concentration of HAAs from chlorination of the HPO and TPIB fractions before and after MIEX® treatment (halogenation conditions: 2 mg L^{-1} DOC, 6 mg L^{-1} Cl_2 dose, 0.2 mg L^{-1} Br^-, pH 7, 25°C, 168 hours).

Sample	Concentration of Individual HAAs (µg L^{-1})									Total HAAFP (µg L^{-1})	Specific HAAFP (µg/mg C)
	MCAA	MBAA	DCAA	TCAA	BCAA	DBAA	BDCAA	CDBAA	TBAA		
HPO	-	-	78	97	28	5	24	2	-	235	118
HPO after MIEX®	-	-	99	120	31	6	20	1	-	278	139
TPIB	-	-	7	5	4	1	1	-	-	18	9
TPIB after MIEX®	-	-	3	-	4	3	-	-	-	10	5

* ND – not detected

The oxidant demands of the MIEX®-treated fractions were lower than the untreated fractions (Table 4.8). Since the DOC concentration has been normalised to 2 mg L^{-1} prior to the disinfection experiments, the oxidant demand is already normalised to the DOC concentration, and comparisons of oxidant demands before and after MIEX® treatment are comparisons of specific oxidant demands. The oxidant demand concentrations in Table 4.8 show that MIEX® treatment has preferentially removed the oxidant-reactive (here chlorine- and bromine-reactive) fractions of NOM in these water samples. Specific oxidant demand results in Chapter 3 (Table 3.4) also showed a lower oxidant demand after MIEX® treatment. A previous study at the Wanneroo GWTP (Warton et al. 2007, a) showed a reduction in specific oxidant demand after MIEX® treatment, as observed in this study. Preferential removal of the oxidant-reactive (here chlorine- and bromine-reactive) fraction of NOM is a favourable

parameter for a water treatment process, since a more stable oxidant residual (often termed 'chlorine residual') can be achieved in the product water, with lower levels of chlorination needed for the distribution system. With lower chlorination doses prior to distribution, the formation of disinfection by-products should be reduced.

The formation of significant concentrations of THMs and HAAs (Tables 4.9 and 4.10) indicates that the HPO and TPI fractions are both reactive with chlorine. The 7-day THMFP of the HPO fraction and the HPO fraction after MIEX® treatment were essentially identical, indicating that the reactivity of DOC for THM formation in the two samples is the same and that the MIEX® treatment has not preferentially removed THM precursors from the HPO fraction. Similar THMFPs were seen for the UF fraction (283 μg L^{-1}) and the UF fraction after MIEX® treatment (290 μg L^{-1}) in Chapter 3, Section 3.3.3.4. Physicochemical factors controlling treatability do not relate to reactivity with chlorine, as the DOC concentration was reduced by 68 % for the HPO fraction compared to the UF fraction (12 %) after MIEX® treatment, yet, similar THMFPs were observed for each fraction before and after MIEX® treatment. Hence, MIEX® treatment does not appear to offer an option for selective removal of reactive DBP precursors over non-reactive precursors. In the study of Bond et al. (2010) using model compounds, treatability of the NOM surrogates was explained by physicochemical properties of the compounds. In the case of MIEX® treatment, the degree of anionic charge was the key factor in removal, whereas DBP formation can not be predicted using the same properties. It was not possible to selectively remove reactive DBP precursors in MIEX® treatment (Bond et al. 2010), consistent with the findings in this study.

The DOC concentrations were normalised to 2 mg L^{-1} for all fractions in this DBPFP experiment to study the propensity of each W300 water fraction to form DBPs. Since three out of the four THMFP concentrations (Table 4.9) are above the ADWG value of total THMs < 250 μg L^{-1}, the NOM samples have a high propensity to form THMs. The untreated HPO and TPIB fractions of W300 water showed similar THM formation potentials, and showed that they are similar in composition by the characterisation techniques (Section 4.3.2). HPO NOM fractions are reported to typically have the greatest THMFP (Budd et al. 2005; Croué et al. 1999, a), with humic substances reported to be the major precursors (Croué et al. 1999, a). Even

though other characterisation techniques in this study have shown that the HPO and TPI fractions of NOM in W300 water are chemically consistent with groundwater sources, the specific THMFP of the untreated HPO and TPIB fractions are higher than other groundwaters previously reported (Bolto et al. 2002; Drikas et al. 2003; Croué et al. 1993, a).

In this DBPFP experiment, chloroform was the major THM product formed for the HPO and the HPO after MIEX® fractions. Chloroform was the major THM produced for the TPIB fraction, with dichlorobromomethane the major product for the TPIB after MIEX® treatment fraction. The shift towards the more brominated forms in the TPIB fraction after MIEX® treatment must be due to an increased reaction of the functional groups present and bromine (Liang and Singer 2003).

HAA formation is similarly dependent on pH, bromide ion concentration, the concentration and characteristics of the NOM, temperature, chlorine dose, chlorine residual and contact time. The HPO fraction showed a much larger specific HAAFP than the TPIB fraction both before and after MIEX® treatment (Table 4.10), indicating that the NOM within the HPO fractions contained relatively more HAA precursors than the NOM within the TPIB fraction. The HPO fraction produced more di-and tri-halogenated HAAs than the corresponding TPIB fraction, with the major HAAs formed being the chlorinated HAAs: dichloroacetic acid (DCAA) and trichloroacetic acid (TCAA). Other HAAs detected were: bromochloroacetic acid (BCAA), dibromoacetic acid (DBAA), bromodichloroacetic acid (BDCAA) and chlorodibromoacetic acid (CBDAA). Again, it should be emphasised that in this DBPFP study, the DOC concentration was normalised to 2 mg L^{-1} for all fractions to study the propensity to form DBPs for each fraction from the selected bore, W300. The production of similar concentrations of HAAs for each of the HPO fraction and the TPIB fraction before and after MIEX® treatment suggests that MIEX® treatment did not selectively remove reactive HAA precursors over non-reactive precursors. Interestingly, the HAAFP of the UF fraction (Chapter 3, Table 3.6) was in contrast to the HAAFP measured in this study (Table 4.10), as the potential for HAA formation for the UF fraction was reduced after MIEX® treatment, indicating preferential removal of HAA precursors during MIEX® treatment. The HAAFP of the HPO fraction and the HPO fraction after MIEX® treatment were very high and similar in

mass concentration to the corresponding THMFPs, but DBPFP experiments are considered to represent a worst-case scenario (Warton et al. 2007, b).

The bromine incorporation factor (BIF) is the measure of the extent of bromine incorporation into the different classes of DBPs (such as THMs and HAAs). The molar ratio is calculated as described in Section 3.2.2 by normalising the bromine incorporation factor to a value between zero (no incorporation) and one (full incorporation) for each DBP class (Obolensky and Singer 2005). The THM and HAA BIF values for the HPO and TPI fractions and the HPO and TPIB after MIEX® treatment fractions are shown in Table 4.11.

Table 4.11 BIF (THMs) and BIF (HAAs) obtained after 7 day chlorination experiment.

Sample	BIF (THMs)	BIF (HAAs)
HPO	0.17	0.04
HPO after MIEX®	0.18	0.03
TPIB	0.25	0.06
TPIB after MIEX®	0.38	0.16

For both THMs and HAAs, the extent of bromine substitution varied for the HPO and TPIB fractions. The HPO fraction and the HPO after MIEX® treatment showed similar BIF values for each of the classes of THMs and HAAs, while MIEX® treatment of the TPIB fraction led to an increase in the proportion of brominated THMs and HAAs, similar to the behaviour of the UF fraction (Section 3.2.2). Hypobromous acid is more reactive to hydrophilic and aliphatic structures (Liang and Singer 2003), suggesting these structural precursors are more rich in the TPIB fraction, with MIEX® treatment exhibiting poor removal of these precursors.

From the DBPFP experiments, the HPO and the HPO after MIEX® treatment fractions have been demonstrated to be highly reactive to the formation of DBPs. As mass concentrations, the total THM concentrations were comparable to the total HAA concentrations for the HPO fraction and these concentrations were not notable reduced for the HPO after MIEX® treatment fraction, suggesting MIEX® treatment has not preferentially removed THM or HAA precursors from the HPO fraction. But,

MIEX® treatment of the TPIB fraction did significantly reduce the potential for THM formation.

4.3.4 Conclusions

Isolation of NOM from a local groundwater source using XAD-8/XAD-4 resin fractionation was used with some success. The solid freeze-dried HPO and TPI fractions, isolated using the XAD-8/XAD-4 resin fractionation protocol, were obtained from 132 L of a high DOC concentration (23 mg L^{-1}) groundwater. Desalting of the TPIB fraction was challenging, hindering characterisation of this fraction by the analytical methods employed in this study. Characterisation of the HPO and TPI fractions by FTIR and ^{13}C NMR spectroscopic analysis revealed the fractions to have a significant contribution of aliphatic content, most likely from lipid and biopolymer precursors. Further characterisation of the fractions by pyrolysis-GC-MS, thermochemolysis-GC-MS and MSSV-pryolysis-GC-MS revealed that the HPO fraction had a significant polysaccharide input. The higher nitrogen and oxygen content present in the TPIB and TPIN fractions allowed more nitrogen and oxygen containing groups (such as tannins and proteins) to be revealed by the pyrolysis and thermochemolysis techniques.

The fractions showed different affinity for the MIEX® resin. Treatment of the HPO and TPI fractions by preconditioned MIEX® resin led to significant reductions in the DOC concentration, UV_{254} absorbance and colour. The MIEX® resin was effective for removal of organic matter in the more non-polar (HPO) and intermediate polarity (TPIB and TPIN) fractions of NOM.

In the DBPFP study, the HPO fraction showed a similar propensity to form THMs and HAAs before and after MIEX® treatment, so whilst MIEX® removed 68 % of the DOC concentration from this fraction, it did not preferentially remove the organic precursors of the THM products. In contrast, MIEX® treatment of the TPIB fraction (69 % DOC removal) did show some preferential removal of the precursors for the THMs and HAAs, but showed a shift towards greater reactivity with bromine in THM formation. This indicates THM and HAA precursors within the quantitatively significant HPO fraction can not be preferentially removed by MIEX® treatment. In

general, additional treatment processes to the MIEX® process will be required to enhance removal of the recalcitrant structural moieties of the HPO and TPI fractions, with a particular focus on THM precursor removal.

Chapter 5

5.0 Characterisation of Resin-Fractionated NOM Remaining After MIEX® Treatment of a High Hydrophobicity / High DOC Groundwater

5.1 Introduction

Various water treatment processes can either directly or indirectly remove organic matter depending on their operational conditions and the characteristics of the NOM. High MW NOM is more amenable to removal than low MW NOM in conventional water treatment (Collins et al. 1986). Water with high MW humic material is a good candidate for chemical coagulation, whilst low MW species are more amenable to ion exchange processes, such as a MIEX® process (Singer and Bilyk 2002). An increased removal of NOM can be obtained by a MIEX® process coupled with a coagulation process compared to a coagulation process alone (Singer and Bilyk 2002; Warton et al. 2007, a). There have been numerous published papers on the performance of MIEX® resin at a pilot, bench or full scale application (Morran et al. 1996; Nguyen et al. 1997; Pelekani et al. 2001; Singer and Bilyk 2002; Drikas et al. 2011, Warton et al. 2007, a; Boyer et al. 2008, a; Boyer and Singer 2005; Allpike et al. 2005). The study by Warton et al. (2007, a) was the first of its kind describing the behaviour of the MIEX® process on a full scale plant level using several parameters to assess its performance.

There does not appear to be any previous studies that have fractionated MIEX® treated water to investigate the reactivity of the residual NOM, which is the focus of the work described in this Chapter. Previous studies have characterised the nature

and abundance of structural units in the NOM remaining after treatment (Bond et al. 2010; Chow et al. 1999; Allpike 2008; Page et al. 2003). Chow et al. (1999) used pyrolysis-gas chromatography-mass spectrometry (py-GC-MS), FTIR spectroscopy and high pressure size exclusion chromatography to characterise NOM isolated from raw water, as well as NOM remaining after alum coagulation treatment, from the Myponga and Hope Valley reservoirs located in South Australia. It was observed that the mid to high MW fraction of NOM (> 1000 Da) was removed after alum treatment. Bond et al. (2010) showed coagulation preferentially removed high MW hydrophobic acids and, under conditions representative of full-scale operation, MIEX® provided negligible further removal of the hydrophobic acids. Any improvement in NOM removal performance was reported to be likely to arise from removal of transphilic and hydrophilic acids (Bond et al. 2010). In the study by Page et al. (2003), raw water from several reservoirs in South Australia were coagulated by a jar test procedure, and the NOM samples isolated from the raw and the treated waters were characterised by a py-GC-MS technique. Most of the alum treated samples contained NOM with high relative quantities of polysaccharide-derived material, with the proportion of alkylbenzene, alkylphenol, indole and naphthalene derivatives appearing to change as a result of alum treatment. In the study of Allpike (2008), it was found that the organic matter remaining after MIEX® and after MIEX®-coagulation appeared to show that there had been a slight preference for removal of aromatic organic matter, whereas enhanced coagulation did not appear to preferentially remove aromatic organic matter. In regard to the treatment of water for distribution at a drinking water treatment plant, MIEX®-only treatment was able to remove a significant portion of DOC, colour and UV_{254}-absorbing species, but for the water source under investigation, MIEX®-only treatment was not as effective as enhanced coagulation treatment for DOC, colour and UV_{254} removal. The recalcitrant fraction of NOM after MIEX® treatment appeared to be the intermediate to high MW fraction which Allpike (2008) reported may be effectively removed by other processes such as coagulation or membrane filtration.

5.1.1 Scope of This Study

To complement the procedure undertaken in Chapter 4 where the NOM in W300 groundwater was fractionated by an established XAD resin adsorption method and

the HPO and TPI fractions separately treated by MIEX®, the work undertaken in this Chapter involved treating W300 water by a MIEX® resin process with the NOM remaining in the water after MIEX® treatment being subjected to XAD resin fractionation, to investigate the nature and reactivity of the recalcitrant material remaining after MIEX® treatment. A schematic of the treatment, isolation and characterisation process is shown in Figure 5.1. The reactivity of the fractions isolated post treatment will be compared to the reactivity of the separately treated fractions of Chapter 4, to aid understanding, prediction and perhaps control of NOM reactivity under water treatment conditions. This improved understanding of treatment of various fractions may ultimately result in optimised treatment strategies, contributing to increased quality of drinking water to consumers.

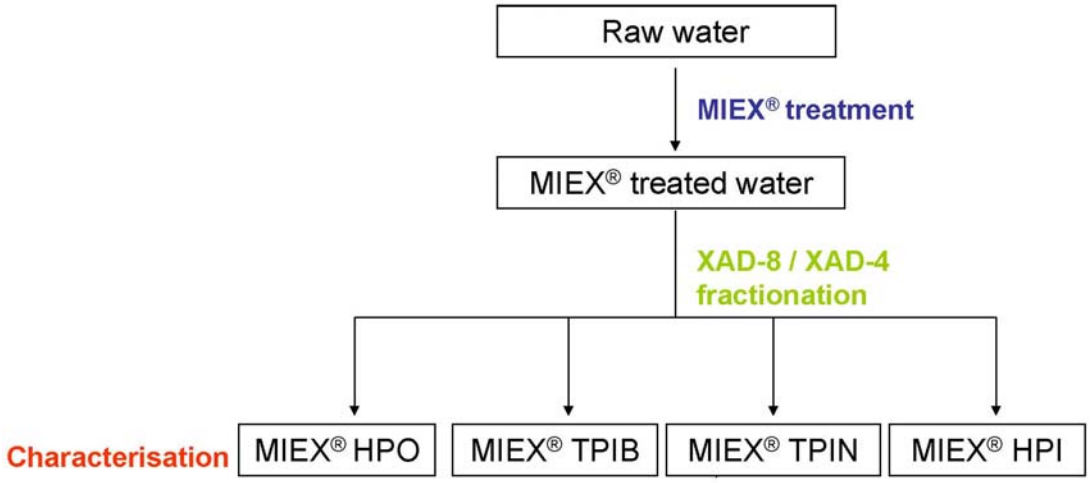

Figure 5.1 The treatment, isolation and characterisation methodology for Chapter 5.

5.2 Experimental

5.2.1 Water Samples

The collection, filtration and storage of the water samples used in this study are described in Section 3.2.1.

5.2.2 Cleaning Procedures

The procedure for cleaning of glassware was the same as that described in Section 2.2.2.2.

5.2.3 MIEX® Treatment of the Raw Water

5.2.3.1 Preconditioning of the MIEX® Resin

Preconditioning of the MIEX® resin has been discussed in detail in Section 3.2.4.1.

5.2.3.2 Treatment of Raw Water by Preconditioned MIEX® Resin

Preconditioned MIEX® resin (42 mL) was used to treat a raw water sample (W300, 1 L) for 15 minutes with stirring, and the aqueous layer was then decanted from the resin. This process was repeated twenty times with 1 L aliquots of W300 water and the same MIEX® resin. The MIEX® resin was then regenerated by stirring with 10 % aqueous sodium chloride solution (600 mL) for 30 minutes and then with MilliQ water (600 mL) for 10 minutes.

After regeneration, the same resin (42 mL) was used to treat another 20 L of raw water in twenty 1 L batches before further regeneration was required. This process was repeated until 400 L of raw water was processed to produce the total MIEX® treated water sample. The MIEX® treated water sample was then filtered through a 0.45 μm glass fibre filter, concentrated under reduced pressure on a rotary evaporator to 70 L, and stored at 4ºC until required.

5.2.4 NOM Resin Fractionation and Isolation Protocol

The XAD-8/XAD-4 resin preparation, cleaning and pH adjustment process are described in detail in Sections 2.2.3 and 4.2.3, respectively.

5.2.4.1 Preparative Fractionation Process

The preparative fractionation process was the same as described in Section 4.2.3.2, except the NOM remaining in the MIEX® treated water sample was fractionated instead of the NOM in filtered W300 water. The fractionation procedure produced four fractions termed: MIEX® HPO, MIEX® TPIB, MIEX® TPIN and MIEX® HPI. A schematic of the isolation process and the four fractions is shown in Figure 5.2.

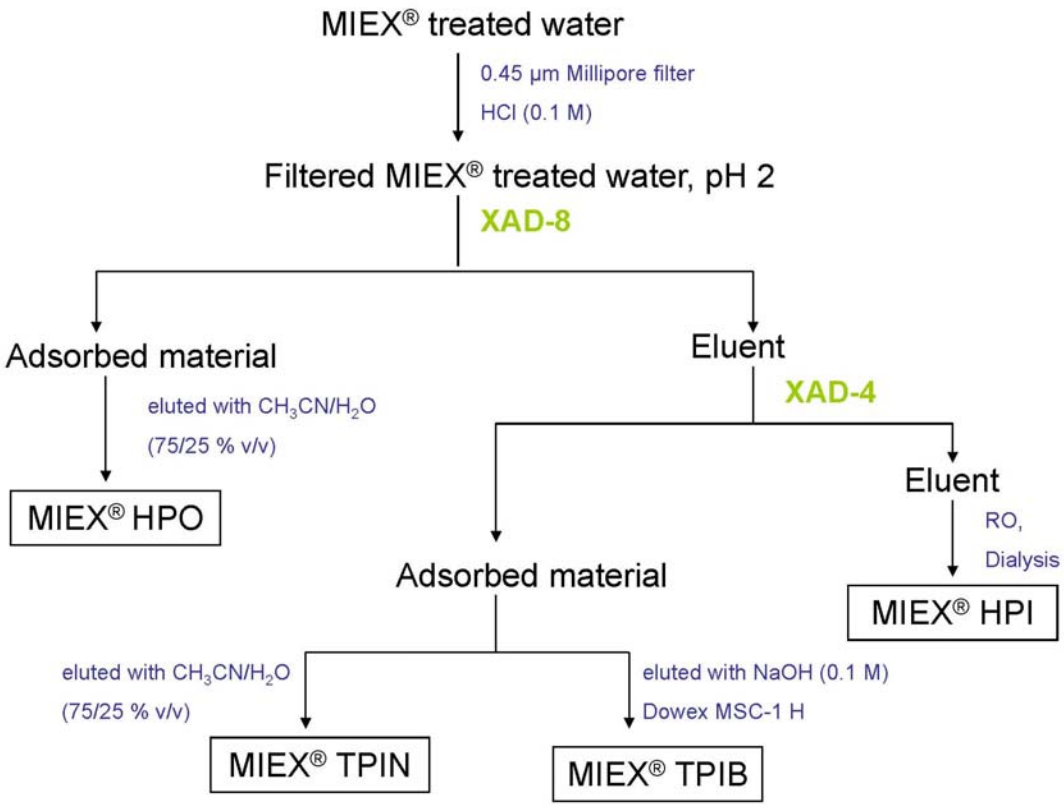

Figure 5.2 The XAD-8/XAD-4 preparative resin isolation procedure. Four fractions of NOM from the MIEX® treated water were obtained.

The fractionation procedure was repeated twice (2 × 33 L) in order to isolate enough transphilic base fraction (MIEX® TPIB) for characterisation and treatment purposes.

5.2.5 Methodology for Characterisation of NOM

All general water parameter measurements and spectroscopic analyses were conducted using previously described methods as follows: elemental analyses of the dried isolates were measured by the procedure outlined in Section 3.2.5.1; DOC concentrations, UV/Visible spectroscopy, bromide ion concentrations, and HPSEC were all analysed as outlined in Sections 2.2.2 – 2.2.7.

Flash pyrolysis-GC-MS, thermochemolysis-GC-MS and micro-scale sealed vessel (MSSV) pyrolysis-GC-MS were conducted as outlined in Sections 4.2.5.1 – 4.2.5.3.

FTIR, solid-state ^{13}C NMR and fluorescence spectroscopic analyses were conducted as outlined in Sections 3.2.5.2 – 3.2.5.4.

5.2.6 Disinfection By-Product Formation Potential Experiments

The various solutions used for DBP formation potential measurement were prepared as outlined in Section 3.2.6.1.

5.2.6.1 Stock Solutions of the MIEX® HPO and MIEX® TPIB Fractions

Stock solutions (1 L) of the MIEX® HPO and MIEX® TPIB fractions in water were produced by initial dissolution of the dried isolate of each fraction (50 – 100 mg) in aqueous sodium hydroxide solution (0.01 M, 1 mL) followed by the addition of MilliQ water. The solutions were filtered through a 0.45 µm glass fibre filter and the DOC concentrations of the MIEX® HPO and MIEX® TPIB fractions measured, as described in Section 2.2.4, to be 29.6 mg L^{-1} and 5.2 mg L^{-1}, respectively.

5.2.6.2 Chlorination Experiments for the MIEX® HPO and MIEX® TPIB Fractions

Aliquots of the MIEX® HPO (67 mL, 29.6 mg L^{-1}) and MIEX® TPIB (383 mL, 5.2 mg L^{-1}) stock solutions were added into separate amber glass bottles and bromide ion stock solution (200 µL, 1000 mg L^{-1}) was added into each bottle. The pH was adjusted to 7.0 through the addition of phosphate buffer and the solutions were diluted with MilliQ water and chlorine stock solution (6 mL, 1000 mg L^{-1}) added to produce an initial chlorine concentration of 6 mg L^{-1} (total volume 1 L), a similar dose to that applied for disinfection at the Wanneroo GWTP. The reaction mixtures were stored in the dark at 25°C for seven days. At various times over 7 days, the residual chlorine equivalent concentrations were measured in duplicate and aliquots (~40 mL) of each reaction mixture were quenched with an aqueous sodium sulfite solution (500 µL, 100 g L^{-1}) and stored in the dark at 5 °C until THM analysis was performed. After 7 days, an additional aliquot (40 mL) of each reaction mixture was quenched with an aqueous sodium sulfite solution (500 µL, 100 g L^{-1}) and stored in the dark at 5 °C until HAA analysis was performed. The initial free chlorine concentration was chosen so as to produce a final 7-day free chlorine equivalent concentration of 0.5 – 1.5 mg L^{-1} for each sample.

5.2.7 Analysis of Disinfection By-Products

HS SPME-GC-MS analysis of the THMs and analysis of the HAAs by liquid-liquid extraction and derivatisation followed by GC-MS were conducted as described in Section 3.2.7.

5.3 Results and Discussion

5.3.1 MIEX® Resin Preconditioning and MIEX® Treatment of W300 Raw Water

Virgin MIEX® resin was sampled from the Wanneroo Groundwater Treatment Plant (GWTP) at the same time as W300 raw water sampling. The virgin MIEX® resin was treated with raw water (W300) to preload the resin with W300 NOM to simulate the plant treatment process on a laboratory scale, using conditions to model full-scale MIEX® treatment at the Wanneroo GWTP. To simulate the MIEX® process on a bench-scale, the Jar Test Protocol developed by Orica Advanced Water Technologies (Holmquist 2006) was used. For this purpose, MIEX® resin (16.6 mL) was preconditioned by treating the resin with repeated aliquots (1.65 L) of the groundwater from bore W300 (total 50 L) before the resin was regenerated.

The preconditioned MIEX® resin was then used to treat the raw water in batches of 20 L before further regeneration was required. This process was repeated until 400 L of raw water was processed to produce the total MIEX® treated water sample. An aliquot of the raw water, and an aliquot of the MIEX® treated water sample, prior to rotary evaporation, was sub-sampled and the DOC concentration, UV_{254}, $SUVA_{254}$ and colour parameters are shown in Table 5.1.

Table 5.1 DOC concentration, UV_{254}, $SUVA_{254}$ and colour parameters for W300 raw water before and after MIEX® treatment.

Sample	DOC (mg L^{-1})	UV (cm^{-1})	$SUVA_{254}$ (m^{-1} L / mg C)	Colour (HU)
Raw Water (W300)	23.3	5.20	4.5	220
MIEX® treated water	9.8	2.63	5.4	101

The DOC concentration in the raw water was significantly reduced (58 %) after MIEX® treatment. This degree of removal was consistent with a previous study (Warton et al. 2007, a) in which water samples were collected from several points in the treatment stream at the Wanneroo GWTP on two occasions, one in winter and one in summer. In the summer blend water, 49 % of DOC was removed by MIEX® treatment, whilst the winter blend showed 54 % removal. Other pilot plant studies on groundwaters, surface waters and reservoirs (Drikas et al. 2003; Budd et al. 2003; Fabris et al. 2007; Boyer and Singer 2005) have shown MIEX® treatment producing removals of 36 – 80 % of the DOC concentration. Hence, the bench-scale preconditioning protocol used in this study does seem to reasonably replicate large-scale MIEX® treatment.

A slight increase in $SUVA_{254}$ following MIEX® treatment reflects some selectivity in the DOC removal. This result is in contrast to a long term case study of MIEX® pre-treatment at the Mt Pleasant WTP (Drikas et al. 2011) which showed MIEX® pre-treatment consistently produced water with a lower $SUVA_{254}$ because more UV-absorbing organic compounds were preferentially removed by MIEX®. An increase in $SUVA_{254}$ was also observed in the study of Warton et al. (2007 a), during studies of the water blend at the Wanneroo GWTP in summer. The $SUVA_{254}$ was strongly influenced, however, by UV_{254}-absorbing species of very high MW (> 67 kDa) rather than DOC in the 1 to 10 kD MW region as shown in the size exclusion chromatograms (Warton et al. 2007 a). This high MW peak in the SEC-UV_{254} chromatogram was also observed in the corresponding winter blend study, and seems to be peculiar to local Western Australian waters (Warton et al. 2007 a). A similar, but relatively lower in abundance high MW peak was seen in the SEC for the W300 raw water, and this material did not appear to be removed by MIEX® treatment (Section 5.3.1.1, Figure 5.3). The lack of removal of this high MW peak through MIEX® treatment, may have caused the slight increase in $SUVA_{254}$ post treatment. Huber and Frimmel (1996) proposed that the high MW peak represents colloidal organic and inorganic substances: substances which are largely unaffected by anion exchange processes (Allpike et al. 2005). Conversely, MIEX® treatment removed a large proportion of the coloured DOC in the raw water (54 %), indicating its efficiency in removing the coloured or humic dominated fraction of DOC (Edwards and Amirtharajah 1985; Bennett and Drikas 1993). Coloured water is an aesthetic

problem for consumers and efficient removal, as achieved by MIEX® treatment, is an important consideration in water treatment processes.

5.3.1.1 Size Exclusion Chromatographic Analysis

The size exclusion chromatographic profiles of the raw water before and after MIEX® treatment with organic carbon (SEC-OCD) and UV detection at 254 nm (SEC-UV_{254}) are shown in Figure 5.3a and b, respectively. The broad MW distribution of the SEC-UV_{254} profiles (Figure 5.3b) are generally consistent with the waters described in Section 2.2.3, as well as previous studies of Wanneroo groundwater (Warton et al. 2007, a; Allpike et al. 2005), and other water sources such as lakes (Peuravuori and Pihlaja 1997; Vrijenhoek et al. 1998) and rivers (Vrijenhoek et al. 1998). The profiles have been resolved into 8 different MW regions according to a previously reported numbering system (Allpike et al. 2005; Huber and Frimmel 1996). The raw water shows some colloidal material (region 1), a relatively large proportion of unresolved high MW humic substances (regions 2 – 4), a moderate amount of lower MW monoprotic organic acids (regions 5 – 7) and negligible signal at lowest apparent MW (region 8).

The SEC-OCD and SEC-UV_{254} profiles of the raw and MIEX® treated water samples indicate a moderate proportion of DOC was removed by MIEX® treatment, with the medium MW range (6000 – 1000 Da) material showing greatest reduction. The high MW region 1 was relatively unaffected by MIEX® treatment. This region represents colloidal (and inorganic) material which is largely unaffected by the anion exchange process (Allpike et al. 2005). The persistence of this material and loss of medium-low MW organic material will lead to an increase in $SUVA_{254}$ as shown in Table 5.1, since colloidal material has been shown to have a high UV absorbance activity due to light scattering effects (Huber and Frimmel 1996). Regions 2 – 4 were only slight removed during MIEX® treatment. Humic and fulvic hydrophobic materials are concentrated in this SEC region (Allpike et al. 2005). It has been reported that NOM in groundwaters on the Swan Coastal Plain is thought to consist largely of tannin derived substances, probably from condensed tannins composed predominantly of phenolic moieties, with relatively minor carboxylic acid content (Heitz 2002). Phenolic moieties are not efficiently removed by the MIEX® ion exchange

mechanism as they are likely to be present in their protonated (uncharged) form at the pH of treatment.

Regions 5 – 7 were most significantly reduced by MIEX® treatment. This is consistent with anionic species, such as carboxylic acids, which are concentrated in this region, being readily removed by the ion exchange process.

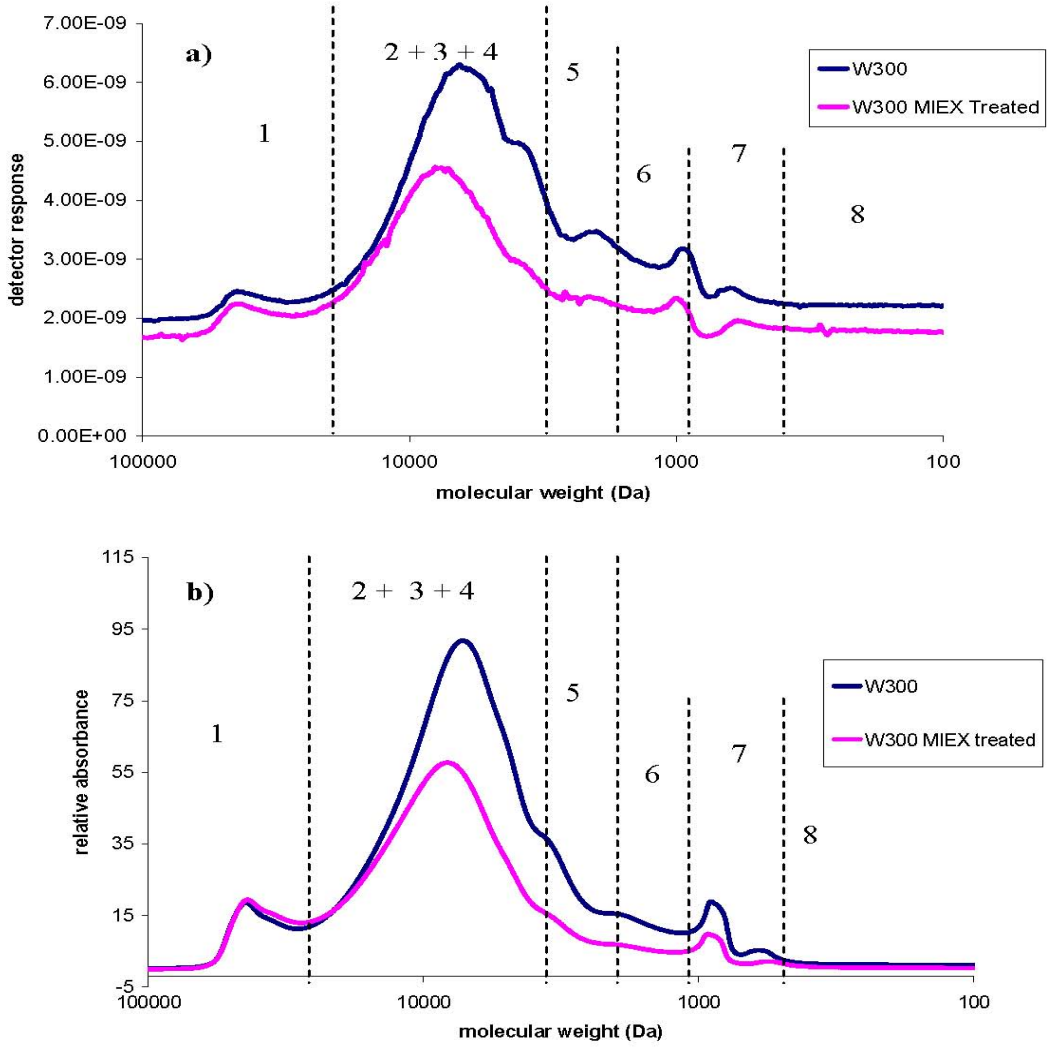

Figure 5.3 Molecular weight distribution of the raw water before and after MIEX® treatment measured by a) SEC-OCD and b) SEC-UV_{254} detection. Numbers correspond to eight distinct MW regions as described by Huber and Frimmel 1996 and Allpike et al. 2005.

5.3.1.2 Fluorescence Excitation-Emission Spectroscopy

Various fluorescence spectroscopy techniques have been used to characterise NOM samples (Chen et al. 2003, b). Fluorescence can provide important chemical information because all NOM samples have unique fluorescence signatures, reflecting the structure and functionality of the sample (Swietlik and Sirorska 2004). The fluorescence excitation-emission (EEM) profiles of the raw water before and after MIEX® treatment are shown in Figure 5.4, with all supporting literature explaining the major fluorescent components discussed in detail in Section 3.3.2. The peaks running diagonally through the emission range of 400 – 500 nm and an excitation range of 200 – 260 nm are instrument artefacts of glass and water interactions present in all EEM spectra. The peaks running diagonally through the emission range of 250 – 380 nm at an excitation range of 270 – 290 nm are due to Rayleigh/Tyndall scattering lines (Caron and Smith 2011).

Prior to treatment, the raw water (Figure 5.4a) showed a high amount of humic-like (Ex: ≥ 280 nm – Em: > 380 nm) and fulvic-like (Ex: < 250 nm – Em: > 350 nm) material (Chen et al. 2003, b). The spectral intensity in Figure 5.4 is represented by the contour lines: the closeness of lines increasing with increasing intensity. The high EEM intensity of the raw water and the only slightly lower intensity of the MIEX® treated water, reflect the high DOC concentrations of these two samples (Hua et al. 2007). A high DOC concentration is normally found in waters with higher fluorescence intensity and broader fluorescence centres (Hua et al. 2007). The DOC concentrations of the raw water (23 mg L^{-1}) and the MIEX® treated water (10 mg L^{-1}) are considered high for fluorescence spectroscopic analysis. The closeness of the contour lines and occurrence of two peaks, a large one at Ex: 330 nm – Em: 420 nm and a less abundant one at Ex: 260 nm – Em: 420 nm, in the EEM spectra of the raw water (Figure 5.4a) are indicative of humic- and fulvic-like material (Hua et al. 2007; Her et al. 2003; Kim et al. 2006). After MIEX® treatment (Figure 5.4b), the humic- and fulvic-like material was of a slightly lower intensity. Partial removal of these structures might also be reflected by the moderate reduction of material in SEC regions 2 – 4 (Figure 5.3). But, as the fluorescence EEM spectra of the raw water and MIEX® treated water are similar, suggesting similar chemical characteristics, MIEX®

treatment appears to have had little effect on EEM spectral characteristics of NOM in this water source.

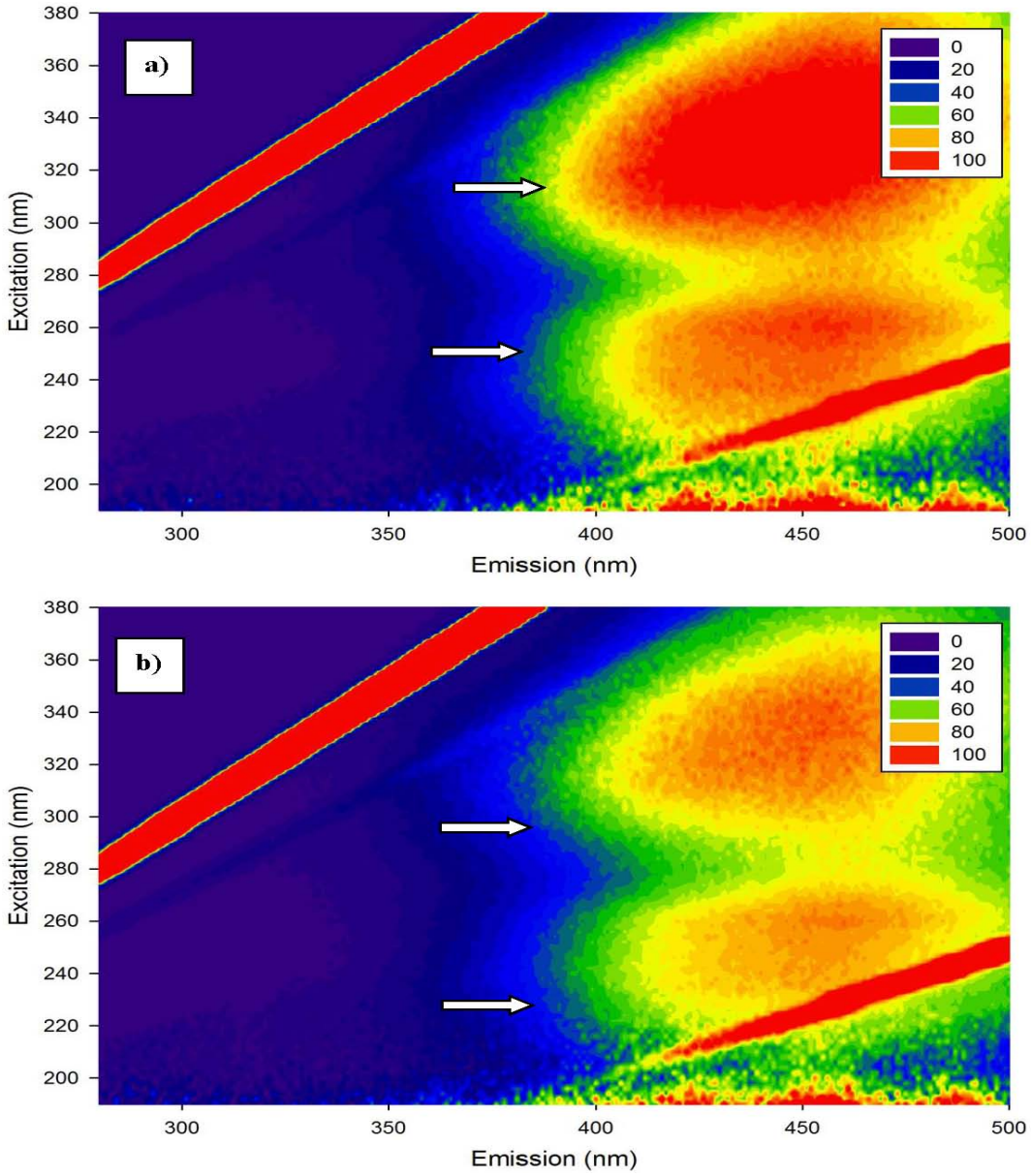

Figure 5.4 Excitation-emission (EEM) fluorescence spectra of the a) raw water and b) MIEX® treated water. White arrows represent 'humic-like' components within the spectra. 'Protein-like' components within the spectra could not be identified due to the high concentration of 'humic-like' material.

5.3.2 Isolation of XAD Fractions from NOM Remaining After MIEX® Treatment

After MIEX® treatment of W300 groundwater (400 L), the treated water was concentrated to 70 L and the NOM in the concentrated sample was fractionated with the XAD-8/XAD-4 resin procedure. Four separate fractions, MIEX® HPO, MIEX® TPIB, MIEX® TPIN and MIEX® HPI were isolated. The first three fractions were isolated in solid form and the MIEX® HPI (the final eluent from the procedure) remained as a liquid, with the total DOC recovered from the XAD-8/XAD-4 method being 30 %, consistent with the recovery observed in Chapter 4 of 35 % (Section 4.3.1) and previous resin fractionation studies (Leenheer et al. 1987). In comparison to the DOC recovery (61 %) achieved using the UF isolation method in Chapter 3, the XAD-8/XAD-4 resin procedure did not allow a higher recovery of total DOC. The mass and relative proportions of isolated XAD fractions are shown in Table 5.2.

Table 5.2 Isolated mass and relative proportions of the NOM fractions.

Sample	Isolated Mass (mg)	Calculated Weight of C in Isolate based on Elemental Analysis % C (mg)	Proportion of Total Recovered C as a Percentage^
MIEX® HPO	2050	1005	88 %
MIEX® TPIB	248	123	11 %
MIEX® TPIN	20	8	0.8 %
MIEX® HPI	4*	N/A	0.2 %

N/A – not calculated
^ Based on mg C of each isolate (from the elemental analysis) / total mass of C of all isolates (from the elemental analysis)
*This fraction was not isolated as a solid form. The isolated mass was calculated to be 4 mg of organic carbon based on the concentration of DOC in the aqueous isolate.

The relative proportions of XAD fractions from the NOM remaining after MIEX® treatment showed some differences to the relative proportions of XAD fractions isolated from the untreated NOM (Table 4.1). Following MIEX® treatment, there was a high proportion of HPO, similar amounts of TPI and lower HPI, consistent with the preferential removal of mid to low MW material in MIEX® treatment (Slunjski et al. 2000, b; Lee et al. 2003; Drikas et al. 2003), which concentrates in the TPI and HPI fractions. The degree of anionic charge in the TPI and HPI fractions is the key factor in the removal of these fractions by the MIEX® process (Sharp et al.

2006, a). Any preferential removal of TPI is important, given the ineffectiveness of coagulation in removing TPI fractions (Bond et al. 2010). MIEX® treatment has been previously shown (Huber and Frimmel 1996) to be inefficient in the removal of humic and fulvic hydrophobic material. The relatively inefficient removal of the humic rich HPO fraction after MIEX® treatment concurs with the persistence of high MW organic material identified by SEC analysis (OCD and UV_{254} detection) reported here (Figure 5.3) and previously (Allpike et al. 2005).

5.3.3 Characterisation of Solid XAD Fractions from NOM Remaining After MIEX® Treatment

5.3.3.1 Elemental Analysis and Atomic Ratios

General compositional information was provided by elemental analysis of the three fractions obtained in solid form (MIEX® HPO, MIEX® TPIB, MIEX® TPIN), with the elemental percentage compositions and atomic ratio data of these fractions listed in Table 5.3. The low ash content of the MIEX® HPO fraction (3.01 %) is indicative of high organic matter content and low inorganic content. The low amount (20 mg) of the MIEX® TPIN fraction prohibited measurement of oxygen and ash content.

Table 5.3 Elemental percentage compositions and atomic ratio data of the solid XAD fractions isolated from the MIEX® treated water.

Sample	% C	% O	% H	% N	% S	% Ash	H/C	O/C	N/C
MIEX® HPO	49.03	38.37	4.12	1.18	0.82	3.01	1.00	0.58	0.01
MIEX® TPIB	4.98	15.95	3.87	0.72	7.46	33.35	9.26	2.40	1.28
MIEX® TPIN	41.87	ND*	4.63	1.90	0.48	ND*	1.32	ND*	0.04

* ND - Not determined due to insufficient sample for analysis

The elemental compositions of the three fractions varied considerably (Table 5.3), similar to the large variation in composition from the untreated water fractions (Table 4.2), but the values are still generally typical of groundwater NOM (Croué 1999; Croué et al. 2003; Leenheer et al. 2000). The H/C, O/C and N/C ratios are also typical of reported ratios of HPO and TPI fractions from unpolluted groundwaters (Christensen et al. 1998). The H/C ratio of the MIEX® HPO fraction (~ 1) is indicative of aromatic rich aquatic humic material (Kim et al. 2006). The TPI fractions had higher O/C and N/C values, due to the concentration of heteroatom-

containing compounds in these fractions (Leenheer et al. 2000; Croué et al. 2003). Nitrogen concentrations generally increase with hydrophilic character, whilst carbon and hydrogen levels decline (Leenheer et al. 2000). Malcolm et al. (1995) isolated HPO and TPI fractions from a variety of surface waters in France, England, Norway and the United States and the TPI fractions were reported to have a relatively low chlorine reactivity compared to the humic and fulvic rich HPO fractions. Given the likely higher chlorine reactivity and proportion of the HPO fraction compared to the untreated HPO in Chapter 4, it is the more significant fraction with respect to disinfection by-product (DBP) formation. The DBP formation potential of the XAD fractions from NOM remaining after MIEX® treatment will be discussed in detail in Section 5.3.3.7.

The measured elements of the MIEX® TPIB fraction (C, H, N, O, S, ash) accounted for only 66.3 % of the material, indicating other elements that were not measured as part of the elemental analysis were present in significant quantities. A sub-sample of the MIEX® TPIB fraction was dissolved in MilliQ water, the DOC concentration of this sample was determined, and concentrations of selected metals and other ions in the TPIB fraction were measured by atomic absorption spectroscopy. The results of these analyses are listed in Table 5.4.

Table 5.4 Elemental composition of the TPIB fraction isolated from the MIEX® treated water.

Sample	Concentration (mg L^{-1})										
	Na	**K**	**Mg**	**Ca**	**Al**	**Si**	**Fe**	**Mn**	**Cu**	**Cl**	**DOC**
MIEX® TPIB	7.6	0.02	0.15	1.18	0.23	0.5	0.03	ND*	0.04	20	1.6

* ND – not detected

The results suggest that the MIEX® TPIB fraction contained relatively high concentrations of the elements sodium and chlorine, which would have been volatilised at the combustion temperatures used during the elemental analysis. The high concentrations of sodium and chlorine in the MIEX® TPIB fraction suggest insufficient cleaning of the Dowex MSC-1 H resin, prior to sample application. A similar occurrence was reflected in the elemental analysis of the TPIB fraction of the untreated water (Table 4.3). Desalting the MIEX® TPIB sample was considered, but as it a very laborious technique, with risks including possible sample alteration and

lower sample recovery, the decision was made to use the MIEX® TPIB fractions as obtained.

5.3.3.2 Fourier Transform Infrared Spectroscopic Analysis

FTIR spectra of the MIEX® HPO and MIEX® TPI fractions are presented in Figure 5.5. The three fractions showed similar IR absorption, typical of the profile of humic substances (Stevenson 1994) and the untreated fractions in Chapter 4, reflecting qualitatively similar structural and functional group features. The similarity of the FTIR bands of HPO and TPI fractions has been reported in several previous studies (Stevenson 1994; Rostad et al. 2000; Leenheer 1981). The most prominent features in the HPO spectrum in the current study were aliphatic hydrocarbon absorption bands at 2800 – 3100 cm^{-1} (yellow region), representative of C-H stretching from methyl and methylene carbons, accompanied by a dominant carboxyl peak at 1725 cm^{-1} in the infrared spectrum due to stretching of carboxylic and carbonyl groups (pink region, (Rostad et al. 2000)). This strong carboxyl peak was accompanied by a broad aromatic and ketonic peak at 1620 cm^{-1} (purple region) which can be assigned to aromatic C=C stretching and asymmetric C=O stretching in COO^- groups (Rostad et al. 2000). Consistent with a higher hydrophilic nature as shown by elemental analysis (Table 5.3), the TPI fractions showed more pronounced aliphatic bands at 2900 cm^{-1} (yellow region), O-H stretching around 2800 – 3600 cm^{-1} (green region) and C-O and alcohol stretching at 1050 – 1250 cm^{-1} (blue region).

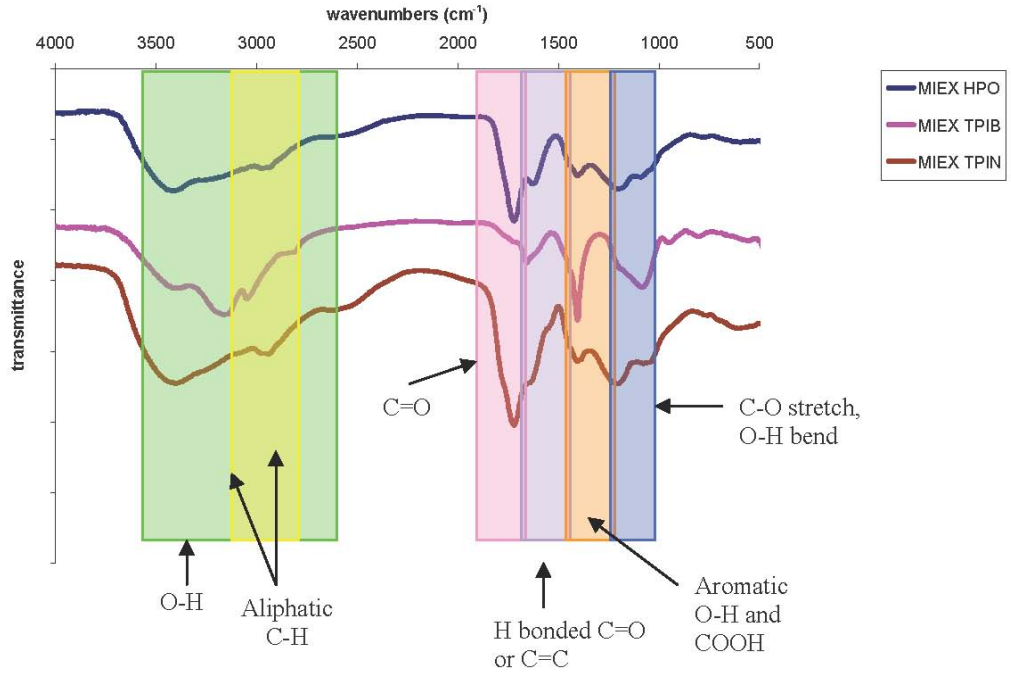

Figure 5.5 FT-IR spectra for the three XAD fractions isolated from MIEX® treated water.

MIEX® treatment of the raw water prior to fractionation did result in some variations in the FTIR spectra of the NOM isolates compared to the raw water isolates (Figure 4.2). Most noticeably, the MIEX® treated samples (Figure 5.5) displayed a significant absorption in the 1000 – 1200 cm^{-1} region, possibly representing C-O stretching of various groups (Takács and Alberts 1999), whereas this absorption was not seen in the raw water isolates. Several functional groups give signals in this region, including bands due to C-O stretching of alcohols, C-O stretching and O-H deformations of carboxylic acids, C-O stretching of esters and C-O-C stretching of ethers (Aiken 1985; Stevenson 1994). The nature of MIEX® treatment (i.e. anion exchange) suggests that hydroxy groups may be particularly susceptible to removal by MIEX®. A reduction in the relative proportion of the band at 1620 cm^{-1} for the TPI fractions isolated from MIEX® treated water compared to fractions from the raw water possibly indicates a reduction in the amount of aromatic carbon in the fractions isolated from MIEX® treated water. Ineffective removal of the high MW, highly aromatic fraction was also observed in the HPSEC results (Figure 5.3).

5.3.3.3 Solid-State ^{13}C Nuclear Magnetic Resonance Spectroscopic Analysis

The solid-state ^{13}C NMR spectra for the MIEX® HPO and MIEX® TPIB fractions are shown in Figure 5.6. The corresponding MIEX® TPIN fraction could not be analysed due to insufficient sample. The low intensity broad peaks in the spectra of the HPO and TPIB fractions were generally similar to the solid-state ^{13}C NMR spectra reported for other aquatic NOM samples (Chen and Edwards 1999; Chen et al. 2002; Chen et al. 2003, a; Rostad et al. 2000; Mash et al. 2004; Lankes et al. 2008) and the corresponding XAD fractions from the untreated water sample in Chapter 4 (Section 4.3.2.3). The MIEX® HPO fraction showed relatively larger signals of aromatic carbon (pink region) and oxygenated aliphatic carbon (such as methoxy groups) (yellow region) than the MIEX® TPIB fraction, consistent with a previous study of HPO and TPI fractions isolated from three water storage reservoirs in the semi-arid area of Southwest USA (Mash et al. 2004). In this previous study (Mash et al. 2004), the HPO fractions from all three reservoirs showed similar solid-state ^{13}C NMR spectra, with the oxygenated aliphatic carbon signal contributing 46 – 48 % of the total peak area, and aromatic carbon contributing 12 – 14 % of the total peak area. The oxygenated aliphatic carbon signal for the TPI fractions from these three reservoirs contributed 39 – 41 % of the total peak area, with the aromatic carbon signal contributing 7 – 9 % of the total peak area. Conversely, the TPI fractions showed a higher contribution of aliphatic material (23 – 24 %), compared to the HPO fractions (16 – 18 %) (Mash et al. 2004), as observed in the current study. The sharp signal at 30 ppm (green region) for the TPIB fraction is indicative of long chain aliphatic moieties (Lankes et al. 2008).

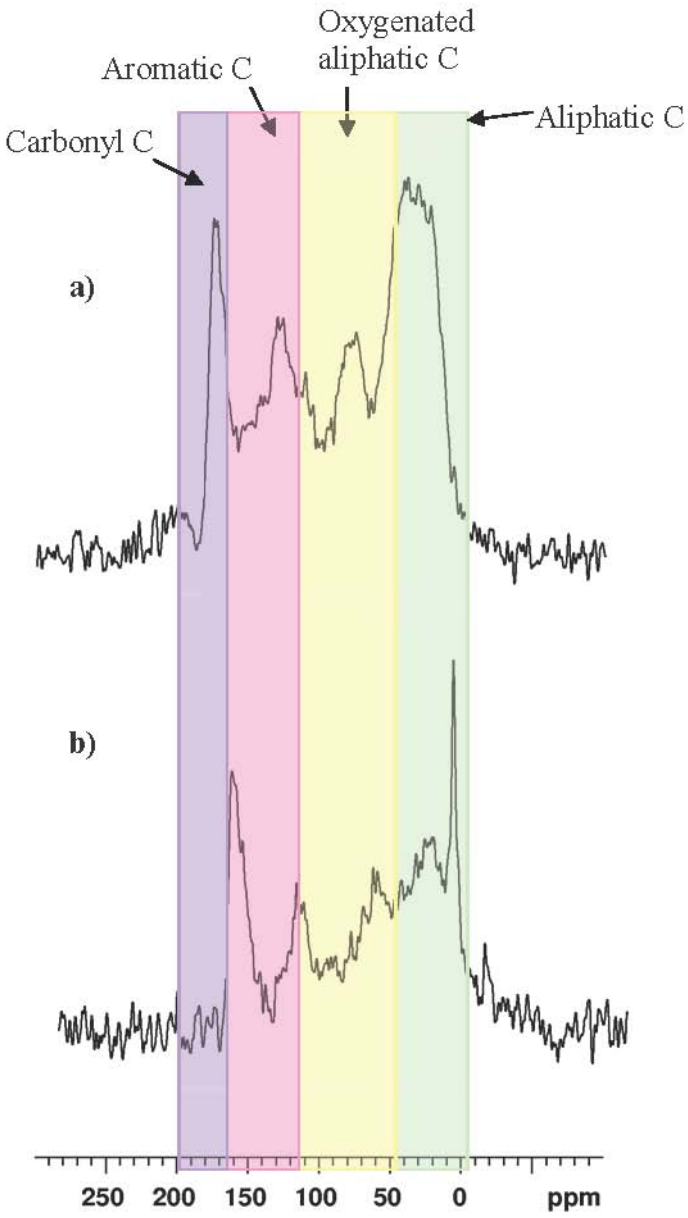

Figure 5.6 Solid-state ^{13}C NMR spectra of the a) HPO and b) TPIB fraction isolated from the MIEX® treated water.

For comparison purposes, the relative signal areas measured for the fractions were integrated over four broad regions and attributed to functional groups, as discussed in detail in Section 4.3.2.3. The relative proportions of carbon types from integration of the two spectra are shown in Figure 5.7. Overall, the distribution of the types of carbon from solid-state ^{13}C NMR spectroscopy were similar for the two samples, but the carbon distribution differed to the untreated fractions in Chapter 4, and other fractions isolated from Wanneroo groundwater (Allpike 2008). The major carbon type for the MIEX® HPO and MIEX® TPIB fractions was oxygenated aliphatic

carbon (32 and 35 %, respectively), with aliphatic carbon the second most abundant carbon type in both fractions. It appears that MIEX® treatment removed a small component of the aromatic fraction, which was also observed in the FTIR spectra (Figure 5.5). Carbonyl carbon was the least abundant carbon type in both fractions, as found in previous studies (Allpike 2008), and in earlier studies of the UF fraction (Chapter 3) and the fractions isolated from untreated water (Chapter 4).

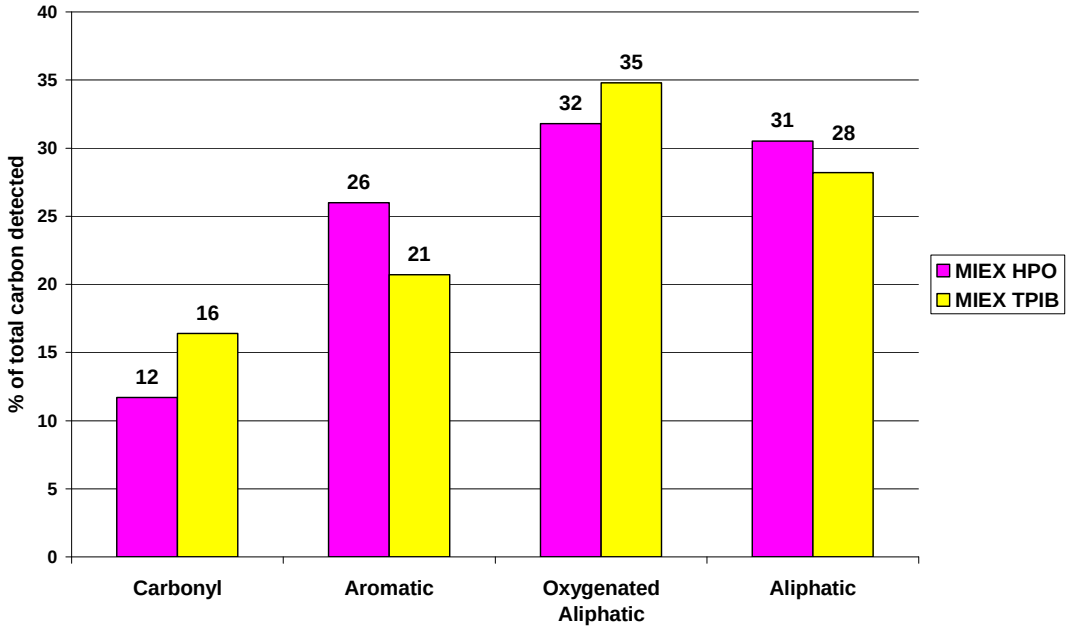

Figure 5.7 Relative proportions of carbon types in the solid-state ^{13}C NMR spectra of the isolated NOM fractions separated from water after MIEX® treatment.

In a study of NOM isolated from three Australian sources (two from Victoria and one from Wanneroo GWTP), Wong et al. (2002) used solid-state ^{13}C NMR spectroscopy to obtain structural characteristics of these samples. In the study by Wong et al. (2002), the ^{13}C NMR spectrum of isolated material from the Wanneroo GWTP was similar to the spectra in the current research (Figure 5.6), dominated by aliphatic carbon. Unfortunately in the previous research, integrated areas of each spectral region were not reported, making a direct comparison of spectral response difficult. Fractionation of the Wanneroo sample resulted in a greater proportion of aliphatic and oxygenated aliphatic carbon for the hydrophobic sample (Wong et al. 2002), as observed for the NOM fractions obtained after MIEX® treatment (Figure 5.7). Overall, treatment of the raw water with MIEX® resin showed increases in the relative amounts of aliphatic carbon and oxygenated aliphatic carbon, with small

decreases in the relative amounts of aromatic carbon and carbonyl carbon. The ion exchange properties of the MIEX® resin mean that it is likely to remove the negatively charged fraction of aquatic NOM.

5.3.3.4 Pyrolysis-Gas Chromatography-Mass Spectrometry

Conventional flash pyrolysis-GC-MS was performed at 650 °C for 10 seconds on the solid samples of the MIEX® HPO, MIEX® TPIB and MIEX® TPIN fractions of NOM remaining after MIEX® treatment. The total ion chromatograms from py-GC-MS of these fractions are shown in Figure 5.8a – c, respectively. The major pyrolysis products from the fractions and their likely biological precursors are listed in Table 5.5. A much larger suite of tentatively identified products are listed in Appendix 2.

The high salt content present in the MIEX® TPIB fraction (Table 5.4) reduced the NOM content in the sample and therefore the product abundance. The high salt content possibly also inhibited product formation in the pyrolysis-GC-MS technique, limiting comparison of this fraction to the other fractions.

Approximately 50% of the pyrolysis products of NOM can usually be assigned to specific biochemical precursors (Leenheer 2009), but as the yields of analysable products from pyrolytic techniques (such as pyrolysis-GC-MS) are often low (< 25 %), conclusions regarding the original structure of the NOM in the samples must be drawn with caution (Kögel-Knabner 2000). The MIEX® HPO fraction showed a relatively high abundance of aromatic hydrocarbons (peaks 15, 20, 25), alkylphenols (31, 37) and PAHs (28, 33, 47), similar to the pyrolysis products observed from other aquatic HPO fractions (Croué et al. 1999, b; Harrington et al. 1996) and the raw HPO fraction (Figure 4.4a). Flash pyrolysis (at 625 °C) was one technique used for characterisation of the Suwannee, South Platte and Blavet River NOM samples in the study of Croué et al. (1999 b), with phenols and cresols shown to be the predominant peaks for the HPO fractions. The high content of phenolic (Templier et al. 2005; Berwick et al. 2010, b) and other aromatic (Joll et al. 1999) compounds in pyrolysis product mixtures from NOM samples derived from groundwaters has been previously reported; indeed aromatic hydrocarbons are common flash pyrolysis products of aquatic NOM and they are derived from several biomolecular sources (Templier et al. 2005). Phenols and cresols can be derived from

polyhydroxyaromatic type structures (Heitz et al. 2001; Croué et al. 1999, b), and are often attributed to intact or partially degraded lignin and tannin constituents of plant tissues (McIntyre and McRae 2005). In contrast to the MIEX® HPO fraction, the MIEX® TPIB and MIEX® TPIN fractions contained lower proportions of phenols, but higher proportions of nitrogenous products, such as acetonitrile (4) and pyrrole (11), reported to be derived from protein and amino sugar precursors (Gadmar et al. 2005; Croué et al. 2003). The higher nitrogen content of the pyrolysis products from the MIEX® TPI fraction compared to the MIEX® HPO fraction was also reflected in the results of elemental analysis (Table 5.3) where the MIEX® TPI fractions were more nitrogen-enriched than the MIEX® HPO fraction. A previous study on fractionation of NOM from a surface water source in France by the XAD-8/XAD-4 resin method also used py-GC-MS to characterise the NOM isolates (Croué et al. 1999, b). It was found that phenol and cresol were the major peaks in the chromatogram of the XAD-8 fraction (equivalent to the HPO fraction in the current study) whilst acetonitrile and pyrrole were more abundant in the chromatogram of the XAD-4 fraction (equivalent to the TPI fractions here) (Croué et al. 1999, b), consistent with the observed products in the current study.

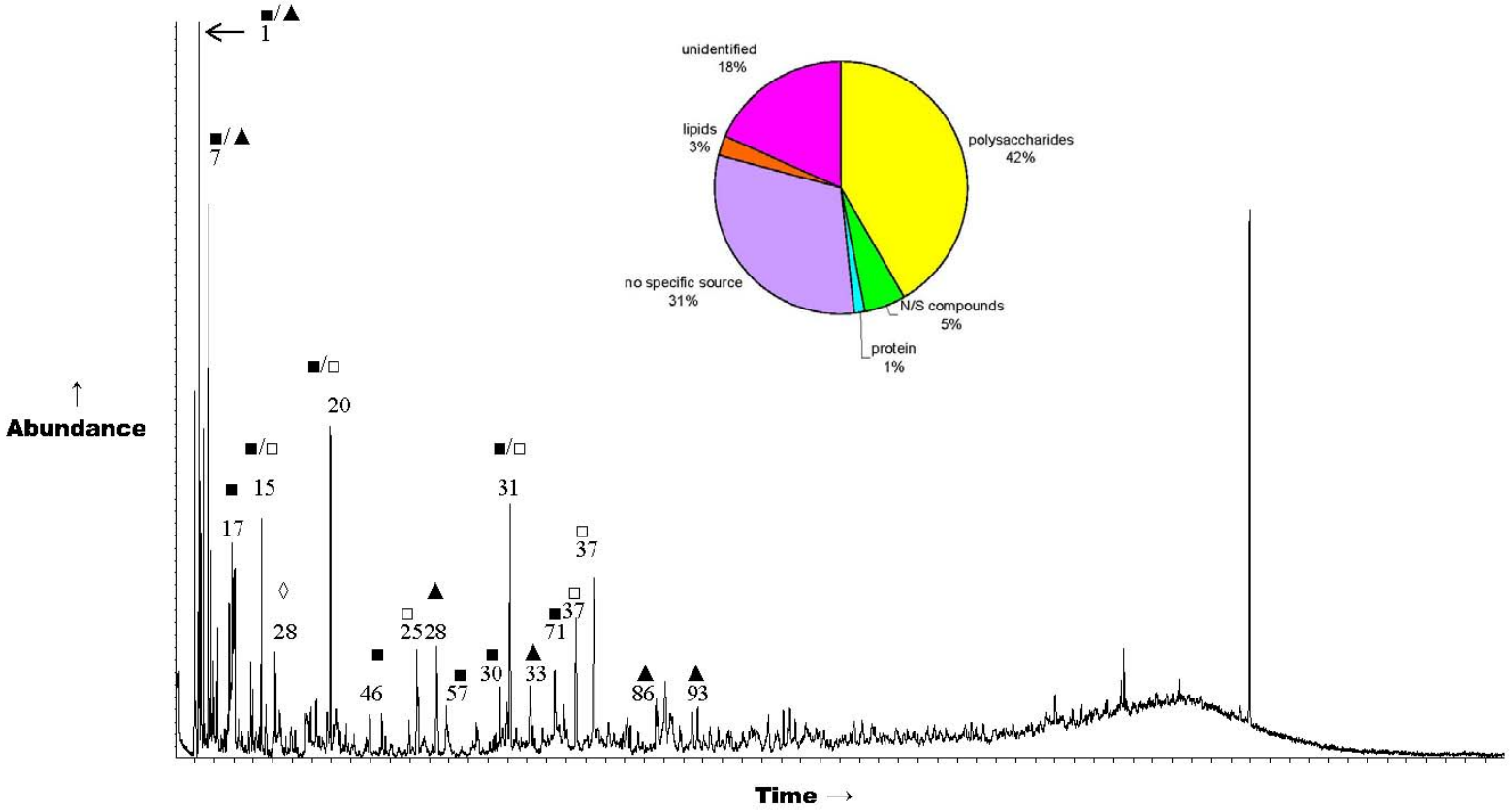

Figure 5.8a Total ion chromatogram from the py-GC-MS of the MIEX® HPO fraction. Peak assignments correspond to products listed in Table 5.5: ■ polysaccharides, ● N/S compounds, □ protein, ◊ lipids, ▲no specific source. The pie chart reflects relative proportions of six major product and precursor types.

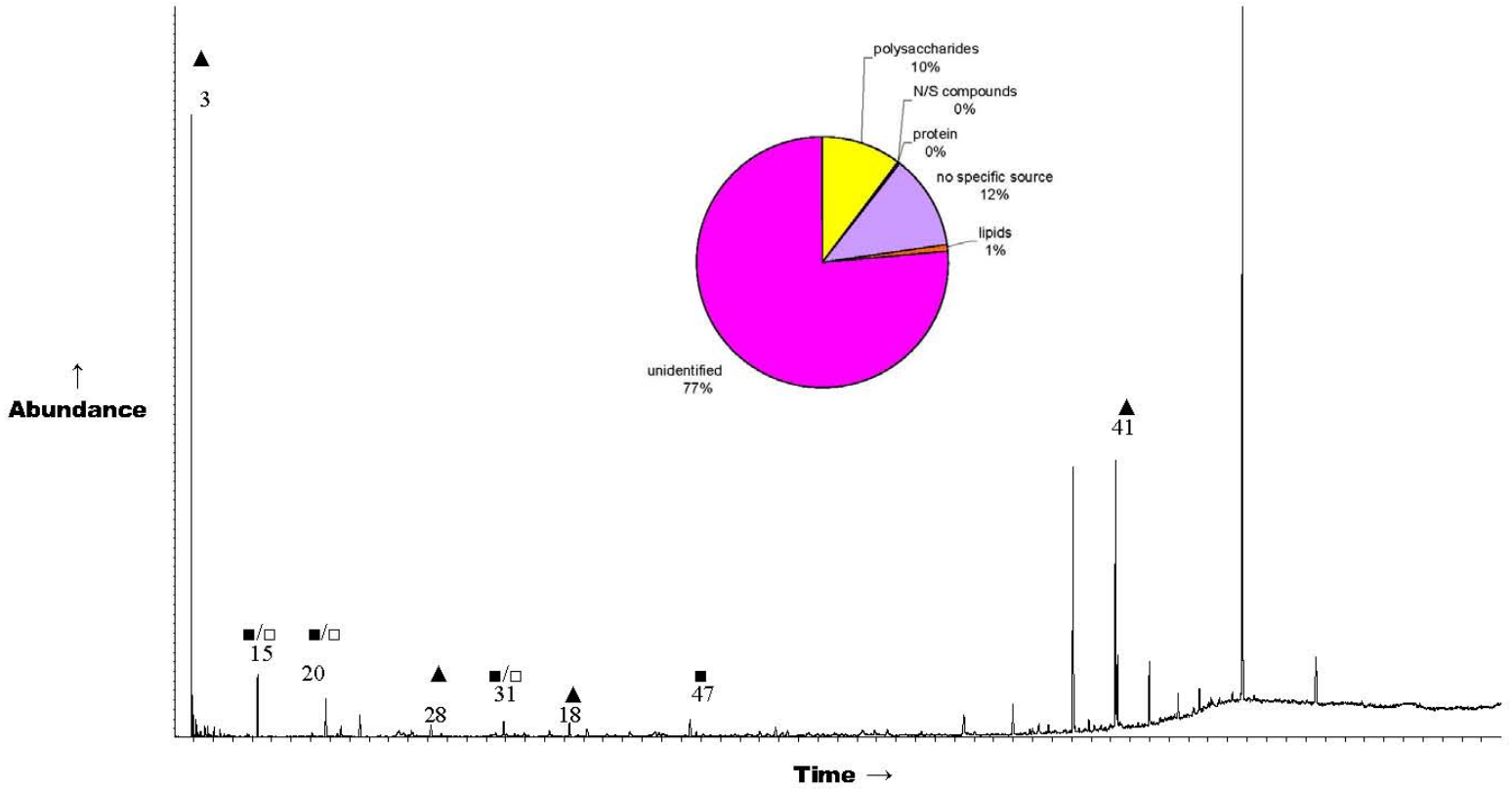

Figure 5.8b Total ion chromatogram from the py-GC-MS of the MIEX® TPIB fraction. Peak assignments correspond to products listed in Table 5.5: ■ polysaccharides, ● N/S compounds, □ protein, ◊ lipids, ▲no specific source. The pie chart reflects relative proportions of six major product and precursor types.

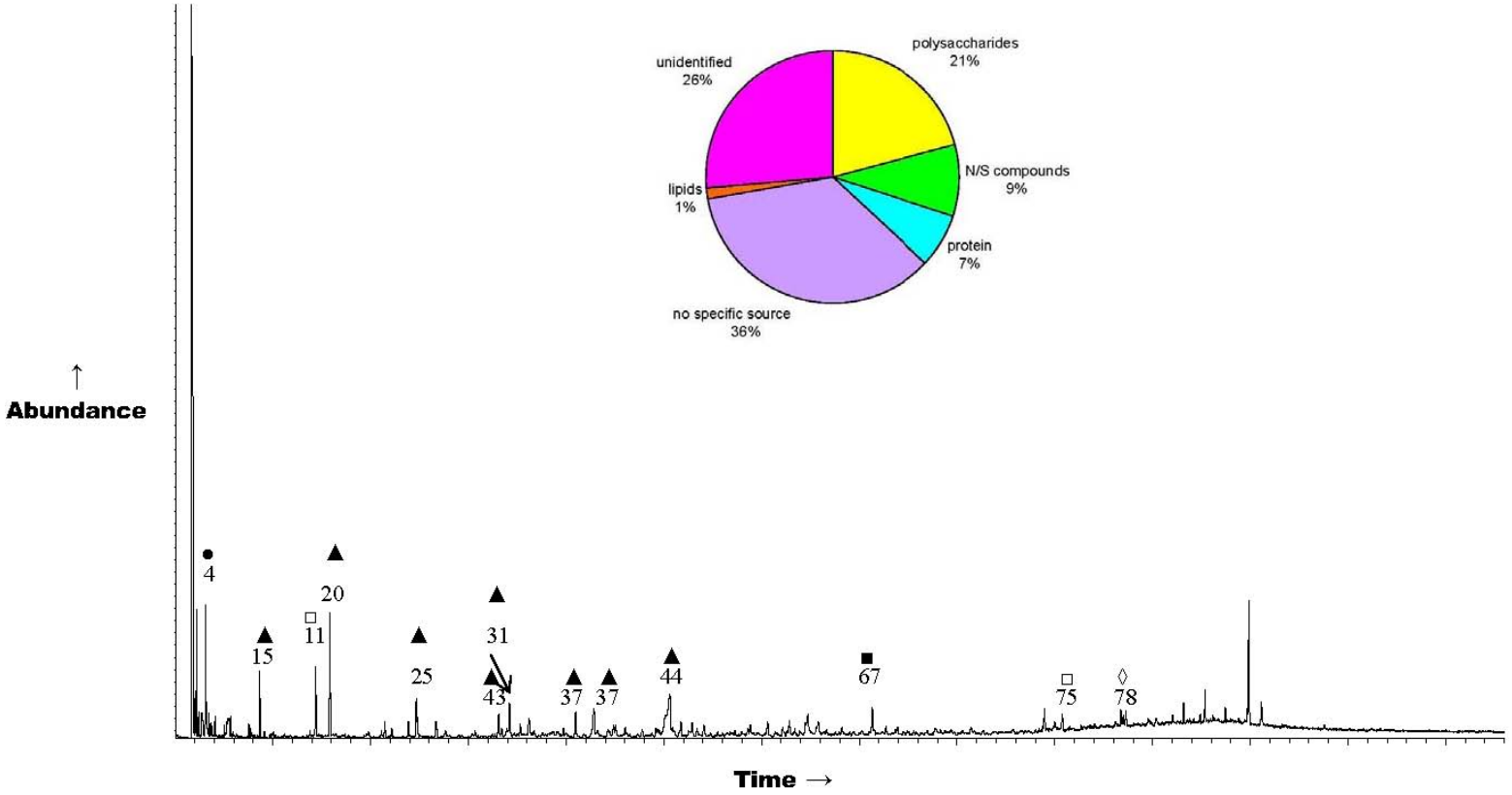

Figure 5.8c Total ion chromatogram from the py-GC-MS of the MIEX® TPIN fraction. Peak assignments correspond to products listed in Table 5.5: ■ polysaccharides, ● N/S compounds, □ protein, ◊ lipids, ▲no specific source. The pie chart reflects relative proportions of six major product and precursor types.

Table 5.5 Major pyrolysis products from the XAD fractions of the NOM isolated from the MIEX® treated water and their likely origin. Full list of tentatively identified products can be found in Appendix 2.

Peak Nº.	Compound	Possible Origin
1	acetaldehyde / methyl propene / 1,3-butadiene	polysaccharides /no specific source
3	propylene	no specific source
4	acetonitrile	N/S compounds
7	cyclobutane / acetone / furan	polysaccharides / no specific source
11	pyrrole	protein
15	benzene	polysaccharides/ protein / lignin
17	2-methyl propanal	polysaccharides
18	indene	no specific source
20	toluene	polysaccharides / protein / lignin
25	xylene	protein / lignin
28	styrene	no specific source
30	2-cyclopenten-1-one	polysaccharides
31	phenol	polysaccharides/ protein / lignin
33	C_3 benzene	no specific source
37	cresol	lignin / tannin / protein
41	cyclotetradecane	no specific source
43	ethyltoluene	no specific source
44	benzoic acid	no specific source
46	2-furancarboxaldehyde	polysaccharides
47	naphthalene	polysaccharides
57	2-methyl-2-cyclopenten-1-one	polysaccharides
67	diacetylbenzene	polysaccharides
71	ethyl hexanol	polysaccharides
75	1,4-diaza-2,5-dioxobicyclo[4.3.0]nonane	protein
78	hexadecanoic acid	lipids
86	dimethylphenol	lignin / tannin
93	dimethylphenol	lignin / tannin

In order to simplify the pyrolysis products from the three different fractions, the tentatively identified products were allocated to one of six groups based on the probable origin of the fragment. Four of the categories related to distinct biological origin or chemical structure, with two other categories referring to “other products” which could be derived from multiple sources or could not be identified by GC-MS. These classifications are based on a modified version of the classification system of Bruchet and colleagues (Bruchet et al. 1989; Bruchet et al. 1990). The proportion of

species within these categories was determined by summing the areas of all peaks within a category and calculating the ratio of this total category peak area to the total area of detected peaks as a percentage. This process was carried out in an identical manner for all three samples, providing a consistent method for comparison. The relative proportions of these groups expressed as a percentage of the total pyrolysis product peak area are shown as pie charts in Figure 5.8a – c. This semi-quantitative approach added to the chemical assessment of different samples, and revealed several distinct differences between the three fractions. The MIEX® HPO fraction was rich in polysaccharides (furans, cyclopentenes), tannins and lipids, with minimal input from protein or nitrogen- or sulfur-containing (N/S) compounds, similar to the untreated HPO fraction (Figure 4.4a). The high abundance of polysaccharides present in the MIEX® HPO fraction was reflected by the high oxygenated-aliphatic and aromatic carbon content seen in the solid-state ^{13}C NMR spectroscopic analysis (Figure 5.7). The MIEX® TPIN fraction was rich in N/S compounds, proteins and polysaccharides. The higher abundance of oxygenated and nitrogenous products was consistent with the higher total nitrogen content and N/C ratio (Table 5.3) observed from the elemental analysis of this sample.

Whereas MIEX® treatment preferentially removed TPI and HPI material, as indicated by the slight redistribution of the fractions following treatment (Table 5.2), little molecular difference was evident in the py-GC-MS profiles of the XAD fractions of the untreated (Figure 4.4) and MIEX® treated water (Figure 5.8). Most of the products detected in the HPO and TPIN fractions of the treated water (Table 5.5) were also detected in the same fractions of the untreated water (Table 4.4). The HPO fraction isolated from the MIEX® treated water (Figure 5.8a) had a higher amount of polysaccharide material, but a lower amount of protein and N/S compounds compared to the HPO fraction isolated from the untreated water (Figure 4.4a). Similar tentative pyrolysate distributions were detected from the respective TPIN fractions (Figure 5.8c and 4.4c). The high salt content present in both the TPIB and MIEX® TPIB fractions (Tables 4.2 and 5.5 respectively) inhibited product formation in the pyrolysis-GC-MS technique, limiting the ability to compare the fractions.

5.3.3.5 On-line Thermochemolysis-Gas Chromatography-Mass Spectrometry

Pyrolysis of NOM in the presence of tetramethylammonium hydroxide (TMAH) promotes the formation of GC- resolvable methyl esters of carboxylic acid structures and methyl ethers of phenolic structures which is beneficial since carboxylic acids and phenols are not efficiently detected by GC-MS during conventional pyrolysis (Saiz-Jimenez et al. 1993). On-line thermochemolysis with TMAH was conducted at 650 °C for 10 seconds on the MIEX® HPO, MIEX® TPIB and MIEX® TPIN fractions. The total ion chromatograms from thermochemolysis-GC-MS analysis of these fractions are shown in Figure 5.9a – c, respectively. Major products and their likely origin are listed in Table 5.6, whilst the full suite of tentatively identified products across the three fractions is listed in Appendix 2.

The high salt content present in the MIEX® TPIB fraction (Table 5.4) reduced the NOM content in the sample and therefore the product abundance. The high salt content possibly also inhibited product formation in the thermochemolysis-GC-MS technique, limiting the comparison of this fraction to the other fractions.

The product mixtures from on-line thermochemolysis complement the product mixtures observed in conventional flash pyrolysis (Figure 5.8a – c), with the detection in on-line thermochemolysis of additional acids (as their methyl esters), such as methyl propanoate, methyl isobutyrate and the methyl ester of 2-methoxypropionic acid, which were not detected by flash pyrolysis. Alkyl substituted aromatic compounds (e.g. alkyl benzenes and naphthalenes) typical of direct pyrolysis were detected, but also a large range of aliphatic and aromatic carboxylic acids common to thermochemolysis studies of NOM (del Rio et al. 1998; Templier et al. 2005). The methyl esters of the low MW carboxylic acids have been attributed to cross linkages between phenolic structures and have been reported to be usually abundant in humic substances (Martin et al. 1995). Aliphatic diacids, as their dimethyl esters, were also detected and are reported to be typical of animal, vegetable and microbial cell metabolites (Templier et al. 2005). The C_{16} and C_{18} fatty acid methyl esters (FAMEs) were the most dominant lipids for each fraction, similar to the HPO, TPIB and TPIN fractions (Section 4.3.2.5, Figure 4.6 and Table 4.5) and other studies of groundwater NOM (Desmukh et al. 2001). Thermochemolysis of these NOM fractions obtained after MIEX® treatment also showed several

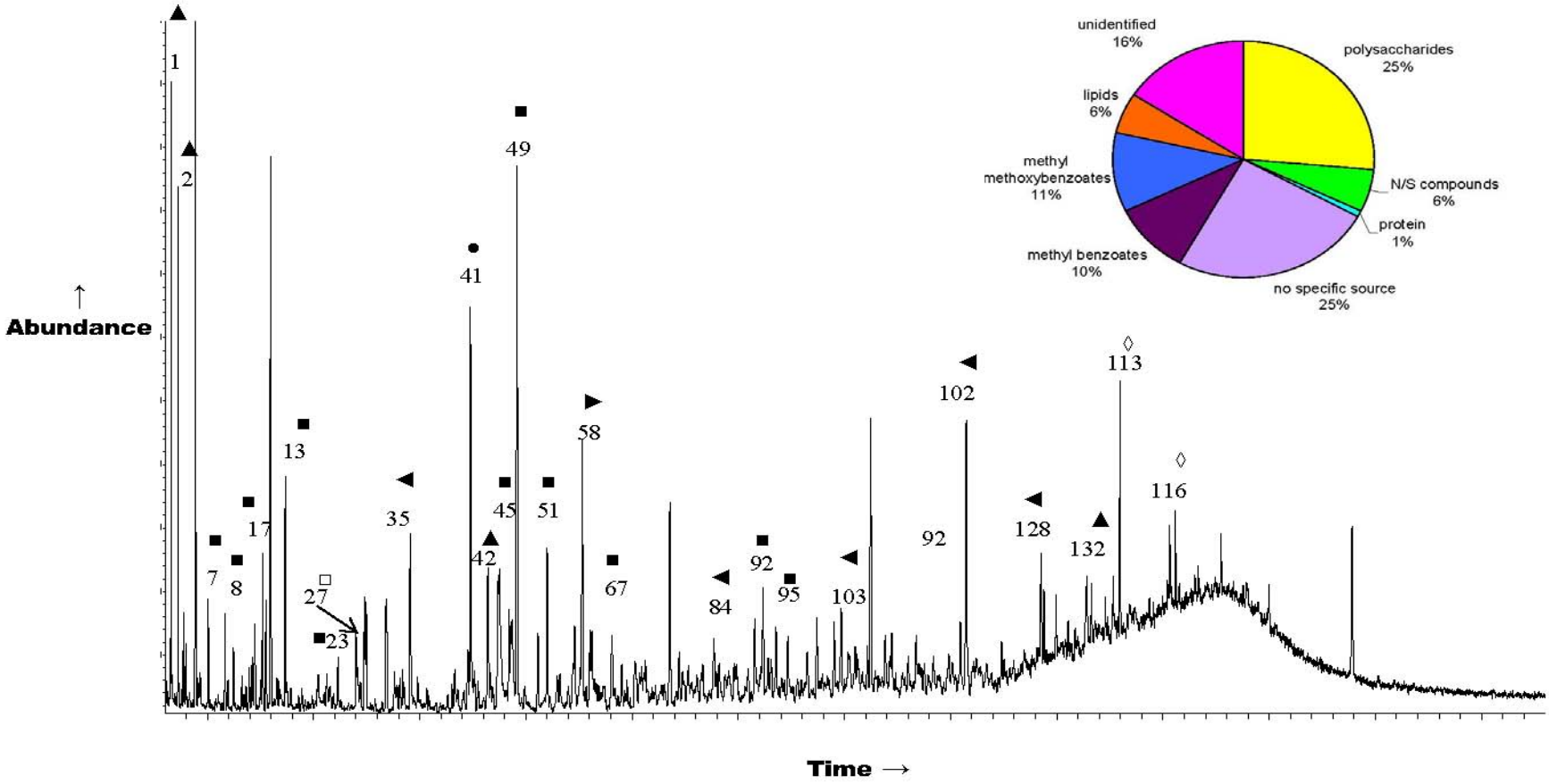

Figure 5.9a Total ion chromatogram from thermochemolysis-GC-MS of the MIEX® HPO fraction. Peak assignments correspond to products listed in Table 5.6: ■ polysaccharides, ● N/S compounds, □ protein, ◊ lipids, ◄ methyl methoxybenzoates, ►methyl benzoates, ▲no specific source. The pie chart reflects relative proportions of eight major product and precursor groups.

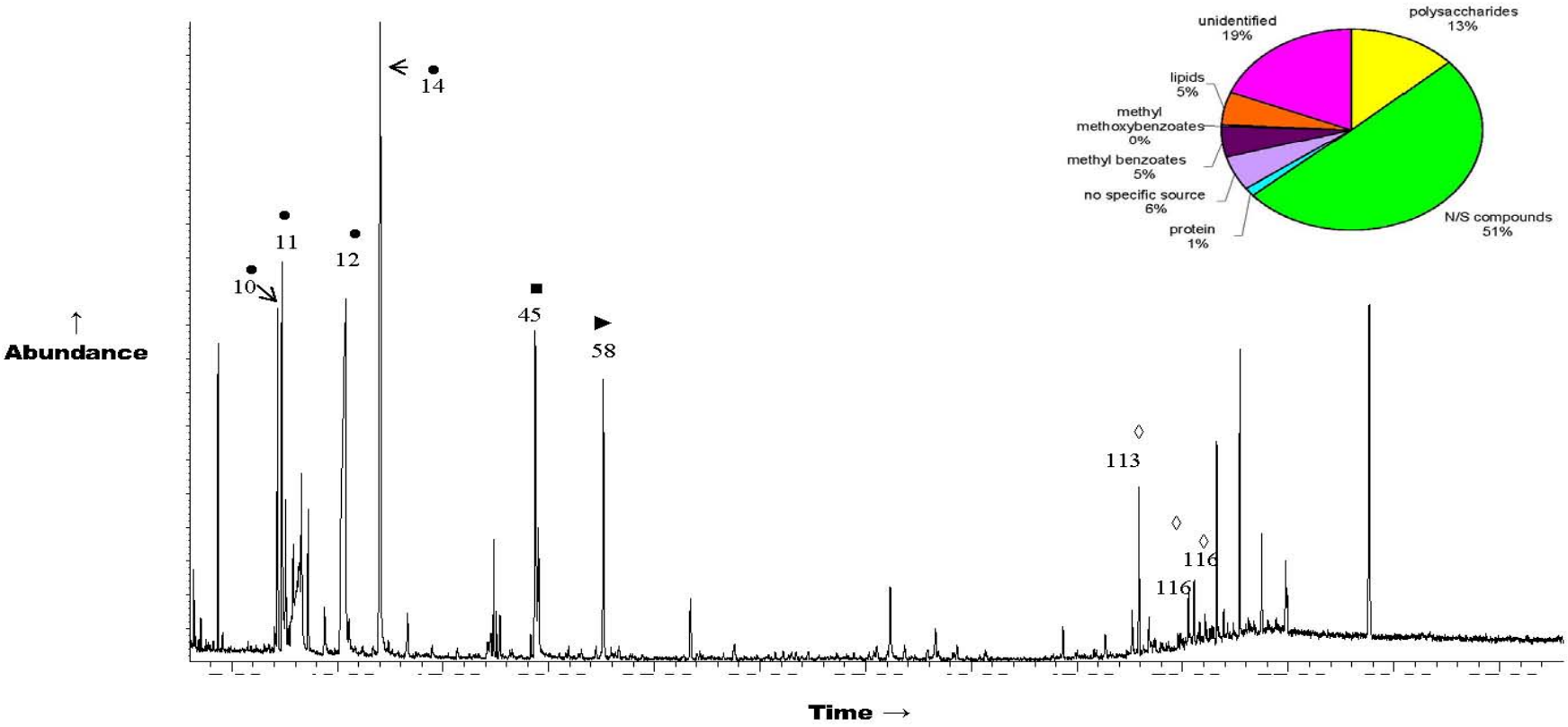

Figure 5.9b Total ion chromatogram from thermochemolysis-GC-MS of the MIEX® TPIB fraction. Peak assignments correspond to products listed in Table 5.6: ■ polysaccharides, ● N/S compounds, □ protein, ◊ lipids, ◄ methyl methoxybenzoates, ►methyl benzoates, ▲no specific source. The pie chart reflects relative proportions of eight major product and precursor groups.

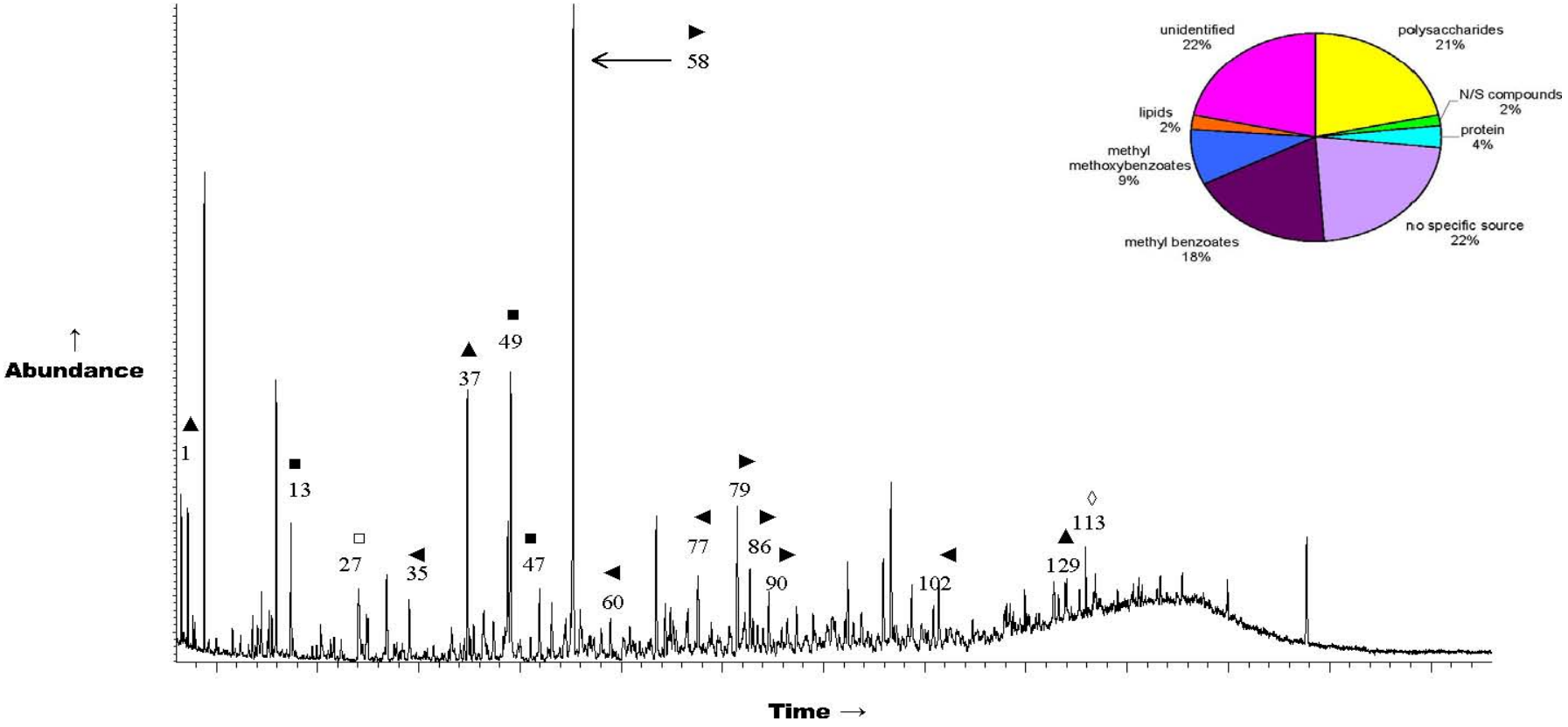

Figure 5.9c Total ion chromatogram from thermochemolysis-GC-MS of the MIEX® TPIN fraction. Peak assignments correspond to products listed in Table 5.6: ■ polysaccharides, ● N/S compounds, □ protein, ◊ lipids, ◄ methyl methoxybenzoates, ►methyl benzoates, ▲no specific source. The pie chart reflects relative proportions of eight major product and precursor groups.

Table 5.6 Major products from the XAD fractions of NOM isolated from the MIEX® treated water and their possible origin. Full list of tentatively identified products can be found in Appendix 2.

Peak N°.	Compound	Possible Origin
1	methyl acrylate	no specific source
2	methyl propanoate	no specific source
7	methyl isobutyrate	polysaccharides
8	methyl methacrylate	polysaccharides
10	(dimethylamino)acetonitrile	N/S compounds
11	dimethylcyanamide	N/S compounds
12	2-methoxy propionic acid methyl ester	polysaccharides
13	*N,N*-dimethylacetamide	N/S compounds
14	*N*-methylacetamide	N/S compounds
23	acetic acid methyl ester	polysaccharides
27	ethylbenzene	protein / lignin
35	anisole	lignin
37	trimethylbenzene	no specific source
41	methyl 2-pentanoate	polysaccharides
42	hexahydro-1,3,5-trimethyl-1,3,5-triazine	N/S compounds
45	C_3 benzene	no specific source
47	ethyl hexanol	polysaccharides
49	dimethyl succinate	polysaccharides
51	dimethyl 2-methylsuccinate	polysaccharides
58	methyl benzoate	methyl benzoates
60	dimethoxybenzene	lignin
67	dimethyl glutarate	polysaccharides
77	dimethoxytoluene	lignin
79	methyl dimethyl benzoate	methyl benzoates
84	dimethoxytoluene	lignin
86	methyl ethylbenzoate	methyl benzoates
90	methyl methoxybenzoate	methyl benzoates
92	methylnaphthalene	polysaccharides
95	methylnaphthalene	polysaccharides
102	methyl dimethoxybenzoate	lignin
103	trimethoxybenzene	lignin
113	methyl hexadecanoate	lipids
116	octadecanoic acid methyl ester	lipids
128	trimethoxybenzoic acid methyl ester	methyl methoxybenzoates
129	phenanthrene	no specific source
132	anthracene	no specific source

high MW polycyclic aromatic hydrocarbons (e.g. phenanthrene, anthracene) not observed with flash pyrolysis, suggesting that the TMAH reagent assists in the thermal release of these PAH structures.

The major thermochemolysis products of the MIEX® HPO fraction included the methyl esters of low MW saturated and unsaturated acids (e.g. methyl acrylate, methyl propanoate), alkyl ($\leq C_3$) phenols, and their methoxy analogues. FAMEs were also detected (peaks 113, 116). All these products are common thermochemolysis products of tannin and lignin structures of terrestrially derived humic substances (Leenheer et al. 2003). Low MW acids (as their methyl esters) and polymethoxybenzenes are usually attributed to cross linking units between phenolic structures of humic macromolecules (Martin et al. 1995). FAMEs are generally formed by transesterification of triglycerides and other lipids (Challinor 1991), and are generally attributed to microbial sources (Frazier et al. 2005). A higher proportion of nitrogenous compounds were detected in the MIEX® TPIB and MIEX® TPIN fractions, such as (dimethylamino)acetonitrile (10), dimethylcyanamide (11) and *N*-methylacetamide (12) consistent with the concentration of relatively polar nitrogen (and other heteroatom) structures present in the thermochemolysis product mixture of the TPI fraction (Table 5.3).

The classification system used for the flash pyrolysis data was also applied to the TMAH thermochemolysis products and the percentages of eight discrete product groups - polysaccharides, N/S compounds, protein, lipids, methyl benzoates, methyl methoxybenzoates, and other products (which refers to those known to be derived from multiple sources and those which could not be identified) - are included in pie charts in Figure 5.9a-c. Qualitative differences were evident between the classification types of the products from the three fractions. The MIEX® HPO fraction was richest in polysaccharides, methyl methoxybenzoates, methyl benzoates and lipids. The MIEX® TPIB fraction was much richer in N/S compounds, but still had significant contributions of polysaccharide, methyl benzoate and lipid material. The MIEX® TPIN fraction was also rich in polysaccharides, as well as protein, methyl methoxybenzoates and methyl benzoates. As NOM becomes enriched in nitrogenous compounds, it becomes more hydrophilic (Templier et al. 2005), consistent with the high relative contribution of N compounds in the thermochemolysis product mixtures from the MIEX® TPIN and MIEX® TPIB fractions and the results of the elemental analysis of these two fractions (Table 5.3).

MIEX® treatment prior to XAD resin fractionation led to several notable changes in the molecular composition of the XAD fractions (Figure 5.9a compared to Figure 4.6a) as indicated by thermochemolysis-GC-MS. MIEX® treatment led to a relative reduction in detectable N/S compounds for the MIEX® HPO fraction. The MIEX® TPIB fraction increased in the relative N/S compound composition, with a corresponding relative decrease in polysaccharide material, compared to the corresponding fraction without MIEX® treatment. No obvious changes were evident for the MIEX® TPIN fraction compared to the corresponding fraction without MIEX® treatment. However, as all the chromatographic techniques employed in this Thesis were used for qualitative rather than quantitative purposes, any changes between composition of the fractions pre and post MIEX® treatment should be verified by other methods.

5.3.3.6 Micro-Scale Sealed Vessel Pyrolysis-Gas Chromatography-Mass Spectrometry

Recent MSSV pyrolysis studies of NOM and related humic fractions has shown that the technique can assist the thermal defunctionalisation of a wide variety of organic biochemicals and provide new speciation data useful for establishing structures and source inputs (Berwick et al. 2007; Greenwood et al. 2006; Berwick 2009; Berwick et al. 2010, a; Berwick et al. 2010, b). MSSV pyrolysis was conducted at 300 °C for 72 hours on the MIEX® HPO, MIEX® TPIB and MIEX® TPIN fractions. Total ion chromatograms from MSSV pyrolysis followed by GC-MS of the MIEX® HPO, MIEX® TPIB and MIEX® TPIN fractions are shown in Figure 5.10. Major products assigned on the basis of mass spectral interpretation are listed in Table 5.7, and all products are listed in Appendix 2.

Each fraction contained high concentrations of alkyl substituted benzenes, phenols, and naphthalenes. As found in the pyrolysis-GC-MS and thermochemolysis-GC-MS chromatograms, the MIEX® HPO and MIEX® TPIN fractions formed products in greater abundances and number than the MIEX® TPIB fraction, with the high salt content present in the MIEX® TPIB fraction (Table 5.4) reducing the NOM content in the sample and therefore the product abundance, as well as possibly inhibiting product formation in the MSSV pyrolysis-GC-MS technique. The MIEX® HPO fraction was dominated by alkyl aromatic compounds (peaks 49, 66, 68; Table 5.7),

and in particular alkylphenols (95, 99, 110, 122, 129), as well as low MW short chain aliphatic compounds (1, 5, 6, 8). The majority of these products were also detected by MSSV pyrolysis-GC-MS of the HPO fraction of the untreated water (Figure 4.7). Alkyl aromatic compounds are common pyrolysis products of aquatic NOM and other humic materials (Saiz-Jimenez et al. 1993). They may arise from a range of sources, but alkylphenols are usually attributed to lignin or tannin sources (Templier et al. 2005; Saiz-Jimenez and De Leeuw 1986; Bruchet et al. 1990). Many cyclic aliphatic higher plant terpenoids undergo aromatisation during natural or artificial maturation (Berwick 2009), and a high aliphatic solid-state ^{13}C NMR signal measured for the MIEX® HPO sample (Figure 5.6) may be indicative of this process. Aromatisation of cyclic terpenoids during MSSV thermal treatment may contribute to the high concentration of aromatic hydrocarbon product. The lack of significant amounts of long chain aliphatic products from MSSV pyrolysis, flash pyrolysis and thermochemolysis suggests the high alkyl carbon content detected by solid-state ^{13}C NMR spectroscopy probably reflects highly branched and cyclic aliphatic structures of terpenoids (Lu et al. 2003).

Naturally occurring terpenoids occur in an extremely wide variety of structural configurations and may be subject to alteration during MSSV thermal treatment. As such, it is difficult to unequivocally correlate individual alkyl naphthalene pyrolysis products to a specific terpenoid precursor. Trimethylnaphthalenes (135) dominated the alkyl naphthalene distribution of the MIEX® HPO fraction, and have been reported in residues after multi-step chemical degradations of immature sediments, rich in higher plant terpenoids (Almedros et al. 1998).

Alkyl benzenes likely include both primary alkyl-linked aromatic structures (Schulten and Gleixner 1999), as well as secondary products from the thermal alteration of other NOM moieties. Reduction of aromatic carboxylic acid groups may be one possible route to alkyl benzenes as solid-state ^{13}C NMR spectroscopic analysis (Figure 5.6) showed that the MIEX® HPO fraction contained moderate carboxyl content. Several aromatic carboxylic acids (as their methyl esters, Section 5.3.3.5) were also detected by thermochemolysis-GC-MS of this fraction. However, the high abundance of alkyl benzenes from this fraction does not correlate to the

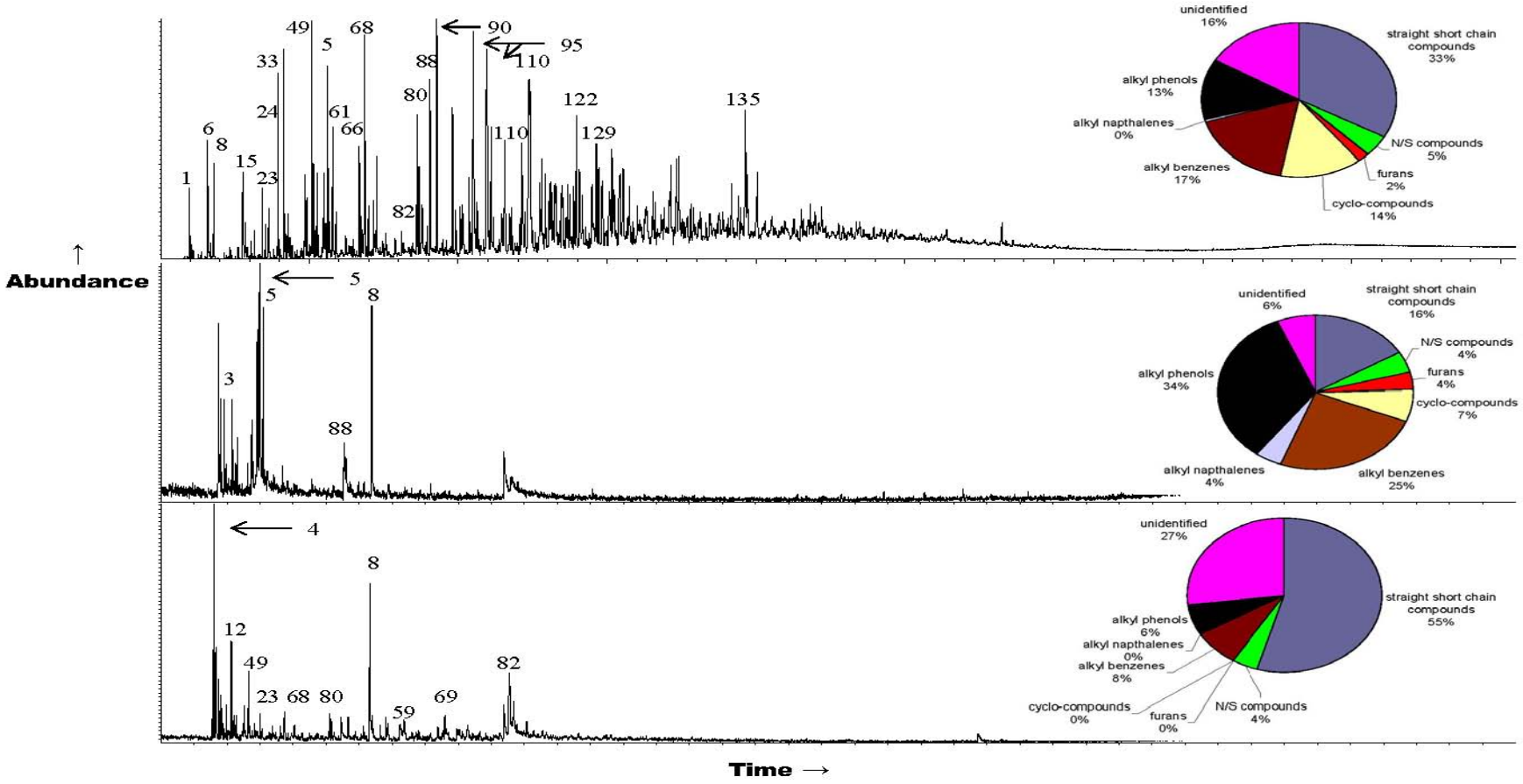

Figure 5.10 Total ion chromatograms obtained by MSSV pyrolysis-GC-MS analysis of the a) HPO, b) TPIB and c) TPIN fractions of NOM remaining in the MIEX® treated water. Peak assignments correspond to products listed in Table 5.7 and Appendix 2. The pie charts reflect relative proportions of eight major product and precursor groups.

Table 5.7 Major products from MSSV pyrolysis-GC-MS of the XAD fractions of NOM isolated after MIEX® treatment.

Peak N°.	Compound	Possible Origin
1	butene	short chain compounds
3	acetone	short chain compounds
4	methanethiol / 1-butene	short chain compounds
5	methyl heptene	short chain compounds
6	propanal	short chain compounds
8	ethyl hexanol	short chain compounds
12	trimethyl pentane	short chain compounds
15	butanone / pentane	short chain compounds
23	dimethylhexadiene	short chain compounds
24	methyl cyclopentene	cyclic compounds
33	heptane	short chain compounds
49	toluene	alkyl benzenes
59	trimethyl-2-cyclopenten-1-one	cyclic compounds
61	ethyl hexane	short chain compounds
66	ethylbenzene	alkyl benzenes
68	xylene	alkyl benzenes
69	dimethylphenol	phenols
80	ethyl toluene	alkyl benzenes
82	tetramethyl furan	furans
88	phenol	phenols
90	trimethyl benzene	alkyl benzenes
95	cresol	phenols
110	dimethylphenol	phenols
122	ethyl-methyl-phenol	phenols
129	trimethyl phenol	phenols
135	trimethyl naphthalene	naphthalenes

relatively low aromatic carbon content detected by solid-state ^{13}C NMR spectroscopy. This suggests that secondary cyclisation and aromatisation of aliphatic and alicyclic terpenoids may be a significant source of alkyl benzenes for this sample (Schulten and Gleixner 1999).

Low MW aliphatic compounds were also prominent MSSV pyrolysis-GC-MS products for all fractions. These aliphatic compounds included C_4-C_8 branched alkanes and alkenes (5, 12, 15, 23, 33) and alkyl cyclopentene (24). Flash pyrolysis also generated high concentrations of low MW aliphatic compounds displaying a range of unsaturation and alkyl substitution from these samples. The high concentration of these pyrolysis products is consistent with the high aliphatic carbon signal measured by solid-state ^{13}C NMR spectroscopy (Figure 5.6). MSSV pyrolysis-

GC-MS of the TPIN and TPIB fractions showed a higher proportion of short chain compounds, a lower proportion of detectable nitrogenous compounds, and a similar proportion of alkylphenols, when compared to the HPO fraction. Conversely, alkyl furans were more abundant for the TPI fractions than for the HPO fraction, consistent with the more abundant oxygenated aliphatic signal seen in the solid-state ^{13}C NMR spectra (Figure 5.7) and the FTIR spectra (Figure 5.5) of the untreated samples.

A semi-quantitative modified classification, as discussed in Section 5.3.3.4 (Bruchet et al. 1989; Bruchet et al. 1990), of common MSSV pyrolysis product groups is shown as pie charts in Figure 5.10. Many of the abundant alkyl aromatic hydrocarbons produced from the MIEX® HPO fraction can be derived from a range of organic precursors and therefore provide limited information about their source of origin. There was a lower proportion of N-containing compounds in the MIEX® HPO fraction compared to the MIEX® TPI fractions (Figure 5.10), consistent with the HPO and TPI fractions of the raw water (Figure 4.7). A previous study on NOM fractions isolated from the Gartempe River in France (Templier et al. 2005) also showed the TPI fraction, in contrast to the HPO fraction, exhibiting a large number of nitrogen-containing compounds in significant relative intensity, including organic compounds containing only nitrogen heteroatoms and organic molecules with both nitrogen and oxygen heteroatoms.

5.3.3.7 Overall Characteristics of the MIEX® HPO, MIEX® TPIB and MIEX® TPIN fractions

MIEX® pre-treatment of W300 groundwater before isolation of NOM fractions by XAD-8/XAD-4 fractionation produced three solid freeze-dried samples, termed MIEX® HPO, MIEX® TPIB and MIEX® TPIN. Reduction of salt concentrations within these fractions was challenging, and a high salt content hindered characterisation of the MIEX® TPIB fraction. Characterisation of the fractions by FTIR and solid-state ^{13}C NMR spectroscopic analysis indicated that the samples had a significant shift in carbon distribution to aliphatic material compared to the untreated samples, indicating that the MIEX® treatment had removed some aromatic material from the samples. Further characterisation by py-GC-MS, thermochemolysis-GC-MS and MSSV-py-GC-MS revealed that the MIEX® HPO

fraction had a significant contribution from alkylphenols and polyaromatic hydrocarbons. The higher nitrogen and oxygen content of the MIEX® TPIB and MIEX® TPIN fractions than the MIEX® HPO fraction found in the elemental analysis was consistent with more nitrogen- and oxygen- containing functionalities (such as those derived from proteins and tannins) being observed in the MIEX® TPIB and MIEX® TPIN product mixtures from the three pyrolysis based methods.

5.3.3.8 Disinfection By-Product Formation Potential

The quantity and speciation of DBPs in finished drinking water can vary with a range of factors, including source water quality (i.e. temperature, pH, bromide concentration and DOC composition and concentration). NOM has been well known as the primary precursor for formation of trihalomethanes (THMs) during chlorination since the 1970s (Bellar et al. 1974; Rook 1974, 1977), and the THM and HAA (haloacetic acid) formation from various organic carbon fractions isolated by XAD resin fractionation has been examined (Kitis et al. 2002; Drikas et al. 2011; Croué et al. 1993, b; Croué et al. 2000). There does not appear to be any previous studies that have fractionated the NOM remaining in MIEX® treated water to investigate the reactivity of this residual NOM. In the current study, the disinfection by-product formation potential (DBPFP) of NOM remaining in the water after MIEX® treatment was examined to determine the potential for the XAD fractions isolated from the NOM in the water after MIEX® treatment to form DBPs.

In the present study, aqueous samples of the MIEX® HPO and MIEX® TPIB fractions (produced by initial dissolution of the dried isolate in MilliQ water) were diluted to achieve DOC concentrations of 2 mg L^{-1}, typical of the DOC concentration at the outlet of the Wanneroo GWTP, and bromide ion (0.2 mg L^{-1}) was added to simulate the bromide concentrations of raw W300 (Table 2.3, Section 2.3.3) since negligible bromide is removed in the Wanneroo GWTP (Warton et al. 2007, a). Disinfection experiments involved addition of chlorine to achieve an initial concentration of 6 mg L^{-1} (a similar chlorine dose to that applied for disinfection of water at the Wanneroo GWTP), addition of buffer to pH 7 and temperature control (25°C), with the concentrations of the residual free chlorine equivalents, THMs and HAAs analysed after 7 days. The 7-day oxidant demands of the MIEX® HPO and MIEX® TPIB samples are shown in Table 5.8, with the 7-day individual and total

THM concentrations shown in Table 5.9, and the corresponding HAA concentrations are shown in Table 5.10.

Table 5.8 Oxidant demands of the MIEX® HPO and MIEX® TPIB fraction (halogentation conditions: 2 mg L^{-1} DOC, 6 mg L^{-1} Cl_2 dose, 0.2 mg L^{-1} Br^-, pH 7, 25°C, 168 hours).

Sample	Oxidant demand (mg L^{-1} free chlorine)	Specific oxidant demand (mg free chlorine/mg C)
MIEX® HPO	4.5	2.3
MIEX® TPIB	4.1	2.1

In these experiments, the oxidant demands of the individual samples were similar to the raw water samples post MIEX® treatment (Table 4.8). Since the DOC concentration has been normalised to 2 mg L^{-1} prior to the disinfection experiments, the oxidant demand is already normalised to the DOC concentration, and comparisons of oxidant demands are therefore comparisons of specific oxidant demands. The oxidant demand of the MIEX® HPO sample was slightly higher than the corresponding MIEX® TPIB sample. Huber and Frimmel (1996) showed that the HPO fraction is likely to contain mainly humic-type material with a large aromatic content, and possibly include significant quantities of phenols and dihydroxybenzenes which have been shown to be highly reactive with chlorine (Gallard et al. 2003). Krasner et al. (1996) established that aromatic compounds, particularly those found in humic material, undergo a number of reactions with chlorine, accounting for the high chlorine demand of this material. In addition, Owen et al. (1995) found that the humic fraction was more reactive with chlorine compared to non-humic material from the same source, as observed in the lower chlorine demand for the MIEX® TPIB fraction.

Table 5.9 Concentrations of THMs from chlorination of the MIEX® HPO and MIEX® TPIB fractions (halogenation conditions: 2 mg L^{-1}DOC, 6 mg L^{-1} Cl_2 dose, 0.2 mg L^{-1} Br^-, pH 7, 25ºC, 168 hours).

Sample	Concentration of Individual THMs (µg L^{-1})				Total THMFP (µg L^{-1})	Specific THMFP (µg/mg C)
	$CHCl_3$	$CHBrCl_2$	$CHBr_2Cl$	$CHBr_3$		
MIEX® HPO	111	93	52	5	261	131
MIEX® TPIB	10	19	24	23	76	58

Table 5.10 Concentrations of HAAs from chlorination of the MIEX® HPO and MIEX® TPIB fractions (halogenation conditions: 2 mg L^{-1}DOC, 6 mg L^{-1} Cl_2 dose, 0.2 mg L^{-1} Br^-, pH 7, 25ºC, 168 hours).

Sample	Concentration of Individual HAAs (µg L^{-1})									Total HAAs (µg L^{-1})	Specific HAAFP (µg/mg C)
	MCAA	MBAA	DCAA	TCAA	BCAA	DBAA	BDCAA	CDBAA	TBAA		
MIEX® HPO	6	1	60	44	32	8	17	2	ND*	172	86
MIEX® TPIB	ND*	ND*	13	3	20	23	1	ND*	ND*	60	30

* ND - not detected

The concentrations of DBPs in Table 5.9 and 5.10 show that the MIEX® HPO and MIEX® TPIB samples are both reactive with chlorine. The higher THM and HAA concentrations from the MIEX® HPO sample compared to the MIEX® TPIB sample are due to the enrichment of reactive humic-type components, other aromatic substituents and unsaturated organic species in this fraction (Liang and Singer 2003; Reckhow et al. 1990; Owen et al. 1995). MIEX® treatment prior to fractionation did reduce the THM concentrations produced for the MIEX® HPO and MIEX® TPIB fractions compared to the HPO, HPO after MIEX®, TPIB, and TPIB after MIEX® fractions (Tables 4.9 and 5.9). Interestingly, the MIEX® TPIB sample produced a higher amount of HAAs (Table 5.10) than the TPIB sample from the untreated water (Table 4.10). This indicates that yield reductions, such as the lower THM and HAA concentrations produced from the MIEX® HPO fraction compared to the concentrations produced from the HPO after MIEX® fraction, could not be envisaged. It is impractical with current treatment technology to selectively target the removal of reactive DBP precursors (Bond et al. 2010), hence the increase in HAAs after MIEX® pre-treatment would also have been difficult to predict, as

physicochemical factors controlling treatability do not relate to reactivity with chlorine (Bond et al. 2010). The TPIB fraction is usually more recalcitrant to conventional treatment (Kitis et al. 2002), and further measures will be required to reduce the concentration of the TPIB fraction if more stringent DBP regulations continue to be implemented.

In this DBPFP experiment, chloroform was the major THM product formed from the MIEX® HPO sample. Dibromochloromethane and bromoform were the most abundant products from the MIEX® TPIB sample. The shift towards the more brominated forms from the MIEX® TPIB sample must be due to an increased reaction of the functional groups present with bromine (Liang and Singer 2003). The shift towards more brominated species was also seen for the TPIB after MIEX® sample compared to the raw water sample in Chapter 4 (Table 4.9), but dichlorobromomethane was the major THM produced for the TPIB after MIEX® fraction.

The MIEX® HPO fraction showed a much larger HAAFP than the MIEX® TPIB sample (Table 5.10), indicating that the NOM within the MIEX® HPO sample contained relatively more HAA precursors than the NOM within the MIEX® TPIB sample. Interestingly, more HAAs were produced for the MIEX® TPIB sample compared to the respective TPIB samples before and after MIEX® treatment in Table 4.10 (TPIB – 18 μg L^{-1}, TPIB after MIEX® – 10 μg L^{-1}). This suggests that MIEX® pre-treatment prior to fractionation did not selectively remove reactive HAA precursors over non-reactive precursors for this sample, even though MIEX® treatment for the TPIB samples (Tables 4.9 and 5.9) indicated removal of some THM precursors. This indicates that some HAA precursors within the MIEX® TPIB fraction are recalcitrant to treatment, and should be targeted by additional treatment.

Some brominated DBPs are more mutagenic and carcinogenic than their chlorinated analogues (Bougeard et al. 2010; Richardson 2003; Chen and Westerhoff 2010; Drikas et al. 2008; Zhang et al. 2000), so a better understanding of the extent of bromine and chlorine substitution into DBPs is required. The extent of bromine incorporation into THMs and HAAs was evaluated here by calculating the bromine incorporation factors (BIFs) as described in Section 3.2.2. BIF values relating to a

comparison of bromine substitution, on a scale of 0 to 1 (Obolensky and Singer 2005), for the THMs and HAAs are shown in Table 5.11.

Table 5.11 BIF values for THMs and HAAs obtained after a 7 day chlorination period.

Sample	BIF (THMs)	BIF (HAAs)
MIEX® HPO	0.27	0.06
MIEX® TPIB	0.59	0.18

For both THMs and HAAs, the extent of bromine substitution varied for the MIEX® HPO and MIEX® TPIB samples. The MIEX® HPO and MIEX® TPIB samples had higher BIF values than the corresponding samples of the untreated water (Table 4.10), indicating a shift towards more brominated DBPs from the samples isolated by resin fractionation of the NOM remaining after MIEX® treatment. The higher BIF values seen for the MIEX® TPIB sample compared to the MIEX® HPO fraction could be due to the efficient reactivity of bromine with aliphatic functional groups which concentrate in the TPIB fraction (Liang and Singer 2003; Sinha et al. 1997).

5.3.4 Conclusions

MIEX® treatment of a large volume of water was used to isolate XAD fractions of NOM remaining after treatment in sufficient quantities for detailed molecular analysis. A range of subtle differences in the molecular composition and properties of the fractions were revealed by molecular analysis. MIEX® treatment changed the distribution of the XAD fractions compared to the raw water fractions (Chapter 4), due to preferential removal of the TPI and HPI fractions. Detailed molecular analysis with a range of methods, including sophisticated spectroscopic analysis, showed an increase in aliphatic character within the composition of the fractions (MIEX® HPO, MIEX® TPIB and MIEX® TPIN) compared to the raw water fractions obtained in Chapter 4.

Reduced concentrations of THMs and HAAs were formed in DBPFP experiments from the XAD fractions isolated after MIEX® treatment compared to the raw water fractions (Chapter 4), but there was a trend towards increasing proportions of

brominated species from the XAD fractions isolated after MIEX® treatment. This can be attributed to the high relative abundance of aliphatic functional groups in these fractions – best identified by FTIR and solid-state ^{13}C NMR spectroscopic analysis – which are generally highly reactive with bromine species. This could be significant for any future increase in focus on brominated DBPs by DBP regulators.

Chapter 6

6.0 Summary of Characterisation Methods, Recommendations and Overall Conclusions

Natural organic matter (NOM) can contribute to various potable water issues and is present in high concentrations in many Australian water supplies. Characterisation of NOM is important for treatment of these waters for potable water purposes. Analytical characterisation data can be correlated from a combination of characterisation methods to derive more detailed structural information about NOM, as well as to validate results obtained from the different methods (Leenheer, 2009). The study described in this Thesis has contributed to the body of characterisation studies being conducted to develop a detailed understanding of the origins, structural features and reactivity of NOM in source waters. A summary of the characterisation methods which have been used in the current study of NOM are discussed in the following subsections. Understanding how NOM behaves in drinking water treatment processes enables optimisation of treatment processes and improved catchment management practices. The information obtained from each characterisation method and its relevance to the water treatment industry are summarised in Section 6.6 (Table 6.2), prior to the overall conclusions of this Thesis.

6.1 Comparison of Methods for Concentration of NOM

This research assessed the efficiency and practicality with which NOM from a local groundwater source could be concentrated and isolated, using ultrafiltration and an XAD-8/XAD-4 resin fractionation procedure. One solid isolate was recovered from ultrafiltration: termed the Raw Water UF. Three solid isolates were recovered in the XAD-8/XAD-4 fractionation procedure: the hydrophobic fraction (HPO), the

transphilic base fraction (TPIB) and the transphilic neutral fraction (TPIN); and the hydrophilic fraction (HPI) was obtained as a liquid isolate in the procedure.

The goal of collecting and concentrating NOM from a water source with 100 % efficiency is impossible to achieve (Croué et al. 1999, b), and the effort required to carry out the separation and concentration steps increases dramatically as that efficiency is approached. Even for the most laborious and efficient techniques currently available, significant losses of NOM can occur due to volatilisation, precipitation of salts and experimental errors (Croué et al. 1999, b).

The two isolation and concentration methods investigated each have both advantages and disadvantages, and neither can be recommended universally. However, ultrafiltration offers the distinct advantage that a large volume of water can be treated in significantly less time and much less laboriously than in the XAD-8/XAD-4 resin fractionation procedure. Ultrafiltration separates the aquatic humic substances from inorganic solutes according to the molecular size of the membrane (Aiken 1985). The isolated NOM fraction is therefore a mixture of organic matter with different sized molecules (Lankes et al. 2008), with the separation influenced by the method conditions (Assemi et al. 2004). While the UF procedure retained 61 % of the total DOC after two passes in the current study, improvements to the procedure should, in general, allow higher recoveries, with lower concentrations of residual salts. In a previous investigation, Couton (2010) reported fouling of an ultrafiltration membrane in an isolation procedure using Wanneroo groundwater, as the membrane was noticeably coloured after a single pass. This colour was removed by washing with 0.1 M NaOH solution, but the NOM contained within the NaOH washings was not recovered in that procedure. Cleaning of the UF membrane with NaOH solution between the repeated filtration steps should reduce the loss of DOC through membrane fouling. Another improvement to the ultrafiltration procedure could include repeated filtration of the retentate (i.e. more than two passes) until the conductivity of the permeate is <5 µS cm^{-1} (Couton 2010), indicating minimal salts are still being removed, producing a NOM isolate with lower inorganic salt concentration.

The XAD-8/XAD-4 resin fractionation procedure required significantly more time and labour than the UF procedure and also involved extensive repetitive washing of

the resins to rinse out reagents, but produced higher purity fractions. The higher purity of the fractions isolated by the XAD-8/XAD-4 resin procedure allowed a greater suite of characterisation techniques to be employed for these fractions compared to the UF fraction. The efficiency of NOM recovery was somewhat lower for the resin fractionation (35 %) than using UF (61 %) in the current study, but could potentially be improved by employing additional steps to collect more NOM. Aiken et al. (1992) used XAD-8 and XAD-4 resins with column capacity factors (*k'*) greater than or equal to 100, respectively, in series to isolate essentially all hydrophobic and transphilic NOM molecules. The column capacity factor (*k*') is used to characterise the affinity of adsorbents for dissolved molecules (Croué et al. 1999, b). Using the procedure from Aiken et al. (1992), recoveries from the XAD-4 resin can be improved by using vacuum evaporation to concentrate the eluent from the XAD-4 resin to the point of salt saturation and then passing the concentrated solution through another column packed with XAD-4 resin with a column capacity factor (*k'*) between 5 – 100 to isolate the NOM molecules (Croué et al. 1999, b). Some molecules adsorb in the second exposure to XAD-4 but not the first exposure because fewer bed volumes of sample are passed through the column in the second exposure (corresponding to a lower *k'* value, Aiken and Leenheer, 1993). In the current study, the column capacity factor was kept constant at a value of 50 for the resin procedure. As NOM is a collection of diverse molecules, different fractions of NOM elute from the column at different times, corresponding to processing a different number of bed volumes of influent (Aiken and Leenheer, 1993). The higher the affinity of a group of NOM molecules for the media surface, the larger is the number of bed volumes of water that can be processed before the molecules break through (Aiken and Leenheer, 1993). By varying the column capacity factor throughout the resin procedure all hydrophobic and transphilic NOM could essentially be recovered.

6.2 Comparison of the Chemical Composition of NOM Isolates

Identification of the types of organic compounds collected by the different isolation processes is important, because conclusions about NOM in the source water are often

drawn based on the analysis of the fractions collected (Leenheer, 2009). In this study, the types of NOM collected by UF and resin adsorption were compared. The sample chosen for this study had a high DOC concentration (23 mg L^{-1}) and a high proportion of aromatic components, and was used as a 'worst case scenario' of possible source water NOM for subsequent characterisation and treatability studies.

Even though this study isolated NOM from one water sample, the analytical approach used to isolate the NOM fractions was based on standard isolation methods that are reproducible on similar water types. The diversity of molecules that constitute NOM and the relatively low concentrations of NOM in water sources often make characterisation difficult. Thus, methods that can accurately characterise NOM are essential. Characterisation of a small number of NOM samples using a 'worst case scenario' water source can result in constraints in data interpretation. Further research could analyse a variety of samples of highly hydrophobic, high DOC source waters to see if relevant NOM classifications from these samples can be better linked to the analytical classifications seen in this study. Even with the limited sample set, this Thesis has contributed to the detailed understanding of the origins and reactivity of NOM of highly hydrophobic, high DOC groundwater sources.

The solid freeze-dried UF isolate obtained from the high DOC concentration / high hydrophobicity groundwater had low carbon content (14 %) and high ash content (35 %). Characterisation of the UF isolate was hindered due to the high ash content, and the recommendations for the ultrafiltration method in Section 6.1 should enable other NOM characterisation studies to produce an isolate with a lower concentration of residual salts. While the quality of the spectra was impeded by the high ash content of the sample, FTIR and solid-state ^{13}C NMR spectroscopic analyses indicated that the sample may have a significant aliphatic content, presumably from lipid and biopolymer precursors. Further characterisation by SEC revealed the UF fraction to have a significant contribution from humic substances of relatively high molecular weight. Hence, isolation of NOM using ultrafiltration has produced a mixture of organic material (both hydrophobic and hydrophilic). This has enabled an overall snapshot of the NOM present in highly hydrophobic / high DOC groundwater sources to be determined.

The NOM fraction eluted from the XAD-8 resin was typically richer in carbon, but depleted in nitrogen and oxygen, compared to the XAD-4 sample, supporting the widely accepted idea that the XAD-8 resin selectively retains the more hydrophobic molecules compared to the XAD-4 resin (Croué et al. 1999, b). The hydrophobic character of the XAD-8 concentrate was manifested by its higher $SUVA_{254}$ and more intense fluorescence EEM, and also by an intense signal from aromatic carbon in the solid-state ^{13}C NMR spectrum and a significant contribution of polysaccharide input detected by pyrolysis-GC-MS, thermochemolysis-GC-MS and MSSV pyrolysis-GC-MS. The solid-state ^{13}C NMR and FTIR spectra of the XAD-4 fractions indicated a significant contribution of aliphatic content from lipid and biopolymer precursors, along with much less aromatic carbon than in the XAD-8 fractions. The higher nitrogen and oxygen content present in the TPIB and TPIN fractions allowed more nitrogen and oxygen containing groups (such as those derived from tannins and proteins) to be revealed by the pyrolysis and thermochemolysis techniques. These structural features support the importance of aliphatic carbon in this fraction and its corresponding hydrophilic character (Croué et al. 1999, b).

Understanding the impact of various forms of NOM on drinking water treatment processes has resulted in a number of isolation methods being developed worldwide, such as the XAD-8/XAD-4 resin fractionation and ultrafiltration methods. For a better understanding of the types of organic compounds present before and after treatment processes, a number of characterisation techniques are used, from the very simple (UV_{254} absorbance and colour), to the more complex, analytical procedures (pyrolysis-GC-MS, Chow et al. 2006). However valuable the characterisation method, the results are not in a form that can be easily interpreted by treatment plant operators. Rapid resin fractionation has found increasing application for NOM characterisation due to its speed, repeatability and minimal sample preparation (Vuorio et al. 1998). Rapid fractionation has allowed a better understanding of NOM removal, as the types of organic compounds removed by the treatment processes can be investigated (Drikas et al. 2011). Hence, even though UF was more useful for evaluating the overall presence of organic material, resin fractionation is more useful for examination of aromatic and hydrophobic humic species. As a result, it is possible that a combination of membrane and resin-based NOM isolation techniques

might be used successfully for characterisation purposes of a highly hydrophobic, high DOC concentration groundwater source.

6.3 Comparison of Methods for NOM Characterisation

As NOM represents a complex mixture of compounds, structural characterisation of NOM is often difficult and requires a multi-faceted approach. New analytical methods continue to be developed to aid the structural analysis of NOM and provide information which can be used to assess the effectiveness of treatment processes. A summary of each characterisation method used in this Thesis is shown in Table 6.1. Each characterisation method allowed new information to be determined about the characteristics of the high DOC groundwater with high hydrophobicity, and each method is summarised in the following subsections.

Table 6.1 Analytical methods used to identify different features of NOM.

Characterisation Method	**Featured Which Can Be Identified**
Elemental analysis	Elemental composition is often used for calculation of the atomic ratios such as O/C, H/C or N/C.
FTIR spectroscopy	Aromatic and aliphatic hydrocarbon, different bonds and functional groups.
Solid-state ^{13}C NMR spectroscopy	Details of carbon structures of NOM (aliphatic carbon, oxygenated aliphatic carbon, aromatic carbon and carbonyl carbon).
Pyrolysis-GC-MS	Produces structural information about the molecular building blocks of NOM.
Online thermochemolysis-GC-MS	Produces structural information about the molecular building blocks of NOM.
MSSV py-GC-MS	Produces structural information about the molecular building blocks of NOM. Can provide information on specific biomarkers of NOM.
Fluorescence EEM	Three major fluorophores can be identified: protein-like, humic-like and fulvic-like fluorophores.
SEC-OCD / SEC-UV254	Molecular weight distribution of NOM; NOM fingerprinting
Oxidant Demand	Chemical reactivity of NOM.
DBPFP	Chemical reactivity of NOM.

6.3.1 Elemental Analysis

Elemental analysis is generally the first technique applied to the study of NOM, and can be reliably conducted only on dry, ash-free isolates. If the ash content of a dry sample is > 5 %, significant errors can occur in the evaluation of organic oxygen (Leenheer, 2009). Oxygen in NOM is commonly reported by difference between 100% minus the sum of the other major elements determined with a C, H, and N analyser. Problems with this difference-oxygen determination are: i) errors with C, H and N determinations are additive and are summed in the O calculation, ii) the minor elements aren't included in this difference calculation, and iii) the ash may include elements already determined such as carbonates, sulfates and oxides (Leenheer, 2009). Direct determination of oxygen on samples with low ash content therefore minimises errors. The high ash content (35 %) seen in the UF fraction indicated that a significant amount of inorganic material was present within the sample. Dialysis had been performed to reduce the amount of inorganic salts in this fraction, but the high ash content present was likely due to insufficient transfer of salts into the permeate during the ultrafiltration and dialysis processes. The low ash content for the HPO and TPIB fractions compared to the UF fraction suggests that the XAD isolation procedure was relatively successful in removing inorganic components from the samples. However, the measured mass of the TPIB fractions (C, O, H, N, S, ash) elementally accounted for a recovery between 45.5 - 66.3 %, indicating other elements not measured as part of elemental analysis were present in significant quantities. This led to the determination of high sodium and chlorine in the samples, measured by atomic absorption spectroscopy. The high concentrations of sodium and chlorine in the samples would have been volatilized at the combustion temperature used during elemental analysis, and so were not included in the recovery calculation. Desalting of the TPIB fractions was considered, but as it is a very laborious technique, with the risks including possible sample alteration and lower sample recovery, the TPIB fractions were used as obtained. Hence, elemental analysis was shown to be a good indicator of the efficiency of isolation and desalting protocols.

Elemental analysis also provided important information such as atomic ratio data to allow NOM fractions isolated from the same source to be compared. The H/C ratio is indicative of the degree of unsaturation, with a higher H/C ratio indicating greater

aliphatic content, while lower H/C ratios indicate greater aromatic character. The H/C ratio values were in the order of UF > TPI > HPO, typical of the aliphatic character present in the samples. The O/C ratio is indicative of the concentration of oxygenated functional groups in the sample, and the N/C ratio is indicative of the concentration of nitrogenous functional groups. As NOM becomes more hydrophilic, it is more enriched in nitrogenous structures and oxygenated functional groups, with the TPI and UF fractions showing higher O/C and N/C ratios compared to the HPO fraction.

Elemental analysis is a rather complex and time consuming method, and requires access to sophisticated analytical instrumentation (Matilainen et al. 2011). Even though this characterisation technique might not be used in water treatment applications due to its expense, the information obtained may be useful to describe and understand the NOM quality and characteristics at various water treatment process steps. The behaviour of NOM in various treatment processes can be better explained and understood if data on structural features involved in NOM are available (Matilainen et al. 2011).

6.3.2 Fourier Transform Infrared Spectroscopy

FTIR spectroscopy has been often used for NOM characterisation as the information provided can complement data from other characterisation techniques. The interpretation of FTIR spectra may be difficult, however, due to the complexity and polyfunctionality of NOM (Matilainen et al. 2011). FTIR analysis is advantageous in that it only uses a small amount of sample (2 mg), as compared to the larger quantities required for elemental analysis (250 mg), so this characterisation technique can be used without significant loss of sample.

All FTIR spectra in this Thesis had several distinguishing features, although the broadness of the infrared absorption bands indicated that each fraction contained a mixture of polyfunctional compounds. Again, the hydrophobic fractions were shown to have strong aromatic C=C stretching and a prominent C=O stretching of carboxylic acids and carbonyl groups. Ineffective removal of the high MW, highly aromatic fraction can be an issue with MIEX® treatment, and another treatment process would need to be considered post MIEX® to remove these NOM compounds.

The removal of high MW organic matter with coagulation is well-documented (e.g. Collins et al. 1986, Owen et al. 1995, Chow et al. 1999, Drikas et al. 2011). Hence, coagulation following MIEX® treatment will remove the high MW material. The more hydrophilic fractions were characterised by relatively strong aliphatic C-H stretching. MIEX® treatment of the raw water prior to fractionation (Chapter 5) did result in some variations in the FTIR spectra of the NOM isolates compared to the raw water isolates. There was a shift in carbon distribution to aliphatic material compared to the raw water samples, indicating that MIEX® treatment had removed some aromatic material from the samples. The MIEX® treated samples also displayed a significant absorption in the 1000 – 1200 cm^{-1} region, representing C-O stretching of various groups such as ethers and esters. van Leeuwen et al. (2002) found very small amounts of this type of low MW components to be removed by treatment, and removal could be improved by change in coagulation conditions (Chow et al. 2004).

The FTIR spectrum of the UF sample also indicated the presence of inorganic constituents such as carbonates, nitrates, phosphates, silica and sulfates in the sample post dialysis, with the detectable peaks in the 800 – 500 cm^{-1} region. These peaks indicate the insufficient transfer of salt into the permeate during the ultrafiltration and dialysis processes. Hence, FTIR spectroscopy was also used to monitor the presence or absence of inorganic solutes in the NOM fractionation and isolation procedures.

6.3.3 Solid-State ^{13}C Nuclear Magnetic Resonance Spectroscopy

Solid-state ^{13}C NMR spectroscopy is one of the most useful spectroscopic methods for investigation of NOM structure because qualitative and quantitative organic structural information can be generated under non-degradative conditions (Peuravuori et al. 2003). The technique is useful for determining details of carbon structures, and is especially useful in combination with elemental composition data, apparent molecular weight or FTIR spectroscopy data of fractionated NOM (Gjessing et al. 1998). However, its use is reliant on a dry, preferably desalted NOM sample. Again, the low carbon and high ash content of the UF fraction contributed to a poorly resolved spectrum for this sample. But, a relatively strong aliphatic carbon signal was able to be identified, and as the signal was very broad, it indicated that the

aliphatic components were short in chain length and/or highly branched (Wilson et al. 1981).

The most significant peaks for the hydrophobic fractions were a broad aliphatic carbon signal, and a more sharply resolved aromatic signal. The transphilic fractions contained less aliphatic and unsaturated carbon and more aromatic carbon than the hydrophobic fractions. The results for solid-state ^{13}C NMR spectroscopy appear perceived to be in contrast to the results found in FTIR spectroscopy, whereby strongly aromatic material was found for the HPO fraction and more aliphatic material was shown in the TPI fraction. But, it must be remembered that the cross-polarizing solid-state ^{13}C NMR spectroscopic technique is most sensitive in the range of aliphatic carbon (10 – 60 ppm, Wong et al. 2002). Normalisation of the carbon signal (applied in Sections 3.3.2.3, 4.3.2.3 and 5.3.3.3) allows a direct comparison of the fractions to occur, avoiding region sensitivity influencing the results.

Solid-state ^{13}C NMR spectroscopy also allowed the fractions obtained in this study to be compared as the relative signal areas measured for the fractions were integrated over four broad regions and attributed to functional groups. Differences from the isolation method used were observed, with the UF fraction carbon type being in the order of oxygenated aliphatic carbon > aliphatic carbon > aromatic carbon > carbonyl carbon. The HPO and TPIB fractions were in the order of oxygenated aliphatic carbon > aromatic carbon > aliphatic carbon > carbonyl carbon. MIEX® treatment prior to resin fractionation showed differences in carbon distribution compared to the untreated fractions. The MIEX® HPO and MIEX® TPIB fractions appear to contain oxygenated aliphatic carbon > aliphatic carbon > aromatic carbon > carbonyl carbon, similar to UF. This knowledge has shown that MIEX® treatment preferentially removed a small component of the aromatic fraction prior to resin fractionation, and is likely to preferentially remove aromatic material of aquatic NOM.

6.3.4 Pyrolysis-Gas Chromatography-Mass Spectrometry

In pyrolysis, large complex molecules included in NOM are broken apart to more analytically available fragments by the application of heat and under anoxic conditions (Matilainen et al. 2011). Pyrolysis combined with gas chromatography

(py-GC-MS) is a useful technique for producing structural information about the molecular building blocks of NOM (Bruchet et al. 1990, Leenheer and Croué 2003). Py-GC-MS analysis requires only a few milligrams of dry sample, free of salt interference. The low carbon and high ash content of the UF fraction did not allow this technique to be performed, and the high salt content present in the TPIB and MIEX® TPIB samples reduced the NOM content in the sample and therefore the py-GC-MS product abundance.

Conversion of about 50 % of NOM mass to identified pyrolysis fragments is typical (Leenheer 2009), and interpretation of fragments from the pyrolytic technique yields information about the distribution of molecules belonging to specific biochemical precursors. The interpretation of NOM py-GC-MS chromatograms may be more subjective than that of solid-state ^{13}C NMR spectra, since only a portion of the pyrolysis fragments are generally used for interpretation. Interpretation of data is also complicated by the fact that some pyrolysis fragments (e.g. phenol, cresol) may have several origins, and others can be produced through secondary reactions.

Despite its limitations with the data interpretation, this technique is a valuable tool for understanding NOM, as it provides a fingerprint of NOM that is distinct from that obtained by other techniques. The hydrophobic fractions showed a relatively high abundance of aromatic hydrocarbons, alkylphenols and PAHs. However, aromatic hydrocarbons are common flash pyrolysis products and are derived from several biomolecular sources, offering limited source diagnostic value (Templier et al. 2005). Limitations therefore exist for analysing complex macromolecules, such as NOM, with this technique. In contrast to the hydrophobic fraction, the distribution of pyrolysis products from the transphilic fractions contained higher proportions of nitrogen- and oxygen-containing products.

All of the tentatively identified products were compared on a semi-quantitative basis employing a previously used classification system to reveal differences between the XAD-derived fractions of a high DOC, highly hydrophobic groundwater source. The hydrophobic fractions were rich in polysaccharides and lipids, with minimal input from protein or nitrogen- or sulfur- containing (N/S) compounds. The transphilic fractions were rich in tannins, protein and polysaccharides. The high abundance of polysaccharides present in the HPO fraction was reflected in the high oxygenated-

aliphatic and aromatic carbon content observed in the ^{13}C NMR spectrum (Section 6.3.3.). The higher abundance of oxygenated and nitrogenous products for the TPI fraction was also consistent with the oxygenated-aliphatic carbon content found in ^{13}C NMR spectroscopy (Section 6.3.3.), and higher organic nitrogen content and N/C ratio (Section 6.3.1).

Whilst MIEX® treatment preferentially removed transphilic and hydrophilic material, based on the redistribution of fractions following treatment, little molecular difference was evident in the py-GC-MS profiles of the untreated and MIEX® treated water. Most of the products identified from the HPO and TPI fractions of the MIEX® treated water were also detected in the same fractions of the untreated water. Py-GC-MS shows promise for the water industry because of the large amount of detailed data provided, but difficulties still remain with interpretation of this data. The technique allowed good comparisons between NOM characteristics identified by other analytical techniques, and helped to reinforce the interpretation of solid-state ^{13}C NMR, FTIR and fluorescence spectra. However, this characterisation method would require further development, prior to any implementation in the water industry.

6.3.5 On-line Thermochemolysis-Gas Chromatography-Mass Spectrometry

Thermochemolysis-GC-MS with tetramethylammonium hydroxide (TMAH) combines thermal degradation and chemical derivatisation, ideally in a single process termed “thermochemolysis”. Thermochemolysis offers the advantage over conventional pyrolysis of preservation of carboxylic acid and ester structures, since acidic protons are methylated. The product suites from on-line thermochemolysis complement those from conventional flash pyrolysis, with the detection of additional acids (as methyl esters).

Product abundance for the TPIB and MIEX® TPIB fractions was hindered by the high salt content of these samples. Sample impurity due to the high ash content in the UF fraction did not allow this technique to be performed. Hence, it is imperative that the isolation method chosen for NOM characterisation studies produces a sample of high purity, free from salt interference, to allow detailed characterisation to occur.

Quantification of pyrolysis products is extremely difficult, because of the vast quantity and range of pyrolysis products obtained (Page et al. 2003). It should be noted that absolute integration of peak areas is unreliable for any quantification because of the different weights of samples and relative amounts of organic material in the samples. Ratios of areas of pyrolysis products to the area of an internal standard is required to give a fingerprint of the pyrolysis products (Page et al. 2003). With this in mind, a broad comparison of the high amount of total TMAH thermochemolysis products detected compared to flash pyrolysis highlights the low suitability of flash pyrolysis to the large polar moiety of humic substances found in NOM. The methyl esters of low MW saturated and unsaturated acids were detected in relatively high abundance for the NOM fractions studied. These low MW acids and polymethoxybenzenes are common thermochemolysis products of NOM and are usually attributed to cross linking units between phenolic structures of humic macromolecules. Thermochemolysis also allowed the detection of a small number of oxygenated cyclic compounds. TMAH has been reported to promote detection of nitrogen- and oxygen-containing structures known to concentrate in the transphilic fractions (Templier et al. 2005).

The MIEX® treated NOM fractions also showed a large range of aliphatic and aromatic carboxylic acids common to thermochemolysis studies of NOM. Aliphatic diacids (as their dimethyl esters) were also detected, and are reported to be typical of animal, vegetable and microbial cell metabolites. Several high MW polycyclic aromatic hydrocarbons were also detected, suggesting that the TMAH reagent assists in the thermal release of these PAH structures.

Important additional structural information can be found with thermochemolysis-GC-MS, representing an excellent complementary method to conventional flash pyrolysis techniques where chromatographic resolution of the polar moiety of humic substances, such as that found in NOM, can be limited. Thermochemolysis-GC-MS shows promise for the water industry because of the large amount of detailed data provided, but difficulties still remain with interpretation of this data. Thermochemolysis, like py-GC-MS, reinforced the interpretation of solid-state ^{13}C NMR, FTIR and fluorescence spectra. However, the thermochemolysis-GC-MS

technique needs further method development for more advanced NOM characterisation, before application to the water treatment industry.

6.3.6 Micro-Scale Sealed Vessel Pyrolysis-Gas Chromatography-Mass Spectrometry

Micro-scale sealed vessel (MSSV) pyrolysis can complement the analytical characterisation afforded by more traditional pyrolysis techniques. Performed in a closed system using moderate temperatures over long time periods, MSSV pyrolysis can provide additional speciation information useful for establishing the structures and source inputs to recent organic material. MSSV removes oxygenated functional groups that give rise to chemical complexity, leaving the core hydrocarbon structures to be analysed.

Each fraction contained high concentrations of alkyl substituted benzenes, phenols and naphthalenes. As found in the pyrolysis-GC-MS and thermochemolysis-GC-MS chromatograms, the hydrophobic and transphilic fractions formed products in greater abundances, but the high salt content present in the TPIB fraction reduced the NOM content in the sample and therefore the product abundance. The low carbon and high ash content of the UF fraction, did not allow this technique to be performed.

The hydrophobic fractions were dominated by alkyl aromatic compounds, and low MW short chain aliphatic compounds. Alkyl aromatic compounds are common pyrolysis products and are usually attributed to lignin or tannin sources. MSSV also allowed the detection of higher MW alkyl phenols (not detected by flash pyrolysis-GC-MS). These high MW alkyl phenols are common products of aquatic and terrestrial humic substances and are attributed to lignin structures.

High abundances of polycyclic aromatic hydrocarbons (including alkyl naphthalenes and alkyl benzenes) were detected for the hydrophobic fractions. Flash pyrolysis, in contrast, yielded very low concentrations of these products. MSSV pyrolysis also showed a higher proportion of N-containing compounds for the transphilic fractions compared to flash pyrolysis-GC-MS.

MSSV py-GC-MS shows promise as a NOM characterisation technique because of the large amount of information provided, but difficulties still remain with

interpretation of the data. This method uses thermal degradation to convert the complex macromolecular NOM structure into smaller fragments that are amenable to identification by GC-MS. However, since the mechanisms of thermal degradation are not yet fully understood, uncertainty still remains over the nature of the precursors to the pyrolysis fragments obtained. Although considerable research has been conducted in this field (Berwick 2009), additional questions remain regarding the mechanisms of formation of products under different heating conditions. Until these questions are answered, the utility of this technique will be largely limited to fingerprinting to provide broad insights into possible structural moieties that might exist within NOM.

6.4 Effects of MIEX® Treatment on the Isolated Fractions

In removing NOM from groundwater, optimisation of the treatment process is important. The main aim of treatment is to produce higher quality water that in turn will create fewer problems in the distribution system. MIEX® is a key NOM removal process in operation at the Wanneroo Groundwater Treatment Plant (GWTP). This study used a high DOC groundwater with a high hydrophobicity for characterisation and treatability studies to assess the performance of the MIEX® process for removal of various fractions. As MIEX® is a relatively new technology in water treatment, the removal effectiveness of the resin for different types of organic matter is not yet well understood. The treatability by MIEX® of each fraction are discussed in detail in the following sections.

6.4.1 DOC Concentration, UV_{254} Absorbance and Colour

NOM content is usually represented by the measurement of DOC concentration and/or absorption of UV light (UV_{254} absorbance). UV_{254} has been identified as a potential surrogate measure for DOC, despite its propensity to only represent the aromatic character. NOM is also the major contributor of the brownish yellow colour in water (Matilainen et al. 2011). Measurement of colour, therefore, can give some indication of the amount of NOM in water (Edwards and Amirharajah, 1985). All of these tests are fast and do not require sophisticated sample pre-treatment or analytical

equipment. These analyses, however, provide information mostly about the amount of NOM, while offering limited information on the character of NOM.

MIEX® treatment of each XAD fraction was conducted by a laboratory simulation of the MIEX® process in operation at the Wanneroo GWTP. Treatment of the Raw Water UF fraction by the MIEX® process led to only a small reduction in DOC concentration (12 %) and a moderate reduction in UV_{254} absorbance (28 %). The high salt content of the UF fraction may have effectively competed for active ion-exchange sites on the resin, limiting the ability of the MIEX® resin to remove DOC from the UF fraction. MIEX® treatment of the fractions isolated by the XAD-8/XAD-4 resin fractionation procedure led to a significant reduction in DOC concentration (55 – 69 %) and UV_{254} absorbance (57 – 87 %), suggesting that MIEX® treatment was effective for targeting removal of the differing polarity NOM fractions.

6.4.2 Fluorescence Excitation-Emission Spectroscopy

Fluorescence spectroscopy provides a sensitive and non-destructive analysis for NOM samples and it is useful for monitoring changes in the molecular structure of humic substances, as all NOM samples have a unique fluorescence signature (Matilainen et al. 2011). The main advantage of fluorescence techniques compared to traditional methods (such as UV-visible spectroscopy) is the better sensitivity and selectivity (Matilainen et al. 2011). The 3-D fluorescence excitation-emission (EEM) spectrophotometric technique visualises a range of different fluorophores covering the excitation and emission wavelengths from ~ 200 nm to ~ 500 nm. This study is the first report of EEM spectra of MIEX®-treated UF and XAD NOM fractions.

Analysis of the UF fraction and the MIEX®-treated UF fraction by fluorescence EEM showed that the MIEX® process removed both humic and fulvic material. The removal of this material can also be correlated to the decrease in UV_{254}-active species (Section 6.4.1). After MIEX® treatment, a small residual of soluble microbial by-product-like material was visible. This indicated that MIEX® was less effective at removing protein-derived structures.

Analysis of the XAD fractions and MIEX®-treated XAD fractions using fluorescence EEM also showed a high removal of humic and fulvic material, mirroring the

reductions observed in DOC concentrations and UV_{254} absorbance (Section 6.4.1). As observed with the UF fraction, EEM analysis of the TPIB fraction indicated soluble microbial metabolites were present after MIEX® treatment, consistent with the idea that the MIEX® process is less effective at removing protein-derived structures. MIEX® treatment of the TPIN fraction only removed a small proportion of the humic and fulvic acid type material, as shown by fluorescence EEM. The different chemical composition of the TPIN fraction in comparison to the HPO and TPIB fraction (as seen in the other characterisation techniques) was demonstrated by the use of fluorescence EEM since fluorescence EEM showed that limited material had been removed by MIEX® treatment of this fraction.

As demonstrated, fluorescence EEM is a sensitive method for analysis of NOM fractions. The current study has shown that the EEM spectra of the fractions were predominantly governed by aromatic (humic/fulvic) functionality. However, the nitrogenous fluorescing species associated with proteins also contributed to the EEM spectra for some samples. Thus, fluorescence EEM can be useful as in-situ method to investigate the predominance of aromatic species in NOM and could be used to monitor biological processes. This characterisation technique is useful for the water treatment industry, as it could be used to probe the origin of NOM and mixing processes in distribution systems, if sources with dissimilar NOM are blended.

6.4.3 Size Exclusion Chromatography

The molecular weight (MW) distribution is one of the fundamental properties required to understand the bulk properties of NOM. High pressure size exclusion chromatography (HPSEC) is an attractive option for determining the MW distribution of NOM, due to its ease of operation, simplicity of sample preparation and high sensitivity requiring minimal sample volumes.

Size exclusion chromatography with both organic carbon detection (OCD) and UV_{254} absorbance detection was used to examine the MW distribution of all fractions both pre- and post-MIEX® treatment. The highly hydrophobic DOC from the groundwater source showed similar MW distributions using both detection methods, indicating that much of the organic carbon in the sample was strongly UV_{254}-active and that with this type of NOM, OCD provided little useful information above the UV_{254}

method. Hence, prior to using HPSEC for NOM samples, it would be useful to characterise the hydrophobicity of the NOM, to determine whether both UV_{254} detection and OCD should be used, or if UV_{254} detection will be sufficient.

Analysis by SEC-OCD and SEC-UV_{254} showed that a moderate to significant proportion of the DOC was removed by MIEX® treatment for all fractions isolated by resin fractionation. MIEX® treatment of the HPO, TPIB and TPIN fractions showed removal of organic matter over a wide range of apparent MW. An intermediate amount of removal of humic material was observed for the UF fraction after MIEX® treatment, compared to the HPO, TPIB and TPIN fractions. Since NOM in groundwater in the Wanneroo borefield is thought (Heitz et al. 2001) to consist largely of tannin-derived substances composed predominantly of phenolic moieties, the minimal removal of humic material (as seen in HPSEC) reinforces the theory (Allpike et al. 2005) that phenolic moieties are not amenable to removal by ion exchange.

HPSEC is a rapid, sensitive method, and does not require sample pre-extraction, making this method directly applicable to drinking water treatment process applications. It has become very useful for NOM characterisation during different steps in drinking water treatment (Allpike et al. 2005, Fabris et al. 2008, Chow et al. 2009). HPSEC profiles provide valuable information in the study of the degree of removal, and the removal mechanisms, of high MW NOM during coagulation (Chow et al. 2009). Hence, HPSEC has been shown to be a highly valuable characterisation tool for the water treatment industry.

6.4.4 Disinfection By-Product Formation Potential

The chemical reactivity of NOM with chlorine as measured by the disinfection by-product formation potential (DBPFP) provides a qualitative assessment of NOM character. DBPFP is a standard method used by the water treatment industry to understand the reactivity of NOM (Franson 1998). Using a highly hydrophobic groundwater source in these DBPFP studies allowed study of a ‘worst case scenario’ for reactivity. It has previously been reported that hydrophobic compounds, such as humic acids, are the primary contributors of DBP precursors in natural waters (Collins et al. 1986, Kitis et al. 2002). The DBPFP studies showed that the raw water

UF isolate and the raw water XAD-isolated fractions (HPO and TPIB) had similar propensities to form THMs and HAAs. Therefore, the reactivity of these fractions has shown that XAD resins and UF are satisfactory isolation methods for isolating the DBP precursors for source waters containing highly hydrophobic NOM.

Chlorine reactivity of the UF fraction before and after MIEX® treatment showed a similar propensity to form THMs, but MIEX® treatment of the UF fraction did significantly reduce the propensity for HAA formation. The formation of THMs and HAAs for the HPO fraction and the HPO fraction after MIEX® treatment was essentially identical, indicating that the reactivity of the DOC in the two samples was very similar. In contrast to the HPO fraction, MIEX® treatment of the TPIB fraction showed some preferential removal of the precursors for THMs and HAAs.

MIEX® treatment before XAD isolation led to a reduced concentration of THMs and HAAs compared to the corresponding DBP concentrations formed from the raw water isolates (UF, HPO and TPIB). The DBPFP also revealed a trend towards increasing proportions of brominated species with MIEX® treatment before resin fractionation. The possibility of a shift towards more brominated DBPs after MIEX® treatment should be monitored in plant-scale applications of the MIEX® process, as brominated DBPs are reported to be of a greater health concern than their chlorinated counterparts.

6.5 MIEX® Treatment Applications

The MIEX® process is an ion exchange process that employs a strong base anion exchange resin to remove NOM from water. NOM removal occurs as a consequence of the negative charge characteristics of many NOM components typically found in water. Use of the high DOC, highly hydrophobic groundwater source evaluated in this study indicated that the MIEX® resin was able to remove NOM over a wide range of apparent molecular weight, consistent with previous studies (Warton et al. 2007, Drikas et al. 2011), and was effective for removal of both hydrophobic and transphilic material in this type of water source. The study results indicate that the MIEX® process can have a range of potential applications to meet site-specific needs of waters of this quality. Consideration must be given to other NOM removal approaches (such as membrane filtration, granular activated carbon) as achievable

levels of NOM removal may be greater with these types of technologies for this type of water source. However, the levels of NOM removal that are available with the MIEX® process may be appropriate at less cost to meet the needs of many utilities. Costs and process applicability of the respective process alternatives will vary depending on site specific factors, so it is important to confirm applicability of each treatment technology with pilot testing. In many cases, the MIEX® process could be integrated within a treatment sequence to provide a component of the overall strategy for NOM removal. It is important that the process be examined for its capability to act in conjunction with other processes to meet the overall goal for NOM removal under these conditions, with potential significant overall improvements in treated water quality.

6.6 Summary of Characterisation Methods For Water Industry Application

Groundwater is the main drinking water source in many regions. The quality of the groundwater will depend on the nature and character, as well as the amount, of NOM in the catchment. A number of different methods were used to describe the nature of NOM from a highly hydrophobic, high DOC groundwater source. Correlation of the data from the multiple characterisation methods has allowed more detailed structural information about NOM of this groundwater type to be obtained. New insights into the structural and functional features of fractionated NOM have been illustrated, which allows a greater understanding of the nature and properties of NOM from a high DOC concentration groundwater source with high hydrophobicity.

The characterisation methods used in this Thesis have been summarised in Table 6.2, together with comments on their application to water industry issues. In some cases, where methods have been relatively well established, these are readily applied to water industry problems (HPSEC, DBPFP, oxidant demand, rapid fractionation). However, in most cases, methods are applicable only to more fundamental research on NOM (py-GC-MS, thermochemolysis-GC-MS, MSSV py-GC-MS), and are not directly applicable to daily water quality issues, although they can provide information that has the potential to improve water treatment technology and management, indirectly and in the longer term. Some techniques (MSSV,

fluorescence EEM) are very new and innovative and require substantial further development. Further development of these techniques has the potential to lead to breakthroughs in the understanding of the fundamental chemistry of NOM.

Table 6.2 Summary of analytical methods and their utility for NOM characterisation and applicability to water industry issues.

Method	What information does it provide?	Comments on direct/indirect application to water industry issues Does it have immediate practical application to water industry?
NOM isolation		
UF	Evaluates overall presence of organic NOM	Not directly applicable to water industry issues, but a useful research tool when used in combination with other methods.
Resin fractionation	Distinguishes between hydrophobic and hydrophilic NOM	XAD-8/XAD-4 resin method is not directly applicable to water industry issues, but a useful research tool when used in combination with other methods. The related rapid fractionation characterisation (but not isolation) method (Chow et al. 2006) is used in water treatment plant research projects as it is a quick method (< 7 hours), requires minimal sample preparation and is a useful tool to evaluate treatment processes (Drikas et al. 2011). The rapid fractionation method can determine the efficiency of water treatment processes, identify NOM fractions recalcitrant to conventional treatment and allow investigation of the formation of disinfection by-products (Chow et al. 2006).
Characterisation techniques		
Elemental analysis	Indicator of purity of NOM samples and isolation protocols. Elemental composition is often used for calculation of the atomic ratios, such as O/H, H/C or N/C.	Not directly applicable to water industry issues, but a useful research tool when used in combination with other methods.
FTIR spectroscopy	Molecular information on NOM functional groups	Not directly applicable to water industry issues, but a useful research tool when used in combination with other methods.
Solid-state ^{13}C NMR spectroscopy	Molecular information on NOM functional groups	Not directly applicable to water industry issues, but a useful research tool when used in combination with other methods.
Pyrolysis-GC-MS	Molecular information on NOM substructures and functional groups, origins of NOM	Not directly applicable to water industry issues, partly due to its complexity and the difficulties that remain in data interpretation. Method is still a useful research tool in combination with other methods.
Online thermochemolysis-GC-MS	Molecular information on NOM substructures and functional groups, origins of NOM	Not directly applicable to water industry issues, partly due to its complexity and the difficulties that remain in data interpretation. Method is still a useful research

		tool in combination with other methods.
MSSV py-GC-MS	Molecular information on NOM substructures and functional groups, origins of NOM	Not directly applicable to water industry issues, partly due to its complexity and the difficulties that remain in interpretation of the data. Method is still a useful research tool in combination with other methods.
Fluorescence EEM	Origins of NOM, Three major groups: protein- , humic- and fulvic-like fluorophores	Fluorescence EEM is potentially directly applicable to water industry issues, providing information on NOM removal in treatment processes.
SEC-OCD / SEC-UV_{254}	Molecular weight distribution of NOM, NOM fingerprinting	SEC-OCD / SEC-UV_{254} is directly applicable to water industry issues, providing information on NOM removal in treatment processes.
Oxidant Demand	Chemical reactivity of NOM with chlorine/bromine can provide a qualitative assessment of NOM character	Oxidant demand is directly applicable to water industry issues, providing information on reactivity of NOM. Oxidant demand is already used by the water industry as a standard method (Franson, 1998).
DBPFP	Chemical reactivity of NOM with chlorine/bromine can provide a qualitative assessment of NOM character	DBPFP is directly applicable to water industry issues, providing information on reactivity of NOM. DBPFP is already used by the water industry as a standard method (Franson, 1998). DBPFP can also be used to examine the potential to exceed guideline concentrations of DBPs in the distribution system.

6.7 Thesis Conclusions

It is well recognised that improved understanding of the chemical structure, functionality and behaviour of NOM is important for development of enhanced water treatment and management technologies. The complexity and ill-defined nature of NOM means that any study of the chemistry of this material brings with it considerable analytical challenges and no single approach can provide definitive answers. In this Thesis, a number of methods to improve the understanding of the molecular chemical structures of NOM from a high DOC, highly hydrophobic groundwater source have been investigated, providing new information on NOM chemistry and behaviour.

A three-fold research approach was used. First, the performance of two NOM isolation methods, ultrafiltration (UF) and XAD-8/XAD-4 resin fractionation, were compared. These techniques were compared based on the efficiency with which NOM was collected and separated. UF was found to be more useful for evaluating the overall presence of organic material, but resin fractionation was found to be more useful for examination of aromatic and hydrophobic humic species. Recommendations for both UF and resin fractionation focus on avoiding the desalting challenges experienced in this study, allowing a greater suite of characterisation methods to be employed for all fractions.

Next, the isolated NOM was compared using several analytical methods. This part of the research shed light on the variability of molecules contributing to NOM of a highly hydrophobic, high DOC groundwater. It also highlighted the potential value and limitations of the analytical methods used in this NOM research. Characterisation of the various fractions by FTIR and solid-state ^{13}C NMR spectroscopic analysis revealed the UF, HPO, TPIB and TPIN fractions to have a significant contribution of aliphatic content from lipid and biopolymer precursors. Further characterisation of the HPO, TPIB and TPIN fractions by pyrolysis-GC-MS, thermochemolysis-GC-MS and MSSV pyrolysis-GC-MS revealed that the HPO fraction had a significant contribution of polysaccharide input. The higher nitrogen and oxygen content present in the TPIB and TPIN fractions allowed more nitrogen and oxygen containing groups (such as those derived from tannins and proteins) to

be revealed by the pyrolysis and thermochemolysis techniques. Issues with data interpretation occurred for the pyrolytic techniques, but these characterisation methods helped to reinforce the information obtained by other characterisation methods. Further method development for more advanced NOM characterisation with the pyrolytic techniques is required before these methods can be applied to the water treatment industry.

Finally, the effects of NOM isolation procedures on the chemical composition and reactivity of the isolates was investigated. All the fractions showed different affinity for the MIEX® resin. Upon MIEX® treatment, the UF fraction showed only a slight reduction in DOC concentration, UV_{254} absorbance and colour, whereas the HPO, TPIB and TPIN fractions showed a significant reduction in these parameters. The high salt content in the UF fraction was likely in competition with the DOC in this fraction for ion exchange sites on the MIEX® resin, limiting the ability of the MIEX® resin to remove DOC from this fraction. In comparison, the MIEX® resin was effective for removal of organic matter in the HPO, TPIB and TPIN fractions of NOM, as the low salt content of these fractions did not interfere in DOC removal by the MIEX® process.

Chlorine reactivity of the UF fraction before and after MIEX® treatment showed a similar propensity to form THMs, but MIEX® treatment of the UF fraction did significantly reduce the propensity for HAA formation. The formation of THMs and HAAs for the HPO fraction and the HPO fraction after MIEX® treatment was essentially identical, indicating that the reactivity of the DOC in the two samples was very similar. In contrast to the HPO fraction, MIEX® treatment of the TPIB fraction showed some preferential removal of the precursors for the THMs and HAAs. It should also be noted that there was a shift towards more brominated HAAs after MIEX® treatment for the UF fraction and more brominated THMs after MIEX® treatment for the TPIB fraction. The possibility of a shift towards more brominated DBPs after MIEX® treatment should be monitored in plant-scale applications of MIEX® treatment, as brominated DBPs are reported to be of a greater health concern than their chlorinated counterparts.

MIEX® treatment of the highly hydrophobic, high DOC groundwater prior to resin fractionation of the NOM remaining after MIEX® treatment did help to reveal subtle

differences in the molecular composition and properties of the fractions. MIEX® treatment changed the distribution of the XAD fractions, due to preferential removal of the TPI and HPI fractions. Detailed molecular analysis with a range of methods, including sophisticated spectroscopic analysis, showed an increase in aliphatic character within the composition of the solid isolates (MIEX® HPO, MIEX® TPIB and MIEX® TPIN) compared to the raw water fractions.

Overall, this Thesis has contributed to the study of NOM, to gain more insight into the fundamental properties of NOM and to develop practical methods to isolate and study NOM. This Thesis has also shown that data from a combination of characterisation methods must be correlated with each other to derive more detailed structural information about NOM and to validate results obtained from different methods.

Appendix 1

Table A.1 Tentatively identified pyrolysis products and unidentified products from the HPO fraction.

Peak Nº	R.T. (mins)	Compound	Peak Nº	R.T. (mins)	Compound
1	1.167	methylpropene / 1,3-butadiene	62	36.919	unknown
2	1.234	methylpropene	63	37.523	cyclododecane
3	1.278	methanethiol	64	38.551	naphthalenol
4	1.379	isocyanic acid	65	39.178	dibenzofuran
5	1.434	acetaldehyde	66	39.547	dodecanoic acid
6	1.646	acetone / acetonitrile	67	40.789	ethyl phthalate
7	1.790	isopentadiene	68	41.405	diphenylenemethane
8	1.891	dimethylcyclopropane	69	44.137	3,3,6,9,9,10-hexamethyl-2,10-diazabicyclo[4.4.0]-1-decene
9	1.969	1,3-butadiene	70	44.272	unknown
10	2.113	1,3-cyclopentadiene	71	44.586	2,4-diphenyl-4-methyl-2(Z)-pentene
11	2.747	acetic acid	72	45.058	tetradecanoic acid
12	2.903	2-butanone	73	45.934	unknown
13	3.026	methylfuran	74	46.170	diphenylmethylpentene
14	3.860	1-methyl-3-cyclopentadiene	75	46.406	anthracene
15	4.416	benzene	76	46.900	pentadecanoic acid
16	4.628	thiophene	77	47.676	unknown
17	5.663	dimethylfuran	78	48.453	hexadecanoic acid
18	5.963	2-cyclopenten-1-one	79	48.565	butyl phthalate
19	7.231	pyrrole	80	51.416	pentadecane
20	7.955	toluene	81	51.619	unknown
21	8.133	methylthiophene	82	53.435	hexadecane
22	10.592	furan	83	55.012	1,2-benzenedicarboxylic acid
23	10.781	methylpyrrole	84	55.630	unknown
24	12.005	ethylbenzene	85	60.204	unknown
25	12.417	xylene	86	61.832	unknown
26	12.796	dimethylthiophene			
27	13.230	methylfuranone			
28	13.442	styrene			
29	13.943	2-methyl-2-cyclopenten-1-one			
30	16.661	2-cyclopenten-1-one			
31	17.185	phenol			
32	17.766	benzonitrile			
33	18.200	C_3 benzene			
34	18.356	benzofuran			
35	19.470	trimethylbenzene			
36	19.949	dimethyl-2-cyclopenen-1-one			
37	20.562	cresol (methylphenol) isomer			
38	21.477	cresol isomer			
39	22.213	unknown			
40	23.116	unknown			
41	23.340	methylbenzofuran			
42	24.655	methylbenzyl alcohol			
43	25.024	benzoic acid			
44	25.180	methylindane			
45	25.337	ethylphenol isomer			
46	26.509	ethylphenol isomer			
47	26.776	naphthalene			
48	27.424	unknown			
49	27.837	dimethylbenzofuran			
50	27.937	unknown			
51	28.484	2-coumarone			
52	29.723	resorcinol			
53	30.393	unknown			
54	31.164	methylnaphthalene isomer			
55	31.320	phthalic anhydride			
56	31.778	methylnaphthalene isomer			
57	32.180	unknown			
58	33.220	unknown			
59	35.197	dimethylnaphthalene isomer			
60	35.678	dimethylnaphthalene isomer			
61	35.846	dimethylnaphthalene isomer			

Table A.2 Tentatively identified pyrolysis products and unidentified products from the TPIB fraction.

Peak Nº	**R.T. (mins)**	**Compound**
1	1.135	2-methylpropene
2	1.246	methanethiol
3	1.390	acetaldehyde
4	1.579	acetonitrile
5	1.746	methylbutadiene
6	1.890	acrylonitrile
7	2.056	1,3-cyclopentadiene
8	2.545	propanenitrile
9	2.656	acetic acid
10	4.309	benzene
11	7.095	pyrrole
12	7.805	toluene
13	8.393	unknown
14	13.211	styrene
15	16.919	phenol
16	17.485	benzonitrile
17	21.181	cresol
18	40.500	ethyl phthalate
19	48.248	decanoic acid
20	54.774	1,2-benzenedicarboxylic acid
21	58.555	unknown

Table A.3 Tentatively identified pyrolysis products and unidentified products from the TPIN fraction.

Peak Nº	R.T. (mins)	Compound	Peak Nº	R.T. (mins)	Compound
1	1.158	dichloromethane / methylpropane	70	28.453	coumaranone
2	1.236	methylpropene / 1,3-butadiene	71	28.699	unknown
3	1.359	butene	72	29.472	ethylacetophenone
4	1.414	methanamine	73	30.347	*trans*-benzalacetone
5	1.503	unknown	74	31.110	methylnaphthalene
6	1.593	unknown	75	31.379	unknown
7	1.682	acetonitrile / acetone	76	32.579	methoxyacetophenone/ ethylbenzoic acid
8	1.860	methylbutadiene	77	33.791	unknown
9	1.949	dimethylcyclopropane	78	34.407	hydroxyacetophenone
10	1.983	acrylonitrile	79	35.204	dimethylnaphthalene
11	2.172	cyclopentadiene	80	35.743	diacetylbenzene
12	2.651	propanenitrile	81	37.147	phthalamide
13	2.785	3-buten-2-one	82	40.779	ethyl phthalate
14	2.941	2-butenone	83	41.049	unknown
15	3.888	cyclohexadiene	84	41.476	unknown
16	3.988	hexatriene	85	43.130	unknown
17	4.166	methylcyclopentene	86	44.313	unknown
18	4.434	benzene	87	44.527	unknown
19	4.679	unknown	88	45.102	tetradecanoic acid
20	4.968	methylpentadiene	89	45.689	1,4-diaza-2,5-dioxobicyclo[4.3.0] nonane
21	5.558	propionic acid	90	46.918	diethyl phthalate
22	5.681	dimethyl furan	91	47.088	1,2-benzenedicarboxylic acid
23	5.836	propenoic acid	92	47.81	unknown
24	6.961	dimethylcyclopentadiene	93	48.307	hexadecanoic acid isomer
25	7.072	pyridine	94	48.545	butyl phthalate
26	7.295	pyrrole	95	48.714	3,9-diazatricyclo[7.3.0.0(3,7)] dodecan-2,8-dione
27	7.986	toluene	96	51.044	decanedioic acid
28	8.866	acetamide	97	52.472	benzene sulfonamide
29	9.933	methylpyridine	98	54.809	phthalic acid
30	10.056	furfural	99	55.637	triphenylphosphine oxide
31	10.635	2-cyclopenten-1-one	100	58.826	unknown
32	10.814	methylpyrrole isomer			
33	11.159	methylpyrrole isomer			
34	11.994	ethylbenzene			
35	12.396	xylene			
36	12.697	cyclopentanol			
37	13.399	styrene			
38	13.890	2-methylcyclopentanone			
39	14.570	dimethylpyrrole			
40	15.250	dimethylpyridine			
41	16.266	unknown			
42	16.589	ethyltoluene isomer			
43	16.746	ethyltoluene isomer			
44	17.058	butanedinitrile			
45	17.259	phenol			
46	17.717	benzonitrile			
47	18.163	alkylbenzene			
48	18.398	methylstyrene			
49	19.001	unknown			
50	19.369	C_3 benzene			
51	19.615	unknown			
52	19.916	dimethylcyclopent-2-en-1-one			
53	20.519	indene			
54	20.586	cresol isomer			
55	20.933	C_4 benzene			
56	21.391	acetophenone			
57	21.525	cresol isomer			
58	21.782	unknown			
59	22.162	ethylstyrene			
60	22.330	methyl succinimide			
61	22.475	tolunitrile isomer			
62	22.598	furandione			
63	23.079	tolunitrile isomer			
64	23.694	tetramethylbenzene			
65	25.126	benzoic acid			
66	26.515	methylacetophenone			
67	26.750	naphthalene			
68	27.098	unknown			
69	27.322	dimethylindazole			

Table A.4 Tentatively identified thermochemolysis-GC-MS products and unidentified products from the HPO fraction.

Peak Nº	R.T. (mins)	Compound	Peak Nº	R.T. (mins)	Compound	Peak Nº	R.T. (mins)	Compound
1	3.311	methyl acrylate	52	21.012	methyl 4,4-dimethoxy-2-methyl butanoate	103	41.097	unknown
2	3.647	methyl propanoate	53	21.522	cresol isomer	104	42.409	decanedioic acid dimethyl ester
3	3.906	1,3-cyclohexadiene	54	22.002	dimethylbutanedioic acid methyl ester	105	43.500	methyl methoxycinnamate
4	4.002	methylcyclopentadiene	55	22.204	allyltoluene	106	44.265	trimethoxybenzoic acid methyl ester
5	4.454	benzene	56	22.320	unknown	107	44.400	tetradecanoic acid methyl ester
6	4.684	methyl-1,3-cyclopentadiene	57	22.560	unknown	108	44.981	unknown
7	5.049	methyl isobutyrate	58	22.666	methyl benzoate	109	45.863	unknown
8	5.845	methyl methacrylate	59	23.022	unknown	110	46.376	pentadecanoic acid methyl ester
9	5.980	methyl butenoate	60	23.119	dimethylanisole	111	46.648	unknown
10	6.248	methyl butyrate	61	23.253	glycine methyl ester/ methyl benzofuran	112	47.668	hexadecanoic acid methyl ester
11	6.642	methyl *cis*-2-butenoate	62	24.052	dimethyl glutarate	113	48.387	methyl diphenylphosphinate
12	6.834	methylpyrrole	63	24.523	1,2-dimethoxybenzene	114	48.669	dodecanoic acid methyl ester
13	6.987	dimethylcyclopentadiene	64	24.706	dimethylphenol isomer	115	50.334	octadecanoic acid methyl ester
14	7.247	dimethylaminoacetonitrile	65	24.792	dimethylphenol isomer	116	52.753	unknown
15	7.631	methoxyacetic acid methyl ester	66	25.148	vinylanisole	117	55.014	1,2-benzenedicarboxylic acid methyl ester
16	7.775	methyl *trans*-crotonate	67	25.967	unknown	118	58.942	unknown
17	7.996	toluene	68	26.794	naphthalene			
18	8.293	3-methylbutanoic acid methyl ester	69	27.227	methyl toluate isomer			
19	8.495	unknown	70	27.381	unknown			
20	8.706	methyl ester of 2-methoxy propionic acid	71	27.612	methyl toluate isomer			
21	10.664	unknown	72	27.834	dimethylbenzofuran			
22	10.780	dimethyl pyrrole	73	28.344	dimethylanisole			
23	11.173	2-pentanoic acid methyl ester	74	28.883	dimethoxytoluene			
24	11.673	dimethylphosphite	75	29.124	unknown			
25	12.028	ethylbenzene	76	29.807	hexanedioic acid dimethyl ester			
26	12.105	methylbutenoic acid methyl ester	77	29.933	unknown			
27	12.239	unknown	78	30.790	methyl dimethylbenzoate			
28	12.422	xylene isomer	79	31.185	methylnaphthalene isomer			
29	12.499	xylene isomer	80	31.802	methylnaphthalene isomer			
30	13.325	trimethoxypropane	81	32.062	unknown			
31	13.421	styrene	82	32.341	methylmethoxybenzene isomer			
32	13.930	2-methyl-2-cyclopenten-1-one	83	32.775	unknown			
33	14.064	dimethyl sulfone	84	33.334	unknown			
34	14.285	unknown	85	33.719	methylmethoxybenzene isomer			
35	14.535	methoxybenzene (anisole)	86	34.230	unknown			
36	14.929	trimethyl phosphate	87	34.538	trimethyl propane-1,2,3-tricarboxylate			
37	16.302	unknown	88	34.866	trimethoxybenzene			
38	16.638	ethyltoluene isomer	89	35.204	unknown			
39	16.783	ethyltoluene isomer	90	35.522	unknown			
40	17.090	unknown	91	36.101	unknown			
41	17.292	unknown	92	36.245	methyl phthalate			
42	17.426	hexahydro-1,3,5-trimethyl-1,3,5-triazine	93	36.939	biphenylene			
43	17.744	benzonitrile	94	37.161	unknown			
44	18.244	trimethylbenzene	95	37.258	trimethoxytoluene			
45	18.753	methylanisole isomer	96	38.010	dimethyl isophthalate			
46	19.214	methyl fumarate	97	38.386	dimethyl terephthalate			
47	19.291	methylanisole isomer	98	38.531	dodecanoic acid methyl ester			
48	19.359	methylanisole isomer	99	38.675	unknown			
49	19.580	dimethyl succinate	100	39.225	unknown			
50	19.955	dimethyl-2-cyclopenten-1-one	101	40.489	methyl dimethoxybenzoate isomer			
51	20.599	cresol isomer	102	40.740	methyl dimethoxybenzoate isomer			

Table A.5 Tentatively identified thermochemolysis-GC-MS products and unidentified products from the TPIB fraction.

Peak Nº	R.T. (mins)	Compound
1	3.253	methyl acrylate
2	3.321	methyl carbonate
3	3.570	methyl propanoate
4	3.839	methylcyclopentadiene
5	4.165	ethylene chloride
6	4.376	benzene
7	4.587	thiophene
8	6.746	methylpyrrole
9	6.986	pyridine
10	7.150	dimethylaminoacetonitrile
11	7.409	dimethylcyanamide
12	7.543	unknown
13	7.697	butenoic acid methyl ester
14	7.908	toluene
15	8.302	butylethylene
16	8.609	unknown
17	9.377	unknown
18	9.848	methylpyridine
19	10.059	*N*-methylacetamide
20	10.501	hexylcrotonate methyl ester
21	11.932	ethylbenzene
22	12.114	unknown
23	12.412	unknown
24	13.343	styrene
25	14.812	trimethylphosphate
26	17.279	hexahydro-1,3,5-trimethyl-1,3,5-triazine
27	17.405	dimethylpropanal
28	17.673	benzonitrile
29	18.806	ethylhexanol
30	19.497	dimethyl succinate
31	20.927	dimethyl methylbutanedioic acid
32	21.167	unknown
33	22.203	unknown
34	22.568	methyl benzoate
35	22.933	unknown
36	23.125	dimethylthioformamide
37	26.330	unknown
38	26.694	naphthalene
39	28.249	unknown
40	28.738	unknown
41	30.695	methyl dimethylbenzoate
42	31.328	carbomethoxybenzaldehyde
43	31.463	unknown
44	31.962	unknown
45	33.612	unknown
46	33.861	unknown
47	34.437	dimethyl itaconate
48	35.137	unknown
49	35.377	unknown
50	35.521	unknown
51	36.145	methyl phthalate
52	37.891	dimethyl terephthalate
53	38.285	dimethyl isophthalate
54	38.419	unknown
55	39.110	nonanedioic acid dimethyl ester
56	42.304	unknown
57	43.878	unknown
58	44.319	tetradecanoic acid methyl ester
59	45.635	unknown
60	46.307	methyl heptadecanoate
61	46.893	unknown
62	47.594	hexadecenoic acid methyl ester
63	49.296	decanoic acid methyl ester
64	50.268	octadecenoic acid methyl ester
65	50.672	unknown
66	51.597	unknown
67	52.686	unknown
68	53.737	hexamethyl cyclotrisiloxane
69	54.933	1,2-benzenedicarboxylic acid methyl ester
70	58.814	squalene

Table A.6 Tentatively identified thermochemolysis-GC-MS products and unidentified products from the TPIN fraction.

Peak Nº	R.T. (mins)	Compound	Peak Nº	R.T. (mins)	Compound	Peak Nº	R.T. (mins)	Compound
1	3.340	methyl acrylate	54	23.041	unknown	107	42.406	decanedioic acid dimethyl ester
2	3.667	methyl propanoate	55	23.128	dimethylanisole	108	44.004	unknown
3	3.926	methyl-1,3-cyclopentadiene	56	23.456	cresol isomer	109	44.101	unknown
4	4.032	methyl-1,3-cyclohexadiene	57	23.727	unknown	110	44.988	unknown
5	4.493	benzene	58	24.055	ethoxytoluene	111	47.126	unknown
6	4.724	hexatriene	59	24.220	dimethyl glutarate	112	47.987	hexadecanoic acid methyl ester
7	5.886	methyl methacrylate	60	24.519	dimethylanisole isomer	113	48.584	butylphthalate
8	6.876	methylpyrrole	61	24.780	dimethylanisole isomer	114	50.602	octadecanoic acid methyl ester
9	7.030	cyclopentadiene	62	25.166	methylindene	115	51.092	decanedioic acid dibutyl ester
10	7.126	pyridine	63	25.640	unknown	116	55.022	1,2-benzenedicarboxylic acid methyl ester
11	7.347	pyrrole	64	25.959	methylacetophenone isomer	117	55.660	triphenylphosphine oxide
12	7.837	methyl crotonate	65	26.530	methylacetophenone isomer	118	58.962	squalene
13	8.049	toluene	66	26.791	naphthalene			
14	8.328	unknown	67	27.236	methyl toluate isomer			
15	8.741	2-methoxy propionic acid methyl ester	68	27.381	unknown			
16	9.962	methylpyridine	69	27.507	unknown			
17	10.298	*N*-methylacetamide	70	27.604	methyl toluate isomer			
18	10.712	unknown	71	27.778	unknown			
19	10.875	methylpyrrole isomer	72	28.340	dimethyl adipate			
20	11.221	methylpyrrole isomer	73	28.843	dimethoxytoluene			
21	12.066	ethylbenzene	74	29.404	methoxybenzaldehyde			
22	12.471	xylene isomer	75	29.521	ethylacetophenone			
23	12.528	xylene isomer	76	29.811	unknown			
24	13.462	styrene	77	29.918	unknown			
25	13.904	ethylpyridine	78	30.402	unknown			
26	13.972	3-methyl-2-cyclopenten-1-one	79	30.799	methyl dimethylbenzoate			
27	14.299	dimethylsulfone	80	31.177	methylnaphthalene			
28	14.578	anisole	81	31.429	ethyl benzoic acid methyl ester			
29	15.300	dimethylpyrrole	82	31.575	methyl cinnamate			
30	16.656	ethyltoluene isomer	83	31.797	methylnaphthalene			
31	16.811	ethyltoluene isomer	84	32.069	unknown			
32	17.340	phenol	85	32.137	methyl vinylbenzoate			
33	17.494	unknown	86	32.350	methyl methoxybenzoate isomer			
34	17.601	unknown	87	32.757	unknown			
35	17.764	unknown	88	33.000	methoxyacetophenone			
36	18.246	benzonitrile	89	33.456	unknown			
37	18.468	methylstyrene	90	33.717	methyl methoxy benzoate isomer			
38	18.786	methylanisole isomer	91	34.630	unknown			
39	19.229	methyl fumarate	92	35.212	unknown			
40	19.384	methylanisole isomer	93	35.474	unknown			
41	19.471	2-ethylhexanol	94	35.620	methylphthalimide			
42	19.596	dimethyl succinate	95	36.115	unknown			
43	19.962	dimethyl-2-cyclopenten-1-one	96	36.241	methyl phthalate			
44	20.049	propylpiperidine	97	36.970	methyl acetylbenzoate isomer			
45	20.570	indene	98	37.232	methyl acetylbenzoate isomer			
46	20.714	cresol isomer	99	38.000	dimethyl terephthalate			
47	21.023	dimethyl methylsuccinate	100	38.389	dimethyl isophthalate			
48	21.438	acetophenone	101	38.544	unknown			
49	21.631	cresol isomer	102	38.933	unknown			
50	22.229	unknown	103	39.215	nonanedioic acid dimethyl ester			
51	22.365	methyl succinimide	104	39.400	unknown			
52	22.538	methylbenzonitrile	105	39.847	unknown			
53	22.722	methyl benzoate	106	40.752	methyl methoxybenzoate isomer			

Table A.7 Tentatively identified MSSV-GC-MS products and unidentified products from the HPO fraction.

Peak Nº	R.T. (mins)	Compound	Peak Nº	R.T. (mins)	Compound
1	1.930	butene	67	13.846	ethylmethylhexadiene
2	2.067	methylpropene	68	13.955	dimethylthiophene isomer
3	2.530	pentene	69	14.281	dimethylthiophene isomer
4	2.730	methylbutane	70	14.492	xylene isomer
5	3.015	2-pentene	71	15.087	trimethylcyclopentanone
6	3.147	propanal	72	15.658	ethylmethylhexadiene
7	3.341	dimethylcyclopropane	73	15.715	isopropylbenzene
8	4.250	cyclopentene	74	16.161	tetramethylfuran
9	4.639	methylpentene isomer	75	16.470	dimethylpyridine
10	4.736	dimethylbutene isomer	76	16.893	propylbenzene
11	5.004	methylpentane isomer	77	17.207	ethyltoluene isomer
12	5.205	methylpentene isomer	78	17.327	ethyltoluene isomer
13	5.462	hexane	79	17.544	trimethylbenzene isomer
14	5.513	butanone	80	18.059	phenol
15	5.696	dimethylbutene isomer	81	18.522	trimethylbenzene isomer
16	5.822	methylfuran	82	19.150	trimethylthiophene
17	6.050	methylpentene isomer	83	19.259	trimethylpyridine
18	6.159	methylcyclopentane	84	19.465	trimethylpyrrole
19	6.302	methylpentene isomer	85	19.579	C_3 benzene
20	6.525	methylcyclopentadiene	86	19.790	methylisopropylbenzene
21	6.759	dimethylpentene isomer	87	20.105	allylbenzene
22	6.816	methylcyclopentene	88	20.236	dimethylcyclopent-2-en-1-one
23	7.045	benzene	89	20.693	diethylbenzene
24	7.199	unknown	90	20.831	propyltoluene
25	7.251	thiophene	91	20.968	cresol isomer
26	7.559	methylpentadiene	92	21.236	trimethyl-2-cyclopenten-1-one
27	7.862	isooctane	93	21.488	acetophenone
28	7.925	dimethylpentene isomer	94	21.676	ethyldimethylthiophene
29	7.977	2-pentanone	95	21.871	cresol isomer
30	8.251	heptane	96	22.168	methylphenylcyclopropane
31	8.342	methylhexene	97	22.334	ethylxylene
32	8.445	dimethylfuran	98	22.865	ethylcumene
33	8.542	dimethylpentadiene	99	23.100	methylbenzofuran
34	8.599	dimethylpentene isomer	100	23.420	diethyltoluene
35	8.668	dimethyl furan	101	23.557	tetramethylbenzene
36	9.051	trimethylcyclopentene	102	24.117	isopropyldimethylbenzene isomer
37	9.165	ethylcyclopentane	103	24.243	ethylphenol isomer
38	9.423	methylcyclohexadiene	104	24.448	isopropyldimethylbenzene isomer
39	9.463	methyl-2-pentanone	105	24.654	methylindane
40	9.640	unknown	106	24.711	dimethylphenol isomer
41	9.714	trimethylcyclobutane	107	25.409	ethylphenol isomer
42	9.765	2-methyl-3-pentanone	108	25.563	dimethylphenol isomer
43	9.817	ethylmethylpentene	109	25.792	dimethylphenol isomer
44	9.903	trimethylcyclopentene isomer	110	26.089	ethylmethyl phenol
45	10.011	trimethylcyclopentene isomer	111	26.443	dimethylphenol
46	10.126	toluene	112	26.786	unknown
47	10.251	methylthiophene isomer	113	26.895	trimethylphenol isomer
48	10.406	methylheptane	114	27.203	dimethylindazole
49	10.514	methylthiophene isomer	115	27.323	dimethylbenzofuran isomer
50	10.84	3-hexanone	116	27.455	dimethylbenzofuran isomer
51	10.949	dimethylhexene	117	27.712	ethylmethylphenol isomer
52	11.074	trimethylcyclopentene isomer	118	27.901	ethylmethylphenol isomer
53	11.206	methylheptene	119	28.089	ethylmethylphenol isomer
54	11.286	unknown	120	28.295	trimethylphenol isomer
55	11.492	trimethylcyclopentene isomer	121	28.535	dimethylindane isomer
56	11.566	dimethylhexene	122	28.969	unknown
57	11.766	trimethylpyrazole	123	29.238	trimethylphenol isomer
58	12.417	methylethylcyclopentene	124	29.621	dimethylindane isomer
59	12.600	tetramethylcyclopentene isomer	125	30.284	methylnaphthalene
60	12.697	2-methylcyclopentanone	126	30.764	unknown
61	12.806	dimethylmethylenecyclopentene	127	31.444	trimethylbenzofuran
62	12.938	tetramethylcyclopentene isomer	128	34.616	dimethylnaphthalene isomer
63	13.326	ethylbenzene	129	34.765	dimethylnaphthalene isomer
64	13.475	ethylthiophene			
65	13.669	xylene isomer			
66	13.721	xylene isomer			

Table A.8 Tentatively identified MSSV-GC-MS products and unidentified products from the TPIB fraction.

Peak Nº	R.T. (mins)	Compound
1	3.629	unknown
2	4.053	unknown
3	5.636	toluene
4	5.979	methylheptene isomer
5	6.107	methylheptene isomer
6	6.321	ethylmethylpentene
7	11.208	benzonitrile
8	12.768	ethylhexanol
9	18.562	ethylbenzonitrile
10	21.063	azepan-2-one
11	41.112	unknown
12	60.944	unknown

Table A.9 Tentatively identified MSSV-GC-MS products and unidentified products from the TPIN fraction.

Peak Nº	R.T. (mins)	Compound
1	3.282	unknown
2	3.346	butene / methylpropene / methanethiol
3	3.464	acetone
4	3.518	dimethylcyclopropane
5	3.614	cyclopentene
6	3.700	propanenitrile
7	3.764	butanone
8	3.840	methylfuran
9	3.936	ethylbutene
10	4.075	methylcyclopentene
11	4.161	benzene
12	4.311	cyclohexene
13	4.365	hexane
14	4.440	pentanone
15	4.493	dimethylcyclopentene
16	4.579	unknown
17	4.622	unknown
18	4.922	methylpyrrole isomer
19	5.083	pyrrole
20	5.341	toluene
21	5.555	methylthiophene
22	5.673	ethylhexene
23	5.759	isopropylfuran
24	5.877	dimethylpentene
25	6.038	dimethylhexadiene
26	6.113	ethylpyrrole
27	6.252	methylpyridine isomer
28	6.359	methylpyridine isomer
29	6.606	ethylmethylcyclopentene
30	6.670	methylpyrrole isomer
31	6.777	methylcyclopentanone
32	6.863	methylpyrrole isomer
33	7.045	unknown
34	7.238	ethylbenzene
35	7.303	dimethylpyrrole
36	7.464	xylene isomer
37	7.818	dimethylpyridine isomer
38	7.871	unknown
39	8.064	xylene isomer
40	8.450	benzylamine
41	8.526	unknown
42	8.933	dimethylpyrrole isomer
43	9.029	ethylpyrrole isomer
44	9.137	dimethylpyrrole isomer
45	9.308	dimethylpyridine isomer
46	9.587	ethylpyrrole isomer
47	9.941	propylbenzene
48	10.027	trimethylpyrrole
49	10.188	ethyltoluene isomer
50	10.284	ethyltoluene isomer
51	10.370	trimethylbenzene isomer
52	10.563	ethylmethylpyrrole
53	10.745	aniline
54	10.906	phenol
55	11.324	trimethylbenzene isomer
56	11.732	ethylmethylpyrrole isomer
57	12.043	ethylmethylpyrrole isomer
58	12.118	trimethylpyrrole
59	12.268	trimethylbenzene isomer
60	12.343	ethylmethylpyrrole isomer
61	12.461	ethylmethylpyridine
62	12.633	ethylhexanol
63	12.783	dimethylcyclopent-2-en-1-one
64	13.266	diethylbenzene isomer
65	13.609	diethylbenzene isomer
66	14.006	unknown
67	14.424	pyrrolidinone
68	14.585	cresol
69	15.047	dimethylethylpyrrole isomer
70	15.187	dimethylethylpyrrole isomer
71	15.337	unknown
72	15.627	unknown
73	15.863	unknown
74	16.131	trimethylethylpyrrole
75	16.249	dimethylbenzamine
76	16.764	ethylphenol isomer
77	17.065	dihydromethylindene
78	17.194	dimethylphenol
79	17.634	unknown
80	17.924	ethylphenol isomer
81	18.525	dimethylindane
82	18.965	unknown
83	19.148	unknown
84	19.288	dimethylbenzofuran
85	19.932	unknown
86	20.759	trimethylphenol
87	21.070	azepan-2-one
88	21.930	unknown
89	22.220	unknown
90	22.521	methylbenzothiazole
91	22.812	diethylpyrazine
92	23.574	unknown
93	24.101	2-methylquinoline
94	30.472	unknown
95	36.208	unknown
96	41.958	3,9-diazatricyclo [7.3.0.0(3,7)]dodecan-2,8-dione
97	49.453	unknown
98	55.262	triphenylphosphine oxide

Appendix 2

Table A2.1 Tentatively identified pyrolysis products and unidentified products from the MIEX® HPO fraction.

Peak Nº	R.T. (mins)	Compound	Peak Nº	R.T. (mins)	Compound	Peak Nº	R.T. (mins)	Compound
1	1.168	methylpropane	55	13.380	2-methyl-2-cyclopenten-1-one	109	35.144	dimethylnaphthalene isomer
2	1.235	acetaldehyde/1,3-butadiene	56	15.417	coumalin	110	35.625	dimethylnaphthalene isomer
3	1.301	methylpropene	57	15.506	citraconic anhydride	111	35.782	dimethylnaphthalene isomer
4	1.346	methanethiol	58	16.386	methylfurfural	112	36.028	benzofuran
5	1.435	isocyanic acid	59	16.608	2-cyclopenten-1-one	113	36.196	unknown
6	1.491	cyclopropane	60	16.776	ethyltoluene	114	36.867	dimethylnaphthalene isomer
7	1.702	cyclobutane/acetone/furan	61	16.965	butanedinitrile	115	38.836	naphthalenol
8	1.847	2-methyl-1,3-butadiene	62	17.133	phenol	116	39.430	trimethylnaphthalene isomer
9	1.936	dimethylcyclopropane	63	17.445	unknown	117	40.415	trimethylnaphthalene isomer
10	2.014	1,3-pentadiene	64	17.701	benzonitrile	118	40.751	ethyl phthalate
11	2.159	1,3-cyclopentadiene	65	18.147	C_3 benzene	119	41.334	trimethylnaphthalene isomer
12	2.537	2-methylpropanone	66	18.292	benzofuran	120	42.858	unknown
13	2.682	cyclopentadiene	67	18.415	methylstyrene	121	44.238	unknown
14	2.771	3-buten-2-one	68	18.793	dimethyl-2-cyclopenten-1-one	122	45.013	tetradecanoic acid
15	2.838	acetic acid	69	19.428	ethylhexanol	123	45.901	tetradecane
16	2.927	2-methylpropanal	70	20.053	methylfuranone	124	46.362	anthracene
17	3.060	acetic acid	71	20.510	cresol isomer	125	47.645	unknown
18	3.250	methylfuran	72	20.933	unknown	126	48.400	hexadecanoic acid
19	3.428	methylpentadiene isomer	73	21.424	cresol isomer	127	48.535	butyl phthalate
20	3.762	unknown	74	21.624	unknown	128	51.378	pentadecane
21	3.862	1-methyl-3-cyclopentadiene	75	22.438	methylindane	129	54.958	1,2-benzenedicarboxylic acid
22	4.140	methylpentadiene isomer	76	22.784	unknown			
23	4.296	3-methyl-2-butanone	77	22.918	unknown			
24	4.418	benzene	78	23.052	dimethylphenol isomer			
25	4.652	cyclopentanone	79	23.164	unknown			
26	5.042	isooctane	80	23.297	methylbenzofuran			
27	5.119	propanoic acid	81	23.676	cyclopentasiloxane			
28	5.342	dimethylfuran	82	23.922	dimethylstyrene			
29	5.665	unknown	83	24.602	dimethylphenol isomer			
30	5.943	unknown	84	24.691	dimethylphenol isomer			
31	6.143	acetamide	85	25.070	benzoic acid			
32	6.633	dimethylcyclopentadiene	86	25.282	ethylphenol			
33	6.934	pyrrole	87	25.818	dimethylphenol isomer			
34	7.212	unknown	88	25.896	tetramethylbenzene			
35	7.769	toluene	89	26.131	unknown			
36	7.936	methylthiophene isomer	90	26.443	dimethylphenol isomer			
37	8.114	methylcyclohexanone	91	26.733	naphthalene			
38	8.226	methylthiophene isomer	92	27.035	dihydrobenzofuran isomer			
39	8.437	unknown	93	27.771	dimethylbenzofuran			
40	8.749	unknown	94	28.318	unknown			
41	9.027	unknown	95	28.441	benzofuranone			
42	9.150	siloxane	96	29.356	unknown			
43	9.695	trimethylfuran	97	29.457	dimethylacetophenone			
44	9.784	2-furancarboxaldehyde	98	30.350	unknown			
45	9.951	unknown	99	30.707	trimethylphenol isomer			
46	10.574	methylpyrrole	100	30.808	trimethylphenol isomer			
47	10.752	unknown	101	31.109	methylnaphthalene isomer			
48	11.064	unknown	102	31.333	trimethylphenol isomer			
49	11.409	ethylbenzene	103	31.444	phthalic anhydride			
50	11.965	xylene isomer	104	31.724	methylnaphthalene isomer			
51	12.366	xylene isomer	105	32.260	methoxyacetophenone			
52	12.433	dimethylthiophene isomer	106	33.199	unknown			
53	12.734	dimethylthiophene isomer	107	33.546	unknown			
54	13.157	styrene	108	34.742	dimethylbenzofuranone			

Table A2.2 Tentatively identified pyrolysis products and unidentified products from the MIEX® TPIB fraction.

Peak Nº	R.T. (mins)	Compound
1	0.965	propylene
2	1.132	2-methylpropene
3	1.565	acetone
4	1.743	methylbutadiene
5	2.042	cyclopentadiene
6	4.284	benzene
7	7.780	toluene
8	8.557	unknown
9	9.523	cyclotrisiloxane
10	11.543	unknown
11	11.765	ethylbenzene
12	12.165	xylene
13	13.164	styrene
14	16.895	phenol
15	17.462	benzonitrile
16	17.940	alkylbenzene
17	19.239	2-ethylhexanol
18	20.261	indene
19	21.160	cresol
20	23.371	unknown
21	24.649	benzoic acid
22	24.849	unknown
23	25.049	unknown
24	25.216	naphthalene
25	26.771	unknown
26	30.017	unknown
27	30.817	methylnaphthalene isomer
28	31.162	phthalic anhydride
29	31.440	methylnaphthalene isomer
30	35.298	dimethylnaphthalene
31	35.899	methyl phthalate
32	36.556	acenaphthylene
33	40.482	ethyl phthalate
34	42.986	unknown
35	43.866	unknown
36	44.000	unknown
37	44.324	2,4-diphenyl-4-methyl-2-(*Z*)-pentene
38	44.804	tetradecanoic acid
39	46.883	1,2-benzenedicarboxylic acid
40	47.151	cyclotetradecane
41	49.980	siloxane
42	50.542	unknown
43	51.455	unknown
44	52.536	unknown

Table A2.3 Tentatively identified pyrolysis products and unidentified products from the MIEX® TPIN fraction.

Peak Nº	R.T. (mins)	Compound	Peak Nº	R.T. (mins)	Compound
1	1.095	methylpropene / 1,3-butadiene	73	48.383	hexadecanoic acid
2	1.206	methanethiol	74	48.507	butyl phthalate
3	1.362	unknown	75	48.631	3,9-diazatricyclo[7.3.0.0(3,7)] dodecan-2,8-dione
4	1.551	acetonitrile	76	51.018	unknown
5	1.729	methylbutadiene	77	51.604	unknown
6	2.040	cyclopentadiene	78	52.687	unknown
7	2.674	unknown	79	53.725	siloxane
8	2.774	acetic acid	80	54.853	unknown
9	2.829	2-butanone	81	54.920	1,2-benzenedicarboxylic acid
10	3.774	methylcyclopentadiene	82	55.573	triphenylphosphine oxide
11	4.330	benzene			
12	4.575	unknown			
13	6.898	unknown			
14	7.198	pyrrole			
15	7.921	toluene			
16	8.199	methylethanamine			
17	9.900	methylpyridine			
18	10.556	2-cyclopenten-1-one			
19	10.734	methylpyrrole isomer			
20	11.090	methylpyrrole isomer			
21	11.946	ethylbenzene			
22	12.347	xylene			
23	13.337	styrene			
24	13.837	2-methyl-2-cyclopenten-1-one			
25	15.349	citraconic anhydride			
26	16.561	ethyltoluene isomer			
27	16.706	ethyltoluene isomer			
28	16.973	butanedinitrile			
29	17.107	phenol			
30	17.652	benzonitrile			
31	18.109	ethyltoluene isomer			
32	18.365	alkylbenzene			
33	18.777	unknown			
34	19.856	dimethyl-2-cyclopenten-1-one			
35	20.491	cresol isomer			
36	21.425	cresol isomer			
37	22.138	unknown			
38	22.428	tolunitrile			
39	22.528	unknown			
40	23.018	methylbenzonitrile			
41	23.898	succinimide			
42	24.588	dimethylphenol			
43	25.112	benzoic acid			
44	25.881	methylacetophenone isomer			
45	26.260	unknown			
46	26.461	methylacetophenone isomer			
47	26.695	naphthalene			
48	27.051	unknown			
49	28.645	unknown			
50	28.979	toluic acid			
51	29.302	unknown			
52	29.425	dimethylacetophenone isomer			
53	30.306	cinnamaldehyde			
54	30.707	unknown			
55	31.075	methylnaphthalene isomer			
56	31.421	phthalic anhydride			
57	31.700	methylnaphthalene isomer			
58	31.956	benzamide			
59	32.246	dimethylacetophenone isomer			
60	32.369	methoxyacetophenone			
61	32.905	ethylbenzoic acid			
62	33.329	unknown			
63	34.110	hydroxyacetophenone			
64	35.126	unknown			
65	35.661	diacetylbenzene			
66	38.910	unknown			
67	39.703	unknown			
68	40.720	diethyl phthalate			
69	42.866	unknown			
70	44.466	unknown			
71	45.004	tetradecanoic acid			
72	45.385	1,4-diaza-2,5-dioxobicyclo [4.3.0]nonane			

Table A2.4 Tentatively identified thermochemolysis-GC-MS products and unidentified products from the MIEX® HPO fraction.

Peak Nº	R.T. (mins)	Compound	Peak Nº	R.T. (mins)	Compound	Peak Nº	R.T. (mins)	Compound
1	3.292	methyl acrylate	63	23.658	dimethylanisole isomer	124	44.260	trimethoxybenzoic acid methyl ester
2	3.618	methyl propanoate	64	24.052	dimethyl glutarate	125	44.387	methyl tetradecanoate
3	3.878	methyl 1,3-cyclopentadiene	65	24.187	dimethylanisole isomer	126	44.969	unknown
4	3.974	1,3-cyclohexadiene	66	24.514	dimethoxybenzene isomer	127	45.534	1,3-benzenedicarboxylic acid methyl ester
5	4.434	benzene	67	24.764	trimethylphenol	128	46.360	anthracene
6	4.559	acetone	68	25.130	methylindene isomer	129	46.633	unknown
7	4.665	thiophene	69	25.332	methylindene isomer	130	47.286	unknown
8	5.030	methyl isobutyrate	70	25.458	dimethoxybenzene isomer	131	47.657	hexadecanoic acid methyl ester
9	5.836	methyl methacrylate	71	25.573	unknown	132	50.324	octadecanoic acid methyl ester
10	5.970	methyl butanoate	72	25.621	dimethoxybenzene isomer	133	51.665	unknown
11	6.623	methyl butenoate	73	26.517	unknown	134	52.744	unknown
12	6.824	methylpyrrole	74	26.777	naphthalene	135	54.999	1,2-benzenedicarboxylic acid methyl ester
13	6.968	1-dimethyl-3-cyclopentadiene	75	27.210	methyl toluate	136	58.904	squalene
14	7.112	dimethyldisulfide	76	27.374	unknown			
15	7.227	dimethylaminoacetonitrile	77	28.058	unknown			
16	7.602	acetic acid methyl ester	78	28.260	dimethoxytoluene isomer			
17	7.755	methyl crotonate	79	28.328	dimethyl adipate			
18	7.976	toluene	80	28.857	dimethoxytoluene isomer			
19	8.274	methyl isovalerate	81	28.973	dimethoxytoluene isomer			
20	8.668	methyl ester of 2-methoxy propionic acid	82	29.108	unknown			
21	9.455	unknown	83	29.378	unknown			
22	10.223	unknown	84	29.552	dimethoxytoluene isomer			
23	10.607	unknown	85	29.802	hexanedioic acid dimethyl ester			
24	11.145	2-methyl pentanoate	86	30.467	unknown			
25	11.999	ethylbenzene	87	30.776	methyl dimethylbenzoate			
26	12.220	unknown	88	31.162	methylnaphthalene isomer			
27	12.403	xylene isomer	89	31.403	methyl ethylbenzoate			
28	12.480	xylene isomer	90	31.558	unknown			
29	13.411	styrene	91	31.780	methylnaphthalene isomer			
30	13.805	unknown	92	32.050	unknown			
31	13.910	2-methyl-2-cyclopentan-1-one	93	32.175	unknown			
32	14.074	unknown	94	32.339	methyl methoxybenzoate isomer			
33	14.189	dimethylsulfone	95	32.773	unknown			
34	14.554	anisole	96	33.246	trimethoxybenzene isomer			
35	14.900	trimethylphosphate	97	33.699	methyl methoxybenzoate isomer			
36	16.523	unknown	98	34.520	unknown			
37	16.648	ethyltoluene isomer	99	34.848	trimethoxybenzene isomer			
38	16.792	ethyltoluene isomer	100	35.176	dimethylnaphthalene isomer			
39	17.282	phenol	101	35.176	dimethylnaphthalene isomer			
40	17.378	hexahydro-1,3,5-trimethyl-1,3,5-triazine	102	35.505	unknown			
41	17.590	unknown	103	35.602	dimethylnaphthalene isomer			
42	17.743	benzonitrile	104	35.853	dimethylnaphthalene isomer			
43	18.214	C_3 benzene	104	36.085	unknown			
44	18.339	benzofuran	105	36.239	methyl phthalate			
45	18.685	ethylhexanol	106	36.925	acenaphthylene			
46	19.205	methyl fumarate	107	37.148	methyl terephthalate			
47	19.301	methylanisole	108	37.235	trimethoxytoluene			
48	19.580	dimethyl succinate	109	37.727	unknown			
49	19.946	dimethyl-2-cyclopenten-1-one	110	37.998	dimethyl terephthalate			
50	20.561	indene	111	38.375	dimethyl isophthalate			
51	21.003	dimethyl 2-methylsuccinate	112	38.762	unknown			
52	21.483	cresol	113	38.955	unknown			
53	21.608	unknown	114	39.206	unknown			
54	22.224	unknown	115	39.902	unknown			
55	22.301	methylsuccinimide	116	40.067	unknown			
56	22.551	unknown	117	40.463	methyl dimethoxybenzoate isomer			
57	22.657	methyl benzoate	118	40.734	methyl dimethoxybenzoate isomer			
58	23.013	unknown	119	41.015	unknown			
59	23.109	dimethylanisole isomer	120	41.683	unknown			
60	23.244	ethylanisole isomer	121	42.525	unknown			
61	23.321	methylbenzofuran	122	43.455	unknown			
62	23.427	ethylanisole isomer	123	44.076	unknown			

Table A2.5 Tentatively identified thermochemolysis-GC-MS products and unidentified products from the MIEX® TPIB fraction.

Peak Nº	R.T. (mins)	Compound
1	3.205	methyl acrylate
2	3.532	methyl propanoate
3	4.357	benzene
4	4.568	thiophene
5	7.015	pyridine
6	7.159	dimethylaminoacetonitrile
7	7.370	dimethylcyanamide
8	7.553	unknown
9	7.821	methylformamide
10	7.908	unknown
11	8.292	unknown
12	8.608	2-methoxy propionic acid methyl ester
13	9.385	unknown
14	10.393	*N*-methylacetamide
15	10.537	unknown
16	12.034	*N*-*N*-dimethylacetamide
17	12.418	unknown
18	13.320	styrene
19	14.481	anisole
20	15.680	unknown
21	17.100	butanedinitrile
22	17.264	phenol
23	17.398	unknown
24	17.513	unknown
25	17.686	benzonitrile
26	19.144	methyl fumarate
27	19.355	ethyl hexanol
28	19.500	dimethyl succinate
29	20.939	unknown
30	22.244	unknown
31	22.580	methyl benzoate
32	23.328	unknown
33	26.705	naphthalene
34	35.520	unknown
35	36.154	methyl phthalate
36	36.835	acenaphthylene
37	37.919	dimethyl terephthalate
38	38.283	dimethyl isophthalate
39	39.320	unknown
40	44.336	unknown
41	46.323	methyl pentadecanoate
42	47.609	hexadecenoic acid methyl ester
43	49.773	unknown
44	49.888	unknown
45	50.283	octadecenoic acid methyl ester
46	50.794	unknown
47	51.063	unknown
48	51.439	unknown
49	51.940	unknown
50	52.701	unknown
51	53.106	cyclotrisiloxane
52	53.742	unknown
53	54.869	unknown
54	54.937	1,2-benzenedicarboxylic acid methyl ester
55	58.825	squalene

Table A2.6 Tentatively identified thermochemolysis-GC-MS products and unidentified products from the MIEX® TPIN fraction.

Peak Nº	R.T. (mins)	Compound	Peak Nº	R.T. (mins)	Compound
1	3.263	methyl acrylate	70	27.174	methyl toluate isomer
2	3.590	methyl propanoate	71	27.328	unknown
3	3.849	methylcyclopentadiene isomer	72	27.434	unknown
4	3.955	methylcyclopentadiene isomer	73	27.559	methyl toluate isomer
5	4.406	benzene	74	27.723	unknown
6	4.636	*N*-*N*-dimethylmethanamine	75	28.215	dimethoxytoluene isomer
7	5.001	methyl isobutyrate	76	28.292	dimethyl adipate
8	5.797	methyl methacrylate	77	28.784	dimethoxytoluene isomer
9	6.201	methyl butyrate	78	29.353	anisaldehyde
10	6.786	methylpyrrole	79	29.450	ethylacetophenone
11	7.036	pyridine	80	29.768	unknown
12	7.228	pyrrole	81	30.116	unknown
13	7.516	propanal	82	30.337	unknown
14	7.593	unknown	83	30.743	methyl dimethylbenzoate
15	7.727	methyl crotonate	84	31.042	methoxyacetophenone
16	7.948	toluene	85	31.119	methylnaphthalene isomer
17	8.687	2-methoxy propionic acid methyl ester	86	31.361	methyl ethylbenzoate
18	8.783	methylcarbamic acid methyl ester	87	31.506	methyl cinnamate
19	9.733	cyclotrisiloxane	88	31.737	methylnaphthalene isomer
20	9.944	methylpyridine	89	31.998	unknown
21	10.156	*N*-methylacetamide	90	32.287	methyl methoxybenzoate isomer
22	10.626	methylfuran	91	32.538	unknown
23	10.808	methylpyrrole isomer	92	32.731	unknown
24	11.163	methylpyrrole isomer	93	32.934	methoxyacetophenone
25	12.037	ethylbenzene	94	33.205	trimethoxybenzene
26	12.219	unknown	95	33.659	methyl methoxybenzoate isomer
27	12.412	xylene isomer	96	34.480	unknown
28	12.489	xylene isomer	97	34.567	unknown
29	13.410	styrene	98	35.166	unknown
30	13.910	2-methyl-2-cyclopentanone	99	35.417	unknown
31	14.188	dimethylsulfone	100	35.775	unknown
32	14.524	methyl methoxybenzene	101	36.065	biphenyl
33	15.735	unknown	102	36.191	methyl phthalate
34	16.618	ethyltoluene	103	36.471	unknown
35	17.060	unknown	104	36.868	acenaphthalene
36	17.252	unknown	105	37.177	unknown
37	17.397	trimethylbenzene	106	37.361	unknown
38	17.551	unknown	107	37.651	unknown
39	17.714	benzonitrile	108	37.941	dimethyl terephthalate
40	18.214	methylstyrene	109	38.329	dimethyl isophthalate
41	18.685	methylanisole isomer	110	38.474	unknown
42	19.175	unknown	111	38.609	unknown
43	19.262	methylanisole isomer	112	38.870	unknown
44	19.397	ethyl hexanol	113	39.151	unknown
45	19.541	dimethyl succinate	114	39.345	unknown
46	20.012	unknown	115	39.838	unknown
47	20.522	indene	116	40.013	unknown
48	20.964	dimethyl 2-methyl succinate	117	40.168	1,3-benzenedicarboxylic acid methyl ester
49	21.387	acetophenone	118	40.420	methyl dimethoxybenzoate isomer
50	21.57	unknown	119	40.681	methyl dimethoxybenzoate isomer
51	22.176	unknown	120	41.059	methyl dimethoxybenzoate isomer
52	22.262	methyl succinimide	121	41.572	unknown
53	22.503	unknown	122	42.192	unknown
54	22.629	methyl benzoate	123	43.928	3-methyl-2,4,5-trioxo-1-(2-*N*-propenyl)imidazolidine
55	22.975	unknown	124	44.035	unknown
56	23.062	dimethylanisole	125	44.366	methyl tetradecanoate
57	23.399	ethylanisole	126	44.939	unknown
58	23.486	unknown	127	45.036	unknown
59	23.659	ethoxytoluene	128	46.380	phenanthrene
61	24.468	dimethoxybenzene isomer	129	46.604	unknown
62	25.093	methylindene	130	46.925	unknown
63	25.421	dimethoxybenzene isomer	131	47.003	unknown
64	25.584	dimethoxybenzene isomer	132	47.637	unknown
65	25.700	dimethoxytoluene	133	47.950	hexadecanoic acid methyl ester
66	25.912	methylacetophenone isomer	134	50.560	octadecanoic acid methyl ester
67	26.336	unknown	135	52.715	unknown
68	26.461	methylacetophenone isomer	136	54.957	1,2-benzenedicarboxylic acid methyl ester
69	26.731	naphthalene	137	58.860	squalene

Table A2.7 Tentatively identified MSSV-GC-MS products and unidentified products from the MIEX® HPO fraction.

Peak Nº	R.T. (mins)	Compound	Peak Nº	R.T. (mins)	Compound
1	1.948	butene	73	14.322	dimethylthiophene isomer
2	2.205	methylpropene	74	14.527	xylene isomer
3	2.548	methylbutene	75	15.025	trimethylcyclopentanone
4	2.754	methylbutane	76	15.122	unknown
5	3.177	propanal	77	15.699	unknown
6	3.365	dimethylcyclopropane	78	15.756	isopropylbenzene
7	3.594	methylbutene / pentene	79	16.202	tetramethylfuran
8	4.280	cyclopentene	80	16.928	propylbenzene
9	4.451	propanethiol	81	17.242	ethyltoluene isomer
10	4.640	dimethylbutene isomer	82	17.368	ethyltoluene isomer
11	4.760	dimethylbutene isomer	83	17.585	trimethylbenzene isomer
12	5.228	methylpentene isomer	84	17.905	trimethylbenzene isomer
13	5.491	hexane	85	18.100	phenol
14	5.543	butanone / pentane	86	18.563	trimethylbenzene isomer
15	5.726	methylpentene isomer	87	19.300	trimethylpyridine
16	5.846	methylfuran	88	19.483	trimethylpyrrole
17	6.074	methylpentene isomer	89	19.626	trimethylbenzene isomer
18	6.189	methylcyclopentane	90	19.831	methyl isopropylbenzene
19	6.549	cyclohexadiene	91	20.146	allylbenzene
20	6.663	dimethylcyclopentene	92	20.277	dimethylcyclopent-2-en-1-one
21	6.846	methylcyclopentene	93	20.734	diethylbenzene
22	7.012	4-methyl-3-penten-2-one	94	20.872	propyltoluene
23	7.074	benzene	95	21.009	cresol
24	7.223	unknown	96	21.277	unknown
25	7.280	thiophene	97	21.512	acetophenone
26	7.589	methylpentadiene	98	21.712	ethyldimethylthiophene
27	7.686	3-methyl-1-cyclopentene	99	21.929	cresol
28	7.898	trimethylpentane	100	22.209	methylisopropylbenzene
29	7.955	methylcyclohexane	101	22.369	trimethyl-2-cyclopenten-1-one
30	8.006	2-pentanone	102	22.901	diethyltoluene
31	8.292	heptane	103	23.135	dimethylphenol
32	8.372	2-methyl-2-hexene	104	23.461	tetramethylbenzene isomer
33	8.475	dimethylfuran	105	23.598	tetramethylbenzene isomer
34	8.578	dimethylcyclopentene	106	24.158	isopropyldimethylbenzene isomer
35	8.629	dimethylpentene	107	24.284	ethylphenol
36	8.698	dimethylfuran	108	24.490	isopropyldimethylbenzene isomer
37	8.846	trimethylpentane	109	24.695	methylindan
38	9.035	dimethylpentanal	110	24.758	dimethylphenol isomer
39	9.081	trimethylcyclopentene	111	25.450	ethylphenol
40	9.452	methylhexatriene	112	25.615	dimethylphenol isomer
41	9.492	methyl-2-pentanone	113	25.838	dimethylphenol isomer
42	9.549	unknown	114	26.130	ethylmethylphenol isomer
43	9.669	unknown	115	26.496	dimethylphenol isomer
44	9.744	methylhexadiene	116	26.827	unknown
45	9.795	2-methyl-3-pentanone	117	27.244	dimethylbenzofuran
46	9.858	ethylmethylpentene	118	27.364	dimethylindazole
47	9.938	trimethylcyclopentene	119	27.502	dimethylbenzofuran
48	10.047	trimethylcyclopentene	120	27.753	ethylmethylphenol isomer
49	10.161	toluene	121	27.947	ethylmethylphenol isomer
50	10.281	methyl thiophene	122	28.136	ethylmethylphenol isomer
51	10.441	methylheptane	123	28.336	trimethylphenol isomer
52	10.549	methyl thiophene	124	28.982	unknown
53	10.875	3-hexanone	125	29.279	trimethylphenol isomer
54	10.984	dimethylhexene	126	29.439	trimethylphenol isomer
55	11.110	trimethylcyclopentene	127	29.662	unknown
56	11.247	methylheptene	128	30.331	methylnaphthalene
57	11.327	unknown	129	30.811	unknown
58	11.533	trimethylcyclopentene	130	31.491	trimethylbenzofuran
59	11.607	ethylhexene	131	34.812	dimethylnaphthalene
60	11.801	trimethylfuran	132	39.275	trimethylnaphthalene
61	12.458	methylethylcyclopentene			
62	12.636	dimethylheptadiene			
63	12.733	methylcyclopentanone			
64	12.973	tetramethylcyclopentene isomer			
65	13.030	unknown			
66	13.201	tetramethylcyclopentene isomer			
67	13.362	ethylbenzene			
68	13.516	ethylthiophene			
69	13.710	xylene isomer			
70	13.762	xylene isomer			
71	13.887	dimethylcyclohexene			
72	13.990	dimethylthiophene isomer			

Table A2.8 Tentatively identified MSSV-GC-MS products and unidentified products from the MIEX® TPIB fraction.

Peak Nº	R.T. (mins)	Compound
1	3.478	unknown
2	3.639	acetone
3	3.820	trimethylsilanol
4	3.874	unknown
5	3.938	unknown
6	4.313	benzene
7	4.387	hexamethyldisiloxane
8	4.516	unknown
9	4.612	heptane
10	5.264	unknown
11	5.489	toluene
12	5.832	dimethylhexene
13	5.971	methylheptene isomer
14	6.185	methylheptene isomer
15	7.372	ethylbenzene
16	10.376	unknown
17	10.451	unknown
18	11.071	phenol
19	12.290	unknown
20	12.761	ethylhexanol
21	13.745	cresol
22	16.310	unknown
23	16.513	unknown
24	16.599	unknown
25	16.749	unknown
26	18.063	unknown
27	19.303	unknown
28	19.976	unknown
29	20.756	azepan-2-one
30	26.144	unknown
31	28.612	unknown
32	29.275	unknown
33	31.529	unknown
34	35.695	unknown
35	37.436	unknown
36	39.851	unknown
37	39.957	unknown
38	41.197	unknown
39	43.526	unknown
40	43.761	unknown
41	44.188	unknown
42	46.218	unknown
43	46.838	unknown
44	47.169	unknown
45	48.558	unknown
46	48.750	unknown
47	52.009	unknown

Table A2.9 Tentatively identified MSSV-GC-MS products and unidentified products from the MIEX® TPIN fraction.

Peak Nº	R.T. (mins)	Compound
1	3.121	unknown
2	3.207	1-butene
3	3.314	acetone
4	3.368	2-pentene
5	3.507	cyclopentene
6	3.593	methylpentene
7	3.636	butanone
8	3.721	methylfuran
9	3.968	methylpentadiene
10	4.054	benzene
11	4.214	cyclohexene
12	4.268	trimethylpentane
13	4.407	heptane / dimethylcyclopentene
14	4.547	hexadienal
15	4.804	unknown
16	4.911	1-methyl-1,4-cyclohexadiene
17	4.954	dimethyldisulfide
18	5.050	methylcyclohexene
19	5.297	toluene
20	5.511	methylthiophene
21	5.640	ethylhexene
22	5.758	unknown
23	6.015	dimethylhexadiene
24	6.144	trimethylpyrazole
25	6.411	unknown
26	6.572	ethylmethylcyclopentene
27	6.711	methylpyrrole
28	6.776	cyclohexanone
29	6.968	methylcyclopentanone
30	7.161	unknown
31	7.236	ethylbenzene
32	7.311	unknown
33	7.461	xylene isomer
34	7.686	dimethylthiophene
35	7.890	unknown
36	8.083	xylene isomer
37	8.490	dimethylfuran
38	9.004	unknown
39	9.432	unknown
40	9.529	unknown
41	10.203	ethyltoluene
42	10.310	C_3 benzene isomer
43	10.471	dimethyltrisulfide
44	10.771	C_3 benzene isomer
45	10.910	phenol
46	11.328	trimethylbenzene
47	11.660	unknown
48	11.746	ethylmethylpyrrole
49	12.131	trimethylpyrrole
50	12.271	trimethylbenzene
51	12.645	ethylhexanol
52	12.796	dimethylcyclopent-2-en-1-one
53	13.278	diethylbenzene
54	13.610	cresol isomer
55	13.749	trimethyl-2-cyclopenten-1-one
56	14.359	unknown
57	14.466	cresol isomer
58	14.691	dihydromethylindene
59	15.206	dimethylethylpyrrole
60	15.356	unknown
61	15.602	methylbenzofuran
62	15.880	unknown
63	16.009	C_4 benzene
64	16.148	unknown
65	16.309	unknown
66	16.758	ethylphenol isomer
67	17.080	dihydromethylindene
68	17.187	dimethylphenol isomer
69	17.915	ethylphenol isomer
70	18.258	dimethylphenol isomer
71	18.515	unknown
72	18.869	dimethylindan
73	18.954	C_2 phenol
74	19.308	unknown
75	19.554	unknown
76	19.683	dimethylindazole
77	19.940	unknown
78	20.132	unknown
79	20.518	C_3 phenol
80	20.754	azepan-2-one
81	21.354	ethylacetophenone isomer
82	22.137	ethylacetophenone isomer
83	22.554	unknown
84	23.101	unknown
85	23.722	unknown
86	24.311	unknown
87	26.967	dimethylnaphthalene
88	27.235	unknown
89	27.792	unknown
90	33.529	unknown
91	49.487	unknown
92	60.974	unknown

References

Abbt-Braun, G., and F. H. Frimmel. 1999. Basic characterization of Norwegian NOM samples - similarities and differences. *Environment International* 25 (2/3): 161-180.

Aiken, G., and J. Leenheer. 1993. Isolation and chemical characterization of dissolved and colloidal organic matter. *Chemistry and Ecology* 8 (3): 135-151.

Aiken, G. R., D. M. McKnight, K. A. Thorn, and E. M. Thurman. 1992. Isolation of hydrophilic organic acids from water using nonionic macroporous resins. *Organic Geochemistry* 18 (4): 567-73.

Aiken, G. R. 1985. Isolation and concentration techniques for aquatic humic substances. In *Humic substances in soil, sediment and water*, ed. G. R. Aiken, D. M. McKnight, R. L. Wershaw and P. MacCarthy, 363-385. New York: Wiley.

Aiken, G. R., D. M. McKnight, R. L. Wershaw, and P. MacCarthy. 1985. *Humic substances in soils, sediments and water*. New York: Wiley

Alberts, J. J., and M. Takács. 2004. Total luminescence spectra of IHSS standard and reference fulvic acids, humic acids and natural organic matter: comparison of aquatic and terrestrial source terms. *Organic Geochemistry* 35 (3): 243-256.

Allpike, B. 2008. Size exclusion chromatography as a tool for natural organic matter characterisation in drinking water treatment. Doctorate, Department of Applied Chemistry, Curtin University of Technology.

Allpike, B. P., A. Heitz, C. A. Joll, and R. I. Kagi. 2007. A new organic carbon detector for size exclusion chromatography. *Journal of Chromatography A* 1157 (1-2): 472-476.

Allpike, B., C. A. Joll, A. Heitz, R. I. Kagi, T. Brinkmann, G. Abbt-Braun, F. H. Frimmel, N. Her, G. Amy, and P. Smith. 2005. Size exclusion chromatography to

characterize DOC removal in drinking water treatment. *Environmental Science and Technology* 39 (7): 2334-2342.

Almedros, G., J. Dorado, F. J. González-Vila, M. J. Blanco, and U. Lankes. 2000. ^{13}C NMR assessment of decomposition patterns during composting of forest and shrub biomass. *Soil Biology and Biochemistry* 32 (6): 793-804.

Amy, G. 2007. *4th IWA Leading Edge Conference and Exhibition on Water and Wastewater Technologies*, Natural organic matter (NOM) profiling as a basis for treatment process selection and monitoring. Singapore, 3-6 June, CD-ROM.

Amy, G., and N. Her. 2004. Size exclusion chromatography (SEC) with multiple detectors: a powerful tool in treatment process selection and performance monitoring. *Water Science and Technology: Water Supply* 4 (4): 19-24.

Amy, G. L., M. R. Collins, C. J. Kuo, and P. H. King. 1987. Comparing gel permeation chromatography and ultrafiltration for the molecular weight characterization of aquatic organic matter. *Journal AWWA* 79 (1): 43-49.

Andrews, S. A., P. M. Huck, and R. T. Coutts. 1994. Identification and quantitation of ozonation by-products of humic substances. In *Humic Substances in the Global Environment and Implications on Human Health*, ed. N. Senesi and T. M. Miano: Elsevier Science.

Ash, G., K. Blakeway, and S. Jefferys. 2012. *Metropolitan Borefields Sampling Results*. TOPS Borefields Group. Water Treatment Process Expertise. Internal report - Water Corporation.

Assemi, S., G. Newcombe, C. Hepplewhite, and R. Beckett. 2004. Characterization of natural organic matter fractions separated by ultrafiltration using flow field-flow fractionation. *Water Research* 38 (6): 1467-1476.

Australian Bureau of Statistics. 2012. http://www.abs.gov.au/ausstats/abs@.nsf/mf/3101.0 (accessed 2nd February).

Baker, A., and R. G. M. Spencer. 2004. Characterization of dissolved organic matter from source to sea using fluorescence and absorbance spectroscopy. *Science of the Total Environment* 333 (1-3): 217-232.

Barber, L. B., J. A. Leenheer, T. I. Noyes, and E. A. Stiles. 2001. Nature and transformation of dissolved organic matter in treatment wetlands. *Environmental Science and Technology* 35 (24): 4805-16.

Barrett, S. E., S. W. Krasner, and G. L. Amy. 2000. Natural organic matter and disinfection by-products: characterization and control in drinking water - an overview. In *Natural Organic Matter and Disinfection By-Products. Characterization and Control in Drinking Water*, ed. S. E. Barrett, S. W. Krasner and G. L. Amy, 2-14. American Chemical Society.

Beck, A. J., and K. C. Jones. 1992. Natural organic substances and contaminant behaviour: progress, conflicts and uncertainty. In *Organic Substances in Soil and Water*, ed. A. J. Beck, 148-194. The Royal Society of Chemistry, Lancaster University.

Belin, C., C. Quellec, M. Lamotte, M. Ewald, and P. Simon. 1993. Characterization by fluorescence of the dissolved organic matter in natural water. Application to fractions obtained by tangential ultrafiltration and XAD resin isolation. *Environmental Technology* 14 (12): 1131-1144.

Bellar, T. A., J. J. Lichtenberg, and R. C. Kroner. 1974. The occurrence of organohalides in chlorinated drinking water. *Journal AWWA* 66 (12): 703-706.

Bennett, L. E., and M. Drikas. 1993. The evaluation of colour in natural waters. *Water Research* 27 (7): 1209-1218.

Berwick, L., P. F. Greenwood, W. Meredith, C. E. Snape, and H. M. Talbot. 2010a. Comparison of microscale sealed vessel pyrolysis (MSSVpy) and hydropyrolysis (Hypy) for the characterisation of extant and sedimentary organic matter. *Journal of Analytical and Applied Pyrolysis* 87 (1): 108-116.

Berwick, L., P. F. Greenwood, and R. J. Smernik. 2010b. The use of MSSV pyrolysis to assist the molecular characterisation of aquatic natural organic matter. *Water Research* 44 (10): 3039-3054.

Berwick, L. J. 2009. Characterisation of aquatic natural organic matter by micro-scale sealed vessel pyrolysis. Doctorate, Department of Applied Chemistry, Curtin University of Technology, Perth.

Berwick, L., P. Greenwood, R. Kagi, and J.P. Croué. 2007. Thermal release of nitrogen organics from natural organic matter using micro scale sealed vessel pyrolysis. *Organic Geochemistry* 38 (7): 1073-1090.

Best, G., M. Singh, D. Mourato, and Y. J. Chang. 2001. Application of immersed ultrafiltration membranes for organic removal and disinfection by-product reduction. *Water Science and Technology: Water Supply* 1 (5/6): 221-231.

Bolto, B., D. Dixon, R. Eldridge, and S. King. 2002. Removal of THM precursors by coagulation or ion exchange. *Water Research* 36 (20): 5066-5073.

Bolto, B. A., G. Abbt-Braun, D. R. Dixon, R. J. Eldridge, F. H. Frimmel, S. Hesse, S. King, and M. Toilf. 1999. Experimental evaluation of cationic polyelectrolytes for removing natural organic matter from water. *Water Science and Technology* 40 (9): 71-79.

Bond, T., E. H. Goslan, S. A. Parsons, and B. Jefferson. 2010. Disinfection by-product formation of natural organic matter surrogates and treatment by coagulation, MIEX® and nanofiltration. *Water Research* 44 (5): 1645-1653.

Booth, S., C. Fonseca, J. Sutherland, P. Carlson, and G. Amy. 2006. *DBP control in high bromide water while using free chlorine during distribution*. AWWA Research Foundation.

Bougeard, C. M. M., E. H. Goslan, B. Jefferson, and S. A. Parsons. 2010. Comparison of the disinfection by-product formation potential of treated waters exposed to chlorine and monochloramine. *Water Research* 44 (3): 729-740.

Boyer, T. H., C. T. Miller, and P. C. Singer. 2008a. Modeling the removal of dissolved organic carbon by ion exchange in a completely mixed flow reactor. *Water Research* 42 (8-9): 1897-1906.

Boyer, T. H., P. C. Singer, and G. R. Aiken. 2008b. Removal of dissolved organic matter by anion exchange: effect of dissolved organic matter properties. *Environmental Science and Technology* 42 (19): 7431-7437.

Boyer, T. H., and P. C. Singer. 2005. Bench-scale testing of a magnetic ion exchange resin for removal of disinfection by-product precursors. *Water Research* 39 (7): 1265-1276.

Bruchet, A., C. Rousseau, and J. Mallevialle. 1990. Pyrolysis-GC-MS for investigating high molecular THM precursors and other refractory organics. *Journal AWWA* 82 (9): 66-74.

Bruchet, A., C. Anselme, J. P. Duguet, and J. Mallevialle. 1989. Effect of humic substances on the treatment of drinking water. In *Aquatic Humic Substances Influence on Fate and Treatment of Pollutants*, ed. E. A. Ghabbour and P. MacCarthy, 93-105. Washington, D.C.: American Chemical Society.

Buchanan, W., F. Roddick, N. Porter, and M. Drikas. 2005. Fractionation of UV and VUV pretreated natural organic matter from drinking water. *Environmental Science and Technology* 39 (12): 4647-4654.

Budd, G. C., B. W. Long, J. C. Edwards-Brandt, P. C. Singer, and M. Meisch. 2005. *Evaluation of MIEX® process impacts on different source waters*. AWWA Research Foundation.

Budd, G. C., P. C. Singer, J. C. Edwards, B. Long, M. E. Meisch, D. J. Rexing, C. A. Owen, J. B. Cook, and B. L. Joslyn. 2003. *2003 AWWA Water Quality Technology Conference, Magnetized ion exchange (MIEX): evaluation of process impacts in different sources*. Philadelphia, Pennsylvania, 2-6 November, CD-ROM.

Cai, Y. 1999. Size distribution measurements of dissolved organic carbon in natural waters using ultrafiltration technique. *Water Research* 33 (13): 3056-3060.

Caron, F., and D. S. Smith. 2011. Fluorescence analysis of natural organic matter fractionated by ultrafiltration: contrasting between urban-impacted water, and radio-contaminated water from a near-pristine environment. *Water Air Soil Pollution* 214 (1-4): 471-490.

Challinor, J. M. 1996. A rapid simple pyrolysis derivatisation gas chromatography-mass spectrometry method for profiling of fatty acids in trace quantities of lipids. *Journal of Analytical and Applied Pyrolysis* 37 (2): 185-197.

Challinor, J. M. 1991. The scope of pyrolysis methylation reactions. *Journal of Analytical and Applied Pyrolysis* 20: 15-24.

Challinor, J. M. 1989. A pyrolysis-derivatisation-gas chromatography technique for the structural elucidation of some synthetic polymers. *Journal of Analytical and Applied Pyrolysis* 16 (4): 323-333.

Chen, B., and P. Westerhoff. 2010. Predicting disinfection by-product formation potential in water. *Water Research* 44 (13): 3755-3762.

Chen, J., E. J. LeBoeuf, S. Dai, and B. Gu. 2003a. Fluorescence spectroscopic studies of natural organic matter fractions. *Chemosphere* 50 (5): 639-647.

Chen, W., P. Westerhoff, J. A. Leenheer, and K. Booksh. 2003b. Fluorescence excitation-emission matrix regional integration to quantify spectra for dissolved organic matter. *Environmental Science and Technology* 37 (24): 5701-5710.

Chen, J., B. Gu, E. J. LeBoeuf, H. Pan, and S. Dai. 2002. Spectroscopic characterization of the structural and functional properties of natural organic matter fractions. *Chemosphere* 48 (1): 59-68.

Chen, H. W., and M. Edwards. 1999. *1999 AWWA Water Quality Technology Conference, Interaction between humic substances and aluminium hydroxides*. Tampa, Florida, 31 October - 3 November, CD-ROM.

Chin, Y., G. Aiken, and E. O'Loughlin. 1994. Molecular weight, polydispersity, and spectroscopic properties of aquatic humic substances. *Environmental Science and Technology* 28 (11): 1853-1858.

Cho, J., G. Amy, J. Pellegrino, and Y. Yoon. 1999. Characterization of clean and natural organic matter (NOM) fouled NF and UF membranes, and foulants characterization. *Water Supply* 17 (1): 183-190.

Chow, C. W. K., P. Kuntke, R. Fabris, and M. Drikas. 2009. Organic characterisation tools for distribution system management. *Water Science and Technology* 9 (1): 1-8.

Chow, C., R. Fabris, K. Wilkinson, F. Fitzgerald, and M. Drikas. 2006. Characterising NOM to assess treatability. *Water* 33 (2): 74-85.

Chow, A. T., S. Gao, and R. A. Dahlgren. 2005. Physical and chemical fractionation of dissolved organic matter and trihalomethane precursors: A review. *Journal of Water Supply: Research and Technology - AQUA* 54 (8): 475-507.

Chow, C., R. Fabris, and M. Drikas. 2004. A rapid fractionation technique to characterise natural organic matter for the optimisation of water treatment processes. *Journal of Water Supply: Research and Technology - AQUA* 53 (2): 85-92.

Chow, C., J. van Leeuwen, R. Fabris, S. King, N. Withers, K. Spark, and M. Drikas. 2000. *ENVIRO 2000*, Enhanced coagulation for removal of dissolved organic carbon with alum - a fractionation approach. Sydney, Australia, 9-13 April.

Chow, C. W. K., J. van Leeuwen, M. Drikas, R. Fabris, K. Spark, and D. Page. 1999. The impact of the character of natural organic matter in conventional treatment with alum. *Water Science and Technology* 40 (9): 97-104.

Christensen, J. B., D. L. Jensen, C. Grøn, Z. Filip, and T. H. Christensen. 1998. Characterization of the dissolved organic carbon in landfill leachate-polluted groundwater. *Water Research* 32 (1): 125-135.

Christy, A. A., A. Bruchet, and D. Rybacki. 1999. Characterization of natural organic matter by pyrolysis/GC-MS. *Environment International* 25 (2/3): 181-189.

Christy, A. A., and P. K. Egeberg. 2000. Characterisation of natural organic matter from the Nordic typing project water samples by chemometric analysis of their near infrared spectral profiles. *Chemometrics and Intelligent Laboratory Systems* 50 (2): 225-234.

Collins, M. R., G. L. Amy, and C. Steelink. 1986. Molecular weight distribution, carboxylic acidity, and humic substances content of aquatic organic matter: implications for removal during water treatment. *Environmental Science and Technology* 20 (10): 1028-32.

Comstock, K., R. Isabel, and P. Pherson. 2003. *2003 AWWA Water Quality Technology Conference*, Pilot-scale evaluation of advanced treatment processes for DBP precursor removal. Philadelphia, Pennsylvania, 2-6 November, CD-ROM.

Cook, R. L. 2004. Coupling NMR to NOM. *Analytical and Bioanalytical Chemistry* 378 (4): 1484-1503.

Couton, D. 2010. Thermochemolysis and its application for characterisation of natural organic matter in groundwaters. Doctorate, Department of Applied Chemistry, Curtin University.

Croué, J. P. 2004. Isolation of humic and non-humic NOM fractions: structural characterization. *Environmental Monitoring and Assessment* 92 (1-3): 193-207.

Croué, J. P., M. F. Benedetti, D. Violleau, and J. A. Leenheer. 2003. Characterization and copper binding of humic and nonhumic organic matter isolated from the South Platte River: evidence for the presence of nitrogeneous binding site. *Environmental Science and Technology* 37 (2): 328-336.

Croué, J. P., A. Bruchet, C. Hwang, and J. Leenheer. 2001. *2001 AWWA Water Quality Technology Conference*, The use of pyrolysis GC/MS as a single analytical tool for the structural characterization of NOM and the identification of DBP precursor sites. Nashville, Tennessee, 11-15 November, CD-ROM.

Croué, J. P., D. Violleau, and L. Labouyrie. 2000. Disinfection by-product formation potentials of hydrophobic and hydrophilic natural organic matter fractions: a comparison between a low- and a high-humic water. In *Natural Organic Matter and Disinfection By-Products. Characterization and Control in Drinking Water*, ed. S. E. Barrett, S. W. Krasner and G. L. Amy, 139-153. American Chemical Society.

Croué, J. P. 1999. *18th Federal Convention Australian Water and Wastewater Association*, Isolation, fractionation, characterization and reactive properties of natural organic matter. Adelaide, Australia, 11-14 April.

Croué, J. P., J. Debroux, G. L. Amy, G. R. Aiken, and J. A. Leenheer. 1999a. Natural organic matter: structural characteristics and reactive properties. In *Formation and Control of Disinfection By-Products in Drinking Water*, ed. P. C. Singer, 65-93. American Water Works Association.

Croué, J. P., G. V. Korshin, and M. Benjamin. 1999b. *Characterization of natural organic matter in drinking water*. AWWA Research Foundation.

Croué, J. P., B. Martin, A. Deguin, and B. Legube. 1994. Isolation and characterisation of dissolved hydrophobic and hydrophilic organic substances of a reservoir water. In *Natural Organic Matter in Drinking Water Origin Character and Removal Workshop Proceedings*: AWWA.

Croué, J. P., B. Martin, P. Simon, and B. Legube. 1993a. Hydrophobic and hydrophilic substances in reservoir waters - extraction, characterization, and determination. *Water Supply* 11 (1): 79-90.

Croué, J. P., E. Lefebvre, B. Martin, and B. Legube. 1993b. Removal of dissolved hydrophobic and hydrophilic organic substances during coagulation/flocculation of surface waters. *Water Science and Technology* 27 (11): 143-152.

Davidson, W. A. 1995. *Hydrogeology and groundwater resources in the Perth region, Western Australia*. Vol. Bulletin 142: Geological Survey of Western Australia.

Davis, W. M., C. L. Erickson, C. T. Johnston, J. J. Delfino, and J. E. Porter. 1999. Quantitative Fourier Transform infrared spectroscopic investigation of humic substance functional group composition. *Chemosphere* 38 (12): 2913-2928.

De Paolis, F., and J. Kukkonen. 1997. Binding of organic pollutants to humic and fulvic acids: influence of pH and the structure of humic material. *Chemosphere* 34 (8): 1693-1704.

del Rio, J. C., D. E. McKinney, H. Knicker, M. A. Nanny, R. D. Minard, and P. G. Hatcher. 1998. Structural characterization of bio- and geo-macromolecules by off-line thermochemolysis with tetramethylammonium hydroxide. *Journal of Chromatography A* 823 (1-2): 433-448.

Department of Water. 2010. www.water.wa.gov.au (accessed 10th August).

Desmukh, A. P., B. Chefetz, and P. G. Hatcher. 2001. Characterization of organic matter in pristine and contaminated coastal marine sediments using solid-state ^{13}C NMR, pyrolytic and thermochemolytic methods: a case study in the San Diego Harbor area. *Chemosphere* 45 (6-7): 1007-1022.

Dria, K. J., J. R. Sachleben, and P. G. Hatcher. 2002. Solid-state carbon-13 nuclear magnetic resonance of humic acids at high magnetic field strengths. *Journal of Environmental Quality* 31 (2): 393-401.

Drikas, M., M. Dixon, and J. Morran. 2011. Long term case study of MIEX pre-treatment in drinking water; understanding NOM removal. *Environmental Science and Technology* 45 (4): 1539-1548.

Drikas, M., P. Singer, C. Chow, and M. Holmes. 2008. Disinfection by-products: an Australian review. *Water* 35 (1): 80-85.

Drikas, M., C. W. K. Chow, and D. Cook. 2003. The impact of recalcitrant organic character on disinfection stability, trihalomethane formation and bacterial regrowth: an evaluation of magnetic ion exchange resin (MIEX®) and alum coagulation. *Journal of Water Supply: Research and Technology - AQUA* 52: 475-487.

Drikas, M. 1997. NOM (natural organic matter) the curse of the water industry. *Water* 24 (5): 29-33.

Edwards, G. A., and A. Amirtharajah. 1985. Removing color caused by humic acids. *American Water Works Association Journal* 77 (3): 50-57.

Fabris, R., C. W. K. Chow, M. Drikas, and B. Eikebrokk. 2008. Comparison of NOM character in selected Australian and Norwegian drinking waters. *Water Research* 42 (15): 4188-4196.

Fabris, R. B., C. W. K. Chow, and M. Drikas. 2007. *4th IWA Leading Edge Conference and Exhibition on Water and Wastewater Technologies, Combined treatments for enhanced natural organic matter removal*. Singapore, 3-6 June, CD-ROM.

Fearing, D. A., J. Banks, S. Guyetand, C. Monfort Eroles, B. Jefferson, D. Wilson, P. Hillis, A. T. Campbell, and S. A. Parsons. 2004. Combination of ferric and MIEX® for the treatment of a humic rich water. *Water Research* 38 (10): 2551-2558.

Filley, T. R., K. G. J. Nierop, and Y. Wang. 2006. The contribution of polyhydroxyl aromatic compounds to tetramethylammonium hydroxide lignin-based proxies. *Organic Geochemistry* 37 (6): 711-727.

Francioso, O., S. Sánchez-Cortés, D. Casarini, J. V. Garcia-Ramos, C. Ciavatta, and C. Gessa. 2002. Spectroscopic study of humic acids fractionated by means of tangential ultrafiltration. *Journal of Molecular Structure* 609 (1-3): 137-147.

Franson, M. A. H. 1998. *Standard Methods for the Examination of Water and Wastewater*. 20th ed. Washington: American Public Health Association.

Franzmann, P., A. Heitz, L. R. Zappia, J. E. Wajon, and K. Xanthis. 2001. The formation of malodorous dimethyl oligosulphides in treated groundwater: the role of biofilms and potential precursors. *Water Research* 35 (7): 1730-1738.

Frazier, S. W., L. A. Kaplan, and P. G. Hatcher. 2005. Molecular characterization of biodegradable dissolved organic matter using bioreactors and [$^{12}C/^{13}C$] tetramethylammonium hydroxide thermochemolysis GC-MS. *Environmental Science and Technology* 39 (6): 1479-1491.

Frazier, S. W., K. O. Nowack, K. M. Goins, F. S. Cannon, L. A. Kaplan, and P. G. Hatcher. 2003. Characterization of organic matter from natural waters using tetramethylammonium hydroxide thermochemolysis GC-MS. *Journal of Analytical and Applied Pyrolysis* 70 (1): 99-128.

Frimmel, F. H., and G. Abbt-Braun. 1999. Basic characterization of reference NOM from central Europe- similarities and differences. *Environment International* 25 (2/3): 191-207.

Gadel, F., and A. Bruchet. 1987. Application of pyrolysis-gas chromatography-mass spectrometry to the characterization of humic substances resulting from decay of aquatic plants in sediments and waters. *Water Research* 21 (10): 1195-1206.

Gadmar, T. C., R. D. Vogt, and L. Evje. 2005. Artefacts in XAD-8 NOM fractionation. *International Journal of Environmental Analytical Chemistry* 85 (6): 365 - 376.June 12, 2007).

Gaffney, J. S., N. A. Marley, and S. B. Clark. 1996. Humic and fulvic acids and organic colloidal materials in the environment. In *Humic and Fulvic Acids: Isolation, Structure and Environmental Role*, ed. J. S. Gaffney, N. A. Marley and S. B. Clark, 2-15. Washington, D.C.: American Chemical Society.

Gallard, H., F. Pellizzari, J. P. Croué, and B. Legube. 2003. Rate constants of reactions of bromine with phenols in aqueous solution. *Water Research* 37 (12): 2883-2892.

Gélinas, Y., J. A. Baldock, and J. I. Hedges. 2001. Demineralization of marine and freshwater sediments for CP/MAS ^{13}C NMR analysis. *Organic Geochemistry* 32 (5): 677-693.

Gjessing, E. T., J. J. Alberts, A. Bruchet, P. K. Egeberg, E. Lydersen, L. B. McGown, J. J. Mobed, U. Münster, J. Pempkowiak, M. Perdue, H. Ratnawerra, D. Rybacki, M. Takács, and G. Abbt-Braun. 1998. Multi-method characterisation of natural organic matter isolated from water: characterisation of reverse osmosis-isolates from water of two semi-identical dystrophic lakes basins in Norway. *Water Research* 32 (10): 3108-3124.

Greenwood, P. F., J. A. Leenheer, C. McIntyre, L. Berwick, and P. D. Franzmann. 2006. Bacterial biomarkers thermally released from dissolved organic matter. *Organic Geochemistry* 37 (5): 597-609.

Grøn, C., L. Wassenaar, and M. Krog. 1996. Origin and structures of groundwater humic substances from three Danish aquifers. *Environment International* 22 (5): 519-534.

Guignard, C., L. Lemée, and A. Ambles. 2005. Lipid constituents of peat humic acids and humin. Distinction from directly extractable bitumen components using TMAH and TEAAc thermochemolysis. *Organic Geochemistry* 36 (2): 287-297.

Harrington, G. W., A. Bruchet, D. Rybacki, and P. C. Singer. 1996. Characterization of natural organic matter and its reactivity with chlorine. In *Water Disinfection and Natural Organic Matter*, ed. R. A. Minear and G. Amy, 138-158. Washington DC: American Chemical Society.

Hatcher, P. G., K. J. Dria, S. Kim, and S. W. Frazier. 2001. Modern analytical studies of humic substances. *Soil Science* 166 (11): 770-794.

Heitz, A. 2002. Malodorous dimethylpolysulfides in Perth drinking water. Doctorate, School of Chemistry and Applied Science, Curtin University of Technology, Perth.

Heitz, A., C. Joll, R. Alexander, and R. I. Kagi. 2001. Characterisation of aquatic natural organic matter in some Western Australian drinking water sources. In *Understanding and Managing Organic Matter in Soils, Sediments and Waters*, ed. R. S. Swift and K. M. Spark, 429-436. Adelaide, Australia: International Humic Substances Society.

Her, N., G. Amy, J. Chung, J. Yoon, and Y. Yoon. 2007. Characterizing dissolved organic matter and evaluating associated nanofiltration membrane fouling. *Chemosphere* 70 (3): 495-502.

Her, N., G. Amy, D. McKnight, J. Sohn, and Y. Yoon. 2003. Characterization of DOM as a function of MW by fluorescence EEM and HPLC-SEC using UVA, DOC and fluorescence detection. *Water Research* 37 (17): 4295-4303.

Hirschberg, K.-J. B. 1989. Proceedings of the Swan Coastal Plain Management Conference, Groundwater contamination in the Perth metropolitan region. Perth: Western Australian Water Resources Council.

Holmquist, A. 2006. *Testing Procedures for MIEX® Resin*. Orica Advanced Water Technologies. Commercial in confidence.

Hua, B., K. Veum, A. Koirala, J. Jones, T. E. Clevenger, and B. Deng. 2007. Fluorescence fingerprints to monitor total trihalomethanes and N-nitrosodimethylamine formation potentials in water. *Environmental Chemical Letters* 5 (2): 73-77.

Hua, G., D. A. Reckhow, and J. Kim. 2006. Effect of bromide and iodide ions on the formation and speciation of disinfection byproducts during chlorination. *Environmental Science and Technology* 40 (9): 3050-3056.

Huber, S. A., and F. H. Frimmel. 1996. Size-exclusion chromatography with organic carbon detection (LC-OCD): a fast and reliable method for the characterization of hydrophilic organic matter in natural waters. *Vom Wasser* 86: 277-290.

Huffman Jr, E. W. D., and H. A. Stuber. 1985. Analytical methodology for elemental analysis of humic substances. In *Humic substances in soil, sediment and water. Geochemistry, isolation and characterization*, ed. G. R. Aiken, D. M. McKnight, R. L. Wershaw and P. MacCarthy, 433-455. Wiley.

Humbert, H., H. Gallard, V. Jacquemet, and J. P. Croué. 2007. Combination of coagulation and ion exchange for the reduction of UF fouling properties of a high DOC content surface water. *Water Research* 41 (17): 3803-3811.

Hwang, C. J., M. J. Sclimenti, S. W. Krasner, J. P. Croué, A. Bruchet, and G. L. Amy. 1999. *1999 AWWA Water Quality Technology Conference*, Characterization and reactivity of hydrophilic natural organic matter (NOM) in a low-humic water. Tampa, Florida, 31 October - 3 November, CD-ROM.

Joll, C. A., D. Couton, A. Heitz, and R. I. Kagi. 2004. Comparison of reagents for off-line thermochemolysis of natural organic matter. *Organic Geochemistry* 35 (1): 47-59.

Joll, C. A., A. Heitz, W. Simanjuntak, R. Alexander, and R. I. Kagi. 1999. *Proceedings of the American Water Works Association 1999 Annual Conference and Exhibition*, Characterisation of natural organic matter in some Western Australian drinking water sources and the relationship of NOM to organic-related bulk water parameters. Chicago, Illinois, USA, 20-24 June, CD-ROM.

Kanokkantapong, V., T. F. Marhaba, B. Panyapinyophol, and P. Pavasant. 2006. FTIR evaluation of functional groups involved in the formation of haloacetic acids during the chlorination of raw water. *Journal of Hazardous Materials* 136 (2): 188-196.

Kim, H.-C., M.-J. Yu, and I. Han. 2006. Multi-method study of the characteristic chemical nature of aquatic humic substances isolated from the Han River, Korea. *Applied Geochemistry* 21 (7): 1226-1239.

Kitis, M., T. Karanfil, A. Wigton, and J. E. Kilduff. 2002. Probing reactivity of dissolved organic matter for disinfection by-product formation using XAD-8 resin adsorption and ultrafiltration fractionation. *Water Research* 36 (15): 3834-3848.

Knicker, H., and M. A. Nanny. 1997. Nuclear magnetic resonance spectroscopy: basic theory and background. In *Nuclear Magnetic Resonance Spectroscopy in Environmental Chemistry*, ed. M. A. Nanny, R. A. Minear and J. A. Leenheer, 3-15. New York: Oxford University Press.

Koechling, M. T., and R. S. Summers. 1996. *Proceedings-Water Quality Technology Conference*, Evaluation of ultrafiltration and hydrophobic separation for characterizing natural organic matter.

Kögel-Knabner, I. 2000. Analytical approaches for characterizing soil organic matter. *Organic Geochemistry* 31 (7-8): 609-625.

Korshin, G. V., C.-W. Li, and M. M. Benjamin. 1997. Monitoring the properties of natural organic matter through UV spectroscopy: a consistent theory. *Water Research* 31 (7): 1787-1795.

Krasner, S. W., J. P. Croué, J. Buffle, and E. M. Perdue. 1996. Three approaches for characterizing NOM. *Journal AWWA* 88 (9): 66-79.

Kristiana, I., B. Allpike, C. A. Joll, A. Heitz, and R. Trolio. 2010. Understanding the behaviour of molecular weight fractions of natural organic matter to improve water treatment processes. *Water Science and Technology: Water Supply* 10 (1): 59-68.

Lankes, U., H.-D. Ludemann, and F. H. Frimmel. 2008. Search for basic relationships between "molecular size" and "chemical structure" of aquatic natural organic matter - answers from 13C and 15N CPMAS NMR spectroscopy. *Water Research* 42 (4-5): 1050-1060.

Lee, S., B. Kwon, M. Sun, and J. Cho. 2005. Characterization of NOM included in NF and UF membrane permeates. *Desalination* 173 (2): 131-142.

Lee, N., S. Sinha, G. Amy, and M. Bourke. 2003. *2003 AWWA Annual Conference*, Removal of polar natural organic matter (NOM) with a magnetically impregnated ion exchange (MIEX®) media. Anaheim, California, 15-19 June, CD-ROM.

Lee, N., S. Sinha, G. Amy, and M. Bourke. 2002. *2002 AWWA Water Quality Technology Conference*, Evaluation of magnetic ion exchange resin treatment for preferential removal of NOM fractions. Seattle, Washington, USA, 10-14 November, CD-ROM.

Leenheer, J. A. 2009. Systematic approaches to comprehensive analyses of natural organic matter. In *Annals of Environmental Science*, 1-130. Boston, MA: Northeastern University.

Leenheer, J. A., and J. P. Croué. 2003. Characterizing aquatic dissolved organic matter. *Environmental Science and Technology* 37 (1): 18A-26A.

Leenheer, J. A., M. A. Nanny, and C. McIntyre. 2003. Terpenoids as major precursors of dissolved organic matter in landfill, leachates, surface water, and groundwater. *Environmental Science and Technology* 37 (11): 2323-2331.

Leenheer, J. A., J. P. Croué, M. Benjamin, G. V. Korshin, C. J. Hwang, A. Bruchet, and G. R. Aiken. 2000. Comprehensive isolation of natural organic matter from water for spectral characterizations and reactivity testing. In *Natural Organic Matter and Disinfection By-Products. Characterization and Control in Drinking Water*, ed. S. E. Barrett, S. W. Krasner and G. L. Amy, 68-83. American Chemical Society.

Leenheer, J. A., R. L. Wershaw, and M. M. Reddy. 1995. Strong-acid, carboxyl-group structures in fulvic acid from the Suwannee River, Georgia. 1. Minor structures. *Environmental Science and Technology* 29 (2): 393-398.

Leenheer, J. A., P. A. Brown, and E. A. Stiles. 1987. Isolation of nonvolatile, organic solutes from natural waters by zeotrophic distillation of water from *N,N*-dimethylformamide. *Analytical Chemistry* 59 (9): 1313-19.

Leenheer, J. A. 1981. Comprehensive approach to preparative isolation and fractionation of dissolved organic carbon from natural waters and wastewaters. *Environmental Science and Technology* 15 (5): 578-587.

Leenheer, J. A., and E. W. D. Huffman. 1976. Classification of organic solutes in water using macroreticular resins. *Journal of Research of the U.S. Geological Survey* 4 (6): 737-751.

Lehtonen, T., J. Peuravuori, and K. Pihlaja. 2000a. Characterisation of lake-aquatic humic matter isolated with two different sorbing techniques: tetramethylammonium hydroxide treatment and pyrolysis-gas chromatography / mass spectrometry. *Analytica Chimica Acta* 424 (1): 91-103.

Lehtonen, T., J. Peuravuori, and K. Pihlaja. 2000b. Degradation of TMAH treated aquatic humic matter at different temperatures. *Journal of Analytical and Applied Pyrolysis* 55 (2): 151-160.

Li, A., J. Hu, W. Zhang, and X. Wang. 2009. Polarity based fractionation of fulvic acids. *Chemosphere* 77 (10): 1419-1426.

Li, L., Z. Zhao, W. Huang, P. Peng, G. Sheng, and J. Fu. 2004. Characterization of humic acids fractionated by ultrafiltration. *Organic Geochemistry* 35 (9): 1025-1037.

Liang, L., and P. C. Singer. 2003. Factors influencing the formation and relative distribution of haloacetic acids and trihalomethanes in drinking water. *Environmental Science and Technology* 37 (13): 2920-2928.

Lu, X. Q., N. Maie, J. V. Hanna, D. L. Childers, and R. Jaffé. 2003. Molecular characterization of dissolved organic matter in freshwater wetlands of the Florida Everglades. *Water Research* 37 (11): 2599-2606.

Lu, X. Q., J. V. Hanna, and W. D. Johnson. 2001. Evidence of chemical pathways of humification: a study of aquatic humic substances heated at various temperatures. *Chemical Geology* 177 (3-4): 249-264.

Lu, X. Q., J. V. Hanna, and W. D. Johnson. 2000. Source indicators of humic substances: an elemental composition, solid state ^{13}C CP/MAS NMR and py-GC/MS study. *Applied Geochemistry* 15 (7): 1019-1033.

Ludlow, M., D. Louden, A. Handley, S. Taylor, B. Wright, and I. D. Wilson. 1999. Size-exclusion chromatography with on-line ultraviolet, proton nuclear magnetic resonance and mass spectrometric detection and on-line collection for off-line Fourier Transform infrared spectroscopy. *Journal of Chromatography A* 857 (1-2): 89-96.

Ma, H., H. E. Allen, and Y. Yin. 2001. Characterization of isolated fractions of dissolved organic matter from natural waters and a wastewater effluent. *Water Research* 35 (4): 985-996.

Malcolm, R. L., J. P. Croué, and B. Martin. 1995. Isolation of XAD-4 acids from natural waters and their importance as precursors to TOX and THM upon chlorination. In *Naturally-Produced Organohalogens*, ed. A. Grimvall and E. W. B. de LeerNetherlands: Kluwer Academic Publishers.

Malcolm, R. L., and P. MacCarthy. 1992. Quantitative evaluation of XAD-8 and XAD-4 resins used in tandem for removing organic solutes from water. *Environment International* 18 (6): 597-607.

Malcolm, R. L. 1989. Factors to be considered in the isolation and characterization of aquatic humic substances. In *Humic Substances in the Aquatic and Terrestrial Environment*, ed. B. Allard, H. Borén and A. Grimvall: Springer Verlag.

Mao, J., R. M. Cory, D. M. McKnight, and K. Schmidt-Rohr. 2007. Characterization of a nitrogen-rich fulvic acid and its precursor algae from solid state NMR. *Organic Geochemistry* 38 (8): 1277-1292.

Marhaba, T. F., Y. Pu, and K. Bengraine. 2003. Modified dissolved organic matter fractionation technique for natural water. *Journal of Hazardous Materials* 101 (1): 43-53.

Marhaba, T. F. 2000. Fluorescence technique for rapid identification of DOM fractions. *Journal of Environmental Engineering* 126 (2): 145-152.

Marhaba, T. F., D. Van, and R. L. Lippincott. 2000. Changes in NOM fractionation through treatment: a comparison of ozonation and chlorination. *Ozone Science and Engineering* 22 (3): 249-66.

Martin, F., J. C. del Rio, F. J. González-Vila, and T. Verdejo. 1995. Pyrolysis derivatization of humic substances 2. Pyrolysis of soil humic acids in the presence of tetramethylammonium hydroxide. *Journal of Analytical and Applied Pyrolysis* 31: 75-83.

Mash, H., P. Westerhoff, L. A. Baker, R. A. Nieman, and M. Nguyen. 2004. Dissolved organic matter in Arizona reservoirs: assessment of carbonaceous sources. *Organic Geochemistry* 35 (7): 831-843.

Matilainen, A., E. T. Gjessing, T. Lahtinen, L. Hed, A. Bhatnagar, and M. Sillanpää. 2011. An overview of the methods used in the characterisation of natural organic matter (NOM) in relation to drinking water treatment. *Chemosphere* 83 (11): 1431-1442.

McIntyre, C., and C. McRae. 2005. Proposed guidelines for sample preparation and ESI-MS analysis of humic substances to avoid self-esterification. *Organic Geochemistry* 36 (4): 543-553.

Morran, J. Y., D. B. Bursill, M. Drikas, and H. Nguyen. 1996. *AWWA Watertec Convention*, A new technique for the removal of natural organic matter. Sydney, Australia.

Morrison, R. T., and R. N. Boyd. 1992. *Organic chemistry*. 6th ed. New Jersey: Prentice Hall.

Mycke, B., K. Hall, and P. Leplat. 1994. Carbon isotopic composition of individual hydrocarbons and associated gases evolved from micro-scale sealed vessel (MSSV) pyrolysis of high molecular weight organic material. *Organic Geochemistry* 21 (6-7): 787-800.

Nanny, M. A. 1997. Sorption processes in the environment nuclear magnetic resonance spectroscopy as a new analytical method. In *Nuclear Magnetic Resonance Spectroscopy in Environmental Chemistry*, ed. M. A. Nanny, R. A. Minear and J. A. Leenheer, 19-25. New York: Oxford University Press.

Newcombe, G., M. Drikas, S. Assemi, and R. Beckett. 1997. Influence of characterised natural organic material on activated carbon adsorption: I. Characterisation of concentrated reservoir water. *Water Research* 31 (5): 965-972.

Nguyen, H., M. Slunjski, M. F. Bourke, and M. Drikas. 1997. *17th Federal Convention Australian Water and Wastewater Association*, DOC removal by MIEX® process - scaling-up and other development issues. Melbourne, Australia, 16-21 March.

NHRMC, Australian Drinking Water Guidelines. 2011. http://www.nhmrc.gov.au/publications/_files/awgfull.pdf (accessed 24th January 2012).

Nissinen, T. K., I. T. Miettinen, P. J. Martikainen, and T. Vartiainen. 2001. Molecular size distribution of natural organic matter in raw and drinking waters. *Chemosphere* 45 (6-7): 865-873.

Norwood, D. L., R. F. Christman, and P. G. Hatcher. 1987. Structural characterization of aquatic humic material. 2. Phenolic content and its relationship to chlorination mechanism in an isolated aquatic fulvic acid. *Environmental Science and Technology* 21 (8): 791-798.

Obolensky, A., and P. C. Singer. 2005. Halogen substitution patterns among disinfection byproducts in the information collection rule database. *Environmental Science and Technology* 39 (8): 2719-2730.

Owen, D. M., G. L. Amy, Z. K. Chowdhury, R. Paode, G. McCoy, and K. Viscosil. 1995. NOM characterization and treatability. *Journal AWWA* 87 (1): 46-63.

Page, D. W., J. A. van Leeuwen, K. M. Spark, and D. E. Mulcahy. 2003. Application of pyrolysis-gas chromatography / mass spectrometry for characterisation of dissolved organic matter before and after alum treatment. *Journal of Analytical and Applied Pyrolysis* 67 (2): 247-262.

Pelekani, C., M. Drikas, and D. B. Bursill. 2001. Application of direct filtration to MIEX® treated River Murray water. *Water* 28 (4): 42-45.

Peuravuori, J., P. Ingman, and K. Pihlaja. 2003. Critical comments on accuracy of quantitative determination of natural organic matter by solid state ^{13}C NMR spectroscopy. *Talanta* 59: 177-189.

Peuravuori, J., and K. Pihlaja. 1997. Molecular size distribution and spectroscopic properties of aquatic humic substances. *Analytica Chimica Acta* 337 (2): 133-49.

Piccolo, A. 2001. The supramolecular structure of humic substances. *Soil Science* 166 (11): 810-832.

Reckhow, D. A., P. C. Singer, and R. L. Malcolm. 1990. Chlorination of humic materials: byproduct formation and chemical interpretations. *Environmental Science and Technology* 24 (11): 1655-1664.

Richardson, S. D. 2003. Water analysis: emerging contaminants and current issues. *Analytical Chemistry* 75 (18): 2831-2857.

Rivero, C., N. Senesi, J. Paolini, and V. D'Orazio. 1998. Characteristics of humic acids of some Venezuelan soils. *Geoderma* 81 (3-4): 227-239.

Rodriguez, M. J., J.-B. Sérodes, and P. Levallois. 2004. Behaviour of trihalomethanes and haloacetic acids in a drinking water distribution system. *Water Research* 38 (20): 4367-4382.

Rook, J. J. 1977. Chlorination reactions of fulvic acids in natural waters. *Environmental Science and Technology* 11 (5): 478-482.

Rook, J. J. 1974. Formation of haloforms during chlorination of natural waters. *Water Treatment and Examination* 23 (2): 234-243.

Rostad, C. E., J. A. Leenheer, B. Katz, B. S. Martin, and T. I. Noyes. 2000. Characterization and disinfection by-product formation potential of natural organic matter in surface and groundwaters from northern Florida. In *Natural Organic Matter and Disinfection By-Products. Characterization and Control in Drinking Water*, ed. S. E. Barrett, S. W. Krasner and G. L. Amy, 154-172. American Chemical Society.

Saiz-Jimenez, C. 1994. Analytical pyrolysis of humic substances: pitfalls, limitations, and possible solutions. *Environmental Science and Technology* 28 (11): 1773-1780.

Saiz-Jimenez, C., B. Hermosin, and J. J. Ortega-Calvo. 1993. Pyrolysis/methylation: A method for structural elucidation of the chemical nature of aquatic humic substances. *Water Research* 27 (11): 1693-1696.

Saiz-Jimenez, C., and J. W. De Leeuw. 1986. Chemical characterization of soil organic matter fractions by analytical pyrolysis-gas chromatography-mass spectrometry. *Journal of Analytical and Applied Pyrolysis* 9: 99-119.

Schnitzer, M., and K. Ghosh. 1979. Some recent advances in the chemistry and reactions of humic substances. *Journal of Indian Chemical Society* 56 (11): 1090-1093.

Schulten, H.-R., and G. Gleixner. 1999. Analytical pyrolysis of humic substances and dissolved organic matter in aquatic systems: structure and origin. *Water Research* 33 (11): 2489-2498.

Senesi, N. 1990. Molecular and quantitative aspects of the chemistry of fulvic acids and its interactions with metal ions and organic chemicals: Part II. The fluorescence spectroscopy approach. *Analytica Chimica Acta* 232: 77-106.

Sharp, E. L., S. A. Parsons, and B. Jefferson. 2006a. Coagulation of NOM: Linking Character to Treatment. *Water Science and Technology* 53: 67-76.

Sharp, E. L., S. A. Parsons, and B. Jefferson. 2006b. Seasonal variations in natural organic matter and its impact on coagulation in water treatment. *Science of the Total Environment* 363 (1-3): 183-194.

Sharp, E. L., P. Jarvis, S. A. Parsons, and B. Jefferson. 2006c. Impact of fractional character on the coagulation of NOM. *Colloids and Surfaces A: Physicochemical and Engineering Aspects* 286 (1-3): 104-111.

Sihombing, R., P. F. Greenwood, M. A. Wilson, and J. V. Hanna. 1996. Composition of size exclusion fractions of swamp water humic and fulvic acids as measured by solid state NMR and pyrolysis-gas chromatography - mass spectrometry. *Organic Geochemistry* 24 (8-9): 859-873.

Singer, P. C., T. H. Boyer, A. Holmquist, J. Morran, and M. Bourke. 2007a. *2007 AWWA Water Quality Technology Conference and Exhibition*, Integrated analysis of NOM removal by magnetic ion exchange. Charlotte, North Carolina, 4-8 November, CD-ROM.

Singer, P. C., M. Schneider, J. Edwards-Brandt, and G. C. Budd. 2007b. MIEX® for removal of DBP precursors: Pilot-plant findings. *Journal AWWA* 99 (4): 128-139.

Singer, P. C. 2002. Occurrence of haloacetic acids in chlorinated drinking water. *Water Science and Technology: Water Supply* 2 (5): 487-492.

Singer, P. C., and K. Bilyk. 2002. Enhanced coagulation using a magnetic ion exchange resin. *Water Research* 36 (16): 4009-4022.

Singer, P. C. 1999. Humic substances as precursors for potentially harmful disinfection by-products. *Water Science and Technology* 40 (9): 25-30.

Sinha, S., G. L. Amy, and J. Sohn. 1997. *Proceedings - AWWA Annual Conference, Reactivity of NOM fractions in forming chlorinated DBPs*.

Slunjski, M., M. Bourke, and B. O'Leary. 2000a. *International Humic Substances Society, Australian Chapter Seminar*, 18 February, MIEX® DOC process for removal of humics in water treatment.

Slunjski, M., K. Cadee, and J. Tattersall. 2000b. *Aquatech Amsterdam 2000*, MIEX® resin water treatment process. Amsterdam, Netherlands, 26-29 September.

Smart, P. L., B. L. Finlayson, W. D. Rylands, and C. M. Ball. 1976. The relation of fluorescence to dissolved organic carbon in surface waters. *Water Research* 10 (9): 805-811.

Smith, P., B. O'Leary, J. Tattersall, and B. Allpike. 2003. *OZWATER Convention and Exhibition*, The MIEX® process - a year of operation. Perth, Australia, 6-10 April, CD-ROM.

Soh, Y. C., F. Roddick, and J. van Leeuwen. 2007. *2nd IWA ASPIRE Conference and Exhibition*, The impact of alum coagulation on the character, biodegradability and disinfection by-product formation potential of reservoir NOM fractions. Perth, Western Australia, 28 October-1 November, CD-ROM.

Specht, C. H., and F. H. Frimmel. 2000. Specific interactions of organic substances in size-exclusion chromatography. *Environmental Science and Technology* 34 (11): 2361-2366.

Stevenson, F. J. 1994. *Humus Chemistry: Genesis, Composition, Reactions*. 2nd ed. Brisbane: John Wiley and Sons, Inc.

Swietlik, J., and E. Sirorska. 2004. Application of fluorescence spectroscopy in the studies of natural organic matter fractions reactivity with chlorine dioxide and ozone. *Water Research* 38 (17): 3791-3799.

Takács, M., and J. J. Alberts. 1999. Changes in chemical composition, FTIR and fluorescence spectral characteristics of humic acids in peat profiles. In *Understanding humic substances. Advanced methods, properties and application*, ed. E. A. Ghabbour and G. Davies, 169-77. The Royal Society of Chemistry.

Templier, J., S. Derenne, J. P. Croué, and C. Largeau. 2005. Comparative study of two fractions of riverine dissolved organic matter using various analytical pyrolytic methods and a 13C CP/MAS NMR approach. *Organic Geochemistry* 36 (10): 1418-1442.

Thurman, E. M. 1985. Humic substances in groundwater. In *Humic Substances in Soil, Sediment and Water. Geochemistry, Isolation, and Characterization*, ed. G. R. Aiken, D. M. McKnight and R. L. Wershaw, 87-103. Wiley Interscience.

Thurman, E. M., and R. L. Malcolm. 1981. Preparative isolation of aquatic humic substances. *Environmental Science and Technology* 15 (4): 463-66.

Thurman, E. M., R. L. Malcolm, and G. R. Aiken. 1978. Prediction of capacity factors for aqueous organic solutes adsorbed on a porous acrylic resin. *Analytical Chemistry* 50 (6): 775-79.

van Leeuwen, J., C. Chow, R. Fabris, N. Withers, D. Page, and M. Drikas. 2002. Application of a fractionation technique for better understanding of the removal of natural organic matter by alum coagulation. *Water Science and Technology: Water Supply* 2 (5-6): 427-433.

Volk, C., and M. W. LeChevallier. 2000. Assessing biodegradable organic matter. *Journal AWWA* 92 (5): 64-76.

Vrijenhoek, E. M., A. E. Childress, M. Elimelech, T. S. Tanaka, and M. D. Beuhler. 1998. Removing particles and THM precursors by enhanced coagulation. *Journal AWWA* 90 (4): 139-150.

Vuorio, E., R. Vahala, J. Rintala, and R. Laukkanen. 1998. The evaluation of drinking water treatment performed with HPSEC. *Environment International* 24 (5/6): 617-623.

Wajon, J. E., R. Alexander, R. I. Kagi, and B. Kavanagh. 1985. Dimethyl trisulphide and objectionable odours in potable waters. *Chemosphere* 14 (1): 85-89.

Warton, B., A. Heitz, B. Allpike, and R. Kagi. 2008. Size-exclusion chromatography with organic carbon detection using a mass spectrometer. *Journal of Chromatography A* 1207: 186-189.

Warton, B., A. Heitz, L. R. Zappia, P. D. Franzmann, D. Masters, C. A. Joll, M. Alessandrino, B. Allpike, B. O'Leary, and R. I. Kagi. 2007a. Magnetic ion exchange drinking water treatment in a large-scale facility. *Journal AWWA* 99 (1): 89-101.

Warton, B., R. Trolio, R. Gupta, A. Heitz, B. Allpike, R. Walker, S. McNeil, J. Lo, C. Joll, and R. Kagi. 2007b. *AWA Ozwater Conference and Exhibition*, Current and future predictive tools for management of trihalomethane formation in drinking water. Sydney, Australia, 4-8 March, CD-ROM.

Water Corporation of Western Australia. 2010. www.watercorporation.com.au (accessed 10th August).

White, G. C. 1999. Handbook of chlorination and alternative disinfectants. 4th ed: Wiley-Interscience.

Wilson, M. A. 1989. Solid-state nuclear magnetic resonance spectroscopy of humic substances: basic concepts and techniques. In *Humic Substances II In Search of Structure*, ed. M. H. B. Hayes, P. MacCarthy, R. L. Malcolm and R. S. Swift, 310-338. Brisbane: Wiley Interscience.

Wilson, M. A., P. F. Barron, and A. H. Gillam. 1981. The structure of freshwater humic substances as revealed by ^{13}C-NMR spectroscopy. *Geochimica et Coshimica Acta* 45 (10): 1743-1750.

Wong, H., K. M. Mok, and X. J. Fan. 2007. Natural organic matter and formation of trihalomethanes in two water treatment processes. *Desalination* 210 (1-3): 44-51.

Wong, S., J. V. Hanna, S. King, J. Carroll, R. J. Eldridge, D. R. Dixon, B. A. Bolto, S. Hesse, G. Abbt-Braun, and F. H. Frimmel. 2002. Fractionation of natural organic matter in drinking water and characterization by ^{13}C cross-polarization magic-angle spinning NMR spectroscopy and size exclusion chromatography. *Environmental Science and Technology* 36 (16): 3497-3503.

Zhang, X., S. Echigo, R. A. Minear, and M. J. Plewa. 2000. Characterisation and comparison of disinfection by-products of four major disinfectants. In *Natural organic matter and disinfection by-products: characterisation and control in drinking water*, ed. S. E. Barrett, S. W. Krasner and G. L. Amy, 299-314. American Chemical Society.

Zhou, Q., S. E. Cabaniss, and P. A. Maurice. 2000. Considerations in the use of high-pressure size exclusion chromatography (HPSEC) for determining molecular weights of aquatic humic substances. *Water Research* 34 (14): 2505-3514.